Evaluation of Antivirals against Alphaviruses using the example of Chikungunya Virus

von

Friederike Ilse Lore Hucke

2022

Inaugural-Dissertation zur Erlangung der Doktorwürde

der Tierärztlichen Fakultät der Ludwig-Maximilians-Universität

München

Evaluation of Antivirals against Alphaviruses using the example of Chikungunya Virus

von Friederike Ilse Lore Hucke

aus Lahr im Schwarzwald

München 2022

Aus dem Veterinärwissenschaftlichen Department der Tierärztlichen

Fakultät der Ludwig-Maximilians-Universität München

Lehrstuhl für Virologie

Arbeit angefertigt unter der Leitung von

Univ.-Prof. Dr. Dr. h.c. Gerd Sutter

Arbeit angefertigt am Institut für Mikrobiologie der Bundeswehr,

München

Mentor: FTLA Dr. J. J. Bugert

Gedruckt mit Genehmigung der Tierärztlichen Fakultät

der Ludwig-Maximilians-Universität München

Dekan: Univ.-Prof. Dr. Reinhard K. Straubinger, Ph. D.

Berichterstatter: Univ.-Prof. Dr. Dr. h.c. Gerd Sutter

Korreferent: Priv.-Doz. Dr. Sonja Härtle

Tag der Promotion: 30. Juli 2022

Die vorliegende Arbeit wurde gemäß § 6 Abs. 2 der Promotionsordnung für die Tierärztliche Fakultät der Ludwig-Maximilians-Universität München in kumulativer Form verfasst.

Folgende wissenschaftliche Arbeiten sind in dieser Dissertationsschrift enthalten:

Hucke, F. I. L., Bestehorn-Willmann, M., Bassetto, M., Brancale, A., Zanetta, P., & Bugert, J. J. (2022). **CHIKV strains Brazil (wt) and Ross (lab-adapted) differ with regard to cell host range and antiviral sensitivity and show CPE in human glioblastoma cell lines U138 and U251**. *Virus Genes,* **58,** 188–202 (2022). https://doi.org/10.1007/s11262-022-01892-x. Reproduced with permission from Springer Nature.

Hucke, F. I. L., Bestehorn-Willmann, M., & Bugert, J. J. (2021). **Prophylactic strategies to control chikungunya virus infection**. *Virus Genes*, *57*(2), 133–150. https://doi.org/10.1007/s11262-020-01820-x.

Hucke, F.I.L., & Bugert, J. J. (2020). **Current and Promising Antivirals Against Chikungunya Virus**. *Frontiers in Public Health*, *8*, 618624. https://doi.org/10.3389/fpubh.2020.618624.

Weitere Arbeiten die nicht in der Dissertationsschrift enthalten sind:

Bugert, J. J., Hucke, F. I.L., Zanetta, P., Bassetto, M., & Brancale, A. (2020). **Antivirals in medical biodefense.** *Virus Genes*, *56*(2), 150–167. https://doi.org/10.1007/s11262-020-01737-5.

Meiner Familie

CONTENTS

I.   ABBREVIATIONS

ADP	Adenosindiphosphate
Asn	Asparagine
BSL	Biosafety level
CC_{50}	Cytotoxicity concentration 50%
°C	Degrees Celsius
CDC	*Centres for Disease Control and Prevention*
CHIKF	Chikungunya fever
CHIKV	Chikungunya virus
CMC	Carboxymethylcellulose
CNS	Central nervous system
Cp	Capsid protein
CPE	Cytopathic effect
CPV	Cytopathic vacuole
cRNA	Copy-RNA
Ct	Cycle threshold
Cys	Cysteine
ddH_2O	Double-distilled water
DENV	Dengue virus
DMEM	Dulbecco's Modified Eagle Medium
DMSO	Dimethyl sulfoxide
DNA	Desoxyribonuclein acid
DNase	Desoxyribonuclease
dNTP	Desoxyribonucleosid-triphosphat
DPBS	*Dulbecco's Phosphate Buffered Saline*
dpi	Days *post* infection
dpt	Days *post* treatment
Dr.	Doktor
ds	Double-stranded
e.g.	For example
EC_{50}	Half maximal effective concentration
EEEV	Eastern equine encephalitis virus
EIDs	Emerging infectious diseases
ELISA	Enzyme-linked immunosorbent assay
et al.	And others
FBS	Foetal Bovine Serum
FDA	U.S. Food and Drug Administration
Fig.	Figure

G3BP	Ras-GTPase-activating protein (Src-homology 3 (SH3) domain)-binding proteins
GAGs	Glycosaminoglycans
GTP	Guanosine triphosphate
HCQ	Hydroxychlorquinine
HCV	Hepatitis C virus
HG	High glucose
His	Histidine
HTS	High-throughput screening
IC_{50}	Half maximal inhibition concentration
IFA	Immunofluorescence assay
IFN	Interferon
IMPDH	Inosine monophosphate dehydrogenase
kb	Kilobase
kDa	Kilodalton
LB	Lysogeny broth
LG	Low glucose
LMU	Ludwig-Maximilians-Universität
log	Logarithm
M	Molar
Met	Methionine
min	Minutes
μL	Microliter
μm	Micrometre
μM	Micromolar
mL	Millilitre
mm	Millimetre
MOI	Multiplicity of infection
MPA	Mycophenolic acid
mRNA	Messenger-RNA
MTase	Methytransferase
MTS	3-(4,5-dimethylthiazol-2-yl)-5-(3-carboxymethoxyphenyl)-2-(4-sulfophenyl)-2H-tetrazolium
NA	Nucleoside analogue
NaCl	Natrium-chloride
NC	Nucleocapsid
NCBI	National Centre for Biotechnology Information
ng	Nanogram
NHP	Non-human primates

nm	Nanometre
NP	Nucleoside phosphonate analogue
nsP(s)	Non-structural protein(s)
NTDs	Neglected tropical diseases
OD	Optical density
ONNV	O'nyong-nyong virus
ORF	Open reading frame
pi	*Post* infection
PCR	Polymerase chain reaction
%	Percent
pg	Picogram
PKR	Protein kinase R
+ssRNA	Positive-sense, single-stranded RNA
PM	Plasma membrane
PMS	N-methyl dibenzopyrazine methyl sulfate
PRR	Pattern recognition receptor
qRT-PCR	Quantitative reverse transcriptase polymerase chain reaction
R&D	Research and development
RBV	Ribavirin
RC	Replication complex
RCA	Rolling circle amplification
RdRp	RNA-dependent RNA polymerase
RKI	Robert Koch Institut
RNA	Ribonucleic acid
RNAi	RNA interference
rpm	Rounds per minute
RRV	Ross River virus
RT	Room temperature
RT-PCR	Reverse transcriptase polymerase chain reaction
RTP	Ribofuranosyl 5'-triphosphate
sec	Seconds
SFV	Semliki Forest virus
SI	Selectivity index
SINV	Sinbis virus
siRNA	Small interfering RNA
ss	Single stranded
T75	75 cm^2 cell culture bottle
Tab.	Table

TATase	Terminal adenylyl-transferase
TBEV	Tick borne encephalitis virus
TE-buffer	Tris-ethylendiamin-tetraacetat-buffer
TEM	Transmission electron microscope
Trp	Tryptophan
Tyr	Tyrosine
™	Unregistered trademark
US	United States
VEEV	Venezuelan equine encephalitis virus
VLP	Virus-like particle
WEEV	Western equine encephalitis virus
WHO	World Health Organisation
wt	Wildtype
×	Multiplied
x g	x gravitational force
XTT	Sodium 3´- [1- (phenylaminocarbonyl)- 3,4-tetrazolium]-bis (4-methoxy6-nitro) benzene sulfonic acid hydrate
YFV	Yellow fever virus
ZBD	Zentraler Bereich Diagnostik
ZIKV	Zika virus
ZKÜ	Zellkulturüberstand

II.   INTRODUCTION

Alphaviruses are enveloped single-stranded RNA arboviruses of the *Togaviridae* family and are geographically widely distriguted [1, 2]. They cause various diseases in humans and animals such as encephalitis, arthritis fever, rash and arthralgia [1].

Among the medically relevant members of the alphaviruses are Venezuelan, Western, and Eastern Equine Encephalitis viruses (VEEV, WEEV, and EEEV), Ross River virus (RRV) and Chikungunya virus (CHIKV). The Equine Encephalitis viruses are categoriesed as potential agents for bioterrorism since they can all be transmitted via aerosols, causing severe disease [3-7].

Chikungunya virus (CHIKV) is categorised as a(n) (re)emerging disease and is mainly transmitted by *Aedes* spp. mosquitoes [8]. CHIKV is the causative agent of chikungunya fever (CHIKF) which is characterised by high fever, headache and myalgia and polyarthralgia [9]. Especially the polyarthralgia may last for months or even years and leave patients with a severely deteriorated quality of life. CHIKV has repeatedly been responsible for outbreaks that caused serious economic and public health problems in the affected countries [8]. To date, no vaccine or specific antiviral therapies are available.

This thesis focusses on *in vitro* antiviral testing against a wild type CHIKV isolate and selecting possible hit to lead compounds. Climate change leads to the introduction of vectors in more temperate zones and thus it is possible that new diseases emerge with these vectors [10]. Consequently, the need for specific antivirals to treat such emerging diseases like CHIKV is current. Most of these *in vitro* antiviral assays are conducted in Vero cells, a cell line that originated from the kidney of an African green monkey [11]. Although this cell line is the model cell line to probagate CHIKV in, it lacks the clinical relevance of the disease and is not of human origin. Therefore, another goal of the thesis was to identify a human cell line with clinical relevance (especially for neurogenic CHIKV disease) to test antivirals in. This study was the first to describe the human glioblastoma cell line U138 in extensive antiviral tests against CHIKV. Furthermore, different assay methods were compared for their usefulness in antiviral tests against CHIKV in Vero-B4 and U138 cells.

III. LITERATURE REVIEW

1. Emerging and neglected tropical diseases; medical biodefence

The terms 'emerging, and re-emerging diseases' refer to diseases with infectious character and of which the incidence rate in humans has either increased in the past 20 years or might increase in the near future [12]. Emerging infectious diseases (EIDs) are epidemic, whereas neglected tropical diseases (NTDs) are endemic. EIDs and NTDs share essential health determining factors like neglect, poverty, a lack of access to clean water and sanitation facilities as well as limited or no provision of healthcare. Furthermore, many NTDs and EIDs have a zoonotic nature [13]. According to the WHO (World Health Organization), NTDs are a diverse group of communicable diseases that prevail in tropical and subtropical conditions in 149 countries and may cause severe effects on human health and lead to vast economic costs [12, 14]. The WHO classifies CHIKV as one of the 20 major NTDs responsible for various forms of disabilities and deaths especially in developing nations. These 20 NTDs afflict more than one billion people and cost developing nations billions of dollars every year [12]. Furthermore, CHIKV is also one of three diseases that were designated as 'serious and necessitating further action as soon as possible' in the WHOs 'R&D Blueprint for Action to Prevent Epidemics' (May 2016). This R&D Blueprint is a programme fostered by the WHO for accelerating research and development (hence R&D) concerning epidemic agents where there are no or insufficient preventive, and curative solutions [15].

Apart from finding means of treatment for the general public, it is also crucial to find ways to treat troops deployed in tropical settings where CHIKV is endemic. Currently (as of January 2020) the German Armed Forces have 42 troops deployed in regions where CHIKV is endemic and 1056 troops in Mali, a nation which southernly borders on CHIKV endemic countries. Frickmann and Herchenröder [16] have summarised the epidemiological findings on the occurrence of CHIKV in military personnel deployed in tropical settings. Frickmann found out that the infection risk for military personnel in the endemic setting is low but rises to the same level of that of local population during outbreaks. During the 2005/2006 La Réunion CHIKV outbreak, 19.3% of the French military personnel that were deployed there, developed Chikungunya fever (CHIKF) and 93.7% of the symptomatic patients had a chronic form of the disease with pains in joints and/or bones that had considerable impact on their duty [16].

As CHIKV can lead to severely incapacitating polyarthralgia that may last several months to years, emergency preparedness and response as well as combat readiness may be impaired considerably. Until a licensed vaccine or virus-specific treatment are available, military

personnel deployed in tropical and subtropical regions with endemic CHIKV can only rely on permethrin-treated uniforms, repellents and the use of bed-nets to prevent CHIKV infection [16, 17].

In addition, the neurotropic alphaviruses VEEV, EEEV and WEEV are of special interest, since they are designated as Category B biothreat agents that could be used as possible weapons against humans [18, 19]. The neurotropic New World alphaviruses are potential agents for bioterrorism since they can all be transmitted via aerosols, causing severe disease [3-7]. This is well documented in over 180 lab-acquired infections and the fact that the former Soviet Union and America once developed VEEV into a biological weapon [20, 21]. While EEEV is probably the most virulent of the encephalitic alphaviruses, with a case-fatality rate in humans estimated in the range of 50–70%, VEEV is the most infectious one [22]. Aerosol exposure to as few as 10 to 100 VEEV particles results in symptomatic disease in nearly all humans [6]. Among the symptoms of aerosol acquired VEEV are severe headache, chills, myalgia, weakness, malaise, fatigue, lower back pain, photophobia, anorexia, nausea and vomiting but severe encephalitis was not observed [6]. The VEEV complex is a group of 14 antigenic varieties divided into 7 species. Naturally acquired VEEV infections can lead to severe encephalitis causing convulsions, hemiparesis, behavioural changes, and alteration of consciousness or even coma [23]. Although mortality in humans is below 1%, up to 14% of the infected patients develop a neurological form of the disease, which may leave the patient mentally impaired for weeks or even permanently.

The NATO handbook on the medical aspects of NBC defensive operations (1996) originally also listed CHIKV as a potential biological weapon. The Biological Weapons Convention (BWC) of 2001, however, does no longer mention CHIKV [18], possibly due to the fact that spread of aerosolised CHIKV only results in minimal observed clinical disease and is thus not as effective as the neurotropic alphaviruses, especially VEEV [24]. Yet, since CHIKV shares a highly conserved non-structural protein 2 with the other members of the *Alphavirus* genus, potential antiviral compounds that target these conserved motives might also work against the neurotropic alphaviruses.

2.   Alphaviruses

2.1.   Taxonomy and distribution

Alphaviruses together with the Rubiviruses are the two genera that make up the *Togaviridae* family. Alphaviruses belong to the arboviruses and encompass about 30 currently recognised *Alphavirus* spp. that divide into eight phylogenetic groupings which are geographically

distributed in a very wide range [1, 2]. Consequently, the members of the *Alphavirus* genus exist in several geographical variants. They have been categorised accordingly as 'Old World' and 'New World' viruses [25, 26].

Alphaviruses can cause various diseases in humans and animals such as encephalitis, arthritis fever, rash and arthralgia. Although the incidence is not considered to be very high, the severity of disease caused by some members of the *Alphavirus* genus is significant and debilitating. Clinical sequelae can occur months or even years after the original infection in some patients [1].

Among the medically relevant members of the alphaviruses are Venezuelan, Western, and Eastern Equine Encephalitis viruses (VEEV, WEEV, and EEEV), Ross River virus (RRV) and Chikungunya virus (CHIKV). The equine encephalitis viruses all cause encephalic diseases in horses and humans in the Americas, thus belonging to the 'New World' category, while RRV and CHIKV are both 'Old World' viruses. The two categories have a symptomatic distinction as far as general disease manifestation in humans is concerned. While the 'Old World' viruses generally cause diseases with a clinical manifestation in the joints (acute arthralgia that might evolve into chronic arthritis/rheumatism), the 'New World' viruses primarily cause neurological disease [27]. Consequently, they are sometimes also referred to as arthritogenic and encephalitogenic or neurotropic alphaviruses.

The global distribution of alphaviruses is believed to be the result of a combination of factors. An expanding mosquito population together with the adaption of viruses to other mosquito species as well as increased and fast international travel might have contributed to the spread [28-30].

To date, no licenced anti-viral therapy is available to treat *Alphavirus* infections, but several promising candidates are under investigation. Currently there is no *Alphavirus* vaccine licenced for public use, but several vaccine candidates either made it to clinical trials or seem promising [31-34]. Vector control and active immunisation of equines are recommended in areas with VEEV to protect the human population from getting infected via the bite of a VEEV positive mosquito [35].

Under natural conditions, the life cycle of alphaviruses interchanges between the arthropod vectors and the vertebrate hosts. In arthropods (usually mosquitoes), the virus causes a persistent, life-long and asymptomatic infection with a high virus titre in the salivary glands [36]. This ensures the transmission of the virus during the mosquitos' blood meal to avian or mammalian hosts. In the vertebrate host, alphaviruses induce an acute infection which is marked by viremia caused by high virus titre. The high titre then infects new mosquitoes when

they feed on the viraemic host. In cell culture, the natural transmission cycle can be simulated, depending on the cell type that is being used. In cells of vertebrate origin, alphaviruses develop a highly productive, cytopathic infection that causes cell death within 24 to 48 hours after infection (*post* infection*, pi*). During the infection, typical modifications of the intracellular environment of the infected cells can be observed [37]. In cells derived from mosquitoes (e.g., C6/36 cells) on the other hand, a non-cytopathic, persistent or chronic infection occurs that nonetheless leads to the release of virus in high titres.

Since alphaviruses naturally have a shift from host to vector, they are capable of replicating efficiently under fundamentally different conditions and in various different cell types (insect, avian, mammalian). For example, the body temperature of insects is usually quite low while the physiological body temperature of birds can exceed 40 °C. Tests with Sinbis virus (SINV) infected chicken cells in culture showed that high virus yield was produced over a temperature range from 25 °C (lower temperatures have not been tested) to about 41 °C [37]. This diversity enables alphaviruses to recruit a number of diverse host protein factors to achieve viral replication. Most importantly, alphaviruses have to find ways to avoid the cellular immune response in at least two different organisms in order to ensure an efficient replication and spreading in both cell types. One of the major antiviral responses to counteract viral infection in insect cells is the double-stranded (ds) RNA-mediated interference (RNAi) [38]. In vertebrate cell, the antiviral response is made up by inducing various cellular genes and is activated by pattern recognition receptors (PRRs). These PRRs are able to detect virus-specific dsRNA strands as well as other virus-specific molecules that are produced during virus replication and other processes [39].

2.2. *Alphavirus* structure and genome

All alphaviruses are enveloped and have a diameter of about 70 nm. The virion is formed by an envelope consisting of a lipid bilayer and a lattice made up of 240 heterodimers of the viral envelope proteins E1 and E2 which are organised into 80 trimeric spikes (Figure 1). The E1 and E2 proteins are transmembrane glycoproteins and the C-terminal domain of the E2 protein has direct contact with the virus' nucleocapsid (NC) core [40]. As a result, the virion's outer protein shell is tightly associated with the 240 capsid proteins (Cp) that build up the icosahedral nucleocapsid which is unique to alphaviruses [41]. Resulting from the tight association between the E1/E2 spikes with the NC, *Alphavirus* particles have two icosahedral layers, an outer from the E1/E2 proteins and an inner from the NC core. The NC encloses the positive-sense, single-stranded RNA (+ssRNA) genome. The total genome is between 11,000 and 15,000 nucleotides.

It contains two open reading frames (ORFs), which encode the non-structural (ns) or replicase polyprotein and the structural polyprotein (Figure 1) [37].
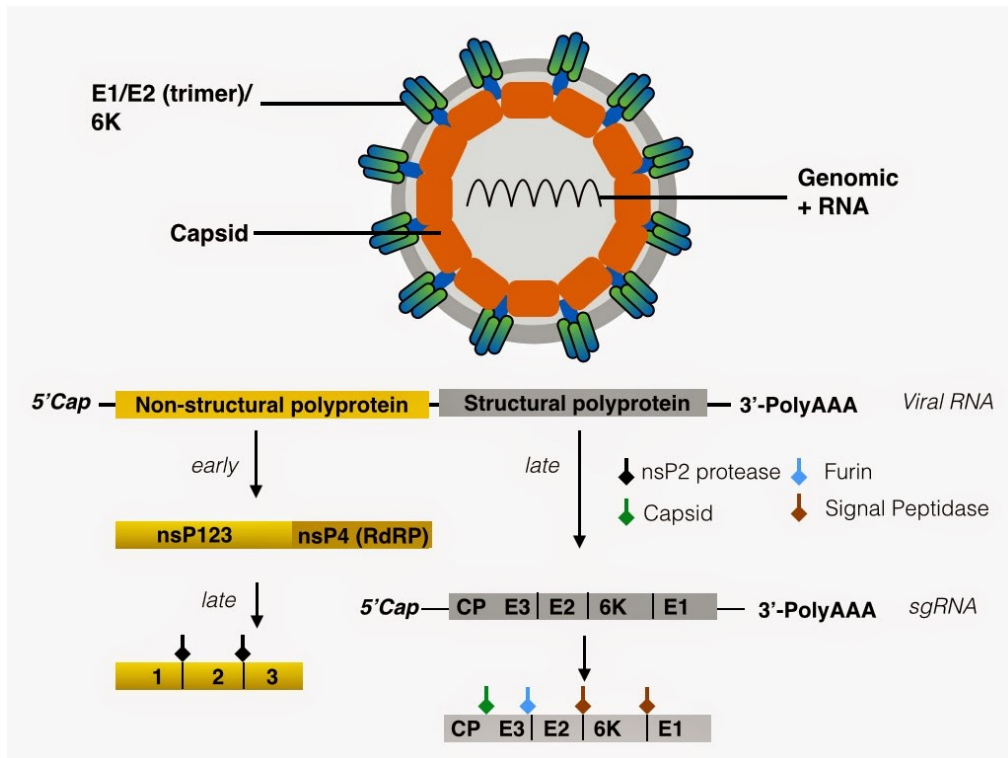
Figure 1: Prototype *Alphavirus* particle and genome.
Like other members of the *Alphavirus* genus, two thirds of the 5' CHIKV genome encode for the four viral nsPs (nsP 1-4) whereas the structural proteins are encoded within a subgenomic 26S RNA, which in turn derives from a precursor 42S RNA. The non-structural (nsP) as well as the structural proteins are expressed as polyproteins and posttranslationally cleaved by cellular and viral proteases. Abbreviations: nsP, non-structural protein; sgRNA, subgenomic RNA; CP, capsid protein. (Picture retrieved from virologytidbits.blogspot.com; accessed on Feb. 21, 2019)

The RNA has a 5'7-methylguanosine cap and a 3'poly-A tail and consequently mimics the structure of cellular mRNA [42]. Two thirds of the 5'-ORF encode for four essential non-structural proteins (nsP1-4) which are required for virus replication and constitute the RNA replicase. The nsPs interact with cellular factors and form the replication complexes (RCs) which are responsible for the synthesis of the double stranded (ds)RNA replicative intermediates. These dsRNAs are the templates for the positive strand viral (42S) genomic and (26S) subgenomic RNAs. The subgenomic RNA thus is the last 1/3 of the viral RNA and is translated into the structural proteins (capsid (Cp), E3, E2, 6K/TF, and E1) [8, 37].

2.3.   Overview of the *Alphavirus* life cycle

The key mechanisms for *Alphavirus* infection are entering cells via endocytosis and low pH-triggered membrane fusion to deliver their RNA genomes into the cytoplasm. To enter host cells, alphaviruses bind to host cell surface receptors which trigger clathrin-mediated endocytosis (Figure 2) [43]. Depending on the virus, a variety of receptors are being used to

initiate endocytosis. Some are known (e.g., the specific receptor for SINV is NRAMP2 (Natural Resistance-Associated Macrophage Protein 2)) while others still have to be identified [44, 45]. Furthermore, some alphaviruses seem not to depend on clathrin-mediated endocytosis, at least in some cell types [46]. Virus binding to the host cell surface may be facilitated by attachment factors like heparan sulphate proteoglycans and DC-SIGN [47, 48]. Following internalisation, the endocytic vesicle containing the virus matures and becomes more and more acidic. The resulting low pH triggers a series of changes of the spikes' conformation that cause the E2/E1 dimers to dissociate. The fusion loop of the E1 protein inserts into the endosomal membrane and the E1 proteins form a homotrimer [43]. This leads to a fusion of the viral membrane with the cell membrane of the endosome and the release of the virus's NC into the cytoplasm (Figure 2).

The NC disassembles and makes the genomic RNA accessible for translation [49-51]. The genomic RNA translates into the non-structural protein 1-4, which form the replication complex (RC) that produces positive sense 42S genomic and 26S subgenomic RNA (Figure 2). The subgenomic RNA is the template for the structural polyprotein that later cleaves into the individual structural proteins (Cp, p62 (which is the precursor of E2 and E3), 6K, TF, E1). Cp associates with the genomic RNA into new NCs while the other structural proteins undergo cleavage, translocation and modifications and accumulate at the plasma membrane (PM). At the PM, the NC associates with the other mature glycoproteins and budding of mature progeny virions takes place [8].
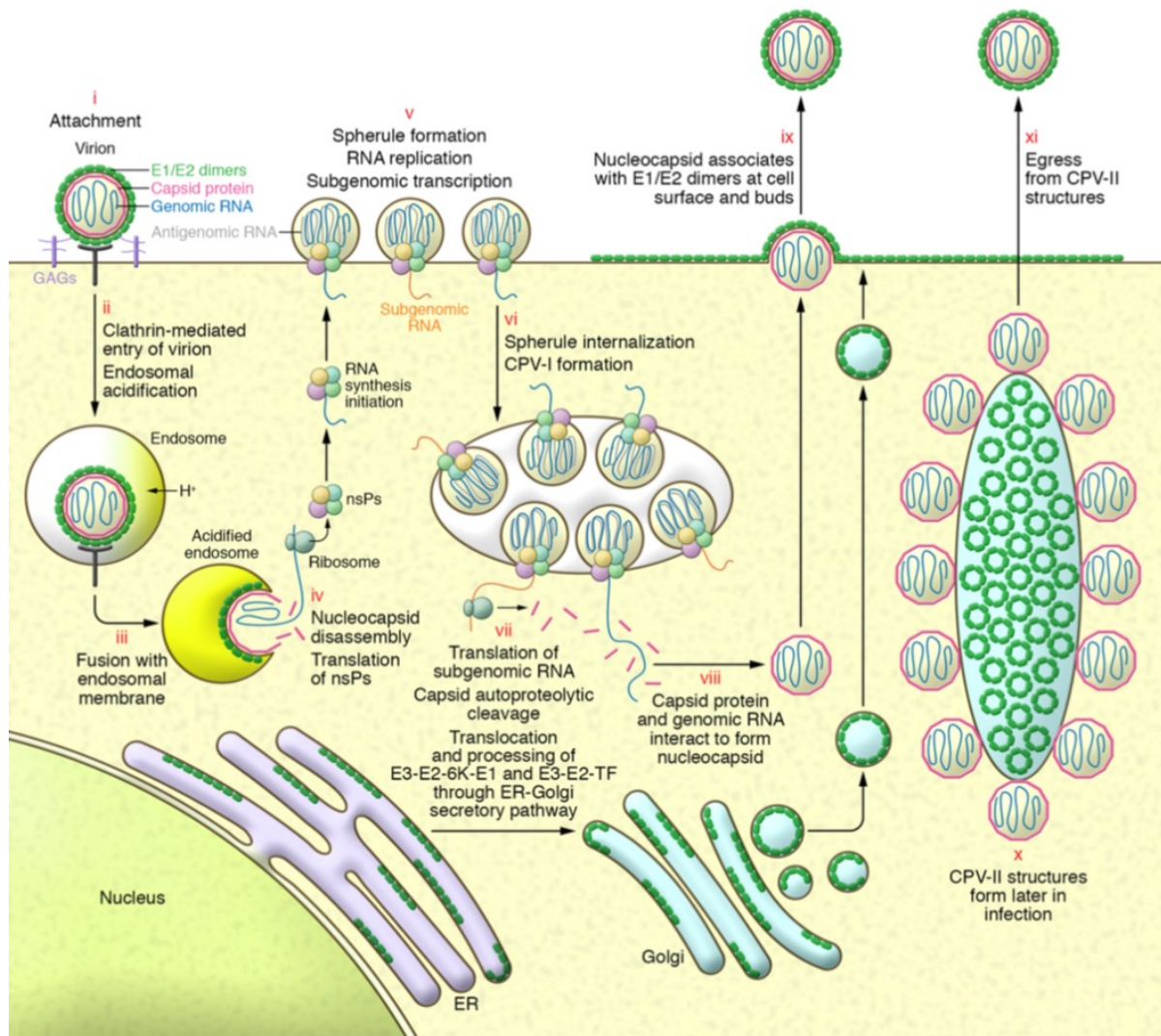
Figure 2: CHIKV replication cycle in mammalian cells as an example for alphaviruses.
(i) The virion binds with the E2 surface protein to the cell surface via an unknown receptor and possibly glycosaminoglycans as attachment factors. (ii) Entrance of CHIKV into the cell is achieved through clathrin-mediated endocytosis. The fusion peptide in E1 is inserted into the endosomal membrane as a result of the acidification of the endosomes. (iii) The fusion of the viral envelope with the membrane of the endosomes leads to the release of the nucleocapsid into the cytosol. (iv) The NC disassembles and thus releases the viral positive-sense genomic RNA which can then be translated into the non-structural proteins (nsPs). (v) The nsP123 polyprotein, the nsP4, the genomic RNA and presumably host proteins assemble at the plasma membrane (PM). The PM is rearranged to form. The replication machinery of the nsP1–4 is located at the neck of the spherule and synthesises genomic, antigenomic and subgenomic RNAs. (vi) Large cytopathic vacuoles (CPV-1) are formed when spherules are internalised. Such CPV-Is can house multiple spherules. (vii) The structural polyprotein is produced when subgenomic RNA is being translated. The autoproteolysis of the capsid releases the capsid into the cytoplasm. The E3-E2-6K-E1/E2-E2-TF polyproteins are translocated into the ER. The structural proteins E2/E1 are posttranslationally modified, transit the secretory system, and accumulate at the PM. (viii) The capsid interacts with genomic RNA and thus forms the icosahedral nucleocapsid. (ix) The nucleocapsids assemble with E2/E1 at the PM, resulting in budding of mature progeny virions. (x) At later stages of infection, CPV-IIs form. They contain hexagonal lattices of E2/E1 and are covered with nucleocapsids. (xi) CPV-IIs are believed to serve as transport vehicles and assembly intermediates where structural proteins are put together. They are also involved in virion budding. Abbreviations: CPV, cytopathic vacuole; ER, endoplasmic reticulum; GAGs, glycosaminoglycans; nsPs, non-structural proteins. (Picture from Silva and Dermody [8])

2.4.   *Alphavirus* replication and non-structural protein regulation

For the synthesis of *Alphavirus* RNA, all four viral nsPs are required individually as well as in the context of ns precursor polyproteins [2]. The processing of the *Alphavirus* ns-polyprotein into the four individual nsPs is highly regulated. For most nsPs their major function has been unravelled, but for some (e.g., nsP3), research is still going on. NsP1 functions as a viral capping enzyme and is the sole anchor that attaches the RC to the inner surface of the plasma membrane [52]. Additionally, there is evidence that nsP1 plays a role in the transport of RCs and in host actin modification [53-55]. The nsP2, having RNA helicase and protease function, is responsible for the processing of the ns-polyproteins [56]. The function of the nsP3 has been unknown for a long time, but the protein is important for RNA replication and for the synthesis of negative sense and sub-genomic RNA [57]. Recent studies found out that it is phosphorylated and interacts with several host proteins, tempering with the host cells' immune response [58, 59]. NsP3 is able to modulate poly- and mono-ADP-ribosylation although to what end is still under investigation [60]. NsP4 is solely responsible for the RNA synthetic properties of the viral replicase complex. It contains the core viral RNA-dependent RNA polymerase (RdRp) domain [52]. However, nsP4 alone cannot synthesise viral RNA without the other nsPs.

Replication:

After being released into the host cell's cytoplasm, the genomic RNA of alphaviruses is being translated and yields the early RCs which are formed by the non-structural polyprotein P123 and nsP4. The RCs are membrane-associated (endosomal and lysosomal membranes) and the polyprotein stage of the nsPs is needed for the proper formation of the RC as well as its association with the membrane (Figure 2). The individual and simultaneously expressed nsPs are not able to form a RC [61]. Virus replication leads to the formation of bulb-shaped membrane invaginations called spherules (diameter, ~50 nm) which are located at the plasma membrane. Alphaviruses as well as other RNA viruses induce a rearrangement of host membranes into so called type-1 cytopathic vacuoles (CPV-Is) (Figure 2 & Figure 3). It is possible that the CPV-I are former endosomes and modified secondary lysosomes [62]. The CPV-Is contain spherules which are typical for alphavirus infections. It has been known for quite some time that the CPV-Is and their spherules are the site of replication (Figure 3) [61-66]. By concentrating replication components and protecting double-stranded RNA intermediates, these spherules provide the microenvironment for RNA synthesis [2].
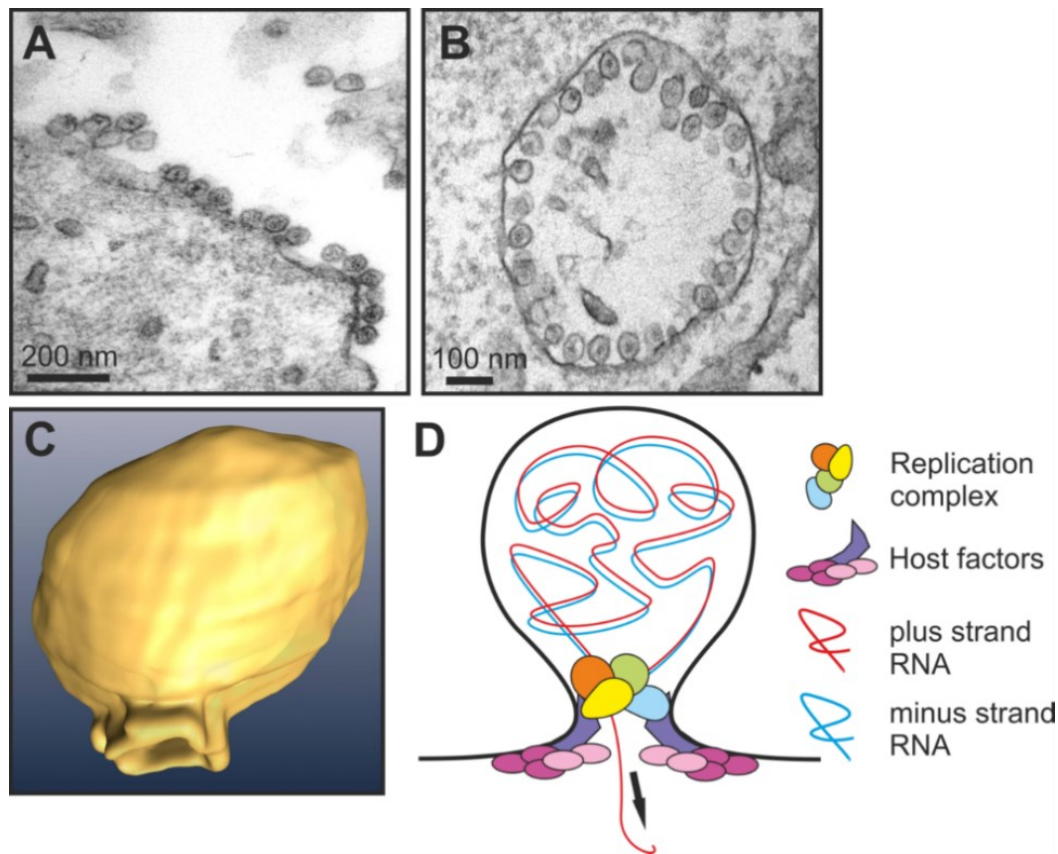
Figure 3: Spherules, membranous replication complexes of Semliki Forest virus (SFV).
A) Spherules located at the plasma membrane at an early time point. B) Type I cytopathic vacuole (CPV-I) of an infected cell, containing numerous spherules lining the membrane. C) 3D reconstruction of a single spherule. D) Schematic of a spherule with replication complex proteins nsP1-4 located hypothetically on the neck region and newly synthesised RNA coming out. The scale bars in A and B are 200 nm and 100 nm respectively. (Picture and text from Pietila, Hellstrom [67])

The early RCs synthesise a complementary minus-strand copy of the 42S genomic RNA. The machinery responsible for the minus strand copy is the nsP123 polypeptide and the individual nsP4 (Figure 4). The nsP123 is later processed into the individual nsP1 that forms the nsP1/P23/nsP4 replicase complex. The nsP23 is very instable and short-lived [68]. The nsP1/P23/nsP4 replication complex is able to produce both negative and positive strand RNA as well as subgenomic RNA (Figure 4). The release of the nsP1 from the P123 polyprotein thus marks the functional transition between the synthesis of negative-sense to positive-sense RNAs [69, 70]. The late RC which is composed of the fully processed individual nsPs1-4, is responsible for the production of positive-sense viral RNAs (genomic and subgenomic plus strands) from the nascent minus-strand RNAs [70, 71].
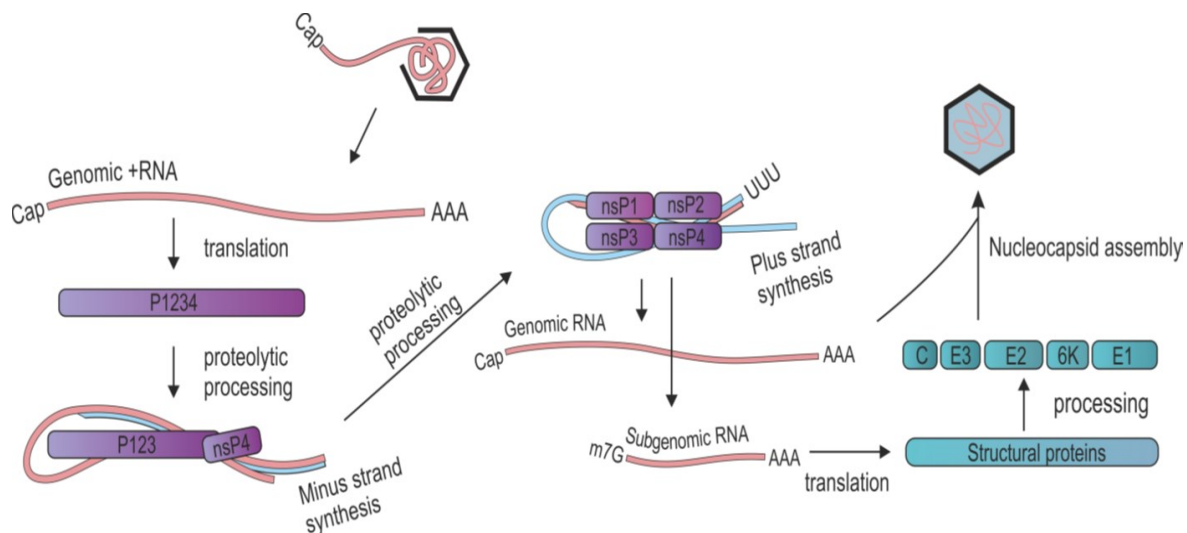
Figure 4: *Alphavirus* polyprotein processing and RNA synthesis.
After entering the cell, the virus particles are disassembled thus releasing the viral plus-strand RNA. Translation of the 5'ORF leads to the synthesis of the nsP1234 polypeptide. After the nsP4 is cleaved from the polyprotein, the early RC synthesises minus strands from the genomic RNA template. Further proteolytic cleavage of the nsP123 polyprotein to the individual nsPs marks the switch to the synthesis of genomic and subgenomic positive-strand RNA. The structural proteins which are needed for nucleocapsid assembly and the packaging of viral genomic (+) RNA are translated from subgenomic RNA. (Picture from Pietila, Hellstrom [67])

The promoters for minus and plus strands are recognised by different parts of nsP4. The other nsPs are needed for binding the RNA strands. Experiments revealed that purified *Alphavirus* nsP4 polymerase is only able to synthesise RNA *de novo* when the nsP123 polyprotein is present as well [72]. Moreover, purified nsP4 has a terminal adenylyl-transferase (TATase) activity which may be responsible for generating the poly(A) tail at the 3'terminal of the genome [72, 73].

So far, the exact structure of the RC has not been determined and it is yet unknown how the viral and possible host components of the RC are arranged. A number of studies that revealed the importance of host-factor involvement for the RNA replication of some alphaviruses have been published in recent years. Some of these host proteins have been demonstrated to interact with viral RNA or nsPs, especially nsP3 [58, 74]. The requirement for host factors during RNA replication offers an additional point of action for antivirals.

Apart from the CVP-I that forms right after the translation of the nsPs, a second type of cytopathic vacuole (CPV-II) is being formed at a late point during infection (Figure 2). The CPV-IIs have a tubular structure and probably originate from the *trans*-Golgi network, as both compartments contain vesicles with viral structural E1/E2 glycoproteins [75, 76]. The role of the CVP-IIs is not clear, they may be an intermediate for virus assembly [77].

2.5.   **Structural proteins, virus assembly, maturation and budding**

For a long time, it was postulated that the 3'ORF encodes for five structural proteins (Capsid (Cp), E1-3, 6K) which are synthesised as a long polyprotein (Figure 1). However, evidence was found that a ribosomal frameshift event occurs during translation of the 6K gene, initiating the production of a novel protein, termed transframe (TF) [78, 79]. Depending on the ribosomal frameshift, a major polyprotein product (E3-E2-6K-E1) and a minor polypeptide product (E3-E2-TF) are translated. The polyproteins are post-translationally cleaved into Cp, E1, 6K or TF and p62 (E2-E3).

The nucleocapsid consists of 240 copies of the Cp protein which is closely associated with the viral RNA. The 80 spikes which cover the NC of alphaviruses are formed in the endoplasmic reticulum (ER) and consist of the heterodimeric glycoproteins E1 and p62 which subsequently trimerise by the cleavage of p62 into E2 and E3 by cellular furin [80]. The nucleocapsid is assembled in the cytoplasm of the host cell. While budding through the cell membrane, the nucleocapsids acquire the lipid bilayer envelope with the virus-encoded glycoproteins E1–E2. The trimeric spikes (E1-E3) seem to facilitate virus attachment and internalisation through the receptor Mxra8 [81]. Glycoprotein E1 is involved in cell fusion and the glycoprotein E2 binds to host receptors. The surface protein E1 belongs to the class II virus fusion proteins. The roles of the 6K and the TF protein have still to be elucidated, but K6 seems to facilitate particle morphogenesis [82]. The TF shares an N-terminus with the 6K and both are believed to form ion channels and seem to play a role in virus assembly, budding and pathogenesis [78, 79, 83-85].

Translation of subgenomic 26S RNA into the structural proteins, virus assembly and maturation

The first protein that is translated from the subgenomic RNA is the Cp which is autoproteolytically cleaved from the nascent polyprotein [37]. As soon as the Cp is released, it packages the 42S genomic RNA and builds up the nucleocapsids. Following the cleavage of Cp, the p62, 6K (TF) and E1 are separated as well [41, 78].

The individual structural proteins are translocated into the ER where they are further processed and undergo conformational changes via posttranslational modifications while they are routed through the secretory pathway via the *trans*-Golgi-network to the plasma membrane (Figure 2) [1]. To ensure this transport, alphaviruses recruit several host factors and remodel the host cells transport machinery. E.g., VEEV and CHIKV rearrange the host cells actin cytoskeleton, presumably to organise the transport of the glycoproteins to the localised budding sites of the alphaviruses [86].

P62, the precursor of E2 and E3, associates with E1 and forms a heterodimer [87]. Furthermore, p62 assists in the folding and the transport of the E1 protein [88]. The formation of the p62/E1 heterodimer protects the E1 from the low pH (~ pH 6.0) of the *trans*-Golgi-network [87, 89]. The cellular protease furin later cleaves p62 into the individual and mature envelope proteins E2 and E3 [37, 90]. The processing of p62 into E2 is not needed for virus assembly and budding [90, 91]. It is eminent for the production of infective virions and marks the destabilisation of the E1/E2 heterodimer which can be easily dissociated when exposed to a low pH (e.g., in endosomes). This is a key step to allow fusion of the viral membrane with the endosomal membrane at the early stages of infection and thus is important to ensure infectivity of the virus [92, 93].

Maturation

The maturation process of alphaviruses is a major point to distinguish them from other related viruses e.g., flaviviruses. The particle components of alphaviruses are proteolytically modified before they assemble into mature viruses at the plasma membrane [94]. The N-terminal regions of the capsid proteins hold a conserved sequence that binds to the 60S ribosomal subunits of the host cell during infection. This initiates the dissociation of the nucleocapsid and the release of the viral RNA [51]. Later, during nucleocapsid assembly, the ribosome binding site is concealed. At the end of the maturation process, the site is exposed again [95, 96]. *Alphavirus* assembly is highly organised [40].

Viruses need to further process their structural proteins in order to produce infectious progeny viruses. Usually, the surface glycoproteins determine the infectivity and tropism of enveloped viruses [90]. The glycoproteins, which are synthesised as precursors, are activated into the mature form by endoproteolytic cleavage. This cleavage is essential for many viruses to ensure infectivity and pathogenicity [97]. Nevertheless, the class II fusion protein E1 of the alphaviruses is not activated by being cleaved itself but by the processing of an interacting companion protein (p62/E2). The cleavage of the companion protein E2 is what finally enables virus fusion and infection [90, 91].

The final step of the virus life cycle takes place when the capsid protein and the genomic RNA interact with the other glycoproteins to assemble into viral particles at the plasma membrane [1]. This final action promotes virus budding at the cells surface.

Budding

Virus budding requires Cp-E2 binding, E2/E1 heterodimer formation, pH protection of E1 by p62/E3-E2, as well as spike lattice assembly [98] [99] [40]. The interaction between the cytoplasmic domain of the E2 protein and the NC triggers virus budding at the PM. Cholesterol

is needed to ensure virus budding [100-102] and, although not specifically required, the presence of 6K and TF also promotes budding [103] [83, 104]. In contrast to other enveloped viruses, budding of alphaviruses does not depend on the host cell machinery [105]. Likewise, packaging of the genomic RNA is not a precondition for virus budding, although the step is needed to ensure infectivity [98, 106].

Alphavirus budding occurs at the PM and recent studies that imaged the process could demonstrate that it did not occur on just any localisation of the PM but on specialised sites [107, 108]. For a more detailed description of the current state of knowledge on the *Alphavirus* exit pathway, I refer to the review of Brown, Wan [40].

3.   Prophylactic strategies to control Chikungunya virus infection

Friederike I. L. Hucke[1], Malena Bestehorn-Willmann[1], Joachim J. Bugert[1]

[1]Bundeswehr Institute of Microbiology, Neuherbergstraße 11, 80937 München, Germany

The manuscript is presented in its published form and has therefore its own reference section. References and abbreviations from the manuscript are not included in the relevant sections at the beginning and the end of this document.

REVIEW PAPER

Prophylactic strategies to control chikungunya virus infection

Friederike I. L. Hucke[1] · Malena Bestehorn-Willmann[1] · Joachim J. Bugert[1]

Abstract

Chikungunya virus (CHIKV) is a (re)emerging arbovirus and the causative agent of chikungunya fever. In recent years, CHIKV was responsible for a series of outbreaks, some of which had serious economic and public health impacts in the affected regions. So far, no CHIKV-specific antiviral therapy or vaccine has been approved. This review gives a brief summary on CHIKV epidemiology, spread, infection and diagnosis. It furthermore deals with the strategies against emerging diseases, drug development and the possibilities of testing antivirals against CHIKV in vitro and in vivo. With our review, we hope to provide the latest information on CHIKV, disease manifestation, as well as on the current state of CHIKV vaccine development and post-exposure therapy.

Keywords CHIKV epidemiology · Antiviral design · Antiviral testing · Vaccines · Monoclonal antibodies

Introduction CHIKV

Taxonomy, structure and genome organisation

Chikungunya virus (CHIKV) is an "old world" alphavirus (family: *Togaviridae*).

Alphaviruses are enveloped viruses with a diameter of about 70 nm and single-stranded positive sense RNA (+ ssRNA). CHIKV belongs to the Semliki Forest virus antigenic complex and is closely related to O'nyong-nyong virus [1]. Other viruses in this particular complex are Sempliki Forest virus, Ross River virus and Mayaro virus. Phylogenetic relationships of alphaviruses are shown in * MERGEFORMAT Fig. 1. The virion is formed by an envelope consisting of a lipid bilayer and a lattice made up of 240 heterodimers of the viral envelope proteins E1 and E2 which are organised into 80 trimeric spikes. The E1 and E2 proteins are transmembrane glycoproteins and the C-terminal domain of the E2 protein has direct contact with the virus's nucleocapsid (NC) core [2]. Thus, the virion's outer protein shell is tightly associated with the 240 capsid proteins (Cp) that build up the icosahedral nucleocapsid (NC).

The CHIKV genome consists of about 11,800 nucleotides and follows the general organisation of all alphaviruses. It contains two open reading frames (ORFs) which encode the non-structural (ns) or replicase polyprotein and the structural polyprotein [6]. The RNA has a 5`7-methylguanosine cap and a 3`poly-A tail and, thus, mimics the structure of cellular mRNA [7]. Two-thirds of the 5'-ORF encode for four essential non-structural proteins (nsP1-4) which are required for virus replication and constitute the RNA replicase. The nsPs interact with cellular factors and form the replication complexes (RCs) which are responsible for the synthesis of the double-stranded (ds)RNA replicative intermediates. These dsRNAs are the templates for the positive strand viral (42S) genomic and (26S) subgenomic RNAs. The subgenomic RNA thus constitute the last third of the viral RNA and is translated into the structural proteins (capsid (Cp), E3, E2, 6 K/TF, and E1) [6, 8]. For a brief characterisation, see * MERGEFORMAT Table 1.

For a more detailed description especially with regard to the fact that the nsPs pose possible targets for antiviral drugs we refer the reviews of Strauss and Strauss [6], Silva and Dermody [8], and Pietila, Hellstrom [9] on the subject of alphavirus and CHIKV structure, replication and life cycle.

Edited by Detlev H. Kruger.

✉ Joachim J. Bugert
   Joachim1Bugert@bundeswehr.org

[1]   Bundeswehr Institute of Microbiology, Neuherbergstraße 11,
   80937 München, Germany
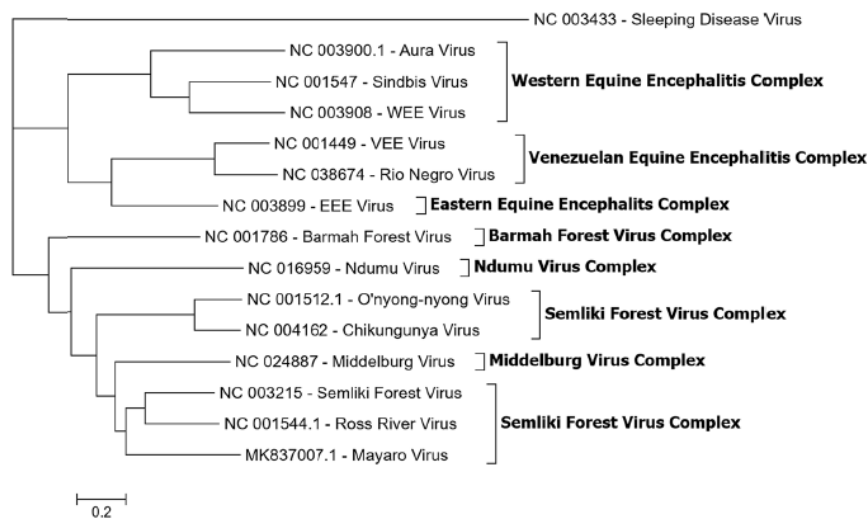
Fig. 1 Molecular phylogeny of the medically most relevant and representative alphaviruses. CHIKV belongs to the Semliki Forest virus antigenic complex and is closely related to O'nyong-nyong virus [3]. The phylogenetic tree was inferred based on a MAFFT-E translational alignment. Fifteen representative nucleotide sequences of the ORF 2 encoding the structural proteins of alphaviruses were used. A maximum likelihood phylogenetic tree was generated using the GTR + F + I + G4 model and 1000 bootstrap replicates. The software used was IQ-TREE [4, 5]. Virus names are shown next to the GenBank accession numbers. *EEE* Eastern equine encephalitis; *VEE* Venezuelan equine encephalitis; *WEE* Western equine encephalitis

Table 1 Functions of the various structural and non-structural Proteins of CHIKV

Protein	Size(aa)	Function
Non-structural Proteins	2474	P1234 precursor protein
nsP1	535	Methyltransferase and guanylyl transferase activities capping and methylation of new viral RNAs; is the only membrane anchor for the replication complex
nsP2	798	C-terminal cysteine (auto)protease activity cleaves initial polyprotein into individual non-structural proteins thus enabling viral replication; has also N-terminal helicase, nucleoside triphosphatase and RNA triphosphatase activities; interferes with the host cells mRNA transcription & translation and inhibits interferon signalling
nsP3	530	Interacts with several host proteins, possibly modulates protein poly- and mono-ADP-ribosylation; influences host cells stress response; Phosphoprotein, important for RNA minus-strand synthesis
nsP4	611	RNA-dependent RNA polymerase (RdRp) essential for viral replication; presumed terminal transferase activity
Structural Proteins	1244	Structural precursor protein
C (Capsid)	261	Forms nucleocapsid core by encapsidating genomic RNA; carboxyl domain is an autocatalytic serine protease
P62/PE2	487	Precursor/Intermediate, later cleaved into E2 and E3 by host furin protease
E1	435	Surface protein; Type II fusion protein; mediates fusion of viral envelope and cellular membrane by fusion peptides
E2	423	Surface protein; major target of neutralizing antibodies; mediates binding to receptors and attachment factors on host cell membrane
E3	64	N-terminal domain is uncleaved leader peptide of E2, suspected to shield fusion peptide in E1 during egress
6 K	61	Leader peptide of E1; presumed ion channel; may enhance particle assembly and release
TF	76	Transframe protein, produced via ribosomal frameshifting, presumed ion channel, may enhance particle release, shares N-terminus with 6 K

Aa amino acid number; *C* capsid; *nsP* non-structural protein; *RdRp* RNA-dependent RNA polymerase; *TF* transframe protein

135

Ecology and epidemiology

Chikungunya virus (CHIKV) is an arthropod borne (arbo-) virus of the Alphavirus genus. It was first described in 1955 by Robinson and Lumsden after an outbreak in present day Tanzania in 1952. The word "chikungunya" is derived from the Makonde word "kungunyala" which means "that which bends up", thus describing the stooped bearing and rigid gait of infected individuals [10]. Since symptoms are very similar to Dengue fever, it is possible that retrospectively, reports of outbreaks could also be attributed to CHIKV reaching possibly even back until 1658 [11].

CHIKV is usually transmitted to humans by infected mosquitos from the *Aedes* genus, mainly *Aedes aegypti*, *Aedes albopictus* and *Aedes polynesiensis*, but *Culex spp.*, *Anopheles spp.*, and *Mansonia spp.* have been found infected with CHIKV as well [12]. CHIKV causes sporadic, more or less periodical outbreaks especially during rainy seasons when mosquito populations are high [13]. The virus can affect both arthropods and vertebrates, with the arthropod staying infected for all their life. CHIKV circulates in a sylvatic/enzootic and in an urban cycle. In Africa, the sylvatic cycle is upheld by forest dwelling mosquitoes like *Ae. furcifer*, *Ae. taylori*, *Ae. africanus* and *Ae. neoafricanus* that infect vertebrates such as monkeys, rodents, and birds. Especially monkeys seem to serve as reservoir and amplification hosts in between epidemics [14].

So far, a sylvatic cycle has not been found in Asia, where the first CHIKV outbreak was reported in 1958. It is assumed that CHIKV maintains its presence by the urban cycle in this region [15]. Yet, the existence of a sylvatic cycle cannot be ruled out, since CHIKV-specific antibodies were found in Asian non-human primates (NHP) [16]. Furthermore, Mavale, Parashar [17] demonstrated that CHIKV-infected male mosquitoes can transmit the virus efficiently to females thus showing that a venereal (and probably a transovarial)

transmission of the virus in the arthropods plays a role for the persistence of CHIKV in this particular region. Acharya, Paul [18] showed that in vitro mosquito cell-generated CHIKV has a lower infectivity in cell culture and caused less severe disease in mice compared to mammalian cell-generated CHIKV. This is due to the loss of glycosaminoglycan receptor binding of CHIKV on mammalian cell surface after the mosquito cell passage [18]. This suggests that transmission of CHIKV amongst the arthropods actually keeps infectivity of the virus downregulated.

Historically, CHIKV was mainly distributed in tropical and subtropical regions of sub-Sahara Africa and Southeast Asia causing sporadic outbreaks. CHIKV was, however, put into focus after a massive outbreak in Kenya in 2004 with close to half a million infected people. This epidemic initiated the spread to more than 22 countries and distributed the virus into regions with moderate climate (Fig. 2) [19]. In India, an outbreak of CHIKV affected more than 1.4 million people in 2005 and was followed by additional epidemics in 2006 and 2007 [20]. Originating in Africa, the 2004 outbreak expanded to the Indian Ocean, India, and Southeast Asia. CHIKV eventually reached Europe in 2007 leading to 205 confirmed cases of CHIKF in Castiglione di Ravenna in Italy [21]. Unlike the previous sporadic outbreaks, the 2004–2010 epidemic displayed autochthonous cases in temperate climates such as in Montpellier, France [22]. In 2013, CHIKV emerged in the Americas, firstly in the Caribbean Islands and reaching the South American continent in 2014 [23]. This led to increasing CHIKF cases and between 2014 and the end of September 2018, a total of 697,564 CHIKV cases have been notified in Brazil (including 94,672 laboratory-confirmed cases). The majority of new CHIKV cases in this year (January until 17. July 2020) have been reported from Brazil, Yemen, Bolivia and Thailand [24].

Until 2004, it has been widely accepted that the *Ae. aegypti* mosquito was the main urban vector of CHIKV [1].

Fig. 2 CHIKV distribution. World map displaying countries where autochthonous (locally initiated) chains of CHIKV transmission have been identified in the past. *In the continental USA, only travel-associated CHIKV infections have been reported in the past three years (2017-March 2020)

This arthropod is well adapted to the urban environment and can multiply fast in a short time. However, during the 2005/2006 outbreak on La Réunion Island the Asian "tiger mosquito" (*Ae. albopictus*) got into focus as far as CHIKV transmission was concerned [25]. With 4–8 weeks, *Ae. albopictus* has a long lifespan (depending on the temperature) and a flight radius of 400–600 m. Both, *Ae. aegypti* and *Ae. albopictus* are diurnal. Yet, the geographical distribution of *Ae. albopictus* is broader than that of *Ae. aegypti*, since it can exist in more temperate zones [26]. Eggs of *Ae. albopictus* are more resistant to drying-up and can stay viable throughout dry seasons. The mosquito recently expanded from Southeast Asia to Madagascar, most islands in the Indian Ocean, Africa, and the Americas. Due to climate change, it even made the transition to the temperate zones of Southern Europe (Italy, France).

Phylogenetic studies and lineages

Before the La Réunion outbreak, phylogenetic analyses based on both partial (E1 glycoprotein) and complete genome analyses revealed the existence of three distinct CHIKV phylogroups (strains) commonly referred to as the West African (WA), East-Central-South African (ECSA) and Asian genotypes [1]. Genome analysis of CHIKV strains isolated during the La Réunion epidemic in 2005 and 2006 revealed that the outbreak was caused by a mutated strain originating from the ECSA isolates [13]. This new mutant was then referred to as the Indian Ocean Lineage (IOL). When CHIKV was introduced into the Caribbean in 2013 it formed another sub-lineage within the Asian lineage (Asian/American) [27]. As far as health issues are concerned, the most relevant lineages are the Asian (including the Asian/American), the IOL sub-lineage and some ECSA strains. Multiple CHIKV outbreaks in the past 15 years go back to these three clades [28].

The question why CHIKV spread over the Indian Ocean and into areas with temperate climate was partly answered by Schuffeneckers discovery of a mutation (referred to as E1-A226V) at residue 226 of the membrane fusion glycoprotein E1. This mutation made CHIKV more adaptable to *Ae. albopictus,* as a study by Tsetsarkin and colleagues could demonstrate [13, 29]. Additionally, reverse genetics identified possible mutations in the E2 glycoprotein (E2-G60D and E2-I211T) which were important for determining CHIKV infectivity in *Ae. albopictus*. Tsetsarkin et al., suspects a strong synergistic effect of the E2-G60D and E2-I211T mutations on CHIKV infectivity for *Ae. albopictus*, when expressed in combination with valine at position E1-226 [30]. In a follow-up study conducted in India another novel E2 mutation, L210Q, was present in all human and mosquito CHIKV isolates collected during 2009 [31]. This substitution was within the region of the E2 protein (amino acids E2 200–220) that determines mosquito cell infectivity for several alphaviruses [32–34].The virus' mutations turned *Ae. albopictus* from a secondary vector to the main transmitter of CHIKV. This enabled the new IOL to spread into regions where this arthropod is distributed. The mutation in the E1 protein had been observed before in Semliki Forest virus (SFV), another alphavirus, where the mutation made SFV less dependent on cholesterol for growth [35]. The efficiency of alphavirus' entry generally depends on the composition of the host cell membrane. Cellular membrane cholesterol is needed for membrane fusion and an efficient exit of progeny virus from infected cells. A mutation that made the virus more independent from cholesterol content in membranes would improve its fitness, especially in insects which have a different lipid composition in the cells. Experimental infection of *Ae. albopictus* with the non-mutated CHIKV strains actually proved that these lineages were not able to replicate as sufficiently in the tiger mosquito as the IOL strain and that the mutated sub-lineage had a significant increase in infectivity, dissemination and transmission by *Ae. albopictus* [29].

Pathogenesis

CHIKV is naturally transmitted to humans through the saliva of infected mosquitoes when they take a blood meal. Additionally, cases of mother to child transmission are known. Once the virus enters the skin, dermal fibroblasts seem to be the main site of viral replication and amplification [36, 37]. Proteins from mosquito saliva promote viral replication by counteracting the induction of antiviral genes, thus hampering the hosts' immune response [37]. Apart from dermal skin fibroblasts, skin keratinocyte and melanocytes are permissive for CHIKV infection as well [38]. Studies with NHP characterised the route CHIKV takes to reach other anatomical regions [39]. At the primary site of infection (skin) CHIKV infects macrophages. Viral particles are captured by dendritic cells (DCs) which transport the virus to the closest lymph nodes. Within the lymph node, viral particles are transferred to monocytes and macrophages which enter the bloodstream. After CHIKV reaches the lymph node, viremia sets in by the active infection of human blood monocytes and other peripheral blood mononuclear cells [40].

Via blood stream, CHIKV reaches the muscles and joints where the infection causes the main symptoms of CHIKF—myalgia and arthralgia. In the muscle, satellite cells seem to be the target for CHIKV, but primary human myoblasts are permissive to the virus infection as well and CHIKV could also be detected in skeletal muscle fibroblasts [41, 42]. CHIKV RNA and proteins could be found in the synovial tissues and fluids during acute and persistent arthralgia and various studies showed that synovial fibroblasts as well as macrophages are susceptible to CHIKV [12, 42].

In CHIKV-infected individuals, cartilage degradation and bone loss take place in the infected joints [43]. CHIKV also replicates and persists in osteoblasts [38].

CHIKV can target a wide range of secondary organs which may lead to severe complications in patients (i.e. renal, respiratory, hepatic, cardiac, and neural syndromes) [12]. CHIKV disseminates into the liver, the spleen, the heart, the kidneys and possibly the lungs [36, 39, 44]. Although CHIKV has not been considered a true neuro-tropic virus, it can cause neurological complications (e.g. meningitis, encephalitis, febrile seizures, Guillain Barré syn-drome, neuro-ocular diseases) especially in the elderly and the very young [45]. In the Indian Ocean outbreak of 2005, a growing number of neurological symptoms associated with CHIKV were observed. Since then the tropism of this agent for the nervous system has been characterised better [46]. In patients displaying severe neurological symptoms, CHIKV could either be isolated from or detected via RT-PCR in the cerebrospinal fluid [45]. In vitro experiments showed, that CHIKV is able to infect and replicate in neurons, astro-cytes, oligodendrocytes and microglia cells [47]. Despite these findings a consensus to the discussion whether the virus affects the nervous system directly or indirectly via a triggered immune-mediated effect has not been reached yet.

Inglis and colleagues concluded that a disrupted glia-neu-ron signalling could be a major driving factor in the develop-ment of CHIKV-associated neuropathology [48], a finding that was also confirmed in mice [49]. For a more detailed understanding of the current knowledge on pathogenesis and tissue tropism of CHIKV as well as on vector and animal host interactions we refer to the review of Matusali et al. [12].

Clinical manifestation

CHIKV causes a febrile disease called Chikungunya fever (CHIKF). Typically, patients develop symptoms after an incubation period of 1–12 days. High fever accompanied with headache, myalgia and joint pain are typical, in some cases haemorrhage and maculopapular rash may occur [8]. Especially musculoskeletal symptoms like persistent disa-bling polyarthralgia are a hallmark of the disease and have repeatedly been observed to go into a chronic state that may last months or even years in up to 50% of the patients [50]. A follow-up study done by Manimunda, Vijayachari [51] dur-ing an epidemic in Karnataka state, India in 2008, revealed that the arthritis caused by CHIKV is a chronic inflammatory erosive arthritis. Interestingly, the most common symptoms in this study were joint pain (98%), fever (85%), swelling around joints (53%), rash (50%), fatigue (49%) and headache (38%). After 9 months, 51% of the patients had been cured, leaving 49% in a chronic state of the disease [51].

If an immunologically naïve population is confronted with CHIKV, the morbidity ranges from 34% (like in La Réunion in 2005) to 63% [52, 53].

Although CHIKV is often self-limiting and has a low mortality rate (0.1%) [54], complications may arise espe-cially in the elderly and the young. The major outbreaks between 2005 and 2016 recorded a significant number of patients suffering from serious complications such as cardio-vascular disorders, involvement of the central nervous sys-tem (CNS), respiratory failure, pre-renal failure, and severe acute hepatitis. The mortality rate among these severe cases ranged from 10.6 to 35% with most patients dying of heart failure, multiple organ failure syndrome or toxic hepatitis [13, 52].

Patients under 1 year or over 65 years of age, have a higher risk of being affected by a CHIKF associated CNS disease (including encephalitis). Among the most frequently diagnosed CHIKV-associated neurological complications are encephalitis, optic neuropathy, neuroretinitis and Guil-lain-Barré-Syndrome, but also occasionally meningoen-cephalitis, myelitis and polyradiculitis [46]. In a cohort study during the CHIKV outbreak on La Réunion between 2005 and 2009, Gérardin (2016) determined the case fatality rate of CHIKV-associated encephalitis to 16.6% among neonates and the proportion of children discharged with persistent dis-abilities (seizures, cerebral palsy) was estimated between 30 and 45%. Various cases were CHIKV has been transmitted vertically from mother to neonate are known. This poses the risk of neurodevelopmental delays, cerebral palsies and microcephaly in the infant [55].

Differential diagnosis, CHIKV diagnostics, and surveillance

The initial signs of CHIKV disease (fever with or without headache and/or arthralgia) are also common in several other diseases. Depending on the patient's history (place of residence, travel history, and exposure), different dis-eases can be considered in the differential diagnoses such as Malaria, Dengue (DENV), Leptospirosis, and other alphavirus infections like Mayaro, Ross River, O'nyong nyong and Sindbis [56]. Apart from being mistaken for another disease, CHIKV infection often go hand in hand with Malaria, Dengue (DENV) or Zika virus (ZIKV) infection and the four diseases share a common set of ini-tial symptoms (headache, fatigue, and myalgia/arthralgia). It is very important for the patient to have quick and reli-able diagnosis because prognosis and patient care differ for these diseases [57]. Especially Malaria and Dengue have the potential for much worse outcomes including death and it is thus eminent to distinguish the pathogens. So far, CHIKF can only be distinguished from Dengue fever by

virus testing and early diagnoses might prevent complications in the patient like haemorrhages, acute respiratory distress syndrome, renal failure and arthritis [58].

Acute CHIKV infections are diagnosed either by virus isolation in cell culture, detecting virus genome or serologically, by detecting specific IgM antibodies [59]. For more detailed information on how to test during what phase of the disease we refer to Barrera, Hunsperger [56]. There are commercial serological assays (enzyme-linked immunosorbent assay (ELISA), immunofluorescence assay (IFA)) and molecular (RT-PCR) detection systems available [60, 61].

Various studies have been conducted in order to find the best diagnostic method. PCR methods seemed to outperform serological assays, which were less sensitive and specific, as they depend to a great extent on the skills of the performing laboratories [59]. Furthermore, due to cross-reactivity of antibodies to common antigens among CHIKV related alphaviruses (e.g. Barmah virus, Ross River virus and Mayaro virus (MAYV)), false positive and false negative results are possible and serologic diagnosis remains a challenge [62]. This is particularly difficult when the viruses have the same geographical distribution and share a set of common symptoms as is the case with CHIKV and MAYV which both are endemic in Brazil and its neighbouring countries [63].

Questionable results should be confirmed with a second assay, e.g. serum virus neutralisation assay (VNT), which is a confirmatory test and considered more specific than ELISA and IFA tests [64].

Even before CHIKV was (re)introduced into the Americas, the Centres for Disease Control and Prevention (CDC) together with the Pan American Health Organization (PAHO) published the guide for 'Preparedness and Response for Chikungunya Virus Introduction in the Americas' [56]. However, although recommendations for surveillance had been provided, some American countries had not established a surveillance system for this particular disease due to lack of clinical and public awareness as well as non-existence of laboratory capacity for testing [65]. According to a retrospective study on Puerto Rico, passive case surveillance seemed most practical and feasible approach to compare epidemiologic trends across regions affected by chikungunya and other emerging infectious diseases [65]. Passive surveillance for a disease happens when a sick person seeks medical care, a doctor suspects a certain pathogen as the causative agent, and the case is reported to public health authorities either before or after laboratory diagnostic testing is done. Passive surveillance is particularly useful to monitor epidemiologic trends in diseases [65]. Yet, the infrastructure for passive case surveillance system might still have to be established, which proves difficult in developing countries with lack of resources. In Puerto Rico, the already existing passive dengue surveillance system that existed since the 1960s was modified to fit the new agent CHIKV [65].

If a disease is already endemic in a country, surveillance of this specific disease is only justified if appropriate actions to ban it are planned [66]. As there is no specific treatment for CHIKF available, the clinical outcome of a patient is only influenced by early detection when a more severe disease can be excluded. In tropical areas where vector activity is to be expected all year long, the same control measures as for DENV might help avoid high infection numbers and a ready detection of a new outbreak could help reduce the burden to public health by raising awareness [66]. Between epidemics, serological surveys are hardly done. Yet some studies for active surveillance have been conducted According to a study that investigated the cause of febrile illness in children during an inter-epidemic period in 5 Asian countries, CHIKV was responsible for 35% of all fevers [67]. Other seroprevalence studies in Africa confirmed that CHIKV was circulating endemically [66]. There was a program from the Pacific Public Health Surveillance Network for specific surveillance strategies of CHIKV, DENV and other febrile diseases including case detection and management, laboratory confirmation, vector control and raising awareness [68]. However, their website has not been updated since May 2016, so no data can be found on the current state of CHIKV surveillance in this area [69].

In Europe and non-endemic countries, CHIKV cases may occur either travel associated or if a viremic traveller enters areas where *Ae. albopictus* is present and finds suitable environmental conditions for the transmission of the virus (which is the case when daily temperature are ≥ 18 ℃) [70]. Thus, travellers returning from endemic areas with febrile illness should be readily tested for Malaria, DENV and CHIKV [66]. According to the European Centre for Disease Prevention and Control (ECDC) the risk assessment states the chance for CHIKV infection in France and Italy, where autochthonous cases have been repeatedly reported, as being moderate [71]. Public awareness should be raised as an essential part of any DENV/CHIKV control program to help identify potential cases and start entomological investigations and possible vector control measures to curb further spread [66].

Strategies against emerging infectious diseases

The following section will give information on drug development and evaluation as well as on vaccines that are currently being investigated in clinical trials against CHIKV. For those interested in current antivirals against alphaviruses in general and other agents relevant in medical biodefence, we recommend the review of Bugert et al. [72].

Drug development

There are three major approaches to finding new drugs: (1) in traditional or phenotypic drug discovery, also called forward pharmacology, potential drugs are screened based on measures of phenotype. (2) Rational drug design, which is also referred to as reverse pharmacology, is based on the knowledge of a biological target which may function at critical intervention points in a disease process and might be blocked by drugs. (3) Repurposing already existing drugs is also a commonly used approach. We will not detail the different approaches but recommend the reviews of Pathel [73], Takenaka [74] and Rester [75].

Methods for in vitro and in vivo evaluation of antiviral compounds

Viruses

Bio-safe surrogates for CHIKV help avoiding the need for BSL-3 facilities. The BHK replicon cell line for example contains a persistently replicating CHIKV replicon [76]. To study virus entry and possible effects of agents on this particular step of CHIKV life cycle requires other models such as CHIKV pseudo-particles that carry the envelope proteins and are tagged with a luciferase reporter [77, 78]. Lucas-Hourani, Lupan [79] screened for CHIKV nsP2 protease inhibitors without using life virus infection. He transfected human HEK-293 T cells with various plasmids that encoded for the sequence of CHIKV nsP2 protein, a luciferase reporter gene and two transcription factors.

Some research groups use the vaccine strain 181/Clone 25 as a model virus. This is a live-attenuated derivative of Southeast Asian human isolate strain AF15561 (GenBank accession no. L37661, listed as TSI-GSD-218). It displays reduced virulence but still has the complete virus' life cycle [80, 81]. Gorchakov, Wang [82] revealed 10 nucleotide differences in the genome compared to its parental strain. Only 5 mutations actually caused an amino acid substitution, the rest were silent mutations. This strain could easily re-evolve back into a more infectious strain [82].

Wild-type (WT) strains with a complete life cycle include clinical isolates like the DRDE-06 strain (Gen-Bank: EF210157) [83], DMERI09/08 strain [84], or laboratory CHIKV strains such as ROSS [84, 85], LR2006_OPY1 (GenBank: DQ443544.2) and the Indian Ocean strain 899 (GenBank: FJ959103.1) [86].

Reporter viruses for high-throughput screening, include recombinant CHIKV expressing GFP (e.g. CHIKV-118-GFP) [87] or luciferase genes [76].

For the initial identification and screening of molecules with antiviral activity, cell viability/cytopathogenic effect (CPE) reduction assays are usually employed. These assays also allow the evaluation of the cytotoxic effect of putative antiviral molecules on the cells. African green monkey kidney cells (Vero cell line) are the most commonly used cells in these assays with CHIKV. Other cell types used for CHIKV antiviral screening include baby hamster kidney (BHK) cells, human foetal lung fibroblast (MRC-5) cells, bronchial epithelial cells, human embryonic kidney 293 (HEK-293) cells and human hepatocarcinoma (Huh-7) cells ([86–90]. Nevertheless, the fact that these commonly used cell lines have little clinical relevance in CHIKV disease is a big disadvantage. Some groups used human muscle satellite cells [41]. Labadie, Larcher [39] found out that macrophages are the main cellular reservoirs during the late stages of CHIKV infection in NHP. Teng, Foo [91] showed that monocytes are the major PBMC (primary blood mononuclear cells) subset targeted by CHIKV in the blood. These cells may be more relevant cell lines, especially as they are suspected to contribute to the long-term effects of CHIKV in humans. Yet, since they are a primary cell lines which are not immortalised, they are not well suited for high-throughput screening (HTS). Furthermore, human dermal fibroblasts seem to be the initial target cells in CHIKV infection, as they are the first to be infected after a mosquito bite [36, 42]. Abdelnabi and colleagues successfully used the human skin fibroblast cell line CRL-2522 as a model for testing CHIKV antivirals [92].

The effect of CHIKV on the cells (CPE) can be either evaluated microscopically and/or quantitatively measured by colorimetric assays e.g. resazurin fluorescence reduction assay [90], the MTS/PMS method [86] or neutral red dye uptake [83]. Additionally, in assays with adherent cell lines, xCELLigence real-time cell analysis (RTCA) screening is an accurate method to investigate the properties of antiviral compounds in infected and non-infected cells, [93]. This method is an established electronic cell sensor array using impedance measurement to detect the number of adhered (and thus viable) cells. It has the big advantage of measuring the cell viability continuously, whereas the aforementioned colorimetric assays are endpoint assays and do not provide information on the initiation of CPE or the changes in reaction rate of the virus propagation over time.

Animal models

There is a variety of mouse models to study CHIKV pathogenesis. Adult immunodeficient mice such as AG129 are being used for lethal infection models [86]. Pal, Dowd [94] used *Ifnar*$^{-/-}$ mice to assess the antiviral efficacy of small molecules and monoclonal antibodies against CHIKV-induced death. To study the efficacy of drug therapy against arthritis and inflammation caused by CHIKV, non-lethal infection models with immunocompetent mice such as C57BL/6 and Swiss albino mice are being employed [77,

95]. Other research groups use cynomolgus macaques (*Macaca fascicularis*) or rhesus macaques (*Macaca mulatta*) to study CHIKV, since these NHP show similar signs of CHIKF as humans, including fever and skin rashes [96]. In his study with immunocompetent macaques, Labadie showed that long-term CHIKV infection was observed in joints, muscles, lymphoid organs, and liver, and that this fact might contribute to the long-term symptoms in humans. Yet, severe signs such as arthritis, meningoencephalitis and death were only observed after infecting the macaques with higher doses of CHIKV [39].

Current strategies against CHIKV

Although mortality rates of CHIKF are rather low with 0.1%, the impact of the diseases on the patient is severe, especially when the virus hits a naïve population. The epidemic on La Réunion in 2005–2006 displayed CHIKF with atypical symptoms going hand in hand with severe morbidity (34.4% of affected patients) and a higher mortality rate (10.6%) [52] while affecting nearly 34% of the overall population of the island [19]. Apart from the suffering which patients have to endure personally, the economic and social impact of the disease seriously affects the communities and the economy [97].

So far, no approved antiviral therapy or vaccine against CHIKV is on the market, leaving patients with supportive therapy only. This usually consists of analgesics, antipyretics, and fluid therapy. Current recommended therapy for CHIKV-infected patients with arthritis/arthralgia encompass non-steroid anti-inflammatory drugs (NSAIDs) to manage pain and inflammation used along with fluid therapy to prevent dehydration [98]. Aspirin should be avoided, since it bears the risk of bleeding and developing Reye's syndrome [99]. Treatment of CHIKF with corticosteroids might cause immunosuppression and worsen the disease. Furthermore, the adverse effects of corticosteroids make their long-term administration additionally risky, thus causing a problem for the treatment of patients with chronic arthralgia or arthritis.

Prevention and control

Bite prevention and vector control are the two hallmarks to avoiding infection in the first place. When travelling to endemic areas, general personal protective measures like wearing long-sleeved clothing or using insect repellent and mosquito nets are important to prevent being bitten by a CHIKV positive mosquito. For some vector-borne diseases like Dengue, Chikungunya, Zika, and West Nile disease, vector control is currently the only method available to protect populations (an existing Dengue vaccine is being avoided due to safety concerns [100]).

Before the invention of broad spectrum insecticides in the 1940s, vector control was mainly achieved by environmental management and larval control based on a thorough understanding of pathogen transmission [101]. Vector-control measures can generally be classified into chemical and non-chemical-based approaches. Both strategies can target immature and adult stages either by killing them (with chemical or biological larvicides/adulticides) or by removing the habitat essential for these stages (e.g. the draining of marshes). To reduce contact of the adult vector with the human host, tropical repellents, insecticide treated bed nets or housing improvements are applied [101].

In the past decades, so-called rear and release strategies were brought into focus. In this approach, the intentional mass rearing and release of modified mosquitoes that mate with the wild counterparts aims to induce genetic change, sterility or reduced vector competence into the target population [102]. There have been several programs to achieve this goal. The release of sterile males that if mating with wild females, result in infertile eggs and reduction and eventual elimination of the vector population was one of the first concepts. Males have been sterilised with radiation, chemical methods, the introduction of genetical modification or microbiological methods [103].

Another approach lies in synthetic gene drives. Gene drives are selfish genetic elements that manipulate gametogenesis and reproduction to increase their own transmission to the next generation [104]. Some synthetic gene drives are used to potentially hamper the function of essential genes which hopefully if released, will lead to a decline of the wild population or conversion of the population into males. Other drives aim to modify the vector population in a way that they are more sensitive to pesticides or reduce the vectors' ability to transmit a virus [104].

Aliota et al. [105] followed this strategy of vector control. His research group tried to curb CHIKV transmission by infecting mosquitoes with the intracellular bacterium *Wolbachia*. The maternally transmitted bacterium *Wolbachia* is an endosymbiont that manipulates host reproduction to enhance its own transmission [106]. This may result in enhanced resistance to pathogens and reduced virus replication in the vector [107]. Aliota introduced the wMel strain of *Wolbachia pipientis* into *Ae. aegypti* mosquitoes and showed that replication and transmission potential of CHIKV were reduced significantly. Similar results have been published for other arboviruses like DENV, Yellow Fever virus and Zika virus, all of which share *Ae. aegypty* as a common vector [108–110]. It seems that the extent of pathogen reduction can be influenced by the strain of bacterium [110]. In endemic regions thus infected mosquitoes could be released and invade the wild mosquito populations and consequently reduce viral transmission. Studies for curbing Dengue virus transmission by releasing *Wolbachia*-infected mosquitoes

into natural *Ae. aegypti* populations have been started in 2017 seem promising. [111, 112]. According to the World Mosquito Program (WMP) studies conducted in Indonesia over a period of 3 years showed that compared to untreated areas, there is a 77% reduction in the incidence of virologically confirmed Dengue fever in *Wolbachia*-treated areas of Yogyakarta, Indonesia (Clinical Trial No. NCT03055585) [113].

If these approaches work out, it might prove an eco-friendly method to curb virus spread without applying chemical insecticides. However, they have their flaws. Rearing and release strategies are expensive, must be well organised, require significant infrastructure, and suffer from an overall negative public opinion, especially when genetically modified mosquito (GMM) are concerned. Furthermore, it is possible, that introduced gene drives evolve back or fail due to drive resistance resulting from standing genetic variation [114].

Prophylaxis and post-exposure therapy

Active immunisation

Compared to other RNA viruses, CHIKV displays a limited diversity between the different strains. Various studies showed that antibodies raised by one CHIKV genotype display a cross-reactivity against all others and there is a broad consensus that CHIKV lineages constitute to a single serotype [28, 115]. This makes CHIKV a viable candidate for generating a vaccine that grants a life-long protection against an infection, with little risk of complications like antibody-dependent enhancement (ADE) as reported from DENV vaccines [116]. Although trying to develop a vaccine since the 1960s, no vaccines have been approved so far, but several candidates are currently being investigated in preclinical and clinical trials [117]. Here, we will only focus on those vaccine candidates that made it to human studies (clinical trials) (Table 2).

Live-attenuated vaccines The advantages of live-attenuated vaccines are that they offer effective and long-lasting immunity, do not have to be given very often and are low in production costs. The first live-attenuated CHIKV vaccine that made it to clinical trials was called TSI-GSD-218 and was developed by successively growing the CHIKV 181/clone 25 in cell culture [80]. It seemed to provide an effective and lasting immunity. However, in the phase 2 trial 8% of the vaccinees developed mild arthralgia [81]. The candidate was abandoned after studies indicated instability of attenuation which raised concerns about safety [8, 82]. Yet, the strain is still used as an attenuated lab strain. This candidate revealed a disadvantage of live-attenuated vaccines: the chance of the virus evolving back into an infective strain. In

case of TSI-GSD-218, attenuation was determined by two amino acid substitutions in the E2 envelope glycoprotein which seemed not to be very stable [8, 82]. Research tried to find other strategies for developing live-attenuated vaccines and finally came up with CHIKV/IRES, a candidate that contains an internal ribosomal entry site (IRES) in place of the subgenomic promotor. This IRES leads to a decrease of the expression of viral structural proteins. As a result, replication in mammalian cells is attenuated and replication in mosquito cells is completely prevented because the IRES does not work in insect cells [8]. The CHIKV/IRES vaccine worked in a safe, highly immunogenic, and effective way in studies with mice and NHP [125, 126]. It furthermore protected mice and NHP against various CHIKV strains and has been preclinically evaluated on safety, efficacy and stability so that now CHIKV/IRES is projected for clinical studies [28, 135].

Another live-attenuated CHIKV vaccine candidate with the number VLA1553 which has been developed by the biotech company Valneva was recently investigated in a phase 1 clinical study to research three dose levels of VLA1553 after a single immunisation (ClinicalTrials.gov; Identifier: NCT03382964). According to the manufacturer, the monovalent, single dose vaccine candidate which was granted Fast Track designation by the FDA in December 2018, had excellent final phase 1 results. Preclinical studies with NHP proved the vaccine candidate to fully protect the animals against WT CHIKV infection after a single dose [118]. Phase 2 supportive studies are ongoing and the candidate has received approval from the FDA to enter phase 3 clinical studies in 2020 [136]. Valneva has recently initiated a pivotal phase 3 trial for the vaccine (NCT NCT04546724). In the randomised, double-blinded, placebo-controlled, multicentre study called VLA1553-301 with approximately 4000 healthy participants, the safety and immunogenicity 28 days after a single-shot vaccination with VLA1553 is to be evaluated. A subset of participants will be tested for sero-protection based on an immunological surrogate (under the Accelerated Approval pathway). Participants will be followed for a total of 6 months [119]. This is the first CHIKV vaccine study to enter phase 3. The parental strain of VLA1553 is the infectious clone CHIKV LR2006-OPY1 and attenuation was achieved by deleting a major part of the gene encoding for nsP3 [120].

Furthermore, in June 2020 an award of US$ 14.1 million was awarded by the Coalition for Epidemic Preparedness Innovations (CEPI) for advancing the development of the live-attenuated vaccine candidate BBV87 [121]. The vaccine has been developed by Bharat Biotech (BBIL) and is an inactivated whole virion vaccine based on a strain derived from an East, Central, South African (ECSA) genotype [121]. The vaccine has completed standard preclinical studies, and an optimum immune response was elicited by the

Table 2 CHIKV vaccine candidates in clinical development

Vaccine name	Developer	Type	Current stage of testing (clinicaltrials.gov identifier)	Refer-ence
TSI-GSD-218 (181/clone25)	US Army Medical Research Institute of Infectious Diseases, University of Maryland	Live-attenuated CHIKV strain (r.d.: 1). Attenuation determined by two amino acid substitutions in the E2 glycoprotein, generated by repeated in vitro passaging	Completed phase 2 Project terminated due to safety concerns	[80–82]
VLA1553	Valneva, Austria	Live-attenuated CHIKV with nsP3 deletion (r.d.: 1)	Recruiting for prospective, randomised, double-blinded, multicenter, pivotal clinical study evaluating the final dose of VLA1553 (phase 3) (NCT04546724)	[118–120]
BBV87	Bharat Biotech (BBIL)	inactivated whole virion vaccine based on a strain derived from an East, Central, South African (ECSA) genotype	Completed phase 1 (Clinical Trial Registry India, CTRI/2017/02/007.755); not yet recruiting for phase 2 and 3 trials (NCT04566484)	[121, 122]
VRC-CHKVLP059-00-VP (primary label), also called: PXVX0317 CHIKV-VLP	US National Institutes of Health, PaxVax	VLPs assembled from CHIKV proteins expressed in mammalian cells (r.d.:2)	Completed phase 2 (NCT02562482, NCT01489358, NCT03483961) Recruiting for phase 2 open-label study (NCT-NCT03992872)	[123, 124]
CHIKV/IRES	University of Texas Medical Branch, Takeda Pharmaceuticals	Recombinant CHIKV with internal ribosome entry site to downregulate structural proteins (r.d.: 1)	Projected for clinical studies	[28, 125, 126]
MV-CHIK	Institute Pasteur, Themis Bioscience	Recombinant live-attenuated measles vaccine expressing CHIKV VLPs derived from the structural protein genes (r.d.: 2)	Phase 2 (NCT03101111, NCT02861586, NCT03635086, NCT03807843)	[127–129]
ChAdOx1 Chik	University of Oxford	replication-deficient simian adenoviral vector expressing CHIKV antigens	Phase 1 (NCT04015648, NCT03590392)	[130]
VAL-181388 mRNA-1388	Moderna Therapeutics Inc	mRNA encoding the CHIKV structural proteins	Active, not recruiting for phase 1 (NCT03325075)	[131, 132]
mRNA-1944	Moderna Therapeutics Inc	mRNA encoding Chikungunya antibody (CHKV-24)	Active, recruiting for phase 1 (NCT03829384)	[133, 134]

CHIKV chikungunya virus; *IRES* internal ribosome entry site; *MV* measle virus; *nsP3*, non-structural protein 3; *r.d.* required/tested dose; *VLP* virus-like particle

adjuvanted vaccine in phase 1 clinical trials in India (Clinical Trial Registry India, CTRI/2017/02/007755). A phase 2/3 adaptive seamless design, randomised, controlled trial has been initiated in September 2020 to evaluate the safety and immunogenicity of a 2 dose-regimen the mentioned CHIKV vaccine in healthy subjects in Panama, Colombia, and Thailand (NCT04566484). The study is not yet recruiting and further details on the vaccine candidate have not been published yet.

Virus-like particles Another vaccine approach deals with virus-like particles (VLPs) which are generated by transfecting a DNA expression plasmid into human cells. The plasmid encodes for CHIKV structural proteins. After expression these structural proteins form particles that resemble intact virions. Yet, since the virions lack genomic viral RNA, they are unable to replicate [137]. One VLP candidate (referred to as VRC 311) completed preclinical trials with NHP and a phase 1 clinical trial proved the vaccine (now labelled VRC-CHKVLP059-00-VP) to be safe, well tolerated and highly immunogenic with a 100% seroconversion rate in all dose cohorts after booster immunisations [123]. Furthermore, it displayed a cross-protection against multiple CHIKV strains [124]. The candidate has currently finished phase 2 clinical trials and results are being evaluated (ClinicalTrials.gov; Identifier: NCT02562482).

Just like cells may express a plasmid that encodes for structural proteins, a virus may be recruited as a vector to express the structural proteins of the VLPs. This approach is called viral-vectored vaccines (VVVs).

One VVV candidate called MV-CHIKV was generated by using a recombinant, live-attenuated measles virus (MV) vector that expresses CHIKV VLPs. These VLPs comprise capsid and envelope structural proteins from the CHIKV strain "La Réunion" [127]. This VVV candidate was accepted for a phase 1 clinical trial and it triggered the production of neutralising antibodies in a dose-dependent manner. It also had a seroconversion of 100% after booster immunisation despite the presence of measles antibodies (which resulted from previous measle vaccinations of some study participants) [128]. The vaccine candidate entered phase 2 clinical trials in 2016 (ClinicalTrials.gov; Identifier: NCT02861586) and the study was completed in 2019. MV-CHIKV turned out to be of good safety, tolerability, and immunogenicity. All treated groups developed neutralising antibodies against CHIKV after one or two immunisations [129]. A study with NHP followed in 2019 in which macaques where challenged with a dose of 1.4×10^5 plaque forming units (PFU) injected subcutaneously 56 days after being vaccinated with MV-CHIKV. None of the previously vaccinated animals showed signs of infection after virus challenge. The developed neutralising antibodies showed a cross-reactivity towards other CHIKV strains. The vaccine

candidate proved to be safe, immunogenic, efficacious and worthy of further development towards licensure [138].

Another recombinant VVV candidate (ChAdOx1 Chik) is currently being evaluated in phase 1 clinical trial (ClinicalTrials.gov; Identifier: NCT03590392). ChAdOx1 Chik is a replication-deficient simian adenoviral vector that expresses CHIKV antigens. No results have been published on this project so far [130].

mRNA encoding for structural proteins that will assemble to VLPs Another approach has been launched by a company called Moderna which uses mRNA encoding for CHIKV structural proteins. The idea is to deliver the mRNA into the host cells where it is recognised by ribosomes. Subsequently the proteins which are encoded on the mRNA are produced. In case of the CHIKV vaccine, the mRNA encodes for the structural proteins that will assemble to VLPs once they are translated. The host organism thus recognises the VLPs as foreign, starts an immune response and produces corresponding antibodies [131]. In a phase 1 trial, the safety, tolerability, and immunogenicity of the Chikungunya vaccine candidate called mRNA-1388 in healthy human subjects is currently being investigated (ClinicalTrials.gov; Identifier: NCT03325075) [132].

Passive immunisation with monoclonal antibodies (mAbs)

Monoclonal antibodies are currently under heavy investigation for their possible use in prophylaxis and post-exposure therapy. So far, none have been licenced for medical use, but some studies seem promising and clinical trials are ongoing [55].

Couderc, Khandoudi [139] demonstrated that isolated anti-CHIKV polyclonal antibodies from patients which were recovering from a CHIKV infection could prevent and treat CHIKV infection in mice. He thus laid the foundation to further investigate antibodies as a means for CHIKV prophylaxis and treatment. In 2014 a clinical trial (clinical trial registration NCT02230163) has been initiated to investigate if transferring anti-CHIKV hyperimmune immunoglobulins that have previously been isolated from CHIKV convalescent donor plasma, may prevent infants with a high risk of mother to child transmission during childbirth from developing a severe form of CHIKF. Although being already initiated in 2014, no results of this study have been published so far. Another phase 1 trial is on its way but not yet recruiting (NCT 04441905) to test the SAR440894 monoclonal antibody (IgG1) directed against the E2 envelope protein of chikungunya virus in a randomised, double-blind study.

Given the fact, that up to all neonatal CHIKV cases in the La Réunion outbreak in 2005/2006 were symptomatic with nearly 20% resulting in a severe form with involvement of the central nervous system and often leading to permanent

damage (seizures, cerebral palsy) [55], the outcome of these studies would be of major interest.

mAbs targeting CHIKV surface envelope (E) proteins The CHIKV virion surface has 80 spikes which are built up of trimers of the glycoproteins E1-E3. The role of these surface proteins is to enable receptor-mediated endocytosis and the endosomal fusion which is induced by low pH. E2 forms the top of the spike and seems particularly important to mediate the attachment, binding, and entry of the virus particles. Thus, this E2 surface protein is considered a critical protein at which neutralising human and mouse mAbs could be targeted. Various groups have already identified either mouse or human neutralising mAbs that bind to E1 or E2 [140, 141].

A number of human mAbs have been analysed extensively in vivo and in vitro and some mAbs (C9, 4J21 and 5M16) provided full protection against CHIKV viremia and CHIKV-associated arthritis when administered prophylactically or even up to 18 h *p.i.* in mice [77, 141].

In his study on CHIKV mouse mAbs, Pal, Dowd [94] could show, that combinations of mouse mAbs which were administered prior to CHIKV exposure, protected immunocompromised mice against CHIKV infection and may limit the occurrence of mAb-resistant virus. The latter being of special concern as the viral loads of CHIKV during infection is very high. Furthermore, the humanised mAb 152 provided protection against lethal CHIKV infection in mice and even proved to be highly effective as a post-exposure treatment. Pal took his studies further and investigated mAb no. 152 and 166 in resus macaques. Combination therapy of these mAbs resulted in reduced viral spread and infection in the NHP. However, the mAbs were not able to clear the viral load completely and viral RNA persisted possibly in cell reservoirs that were responsible for actively replicating CHIKV RNA [94].

Broeckel and her group engineered a recombinant human monoclonal antibody (SVIR001) from a human mAb (no. 4N12) that in previous tests showed prophylactic and post-exposure activity against CHIKV infection in mice. The newly developed SVIR001 had the same antigen binding and neutralisation site as the original 4N12. SVIR001 was tested successfully in mice and resus macaques as a post-exposure therapy against CHIKV. The NHP displayed a rapid elimination of viremia in addition to less severe joint infiltration and fewer CHIKF signs than the control group. Broeckel could show that the macaques treated with SVIR001 had a diminished viral burden at both the site of infection as well as at distant sites. Moreover, the activated innate immune cell numbers and pro-inflammatory cytokine and chemokine levels were significantly reduced in the treated animals [96].

Since studies could prove that the B domain of the E2 surface protein is highly conserved across the alphavirus realm,

the fact that CHIKV polyclonal antibodies show a cross-reactivity and protection against multiple alphaviruses is not surprising [140, 142]. Fox identified 2 mAbs (187 and 265) which are broadly cross-reactive and protected mice against CHIKV, O'nyong-nyong virus (ONNV) and Mayaro virus (MAYV) by blocking viral entry and egress. ONNV shows an 86% envelope protein amino acid similarity and MAYV a 60% similarity to CHIKV. Both related viruses may also cause arthritic symptoms like CHIKV [140].

Although mAbs seem viable candidates for CHIKV therapy, it must be noted that the E1 and E2 epitopes on the virion might not always be accessible to therapeutic antibodies due to the dynamic movement of the proteins on the virion surface. This may affect the efficacy of the mAbs. Aside from that CHIKV might find a way to circumvent mAbs binding to the epitopes and create escape mutants. This viral resistance might be limited by using a combination of different mAbs (e.g. cocktails of neutralising mAbs that specifically recognise CHIKV or broadly neutralising mAbs against CHIKV and its closely related alphaviruses) at the same time, thus using synergistic effects to trap these virions before they can interact with the host receptors [143].

The use of mAbs, however, is time sensitive and in the later stages of CHIKF, passive transfer of antibodies usually does not improve the disease outcome. Furthermore, it is questionable whether mAbs can actually reach all cellular places where CHIKV RNA replication occurs. More research is needed as far as kinetics, doses, combinations, and invasiveness of mAbs are concerned. Last but not least, manufacturing mAbs against CHIKV is not a routine procedure. Cell lines need still to be identified that can effectively produce mAbs according to modern standards. Otherwise, mAb therapy may be too costly and their effective delivery especially to resource-limited areas might be difficult [144].

mRNA encoding for mAbs Another approach for passive immunisation is to deliver mRNA encoding for mAbs into the organism. Kose and colleagues isolated human mAbs from the B cells of a survivor of natural CHIKV infection [133]. Kose created an mRNA sequence that encoded for the mAbs and encapsulated this mRNA into lipid nanoparticles (LNPs). The LNPs were then delivered into mice by infusion. One human mAb, CHIKV-24, was expressed to biologically significant levels in vivo. The group then evaluated the protective capacity of the CHIKV-24 mAb mRNA first in mice, and later in NHP. Treatment with the mAb encoding mRNA protected mice from typical signs of CHIKV infection like arthritis, musculoskeletal tissue infection and death in a dose-dependent manner. Furthermore, it reduced viremia to undetectable levels at 2 days post inoculation in mice. NHP produced a level of mAb concentration that was well above the one needed for protection in mice. The NHP showed a dose–response effect after the first dose

of mRNA and maintained mAb levels after a second dose. Although the NHP were not challenged with WT CHIKV, Klose concluded that the data gathered from his preclinical study suggest that the CHIKV-24 mRNA may be useful to prevent CHIKF in humans [133]. A phase 1 trial is currently taking place to evaluate the safety, tolerability, pharmacokinetics, and pharmacodynamics of mRNA-1944 (ClinicalTrials.gov; Identifier: NCT03829384) [134]. The mRNA is encoding for an anti-CHIKV monoclonal antibody that will be systemically secreted after the mRNA is delivered via infusion into healthy adults.

Challenges in vaccine development and licensure

The economic and financial burden caused by a CHIKV epidemic are particularly high and the impact of CHIKF in these terms could be eliminated with a safe and effective vaccine [116]. Yet, the road to a licensed vaccine is long and faces multiple challenges.

One bottleneck in the development of a CHIKV vaccine is the fact that substantial funding from private, non-profit, and public institutions is necessary to cover the financial costs that arise until a vaccine is ready for the public. Usually the process costs several hundreds of millions of US dollars and companies need a prospect for a return of their investment, which might be questionable when the highest CHIKV burden occurs in developing countries. The above-mentioned focal and sporadic nature of CHIKF outbreaks as well as the establishment of a life-long immunity once the disease has been overcome, are further disincentives to for-profit organisations [116].

Yet, apart from travellers visiting afflicted countries, the military might also have increased interest in a vaccine to protect troops deployed in regions where CHIKV is endemic. Climate change, international travel and other unforeseen factors might promote vector emergence and spread in such a way that even developed countries are at risk of becoming endemic for CHIKV, presenting another potential market for a vaccine. The fact that FDA and the EMA have granted Fast Track- and Priority Medicine status to multiple vaccine candidates should inspire further confidence in the for-profit entities regarding the potential market [145].

Vaccine licensure is regulated by the European Medicines Agency (EMA) and the US Food and Drug Administration (FDA). To receive the approval (a so-called biologics license application (BLA)) for a vaccine (or other biological product) in the USA, the product has to meet the requirements of the Section 351 of the U.S. Public Health Service Act (U.S. Code Title 42—THE PUBLIC HEALTH AND WELFARE). It is eminent to demonstrate that the product is safe, pure and effective and that the facility manufacturing and processing the product meets standards designed to assure that said product stays safe, pure and effective [146]. To prove safety and effectiveness the Code of Federal Regulations states in Title 21, Section § 314.126 how "adequate and well-controlled studies" should be conducted. Trials must be designed in such a way as to distinguish the effect of an investigational product from other influences, such as chance, placebo effect or bias [147]. There are three different approval pathways available under FDA rule and they all require the same level of evidence to prove safety, purity and effectivity. There is the "traditional approval", the "accelerated approval" and the so-called "animal rule" [148].

The "traditional approval" pathway encompasses adequate and well-controlled clinical studies in humans. Recognising the current epidemiological problems and the need for a CHIKV vaccine, the WHO has published a R&D blueprint in which the principles in the design, conduct and analysis of Phase2b/Phase 3 clinical trials to evaluate Chikungunya vaccines are outlined [149].The WHO's suggested trial design is a Phase 3 prospective, double-blind, placebo-controlled, efficacy trial [149]. While this study design is considered the "gold standard" in epidemiologic studies, it seems that the "traditional approval" pathway does not work to receive a BLA for a CHIKV vaccine for various reasons [145].

The unpredictable, sporadic, focal, and relatively short nature of CHIV outbreaks make classical phase 3 trials impossible, which usually take several months in planning. Finding a suitable trial site months or years in advance is not feasible. The population afflicted mostly with severe disease outcome are the elderly and the very young. Clinical trials must take the immune status of these groups into account and the potential vaccines should have an enhanced safety profile. While live-attenuated vaccines are considered less safe due to their chance of regaining virulence, others, like VLPs are safer but less immunogenic [150]. With regard to a reduced immune system status this could prove problematic. Furthermore, while various studies proved the efficacy of neutralising antibodies to grant protection against CHIKV infection, no defined threshold of neutralising antibodies titres could be defined as a correlate of protection. A lack of standardisation of antibody neutralisation protocols prevents comparison of the different vaccine candidates [149].

The US Code of Federal Regulation (CFR) of the FDA thus allows alternative pathways in licensure for situations in which classical trials are not feasible. In a meeting initiated by the FDA and the Vaccine & Related Biological Products Advisory Committee (VRBPAC) in November 2019, alternative licensure pathways of CHIKV vaccines were discussed [151]. The consensus of the meeting was that the epidemiology of CHIKV does not allow for classical clinical efficacy trials and that a combination of seroepidemiological studies and non-human primate animal models might be a reasonable way to assess vaccine efficacy [151]. The so-called accelerated approval and the animal rule pathways, which can be used if a disease causes a serious condition,

are thus legitimate alternatives to the traditional efficacy trials. According to the FDA a serious condition is"a disease or condition associated with morbidity that has substantial impact on day-to-day functioning. Short-lived and self-limiting morbidity will usually not be sufficient, but the morbidity need not be irreversible if it is persistent or recurrent. Whether a disease or condition is serious is a matter of clinical judgement, based on its impact on such factors as survival, day-to-day functioning, or the likelihood that the disease, if left untreated, will progress from a less severe condition to a more serious one" [152]. As CHIKV infection can lead to persistent, disabling polyarthralgia which may last months or even years in up to 50% of the patients [50], CHIKF does qualify as a serious disease. Both alternative pathways may lead to a BLA without proof of efficacy in human clinical trials. However, clinical efficacy trials in humans still need to be conducted for verification after receiving licensure. Accelerated approval licensure is regulated in 21CFR601 Subpart E. The FDA may grant marketing approval of a biological product if an effect can be demonstrated on a surrogate endpoint that is reasonably likely to predict clinical benefit [153]. The question what might serve as a surrogate endpoint still needs to be answered. It may be possible to use a combination of seroepidemiological studies and non-human primate animal models to create an immunogenic surrogate based on neutralising antibodies [148].

The animal rule pathway only applies if neither ''traditional approval'' nor accelerated approval is available. Besides other criteria, efficacy of a vaccine may be proven using a sufficiently well-characterised animal model for predicting the response in humans and if animal study endpoint is clearly related to the desired benefit in humans [154]. However, since there are no animal models fit to mimic the chronic state of CHIKV disease (polyarthralgia and the resulting chronic inflammatory erosive arthritis), it is questionable if demonstrating that a CHIKV vaccine grants sterilising immunity against CHIKV in an NHP model suffices to predict benefits in humans.

Conclusion

With CHIKV transmission depending on arthropod vectors in a complex interaction between virus host and the environment, a thorough understanding of these interactions is essential for the development of strategies to control outbreaks and the geographical spread of vectors. Consideration of factors driving climate change plays an important role, as the vectors might invade habitats that were formerly unsuitable for them.

Countermeasures reviewed here include vector control, prophylaxis, post-exposure therapy or treatment of the disease itself. A number of vaccine candidates look promising

and have completed phase 2 clinical trials. Likewise, post-exposure therapy with monoclonal antibodies might be a valuable option. However, clinical trials are scarce in this particular field and only one trial is currently recruiting. Past epidemics caused by CHIKV demonstrate the impact a neglected or (re)emerging disease may have on a naïve population. Agents like CHIKV that have the potential to disable a population for a longer period and cause possible long-term sequelae pose a threat to the health and the economic system of a country. In the absence of a licensed vaccine, further research in the area of CHIKV disease prophylaxis is of utmost importance to prevent outbreaks and protect vulnerable populations.

References

1. Powers AM et al (2000) Re-emergence of chikungunya and O'nyong-nyong viruses: evidence for distinct geographical lineages and distant evolutionary relationships. J Gen Virol 81(Pt 2):471–479
2. Brown RS, Wan JJ, Kielian M (2018) The alphavirus exit pathway: what we know and what we wish we knew. Viruses 10(2):89
3. Powers AM et al (2000) Re-emergence of chikungunya and o'nyong-nyong viruses: evidence for distinct geographical lineages and distant evolutionary relationships. J Gen Virol 81(2):471–479
4. Minh BQ et al (2020) IQ-TREE 2: new models and efficient methods for phylogenetic inference in the genomic era. Mol Biol Evol 37(5):1530–1534
5. Kalyaanamoorthy S et al (2017) ModelFinder: fast model selection for accurate phylogenetic estimates. Nat Methods 14(6):587–589
6. Strauss JH, Strauss EG (1994) The alphaviruses: gene expression, replication, and evolution. Microbiol Rev 58(3):491–562
7. Khan AH et al (2002) Complete nucleotide sequence of chikungunya virus and evidence for an internal polyadenylation site. J Gen Virol 83(Pt 12):3075–3084
8. Silva LA, Dermody TS (2017) Chikungunya virus: epidemiology, replication, disease mechanisms, and prospective intervention strategies. J Clin Invest 127(3):737–749
9. Pietila MK, Hellstrom K, Ahola T (2017) Alphavirus polymerase and RNA replication. Virus Res 234:44–57
10. Robinson MC (1955) An epidemic of virus disease in Southern Province, Tanganyika Territory, in 1952–53. I. Clinical features. Trans R Soc Trop Med Hyg 49(1):28–32
11. Kuno G (2015) A re-examination of the history of etiologic confusion between dengue and chikungunya. PLoS Negl Trop Dis 9(11):e0004101
12. Matusali G et al (2019) Tropism of the chikungunya virus. Viruses 11(2):175
13. Schuffenecker I et al (2006) Genome microevolution of chikungunya viruses causing the Indian Ocean outbreak. PLoS Med 3(7):e263
14. Althouse BM et al (2018) Role of monkeys in the sylvatic cycle of chikungunya virus in Senegal. Nat Commun 9(1):1046

15. Tsetsarkin KA et al (2011) Chikungunya virus: evolution and genetic determinants of emergence. Curr Opin Virol 1(4):310–317

16. Sam IC et al (2015) Chikungunya virus in macaques, Malaysia. Emerg Infect Dis 21(9):1683–1685

17. Mavale M et al (2010) Venereal transmission of chikungunya virus by Aedes aegypti mosquitoes (Diptera: Culicidae). Am J Trop Med Hyg 83(6):1242–1244

18. Acharya D et al (2015) Loss of glycosaminoglycan receptor binding after mosquito cell passage reduces chikungunya virus infectivity. PLoS Negl Trop Dis 9(10):e0004139

19. Renault P et al (2012) Epidemiology of chikungunya infection on Reunion Island, Mayotte, and neighboring countries. Med Mal Infect 42(3):93–101

20. Yang CF et al (2016) Imported chikungunya virus strains, Taiwan, 2006–2014. Emerg Infect Dis 22(11):1981–1984

21. Angelini R et al (2007) An outbreak of chikungunya fever in the province of Ravenna, Italy. Euro Surveill 12(9):E070906.1

22. Grandadam M et al (2011) Chikungunya virus, southeastern France. Emerg Infect Dis 17(5):910–913

23. Cauchemez S et al (2014) Local and regional spread of chikungunya fever in the Americas. Euro surveillance: bulletin Europeen sur les maladies transmissibles = European communicable disease bulletin 19(28):20854–20854

24. ECDC (2020) Chikungunya worldwide overview: geographical distribution of chikungunya cases reported worldwide, July 2020 Situation update, 17 July 2020. Available from: https://www.ecdc.europa.eu/en/chikungunya-monthly

25. Pages F et al (2009) Aedes albopictus mosquito: the main vector of the 2007 chikungunya outbreak in Gabon. PLoS ONE 4(3):e4691

26. Mogi M et al (2017) The climate range expansion of Aedes albopictus (Diptera: Culicidae) in Asia inferred from the distribution of Albopictus subgroup species of Aedes (Stegomyia). J Med Entomol 54(6):1615–1625

27. Sahadeo N et al (2015) Correction: molecular characterisation of chikungunya virus infections in trinidad and comparison of clinical and laboratory features with dengue and other acute febrile cases. PLoS Negl Trop Dis 9(12):e0004305

28. Langsjoen RM et al (2018) Chikungunya virus strains show lineage-specific variations in virulence and cross-protective ability in murine and nonhuman primate models. mBio 9(2):02449–17

29. Tsetsarkin KA et al (2007) A single mutation in chikungunya virus affects vector specificity and epidemic potential. PLoS Pathog 3(12):e201

30. Tsetsarkin KA et al (2009) Epistatic roles of E2 glycoprotein mutations in adaption of chikungunya virus to Aedesalbopictus and Ae. aegypti mosquitoes. PLoS ONE 4(8):e6835–e6835

31. Niyas KP et al (2010) Molecular characterization of chikungunya virus isolates from clinical samples and adult Aedesalbopictus mosquitoes emerged from larvae from Kerala, South India. Virol J 7:189–189

32. Pierro DJ, Powers EL, Olson KE (2008) Genetic determinants of Sindbis virus mosquito infection are associated with a highly conserved alphavirus and flavivirus envelope sequence. J Virol 82(6):2966–2974

33. Tsetsarkin KA, Weaver SC (2011) Sequential adaptive mutations enhance efficient vector switching by chikungunya virus and its epidemic emergence. PLoS Pathog 7(12):e1002412–e1002412

34. Brault AC et al (2004) Venezuelan equine encephalitis emergence: enhanced vector infection from a single amino acid substitution in the envelope glycoprotein. Proc Natl Acad Sci USA 101(31):11344–11349

35. Vashishtha M et al (1998) A single point mutation controls the cholesterol dependence of Semliki Forest virus entry and exit. J Cell Biol 140(1):91–99

36. Sourisseau M et al (2007) Characterization of reemerging chikungunya virus. PLoS Pathog 3(6):e89

37. Wichit S et al (2017) AedesAegypti saliva enhances chikungunya virus replication in human skin fibroblasts via inhibition of the type I interferon signaling pathway. Infect Genet Evol 55:68–70

38. Zhang R et al (2018) Mxra8 is a receptor for multiple arthritogenic alphaviruses. Nature 557(7706):570–574

39. Labadie K et al (2010) Chikungunya disease in nonhuman primates involves long-term viral persistence in macrophages. J Clin Invest 120(3):894–906

40. Ruiz Silva M et al (2016) Mechanism and role of MCP-1 upregulation upon chikungunya virus infection in human peripheral blood mononuclear cells. Sci Rep 6:32288

41. Ozden S et al (2007) Human muscle satellite cells as targets of chikungunya virus infection. PLoS ONE 2(6):e527

42. Couderc T et al (2008) A mouse model for chikungunya: young age and inefficient type-I interferon signaling are risk factors for severe disease. PLoS Pathog 4(2):e29

43. Lokireddy S, Vemula S, Vadde R (2008) Connective tissue metabolism in chikungunya patients. Virol J 5:31

44. Pal P et al (2014) Chikungunya viruses that escape monoclonal antibody therapy are clinically attenuated, stable, and not purified in mosquitoes. J Virol 88(15):8213–8226

45. Mehta R et al (2018) The neurological complications of chikungunya virus: a systematic review. Rev Med Virol 28(3):e1978

46. Cerny T et al (2017) The range of neurological complications in chikungunya fever. Neurocrit Care 27(3):447–457

47. Das T et al (2015) Multifaceted innate immune responses engaged by astrocytes, microglia and resident dendritic cells against chikungunya neuroinfection. J Gen Virol 96(Pt 2):294–310

48. Inglis FM et al (2016) Neuropathogenesis of chikungunya infection: astrogliosis and innate immune activation. J Neurovirol 22(2):140–148

49. Her Z et al (2015) Loss of TLR3 aggravates CHIKV replication and pathology due to an altered virus-specific neutralizing antibody response. EMBO Mol Med 7(1):24–41

50. Rodriguez-Morales AJ et al (2016) Prevalence of post-chikungunya infection chronic inflammatory arthritis: a systematic review and meta-analysis. Arthritis Care Res (Hoboken) 68(12):1849–1858

51. Manimunda SP et al (2010) Clinical progression of chikungunya fever during acute and chronic arthritic stages and the changes in joint morphology as revealed by imaging. Trans R Soc Trop Med Hyg 104(6):392–399

52. Economopoulou A et al (2009) Atypical Chikungunya virus infections: clinical manifestations, mortality and risk factors for severe disease during the 2005–2006 outbreak on Reunion. Epidemiol Infect 137(4):534–541

53. Simon F, Javelle E, Gasque P (2015) Chikungunya virus infections. N Engl J Med 373(1):93–94

54. Renault P, Josseran L, Pierre V (2008) Chikungunya-related fatality rates, Mauritius, India, and Reunion Island. Emerg Infect Dis 14(8):1327

55. Gerardin P et al (2016) Chikungunya virus-associated encephalitis: a cohort study on La Reunion Island, 2005–2009. Neurology 86(1):94–102

56. Barrera R et al (2011) Preparedness and response for chikungunya virus introduction in the Americas. PAHO/WHO, Washington, DC

57. Omarjee R et al (2014) Importance of case definition to monitor ongoing outbreak of chikungunya virus on a background of

actively circulating dengue virus, St Martin, December 2013 to January 2014. Euro Surveill 19(13):20753

58. Kaur M et al (2018) Coinfection of chikungunya and dengue viruses: a serological study from North Western region of Punjab, India. J Lab Phys 10(4):443–447

59. Jacobsen S et al (2016) External quality assessment studies for laboratory performance of molecular and serological diagnosis of chikungunya virus infection. J Clin Virol 76:55–65

60. Johnson BW, Russell BJ, Goodman CH (2016) Laboratory diagnosis of chikungunya virus infections and commercial sources for diagnostic assays. J Infect Dis 214(suppl 5):S471–S474

61. Kikuti M et al (2020) Evaluation of two commercially available chikungunya virus IgM enzyme-linked immunoassays (ELISA) in a setting of concomitant transmission of chikungunya, dengue and Zika viruses. Int J Infect Dis 91:38–43

62. Kam Y-W et al (2015) Sero-prevalence and cross-reactivity of chikungunya virus specific anti-E2EP3 antibodies in arbovirus-infected patients. PLoS Negl Trop Dis 9(1):e3445–e3445

63. Figueiredo LT (2007) Emergent arboviruses in Brazil. Rev Soc Bras Med Trop 40(2):224–229

64. Gaibani P, Landini MP, Sambri V (2016) Diagnostic methods for CHIKV based on serological tools. Methods Mol Biol 1426:63–73

65. Sharp TM et al (2016) Surveillance for chikungunya and dengue during the first year of chikungunya virus circulation in puerto rico. J Infect Dis 214(suppl 5):S475–S481

66. Gobbi F et al (2015) Emergence and surveillance of chikungunya. Curr Trop Med Rep 2(1):4–12

67. Capeding MR et al (2013) Dengue and other common causes of acute febrile illness in Asia: an active surveillance study in children. PLoS Negl Trop Dis 7(7):e2331

68. Roth A et al (2014) Preparedness for threat of chikungunya in the pacific. Emerg Infect Dis 20(8):e130696

69. PPHSN. Pacific Public Health Surveillance Network 2016 [cited 2020 3. October 2020]; Available from: https://www.pphsn.net/index.htm.

70. Heitmann A et al (2018) Experimental risk assessment for chikungunya virus transmission based on vector competence, distribution and temperature suitability in Europe, 2018. Eurosurveillance 23(29):1800033

71. ECDC (2017) Cluster of autochtonous chikungunya cases in France—23 August 2017. ECDC-European Centre for Disease Prevention and Control, Stockholm

72. Bugert JJ et al (2020) Antivirals in medical biodefense. Virus Genes 56(2):150–167

73. Patel AC (2013) Clinical relevance of target identity and biology: implications for drug discovery and development. J Biomol Screen 18(10):1164–1185

74. Takenaka T (2001) Classical vs reverse pharmacology in drug discovery. BJU Int 88(Suppl 2):7–10

75. Rester U (2008) From virtuality to reality—virtual screening in lead discovery and lead optimization: a medicinal chemistry perspective. Curr Opin Drug Discov Devel 11(4):559–568

76. Pohjala L et al (2011) Inhibitors of alphavirus entry and replication identified with a stable chikungunya replicon cell line and virus-based assays. PLoS ONE 6(12):e28923

77. Selvarajah S et al (2013) A neutralizing monoclonal antibody targeting the acid-sensitive region in chikungunya virus E2 protects from disease. PLoS Negl Trop Dis 7(9):e2423

78. Weber C et al (2015) The green tea catechin, epigallocatechin gallate inhibits chikungunya virus infection. Antiviral Res 113:1–3

79. Lucas-Hourani M et al (2013) A phenotypic assay to identify chikungunya virus inhibitors targeting the nonstructural protein nsP2. J Biomol Screen 18(2):172–179

80. Levitt NH et al (1986) Development of an attenuated strain of chikungunya virus for use in vaccine production. Vaccine 4(3):157–162

81. Edelman R et al (2000) Phase II safety and immunogenicity study of live chikungunya virus vaccine TSI-GSD-218. Am J Trop Med Hyg 62(6):681–685

82. Gorchakov R et al (2012) Attenuation of chikungunya virus vaccine strain 181/clone 25 is determined by two amino acid substitutions in the E2 envelope glycoprotein. J Virol 86(11):6084–6096

83. Khan M et al (2011) Cellular IMPDH enzyme activity is a potential target for the inhibition of chikungunya virus replication and virus induced apoptosis in cultured mammalian cells. Antiviral Res 89(1):1–8

84. Rathore AP et al (2014) Chikungunya virus nsP3 & nsP4 interacts with HSP-90 to promote virus replication: HSP-90 inhibitors reduce CHIKV infection and inflammation in vivo. Antiviral Res 103:7–16

85. Briolant S et al (2004) In vitro inhibition of chikungunya and Semliki Forest viruses replication by antiviral compounds: synergistic effect of interferon-alpha and ribavirin combination. Antiviral Res 61(2):111–117

86. Delang L et al (2014) Mutations in the chikungunya virus non-structural proteins cause resistance to favipiravir (T-705), a broad-spectrum antiviral. J Antimicrob Chemother 69(10):2770–2784

87. Cruz DJ et al (2013) Identification of novel compounds inhibiting chikungunya virus-induced cell death by high throughput screening of a kinase inhibitor library. PLoS Negl Trop Dis 7(10):e2471

88. Bassetto M et al (2013) Computer-aided identification, design and synthesis of a novel series of compounds with selective antiviral activity against chikungunya virus. Antiviral Res 98(1):12–18

89. Bourjot M et al (2014) Trigocherrierin A, a potent inhibitor of chikungunya virus replication. Molecules 19(3):3617–3627

90. Jadav SS et al (2015) Thiazolidone derivatives as inhibitors of chikungunya virus. Eur J Med Chem 89:172–178

91. Teng TS et al (2012) Viperin restricts chikungunya virus replication and pathology. J Clin Invest 122(12):4447–4460

92. Abdelnabi R et al (2017) Protein kinases C as potential host targets for the inhibition of chikungunya virus replication. Antiviral Res 139:79–87

93. Marlina S et al (2015) Development of a Real-Time Cell Analysing (RTCA) method as a fast and accurate screen for the selection of chikungunya virus replication inhibitors. Parasit Vectors 8:579

94. Pal P et al (2013) Development of a highly protective combination monoclonal antibody therapy against chikungunya virus. PLoS Pathog 9(4):e1003312

95. Parashar D et al (2013) Administration of E2 and NS1 siRNAs inhibit chikungunya virus replication in vitro and protects mice infected with the virus. PLoS Negl Trop Dis 7(9):e2405

96. Broeckel R et al (2017) Therapeutic administration of a recombinant human monoclonal antibody reduces the severity of chikungunya virus disease in rhesus macaques. PLoS Negl Trop Dis 11(6):e0005637

97. Feldstein LR et al (2019) Estimating the cost of illness and burden of disease associated with the 2014–2015 chikungunya outbreak in the U.S. Virgin Islands. PLoS Negl Trop Dis 13(7):e0007563

98. CDC. Chikungunya Virus. 2020 19. Sept. 2019 [cited 2020]; Available from: https://www.cdc.gov/chikungunya/geo/index.html

99. Kucharz EJ, Cebula-Byrska I (2012) Chikungunya fever. Eur J Intern Med 23(4):325–329

100. Sridhar S et al (2018) Effect of dengue serostatus on dengue vaccine safety and efficacy. N Engl J Med 379(4):327–340

101. Wilson AL et al (2020) The importance of vector control for the control and elimination of vector-borne diseases. PLoS Negl Trop Dis 14(1):e0007831–e0007831

102. Ritchie SA, Johnson BJ (2017) Advances in vector control science: rear-and-release strategies show promise … but don't forget the basics. J Infect Dis 215(suppl_2):S103–S108

103. Alphey L et al (2010) Sterile-insect methods for control of mosquito-borne diseases: an analysis. Vector Borne Zoonotic Dis 10(3):295–311

104. Wedell N, Price TAR, Lindholm AK (1917) Gene drive: progress and prospects. Proc Biol Sci 2019(286):20192709–20192709

105. Aliota MT et al (2016) The wMel strain of *Wolbachia* reduces transmission of chikungunya virus in *Aedes aegypti*. PLoS Negl Trop Dis 10(4):e0004677

106. Werren JH, Baldo L, Clark ME (2008) *Wolbachia*: master manipulators of invertebrate biology. Nat Rev Microbiol 6(10):741–751

107. Johnson KN (2015) The impact of *Wolbachia* on virus infection in mosquitoes. Viruses 7(11):5705–5717

108. Aliota MT et al (2016) The wMel strain of *Wolbachia* reduces transmission of zika virus by *Aedes aegypti*. Sci Rep 6:28792

109. Hoffmann AA et al (2011) Successful establishment of *Wolbachia* in *Aedes* populations to suppress dengue transmission. Nature 476(7361):454–457

110. van den Hurk AF et al (2012) Impact of *Wolbachia* on infection with chikungunya and yellow fever viruses in the mosquito vector *Aedes aegypti*. PLoS Negl Trop Dis 6(11):e1892

111. Callaway E (2020) The mosquito strategy that could eliminate dengue. Nature. https://doi.org/10.1038/d41586-020-02492-1

112. Ryan P et al (2020) Establishment of wMel *Wolbachia* in Aedes aegypti mosquitoes and reduction of local dengue transmission in Cairns and surrounding locations in northern Queensland, Australia [version 2; peer review: 2 approved]. Gates Open Res 3:1547

113. Anders KL et al (2020) Update to the AWED (Applying *Wolbachia* to Eliminate Dengue) trial study protocol: a cluster randomised controlled trial in Yogyakarta, Indonesia. Trials 21(1):429

114. Callaway E (2017) Gene drives thwarted by emergence of resistant organisms. Nature 542(7639):15

115. Nitatpattana N et al (2014) Long-term persistence of chikungunya virus neutralizing antibodies in human populations of North Eastern Thailand. Virol J 11:183

116. Rezza G, Weaver SC (2019) Chikungunya as a paradigm for emerging viral diseases: evaluating disease impact and hurdles to vaccine development. PLOS Negl Trop Dis 13(1):e0006919

117. Reyes-Sandoval A (2019) 51 years in of chikungunya clinical vaccine development: a historical perspective. Hum Vaccin Immunother 15(10):2351–2358

118. Roques P et al (2017) Attenuated and vectored vaccines protect nonhuman primates against chikungunya virus. JCI Insight 2(6):e83527

119. Valneva (2020) Valneva initiates phase 3 clinical study for its chikungunya vaccine candidate VLA1553. Valneva SE, Saint-Herblain

120. Hallengard D et al (2014) Novel attenuated chikungunya vaccine candidates elicit protective immunity in C57BL/6 mice. J Virol 88(5):2858–2866

121. International Vaccine Institute, I. (2020) CEPI awards up to US$14.1 million to consortium of IVI and Bharat Biotech to advance development of Chikungunya vaccine in collaboration with Ind-CEPI. CEPI, the Coalition for Epidemic Preparedness Innovations, Oslo, Seoul, Telangana

122. Clinical Trials Registry—India, C. (2017) Phase-I open label, dose-escalation clinical trial to evaluate the safety, tolerability and immunogenicity of chikungunya vaccine in healthy adults of 18 to 50 years age. Clinical Trials Registry—India, CTRI, Hyderabad

123. Chang LJ et al (2014) Safety and tolerability of chikungunya virus-like particle vaccine in healthy adults: a phase 1 dose-escalation trial. Lancet 384(9959):2046–2052

124. Goo L et al (2016) A virus-like particle vaccine elicits broad neutralizing antibody responses in humans to all chikungunya virus genotypes. J Infect Dis 214(10):1487–1491

125. Plante K et al (2011) Novel chikungunya vaccine candidate with an IRES-based attenuation and host range alteration mechanism. PLoS Pathog 7(7):e1002142

126. Roy CJ et al (2014) Chikungunya vaccine candidate is highly attenuated and protects nonhuman primates against telemetrically monitored disease following a single dose. J Infect Dis 209(12):1891–1899

127. Brandler S et al (2013) A recombinant measles vaccine expressing chikungunya virus-like particles is strongly immunogenic and protects mice from lethal challenge with chikungunya virus. Vaccine 31(36):3718–3725

128. Ramsauer K et al (2015) Immunogenicity, safety, and tolerability of a recombinant measles-virus-based chikungunya vaccine: a randomised, double-blind, placebo-controlled, active-comparator, first-in-man trial. Lancet Infect Dis 15(5):519–527

129. Reisinger EC et al (2019) Immunogenicity, safety, and tolerability of the measles-vectored chikungunya virus vaccine MV-CHIK: a double-blind, randomised, placebo-controlled and active-controlled phase 2 trial. Lancet 392(10165):2718–2727

130. Medicine, N.N.L.o. *ClinicalTrials.gov*. [cited 2020 05.05.2020]; Available from: https://clinicaltrials.gov/ct2/show/study/NCT03590392

131. Moderna. *Infectious Diseases*. 2019 [cited 2020 January 15]; Available from: https://www.modernatx.com/pipeline/therapeutic-areas/infectious-diseases

132. Liu, A. *Moderna initiates Chikungunya vaccine human test, replaces backup Zika candidate*. 2017 [cited 2019 September 19]; Available from: https://www.fiercepharma.com/vaccines/moderna-initiates-chikungunya-vaccine-human-test-replaces-backup-zika-candidate

133. Kose N et al (2019) A lipid-encapsulated mRNA encoding a potently neutralizing human monoclonal antibody protects against chikungunya infection. Sci Immunol. https://doi.org/10.1126/sciimmunol.aaw6647

134. Moderna (2019) Moderna announces positive phase 1 results for the first systemic messenger RNA therapeutic encoding a secreted protein (mRNA-1944). Business wire, Cambridge

135. Plante KS et al (2015) Extended preclinical safety, efficacy and stability testing of a live-attenuated chikungunya vaccine candidate. PLoS Negl Trop Dis 9(9):e0004007

136. Valneva Press Release (2019) Valneva reports excellent final phase 1 results for its chikungunya vaccine candidate, confirms plans. Valneva, Saint-Herblain

137. Akahata W et al (2010) A virus-like particle vaccine for epidemic chikungunya virus protects nonhuman primates against infection. Nat Med 16(3):334–338

138. Rossi SL et al (2019) Immunogenicity and efficacy of a measles virus-vectored chikungunya vaccine in nonhuman primates. J Infect Dis 220(5):735–742

139. Couderc T et al (2009) Prophylaxis and therapy for chikungunya virus infection. J Infect Dis 200(4):516–523

140. Fox JM et al (2015) Broadly neutralizing alphavirus antibodies bind an epitope on E2 and inhibit entry and egress. Cell 163(5):1095–1107

141. Smith SA et al (2015) Isolation and characterization of broad and ultrapotent human monoclonal antibodies with therapeutic activity against chikungunya virus. Cell Host Microbe 18(1):86–95

142. Kielian M, Saphire EO (2015) Potent antibody protection against an emerging alphavirus threat. Cell 163(5):1053–1054

143. Kuhn RJ et al (2015) Shake, rattle, and roll: impact of the dynamics of flavivirus particles on their interactions with the host. Virology 479–480:508–517

144. Clayton AM (2016) Monoclonal antibodies as prophylactic and therapeutic agents against chikungunya virus. J Infect Dis 214(suppl 5):S506-s509

145. Schrauf S et al (2020) Current efforts in the development of vaccines for the prevention of zika and chikungunya virus infections. Front Immunol 11:592

146. FDA, F.a.D.A. (2018) United States Code, 2018 Edition, Title 42—The public health and welfare. United States Code. U.S. Government Publishing Office, Washington DC

147. FDA, F.a.D.A. (2020) CFR—Title 21—Food and Drugs, Section § 314.126—adequate and well-controlled studies. In: U.S.D.o.H.a.H.S. (HHS) (ed) Code of Federal Regulations (CFR). Food and Drug Administration (FDA), Washington DC

148. Yang S et al (2017) Regulatory considerations in development of vaccines to prevent disease caused by chikungunya virus. Vaccine 35(37):4851–4858

149. WHO (2018) WHO consultation on Chikungunya vaccine evaluation, in R&D blueprint. World Health Organisation (WHO), Geneva

150. DeFilippis VR (2019) Chikungunya virus vaccines: platforms, progress, and challenges. Curr Top Microbiol Immunol. https://doi.org/10.1007/82_2019_175

151. VRBPAC, V.R.B.P.A.C (2018) Vaccines and Related Biological Products Advisory Committee November 8, 2019. FDA US Food & Drug Administration, Silver Spring

152. FDA, F.a.D.A. (2020) CFR—Title 21—Food and Drugs, Section § 312.300 General. In: U.S.D.o.H.a.H.S. (HHS) (ed) Code of Federal Regulations (CFR). Food and Drug Administration (FDA), Washington DC

153. FDA, F.a.D.A. (2020) CFR—Title 21—Food and Drugs, Section § 601.41 Approval based on a surrogate endpoint or on an effect on a clinical endpoint other than survival or irreversible morbidity. In: U.S.D.o.H.a.H.S. (HHS) (ed) Code of Federal Regulations (CFR). Food and Drug Administration (FDA), Washington DC

154. FDA, F.a.D.A. (2020) CFR - Title 21 - Food and Drugs, Section § 601.91 Approval based on evidence of effectiveness from studies in animals. In: U.S.D.o.H.a.H.S. (HHS) (ed) Code of Federal Regulations (CFR). Food and Drug Administration (FDA), Washington DC

4. Current and Promising Antivirals Against Chikungunya Virus

Friederike I. L. Hucke[1], Joachim J. Bugert[1]

[1]Bundeswehr Institute of Microbiology, Neuherbergstraße 11, 80937 München, Germany

The manuscript is presented in its published form and has therefore its own reference section. References and abbreviations from the manuscript are not included in the relevant sections at the beginning and the end of this document.

Current and Promising Antivirals Against Chikungunya Virus

Friederike I. L. Hucke* and Joachim J. Bugert

Department of Virology, Bundeswehr Institute of Microbiology, Munich, Germany

Chikungunya virus (CHIKV) is the causative agent of chikungunya fever (CHIKF) and is categorized as a(n) (re)emerging arbovirus. CHIKV has repeatedly been responsible for outbreaks that caused serious economic and public health problems in the affected countries. To date, no vaccine or specific antiviral therapies are available. This review gives a summary on current antivirals that have been investigated as potential therapeutics against CHIKF. The mode of action as well as possible compound targets (viral and host targets) are being addressed. This review hopes to provide critical information on the *in vitro* efficacies of various compounds and might help researchers in their considerations for future experiments.

Keywords: antiviral design, CHIKV therapy, direct antiviral action, host-targeting antiviral, comparison of *in vitro* efficacies, favipiravir, ribavirin

INTRODUCTION CHIKUNGUNYA VIRUS

Chikungunya virus (CHIKV) is a single-stranded RNA virus with a positive sense genome of about 11,800 nucleotides. CHIKV structure and genome organization follow those of all alphaviruses. The virion has a lipid-bilayer envelope that is tightly associated with an icosahedral nucleocapsid shell (240 capsid copies) which encapsidates genomic RNA (1). The genome contains two open reading frames (ORFs), which encode the non-structural (ns) or replicase polyprotein and the structural polyprotein.

CHIKV is primarily transmitted to humans by the bite of an infected mosquito, mainly of the *Aedes* species. CHIKV causes the so-called chikungunya fever (CHIKF) which is characterized by high fever, headache and the hallmarks of the disease, myalgia and polyarthralgia (1). The latter especially can last for months or even years after the acute phase of the illness has passed, causing a severely deteriorated quality of life for the patient. The resulting stooped bearing and rigid gait of infected individuals are described in the word origin of the disease "kungunyala," which is Makonde for "that which bends up." CHIKV was first described in 1955 by Robinson and Lumsden after an outbreak in present-day Tanzania in 1952 (2).

Until 2004, CHIKV was mainly distributed in tropical and subtropical regions of sub-Sahara Africa and Southeast Asia. It caused sporadic outbreaks mainly during the rainy season. In 2004, however, a massive outbreak in Kenya led to close to half a million infected people. This epidemic initiated the spread to more than 22 countries, including countries with a moderate climate such as France and Italy (**Figure 1**) (5).

Following the bite of a CHIKV infected mosquito, the virus is transported to the nearest lymph node and transferred to monocytes and macrophages which enter the bloodstream. At this point, viremia sets in by the active infection of human blood monocytes and other peripheral blood mononuclear cells. CHIKV then reaches the muscles and joints, where the infection causes the main symptoms of CHIKF—myalgia and arthralgia (6). Apart from muscles and joints, CHIKV may also target a range of secondary organs and thus cause severe complications in patients

FIGURE 1 | Geographical distribution of CHIKV. Word map showing the distribution of autochthonous CHIKV transmissions in the past 7 years (2013–2020) highlighted in green. In the continental United States of America, only travel associated cases have been reported in the past 3 years. As of July 2020, the latest autochthonous cases in Europe have been recorded in France and Italy in 2017 (3, 4).

(i.e., renal, respiratory, hepatic, cardiac, and neural syndromes) (7). As neither specific antiviral drugs nor a licensed vaccine are available, the therapy of CHIKF is based on supportive measures and the treatment of symptoms [non-steroid anti-inflammatory drugs (NSAIDs) and fluid therapy (8)].

For detailed information on CHIKV epidemiology, replication, disease mechanism, and prophylaxis, we refer to the reviews of Silva and Dermody (1), Pietila et al. (9), and Hucke et al. (10).

ANTIVIRALS AGAINST CHIKUNGUNYA VIRUS

Direct-Acting Antivirals

The following chapter will deal with various compounds that are or have been in the focus of research and showed some promising results *in vitro* mainly against CHIKV and/or other relevant alphaviruses. Various compounds made it to *in vivo* studies but so far there is no licensed therapeutic drug acting directly against CHIKV or any other alphavirus. There are many compounds which are currently under investigation for their anti-CHIKV efficacy. However, as the scope of this review is limited, we will only discuss compounds that either showed efficacy in a variety of *in vitro* assays or were repeatedly investigated by different (independent) research groups. It must be noted that compound efficacy can vary considerably, depending on the cell line, virus strain, or assay method that is being used. **Table 1** illustrates this fact and gives an overview of EC_{50}/CC_{50} values of common

substances used as experimental controls in *in vitro* trials. For the interested reader I refer to the reviews of Abdelnabi et al. (38), Subudhi et al. (39) and the review of da Silva-Junior et al. (40), focussing on the medicinal chemistry of synthetic and natural compounds against CHIKV. Furthermore, the review of Bugert et al. (41) inspects antivirals against alphaviruses and other viral agents relevant in medical biodefence.

CHIKV Entry Inhibitors
Chloroquine
Chloroquine is a licensed drug for the prophylaxis and treatment of malaria. Furthermore, it is prescribed for the treatment of systemic lupus erythematosus and rheumatoid arthritis (42). Chloroquine also shows *in vitro* antiviral activity against several viruses, such as human immunodeficiency virus (HIV), severe acute respiratory syndrome (SARS) coronavirus and alphaviruses (43). Khan demonstrated that chloroquine is able to inhibit CHIKV replication in VeroA cells in a dose-dependent manner. Apart from this mode of action, it is also assumed that the drug interferes with the endosome-mediated CHIKV internalization. Bernard et al. (44) showed that chloroquine raises the endosomal pH by interfering with the protonation of the endocytic vesicles and thereby prevents the E1 fusion step needed for the release of CHIKV RNA into the cell cytoplasm. Various research groups used chloroquine as a reference compound in their *in vitro* studies (**Table 2**) (11–15, 45).

Despite the promising results chloroquine displays in *in vitro* studies, clinical trials with the drug failed to prove any benefit

TABLE 1 | Comparison of compounds with anti-CHIKV property.

Compound	EC_{50} (μM)	CC_{50} (μM)	References
CHIKV entry inhibitors			
Chloroquine (reference)	5–11	>36–100	(11–17)
Suramin	8.8–62.1	350 to >700	(18)
Suramin conjugates	1.9–2.7	50 to >200	(19)
nsP1 inhibitors			
Lobaric acid	5.3–16.3	50–76	(20)
[1,2,3]triazolo[4,5-d]pyrimidin-7(6H)-ones (lead)	<1.0	>668	(21)
[1,2,3]triazolo[4,5-d]pyrimidin-7(6H)-one (compound 8)	1.1–5.3	>300	(14)
nsP2 inhibitors			
Bassettos *in silico* lead (compound 1)	5	72	(12)
1,3-thiazolidin-4-one (compound 8)	1.5	>200	(22)
Compound ID1452-2	31	n.d.	(23)
nsP4 inhibitors and inhibitors of viral genome replication			
Ribavirin	2.05–756.8	49 to >500	(16, 24–29)
β-d-N4-hydroxycytidine (NHC)	0.2–1.8	2.5–30.6	(30)
Favipiravir (T-705)	16–245.13	>636	(25, 31)
Defluorinated Favipiravir (T-1105)	7–47	>571	(31)
Sofosbuvir	1–17	402	(24)
Mycophenolic acid (MPA)	0.5–1.6	370	(16, 24, 32)
Protein kinase C inhibitors			
Prostratin	0.2–8	50 to >100	(11, 33)
12-O-tetradecanoylphorbol 13-acetate (TPA)	0.0029	5.7	(11)
Phorbol-12,13-didecanoate	0.006	~4.1	(13)
12-O-decanoylphorbol 13-acetate (DPA)	2.4	4.6	(34)
12-O-decanoyl-7-hydroperoxy-5-ene-13-acetate phorbol	4.0	7.8	(34)
Neoguillauminin A	17.7	~35	(15)
12-deoxy phorbol Compound 1	0.13	12.7	(15)
12-deoxyphorbol Compound 2	0.02	4.85	(15)
12-deoxyphorbol Compound 4	0.02	30.0	(15)
Trigocherrin A	1.5	35	(17)
Multiple/unidentified targets			
Micafungin	17.2–20.63	>100	(35)
Abamectine	1.4 ± 0.9 (Huh-7.5) and 1.5 ± 0.6 (BHK-21)	15.2 ± 1.0 (Huh-7.5) and 28.2 ± 1.1 (BHK-21)	(36)
Ivermectine	1.9 ± 0.8 (Huh-7.5) and 0.6 ± 0.1 (BHK-21)	8.0 ± 0.2 (Huh-7.5) and 37.9 ± 7.6 (BHK-21)	(36)
Berberine	1.9 ± 0.9 (Huh-7.5) and 1.8 ± 0.5 (BHK-21)	>100 (Huh-7.5 and BHK-21)	(36)
coumarin derivatives conjugated with guanosine	9.9–13.9	96.5–212	(37)

The above mentioned compounds have been in the focus of studies during the past 7 years (with the exception of the reference compounds chloroquine and ribavirin). The compounds have been arranged according to their (known) point of interaction. EC_{50} and CC_{50} may display a broad range due differences in cell line, virus strain, and assay method within the study. Unless stated otherwise, EC_{50} and CC_{50} were generated with Vero cell lines.

BHK, baby hamster kidney cells; CC50, cytotoxicity concentration 50%; CHIKV, Chikungunya virus; EC50, half maximal effective concentration; Huh, Human hepatocarcinoma cells; n.d., not determined; nsP, non-structural protein.

for the patient. Trials for prophylaxis or treatment of CHIKV infection either in macaque models or human patients could not demonstrate advantage of chloroquine over meloxicam (an NSAID) administration (46, 47). The discrepancy between *in vitro* and *in vivo* effectiveness of chloroquine has been described before.

TABLE 2 | Efficacy of selected compounds against CHIKV according to different studies.

Compound	Cell line	CHIKV strain; MOI	EC$_{50}$ (µM)	CC$_{50}$ (µM) (SI)	Assay method	References
Ribavirin (RBV)	Vero	Ross C347 strain; MOI = 0.001	341.53		plaque/microscope/trypan blue	(27)
	Vero	vaccine strain 181/clone 25; MOI = 0.0001	408.2	266.5 (SI = 0.65)	Tox: Viral ToxGlo (Promega), Inf: Virus quantification via plaque assay	(25)
	Huh-7	vaccine strain 181/clone 25; MOI = 0.1	10.56	49 (SI = 4.64)	Tox: Viral ToxGlo; Inf: plaque assay	(25)
	A549	vaccine strain 181/clone 25; MOI = 0.1	480.11	205.86 (SI = 0.43)	Tox: Viral ToxGlo; Inf: plaque assay	(25)
	Vero	ECSA clinical isolate; MOI = 2	10.95	n.d.	Tox: MTT; Inf: plaque formation assay, ELISA-like cell-based assay and IFT	(26)
	Vero	vaccine strain 181/clone 25 (NR-13222); MOI = 0.0001	419.43	n.d.	Inf: plaque assay	(28)
	BHK21	CHIKV-0708 Singapore not mutated; MOI = 1	2.05	n.d.	IFT	(29)
	Huh-7	CHIKV (Asian strain); MOI = 0.1	2.5 ± 0.3	298 ± 22 (SI = 120)	RNA level (RT-PCR)	(24)
	Huh-7	CHIKV (Asian strain); MOI = 0.1	5.5 ± 1.5	298 ± 22 (SI = 54)	Virus titer (yield) by plaque	(24)
	Vero E6	ITA07-RA1; MOI = 0.005	423.6 ± 27.5	>500 (SI > 1.18)	MTS (Promega)	(16)
	Vero E6	LS3; MOI = 0.005	756.8 ± 22.4	>500 (SI > 0.66)	MTS (Promega)	(16)
	Vero E6	LS3-GFP; MOI = 0.005	466.7 ± 38.0	>500 (SI > 1.07)	MTS (Promega)	(16)
	BHK21	ITA07-RA1; MOI = 0.005	20.8 ± 1.1	>500 (SI > 24.04)	MTS (Promega)	(16)
	BHK21	LS3; MOI = 0.005	15.6 ± 1.5	>500 (SI > 32.05)	MTS (Promega)	(16)
	BHK21	LS3-GFP; MOI = 0.005	17.5 ± 1.7	>500 (SI > 28.57)	MTS (Promega)	(16)
Favipiravir (T-705)	Vero	vaccine strain 181/clone 25; MOI = 0.0001	184.53	>6365.4 (SI > 34.5)	Tox: Viral ToxGlo (Promega), Inf: plaque assay	(25)
	Huh-7	vaccine strain 181/clone 25; MOI = 0.1	127.3	>6365.4 (SI > 50)	Tox: Viral ToxGlo; Inf: plaque assay	(25)
	A549	vaccine strain 181/clone 25; MOI = 0.1	245.13	>6365.4 (SI > 25)	Tox: Viral ToxGlo; Inf: plaque assay	(25)
	Vero A	Indian Ocean 899; MOI n.s.	60 ± 10	>636 (SI > 10.6)	MTS (Promega)	(31)
	Vero A	LR2006-OPY1; MOI = 0.1	25 ± 1	>636 (SI > 25.44)	MTS (Promega)	(31)
	Vero A	Italy 2008 (clin.); MOI = 0.1	16 ± 6	>636 (SI > 39.75)	MTS (Promega)	(31)
Sofosbuvir	Huh-7	CHIKV Asian strain; MOI = 0.1	1.0 ± 0.1	402 ± 32 (SI = 402)	Inf: RNA level (RT-PCR); Tox: XTT and PMS	(24)
	Huh-7	CHIKV Asian strain; MOI = 0.1	2.7 ± 0.5	402 ± 32 (SI = 149)	Inf: Virus titer (yield) by plaque; Tox: XTT and PMS	(24)
	Stem cells derived astrocytes (iPSCs)	CHIKV Asian strain; MOI = 1	17 ± 5	n.d.	Virus titer (yield) by plaque	(24)

(Continued)

TABLE 2 | Continued

Compound	Cell line	CHIKV strain; MOI	EC$_{50}$ (µM)	CC$_{50}$ (µM) (SI)	Assay method	References
Mycophenolic acid (MPA)	Huh-7	CHIKV Asian strain; MOI = 0.1	0.8 ± 0.05	370 ± 55 (SI = 463)	Inf: RNA level (RT-PCR); Tox: XTT and PMS assay	(24)
	Huh-7	CHIKV Asian strain; MOI = 0.1	1.1 ± 0.2	370 ± 55 (SI = 336)	Inf: Virus titer (yield) by plaque; Tox: XTT and PMS	(24)
	Huh-7	recombinant CHIKV-118-GFP; MOI = 0.5	1.6	> 100 (SI >62)	Resazurin reduction assay	(32)
	Vero E6	ITA07-RA1; MOI = 0.005	0.6 ± 0.03	>50 (SI > 83.3)	MTS (Promega)	(16)
	Vero E6	LS3; MOI = 0.005	0.6 ± 0.01	>50 (SI > 83.3)	MTS (Promega)	(16)
	Vero E6	recombinant LS3-GFP; MOI = 0.005	0.5 ± 0.07	>50 (SI > 100)	MTS (Promega)	(16)
Prostratin	Vero	CHIKV Indian Ocean strain 899; MOI n.s.	2.7 ± 1.2	~60 (SI~22.8)	MTS (Promega)	(11)
	BGM	CHIKV Indian Ocean strain 899; MOI = 0.001	8 ± 1.2	>100 (SI >12.5)	MTS/PMS (Promega)	(33)
	BGM	CHIKV Indian Ocean strain 899; MOI = 0.001	7.6 ± 1.3	>100 (SI > 13.16)	qRT-PCR	(33)
	BGM	CHIKV Indian Ocean strain 899; MOI = 0.001	7.1 ± 0.6	>100 (SI > 14.08)	titration assay	(33)
	human skin fibroblasts CRL-2522	Singapore (SGP011), Caribbean strain (CNR20235) + Reunion Island strain (LR2006 OPY1); MOI = 1	0.2-0.5	50 (SI = 100–250)	luciferase assay, qRT-PCR + titration assay	(33)
Chloroquine	Vero	CHIKV Indian Ocean strain 899	10–11	89–100 (SI = 8-9)	CPE reduction, RT-qPCR, MTS (Promega)	(11, 12, 15, 17)
	Vero E6	ITA07-RA1 MOI = 0.005	7.4 ± 1.1	>36 (SI >4.86)	MTS (Promega)	(16)
	Vero E6	LS3 MOI = 0.005	10.6 ± 1.6	>36 (SI >3.4)	MTS (Promega)	(16)
	Vero E6	LS3-GFP MOI = 0.005	5.0 ± 1.7	>36 (SI >7.2)	MTS (Promega)	(16)

The above mentioned compounds have been repeatedly used in in vitro studies as references. Compound efficacy may considerably between the different studies, depending on the cell line, virus strain, and assay method that is being used. The table aims to give an orientation at what range a control compound might be effective against CHIKV in different cell lines and assay methods.

A549, human lung carcinoma cells; BGM, buffalo green monkey kidney cells; BHK, baby hamster kidney cells; CC50, cytotoxicity concentration 50%; CHIKV, Chikungunya virus; CPE, cytopathic effect; EC50, half maximal effective concentration; ECSA, East/Central/South African strain; GFP, green fluorescent protein; Huh, Human hepatocarcinoma cells; IFT, immunofluorescence test/staining; Inf, infection assay; MOI, multiplicity of infection; MTT/MTS, 3-(4,5-dimethylthiazol 2-yl)-2,5-diphenyltetrazolium bromide (salt) assay; n.d., not determined; n.s., not stated; RT-PCR, reverse transcriptase polymerase chain reaction; SI, selectivity index (= CC50/EC50); Tox, toxicity assay; Vero, African green monkey kidney cells.

Epigallocatechin Gallate (Green Tea Component)

Epigallocatechin gallate (EGCG) is an active polyphenolic catechin and the essential element of green tea (*Camellia sinensis*) extract. Various independent research groups discovered the antiviral properties of EGCG against a number of viruses and recent studies revealed that EGCG also inhibits CHIKV replication *in vitro*. Weber et al. (48) demonstrated that EGCG inhibits CHIKV replication in HEK 293T cells by blocking the entry of CHIKV pseudo-particles that carried the CHIKV envelope proteins.

Thus, EGCG prevented the attachment of CHIKV to the target cells.

More recently, Lu et al. (49) showed the benefits of synergism in the combination treatment of CHIKV infected U2OS cells (human bone osteosarcoma cells) with EGCG and suramin. Lu tested EGCG combined with suramin against the CHIKV strain S27 and two clinical isolates. Besides the synergistic effect of the two compounds, Lu could confirm that the EGCG inhibits virus entry, replication, progeny yield as well as CPE of CHIKV *in vitro*.

Suramin

Suramin, also known as germanin or Bayer-205, is a symmetrical hexasulfonated naphthylurea compound that has been market-authorized by the U.S. Food and Drug Administration (FDA) for the treatment of trypanosomiasis (trypanosome-caused river blindness, onchocerciasis). The drug acts as a competitive inhibitor of sulphated glycosaminoglycans (GAGs) and heparin. As a number of viruses attach to cells via GAGs, suramin may consequently have anti-viral activity by inhibiting virus entry. The drug proved effective against a number of viruses, including DENV and Venezuelan equine encephalitis virus (VEEV) (50, 51). Against CHIKV, suramin proved effective in various *in vitro* studies (18, 52, 53). Suramin diminished CPE, virus replication and yield in a dose-dependent manner. Ho et al. (18) demonstrated that suramin was broadly effective *in vitro* against various CHIKV strains (**Table 1**). Ho used BHK-21, U2OS and MRC-5 cells. His group was the first to prove that the compound inhibits entry and transmission of CHIKV through binding onto E1/E2 glycoproteins. Furthermore, they showed that CHIKV infection was hampered in early stages. Virus binding and fusion was disrupted by the binding of suramin with viral glycoproteins. The compound also interfered with virus release. According to their research the EC_{50} of suramin for the inhibition of CHIKV *in vitro* (EC_{50} of 8.8–62.1 μM) is well within the range of non-toxic serum concentrations in humans (70 μM) when treated for river blindness (54).

Henß et al. (53) were also able to verify that suramin blocks CHIKV at early stages of the infection. Furthermore, her group tested the compound successfully against Ebola virus. All her tests were done *in vitro* (HEK 293T, MCF7, and Huh-7 cells). According to Henß however, the drug's side effects on the patient (nausea, vomiting, reversible urticarial rash, kidney damage, and exfoliative dermatitis; furthermore, suramin is connected to hepatic and bone marrow toxicity) might make suramin inappropriate for the treatment of CHIKV infections, a rather mild disease compared to Ebola. To avoid these side effects, Hwu et al. (19) chemically modified suramin and used 20 new conjugated compounds in a CPE screening assay against CHIKV. He identified six compounds with promising activity against CHIKV.

Inhibitors of Viral Genome Replication and Translation
RNA Interference (RNAi) Targeting CHIKV Genes

Small interfering RNA (siRNA) is able to regulate gene expression by the cleavage of the corresponding messenger RNA (mRNA) (55). The most commonly understood effect of this mechanism is the inhibition of the protein synthesis of certain genes because the mRNA is no longer available. This is referred to as "gene silencing." The discovery that siRNA is able to inhibit specific genes has led to a vast interest in this particular field. SiRNA was hoped to be used as a potential therapy for the treatment of genetic disorders, cancer, viruses, and other diseases. Bitko and Barik (56) showed that RNA interference (RNAi) was able to inhibit a negative-strand RNA virus.

Since RNAi is an endogenous biological process, potentially every gene can be supressed. In addition to that, siRNAs are easier to identify, synthesize and produce on a large scale than

traditional drugs (57). Multiple studies have been conducted to test the possible efficacy of siRNA against viruses *in vitro* and *in vivo* (mice, guinea pigs, macaques and humans) (58). There are two approaches for recruiting RNA interference as antivirals: (1) targeting specific viral sequences; (2) targeting the host cell.

(1) Targeting specific viral sequences with synthetic siRNA:

SiRNA can be created in the laboratory and preferably targets conserved regions. Theoretically any specific viral gene can be disabled. This is an advantage over classical small drug molecules that have to be fitted to a target protein which usually is only present at certain sites in the cell (59).

Dash et al. (60) designed and evaluated siRNA sequences targeting CHIKV nsP3 and E1 genes in Vero cells. They could demonstrate that these siRNAs curbed CHIKV titres by 99.6% in siRNA transfected cells 24 h after infection. However, this reduction could not be sustained at 72h, possibly because of the intracellular degradation of the siRNA. In 2013, Parashar et al. conducted *in vitro* studies in Vero-E6 cells, where he used siRNAs targeting nsP1 and/or E2 mRNA. He succeeded in downregulation of CHIKV replication for more than 90%. *In vivo* studies in CHIKV-infected Swiss albino and C57 BL/6 mice showed a complete inhibition of CHIKV replication when these siRNAs were administered 72 h post-infection (61). Lam et al. (62) could also demonstrate that CHIKV infection could effectively be supressed in the mouse model when pre-treating the animals with (small hairpin) shRNA (a precursor form of siRNA) against CHIKV E1 and nsP1 (62).

More recently, due to its advantages over siRNA and shRNA as far as stability, effectiveness, and toxicity are concerned, the artificial miRNA (amiRNA) based approach is in the focus of research. Bhomia et al. (63) showed the effectiveness of amiRNA for inhibition of Venezuelan equine encephalitis virus (VEEV). Saha et al. (64) successfully tested vector-delivered amiRNA against CHIKV infected Vero cells and efficiently inhibited CHIKV replication. One problem arising from this approach is the development of resistant mutants. A possible solution might be a combination therapy with a cocktail of various siRNAs.

(2) Targeting the host cell with siRNA:

It is also possible to target mRNAs for cellular accessory or entry proteins so that they can no longer be used by the virus during infection. Researchers tried to use the mutationally more stable host proteins as targets instead of the rapidly mutating viral proteins (58).

Rathore et al. were able to show in 2014 that by silencing the heat shock protein 90 (Hsp90) transcripts with siRNA, CHIKV replication is interrupted in cultured cells. Heat shock protein 90 (Hsp90) is known to play a key role in the replication of CHIKV and other viruses and is a highly abundant molecular chaperone (65). Rathore found out that Hsp90 interacts with the nsP3 and nsP4 proteins of CHIKV to promote virus replication (66). For further "Host-targeting Antivirals" (see section Antivirals Against Chikungunya Virus).

Both siRNA approaches (viral or host target approach) share the same issues in bioavailability, delivery, and specificity. siRNA is not very stable. It is rapidly degraded in the cell/organism. Furthermore, when systemically applied, siRNA has to reach the target cells. Effective pharmacological use of siRNA requires

"carriers" that deliver the siRNA to its intended site of action. siRNA displays poor cellular uptake and is not able to pass through the blood-brain-barrier (67). Small hairpin RNAs (shRNAs) present a solution to some of these flaws. shRNAs are ~70 nt long precursor siRNAs that are introduced into the cell by viral or bacterial vectors (e.g., plasmids). After expression in the nucleus, the shRNA is being transported to the cytoplasm where it is further processed by Dicer proteins. It is subsequently loaded into the RISC for specific gene silencing activity in the same manner as synthetic siRNAs (68).

siRNA often turns out to be unspecific. The suppression of other genes (the so-called "off target effects") may lead to unknown consequences due to dangerous mutations and unwanted gene expression (69). SiRNA may also interfere with the host immune response (70). Consequently, the long-term safety of si/shRNA treatment is yet unclear as there are only few *in vivo* RNAi long-term studies (58).

Inhibitors of CHIKV nsP1

The non-structural protein 1 (nsP1) is a palmitoylated protein with methyltransferase (MTase) and guanylyl transferase (GTase) activity. The protein consists of 535 amino acid residues and is responsible for the capping and the methylation of the newly synthesized viral and genomic RNAs (39). The added cap structure on the viral mRNA ensures the translation of the RNA and prevents its degradation from cellular 5'-endonucleases. On its N-terminal domain, the nsP1 has a α-helical amphipathic loop as well as a palmitoylation, which both act as anchors to attach the nsP1 and the nsP1-containing polyproteins/replication complex (RC) to the host's cellular membrane (71). Various studies could show that the palmitoylation of nsP1 is an important feature for the replication of some alphaviruses (72, 73). Depalmoylated Semliki Forest virus (SFV) mutants displayed a diminished pathogenesis in mice (72). Likewise, Zhang and colleagues (74) demonstrated *in vitro* that by inhibiting the enzyme responsible for the palmitoylation of proteins during CHIKV infection, CHIKV replication could be suppressed. There is evidence suggesting that nsP1 has additional functions during alphavirus infections like the development of cell filopodia and the rearrangement of actin filaments (73). Especially the MTase and GTase-like activities of nsP1 present a viable target for antiviral compounds since both enzymatic properties are essential for virus replication. The GT activity of nsP1 is dependent on successful MTase activity (75). Interestingly, unlike cellular MTase and GTase enzymes, the nsP1 does not contain canonical signature motifs and the mechanism of the enzymatic action differs from the cellular cap formation. Thus, there is the possibility of identifying molecules that selectively inhibit viral nsP1 without affecting the host cell capping enzymes' activity (76). Compared to the other nsPs, the research on antivirals that target nsP1 has been poor. Lampio et al. tested 50 guanosine/cap analogs for their activity of inhibiting SFV nsP1 20 years ago (77). Recently, Bullard-Feibelman developed an assay to screen and identify possible CHIKV nsP1 inhibitors (78). Two years later, the same research group presented their results on a high throughput screening (HTS) of 3,051 compounds and their successful identification of promising hit compounds like

the naturally derived compound "lobaric acid" (**Table 1**) (20). Gigante et al. found a strong inhibitor of CHIKV replication among a new family of compounds named [1,2,3]triazolo[4,5-d]pyrimidin-7(6H)-ones (**Table 1**) (21). It was not until 2016 when reverse genetics carried out by Delang et al. could identify the CHIKV nsP1 as the target for this potent compound (79). New derivatives of these compounds also inhibited the GTase activity of CHIKV and VEEV nsP1 (14). A report from Jones et al. (80) postulated that nsP1 was an antagonist of tetherin (an antiviral host factor that helps to retain the viruses at the surface of the infected cells). These findings gave rise to hope that nsP1 could be considered as a target for developing tetherin-mediated therapeutics against CHIKV (80). However, a more recent study on the subject could not confirm Jones' report since no evidence for tetherin-antagonists in alphaviruses was found (81).

Inhibitors of CHIKV nsP2

The CHIKV nsP2 has multiple enzymatic activities and thus plays a central role in CHIKV replication. nsP2 has auto-protease activity at its C-terminal end for cleaving the non-structural viral polyprotein (nsP1234) into the individual nsPs. There is a methyltransferase-like region of unknown function. The N-terminal half has terminal helicase, nucleoside triphosphatase (NTPase), and RNA triphosphatase activities (82). The triphosphatases are involved in RNA capping and also fuel the RNA helicase domain with energy. Additionally, CHIKV nsP2 is a virulence factor as it is able to stop the host cells mRNA transcription and translation, thus tampering with the hosts immune response. This is referred to as "transcriptional shut-off" (83). In fact, a recent study was able to show that nsP2 (as well as nsP3) exhibit RNA interference (RNAi) suppressor activity (84). Viral suppressors of the RNAi pathway (VSR) have been found encoded in various viruses (including flaviviruses) before. Yet, the report of Mathur et al. was the first to show VSR in alphaviruses. Moreover, Fros and colleagues found out that CHIKV nsP2 suppresses the type I/II interferon-stimulated JAK/STAT signaling pathway, which consequently inhibits the hosts antiviral response and defense mechanisms (82). It has previously been shown in other viruses that especially the protease function poses an interesting target for antiviral drugs (85).

Compounds designed in silico. Marcella Bassetto and colleagues applied a structure-based virtual screening strategy to find possible CHIKV nsP2 inhibitors. The molecules in question have been modeled to potentially fit and thus block the nsP2 protease binding site.

Based on this model, Bassetto performed a virtual screening of ~5 million compounds and investigated the structure-activity relationship of the identified hits. After a final visual inspection, 15 derivates were selected to be potential CHIKV nsP2 inhibitors. As only 9 were commercially available, those were evaluated in a virus-cell-based CPE reduction assay. Compound 1 performed best and was predicted to fit the central portion of the nsP2 protease active site (**Table 1**). The compounds' ability to act as a selective CHIKV replication inhibitor was then further

investigated by performing a virus yield assay on Vero cells. The assay confirmed the findings of the CPE reduction assay.

Furthermore, Bassetto created structural analogs of Compound 1 and tried to chemically optimize the properties of the compounds. She designed and synthesized two new derivates with one showing a slightly better antiviral activity profile than compound 1. With her work Bassetto proved that a combination of molecular modeling with different *in silico* techniques and classical medical chemistry methods can lead to the discovery of novel and selective antiviral compounds.

Jadav et al. (86) tested a series of derivates of 1,3-thiazolidin-4-ones for their antiviral activity in a CPE reduction assay on Vero cells. Five compounds showed promising CHIKV inhibition properties. The authors assumed the mode of action may be that of protease inhibition, after they carried out molecular docking simulation with the available X-ray crystal structure of the CHIKV nsP2 protease (86). Here, the computer-aided binding model was used to explain possible mechanism of action, while Bassetto used the docking simulation to model compounds accordingly. Still, neither of these studies actually tested the ability of the predicted compounds to inhibit the protease activity of CHIKV nsP2.

It was the group of Das that actually designed and tested 12 compounds specifically on their ability to block the nsP2 (22). The researchers managed to create a test to validate whether the compounds actually inhibit nsP2. Das designed the compounds specifically to fit the nsP2 active site, using the same method as Bassetto and employing Compound 1 of Bassetto as a template for his products.

The group then systematically analyzed the ability of the compounds to inhibit the protease activity of the purified enzyme in cell-free assays. Two different cell free assays were employed, one being an end-point assay, the second one being continuous. In the end point assay, Das used full-length recombinant CHIKV nsP2 as the protease and a recombinant protein substrate containing the nsP2 cleavage site that was located between enhanced green fluorescent protein (EGFP) and thioredoxin. If the nsP2 was fully functional, the protein substrate was being processed, making it possible to detect the products by separating them by SDS-PAGE and visualizing the results with a Coomassie blue staining. The method on how to express and purify the recombinant proteins has been described earlier by the same group (87).

To verify his finding, Das additionally used a fluorescence resonance energy transfer (FRET)-based assay to compare the efficiencies of different inhibitors. This kind of assay had originally been described for the HIV protease by Matayoshi et al. (88). It is a continuous assay that makes it possible to collect information on the initial period of the reaction. In Das' assay, the nsP2 protease processed a peptide substrate with the nsP3/nsP4 cleavage site of CHIKV P1234 polyprotein (89). The substrate had a quencher at the N terminus and a fluorescent molecule at the C terminus. Cleavage of the substrate by nsP2 protease results in fluorescence that can be detected at an emission wavelength of 490 nm.

With these assays, Das managed to show that the majority of his compounds inhibited the nsP2s ability to process

recombinant protein and synthetic peptide substrates. He also discovered that the original template molecule from Bassetto performed very poorly as a specific nsP2 inhibitor in these cell free assays, despite the fact that it had an EC_{50} of ∼5 µM in cell-based assays against CHIKV (12). Das then tested his compounds successfully in cell-based assays against CHIKV. The fact that some compounds did not inhibit the CHIKV nsP2 protease function in the cell free assays and yet managed to curb CHIKV infection in cell-based assays suggests that the antiviral activity of these compounds may be at least in part due to other mechanisms than the inhibition of protease activity of nsP2 (**Table 1**) (22).

Compounds inhibiting the nsP2 mediated "transcriptional shut-off". Lucas-Hourani et al. (23) developed a phenotypic cell-based functional assay to detect CHIKV nsP2 protease inhibitors. In particular, compounds that inhibited the nsP2 mediated "transcriptional shut-off" mechanism were to be detected. As mentioned before, the nsP2 protease is able to bind to cellular transcription factors and thus induce downregulation of the cell's immune response. In Lucas-Houranis' assay luciferase expression is induced when the cellular functions are working at a normal level. If nsP2 protease is blocked by antivirals, the cells mRNA transcription is properly restored and thus a replication of luciferase takes place, resulting in an increased signal.

The assay is thus based on a recombinant human cell line (HEK-293T) that expresses CHIKV nsP2 together with various reporter gene constructs (on three plasmids). Lucas-Hourani used this transfected cell line to establish an assay suitable for screening compounds for their nsP2 inhibition activity. From a pool of 3,040 molecules, he detected one with no toxicity that particularly blocked nsP2 activity *in vitro* (**Table 1**) (23).

Inhibitors of CHIKV nsP4 and Viral Genome Replication

The nsP4 is the sole protein with a polymerase function and is responsible for the RNA synthesis of the (replication complexes) RCs. The ∼100 residues at the N-terminal region are specific to alphaviruses. The nsP4 has ∼70 kDa and contains the core RNA-dependent RNA polymerase (RdRp) domain at its C-terminal end. The structure of the RdRp is typical and encompasses fingers, palm containing the GDD motif at the active site and thumb domains (90). The RdRp is able to copy the genome into a complementary minus-strand which is in turn copied into genomic and subgenomic RNAs by the polymerase with the help of the other viral nsPs in the RC. Mutation studies revealed a TATase (tyrosine aminotransferase) activity in the RdRp domain. Thus, the nsP4 may be generating the poly(A) tail at the 3'terminal of the genome (91). For more details on the nsP4s role during genome replication and its fundamental function I refer to the review of Pietila et al. (9).

Research has recently focussed on finding antiviral compounds against viruses of the *Flaviviridae* family [hepatitis C virus (HCV), Zika, Dengue, Yellow Fever virus (YFV), tick borne encephalitis virus (TBEV)], most of which are arboviruses. Especially Zika and Dengue can cause coinfections with CHIKV and the initial symptoms of the three diseases look very similar. Since the diagnosis is costly and time consuming, it is crucial to find a pan-antiviral that works against all of them. All three

viruses are +ssRNA viruses and there is a reasonable chance that they share conserved motifs in the orthologous RdRp enzyme (24, 91). The remarkable homology of the nsP4 among the alphaviruses makes it possible that antivirals blocking the nsP4 may exhibit their activity over a broad spectrum of viruses. With human cells lacking this specific polymerase the chances of adverse side effects of RdRp inhibitors are minimized (92).

Nucleoside analogs and proTides. Nucleoside analogs (NAs) are synthetic, chemically modified nucleosides consisting of a sugar and a nucleic acid analog. Nucleotide analogs additionally have one to three phosphate groups attached to the 5′-site. In the cell, they are processed the same way as the natural (endogenous) nucleosides. After their uptake into the cell and their metabolization, the NAs can act on cellular functions. They mimic their physiological counterparts and block cellular division or viral replication by impairing DNA/RNA synthesis (they usually cause termination of the nascent DNA/RNA chain) or by inhibition of cellular or viral enzymes involved in the nucleoside/tide metabolism (93, 94). The FDA has approved more than 25 nucleoside analog drugs used for the therapy of viral infections such as HIV/AIDS (tenofovir), hepatitis B (lamivudine/entecavir), and C (sofosbuvir) or herpes (acyclovir) (93, 95). Besides being antiviral agents, NA drugs are also applied in the therapy of cancer, rheumatologic diseases and even bacterial infections (96).

Before NAs can actually work as antivirals, they have to be phosphorylated in the host organism. Three consecutive phosphorylation reactions are necessary to activate the prodrug. The first reaction to the 5′-monophosphate is usually a rate-limiting step, which also means that if this first phosphorylation does not take place, the drugs remains inactive (97). This might happen either because the virus does not induce a specific kinase or has acquired a mutation in this particular enzyme resulting in resistance to the compound because the host cell is not able to phosphorylate the NA.

Monophosphate NAs have come into focus in order to avoid this problem and improve the therapeutic properties. However, these phosphate analogs (possessing a CO–P bond) proved to be prone to esterase and phosphatase hydrolysis. As an alternative, chemists investigated replacing the phosphate group by an isosteric and isoelectronic phosphonate moiety (CH2-P bond). This led to the discovery of nucleoside phosphonate analogs (NPs), which are chemically and enzymatically more stable than the phosphate analogs (98).

Toxicity and side effects of nucleoside/-tide analog drugs often result from their off-target use by host polymerases and their incorporation into RNA or DNA. The observed toxicities tend to be highly unpredictable and even closely related analogs may prove toxic for different organs (95). Various mechanisms for NAs toxicity have been discovered, the most characteristic is due to their affinity to host mitochondrial gamma polymerase (99). The NAs enter the mitochondria and are either incorporated into the mitochondrial DNA or block its synthesis.

Since NAs, nucleoside 5′-monophosphates or 5′-phosphonates are charged molecules and penetrate the cell membrane very poorly, they are not suited for oral administration. Research tried to improve the pharmacological properties and bioavailability of this class of compounds. This led to the discovery of the ProTides approach by McGuigan in 1998 (100, 101). The researchers designed a novel prodrug in which the phosphate was chemically protected or masked. This group of prodrugs became known as "ProTides" (pronucleotide) and as a result from the masked phosphate, this construct is able to pass the cell membrane via facilitated passive diffusion (94).

In the cell, the ProTide is enzymatically cleaved, thus releasing the masking groups from the nucleoside monophosphate/phosphonate which can be further transformed into the active 5′-triphosphate form of the NA. Various natural and unnatural amino acids can serve as the masking amino acid motif. All ProTide drugs that have reached the clinic, feature l-alanine (94). With the prodrug strategy, medical chemists were able to solve the main pharmacological problems associated with NAs, namely poor cellular uptake and poor metabolism into their phosphorylated forms.

Ribavirin. Ever since its discovery in 1972, ribavirin (1-β-D-ribofuranosyl-1,2,4-triazole-3-carboxamide, also known as Virazole), a synthetic guanosine nucleoside analog, has been used as a compound against various viruses (102).

Ribavirin (RBV) is one of few FDA approved antiviral drugs in clinical use that is effective against respiratory syncytial virus in infants and chronic hepatitis C virus infections in combination with pegylated interferon (IFN)-α (103, 104). Apart from the FDA approved indications, RBV has shown efficacy against a variety of virus infections including haemorrhagic fever and measles (105, 106). Huggins and colleagues could also prove RBV's effectiveness against viruses of the alphavirus family *in vitro* (107). Multiple studies confirmed his findings by testing RBV *in vitro* against CHIKV either as a monotherapy (25) or in combination with doxycycline (26) or IFN-α (27, 28). Especially, Franco et al. (25) demonstrate that the effectiveness of antiviral agents against CHIKV differs considerably between host cell lines (**Table 2**).

Various different mechanisms of action have been attributed to RBV which might explain its broad-spectrum antiviral activity. The major mechanism, by which the replication of RNA viruses is being inhibited, is curbing the cellular guanosine triphosphate (GTP) pools by blocking the inosine monophosphate dehydrogenase (IMPDH) (108). Another indirect mechanism is the immunomodulation of the host's adaptive immune response: RBV triggers a suppression of the T-helper type 2 response and an induction of the T-helper type 1 response (109). The type 1 response is responsible for an increased clearance of infected cells. Additionally, RBV is believed to directly inhibit RNA capping. Other findings suggested that RBV interferes with the guanylyl transferase and/or methyltransferase activity of the nsP1, leading to a production of mRNAs that are not fit for translation (110). RBV is said to directly inhibit the viral polymerases, thus hampering the virus' genome replication (111). This has also been proposed by other studies that suggested RBV to directly inhibits nsP4 RdRp by interacting with its Cys483 residue, resulting in a decrease in replication fidelity (112). This would

confirm the theory that RBV leads to error catastrophe via increased mutation frequency (nucleotide transitions) because of the incorporation of ribavirin triphosphate (RTP) into the newly synthesized viral genomes (113). Others found indications that RBV promotes IFN signaling by modulating specific genes and thus potentiating IFN action (114).

RBV, albeit a success as a broad-spectrum antiviral *in vitro*, has rarely been reported to be the subject of *in vivo* trials against CHIKV in humans. Ravichandran and Manian (115) treated 10 patients with confirmed CHIKV infection. Before treatment the infection had not been resolved after 2 weeks and resulted in crippling lower limb pains and arthritis. The patients were treated with 200 mg RBV twice daily for 7 days. A control group of 10 similar patients was only given analgesics when required. According to Ravichandran and Manian the patients of the RBV group showed a significant improvement in the joint pains and 8 patients out of 10 had a reduction in tissue swelling. Ravichandran concluded that RBV may indeed have a direct antiviral property against CHIKV infection and might lead to a faster recovery of the patients. However, the study had some flaws: (1) only a small number of patients were considered; (2) the study was not a randomized controlled study (a so-called double-blind study) where the RBV group was compared with a group receiving placebo; (3) the drug was administered in the subacute phase of the disease, thus some of the improvement could be attributed to a normal course of healing. A recent *in vitro* study of Mishra et al. (116) suggested that RBV is only effective in the earlier stages of the CHIKV lifecycle; the benefit of giving the drug in a subacute or chronic phase might therefore be questioned.

The doses at which RBV would have to be administered in order to reach its full potential as an antiviral *in vivo* are associated with severe side effects such as haemolytic anemia, pulmonary, dermatologic, and teratogenic effects and can thus only be justified if the infection is life-threatening (117).

RBV's success as an antiviral is probably attributed to its ability to act simultaneously via multiple mechanisms. Usually, when an antiviral interacts at various cellular and viral processes, the chances for drug resistant mutants are diminished. But, in case of RBV, various resistant viruses have been reported, such as Sindbis virus, Hepatitis C Virus and CHIKV, showing yet again, how quickly viruses are able to adapt (52, 110, 118). Taking these developments into account, RBV might still be interesting as a component in an antiviral "cocktail" consisting of multiple drugs with various modes of action, where the dosages of the drugs themselves could be reduced due to synergism and the risk of adverse effects could thus be minimized.

β-d-N4-hydroxycytidine (NHC). A report from Ehteshami et al. (30) stated the outcome of experiments dealing with β-d-N4-hydroxycytidine (NHC), another modified NA. NHC was identified to successfully inhibit CHIKV replication in different replicon cell lines as well as in infectious models *in vitro* (**Table 1**). One year later, another group published that NHC was able to curb the release of genome RNA-containing VEE virions and their infectivity in *in vitro* test with Vero cells (119). This discovery supports the idea that the polymerase activity of the

nsP4 is quite conserved and that drugs targeting this particular activity might show efficacy against various alphaviruses. The antiviral activities of NHC are probably due to the compound acting as a pyrimidine analog that may directly target the viral polymerase and cause chain-termination. Alternatively, the compound might induce accumulation of mutations in virus-specific RNAs which are either lethal or lead to viral genomes that are incapable of replication (30). Urakova suspects a dual effect of NHC on VEEV by causing a modest decrease *in virion* release and a strong decrease *in virion* infectivity. This idea supports the theory that mutations caused during the replication process lead to "error catastrophe" or "lethal defection" (119, 120).

Urakova reported that NHC only triggered the development of a low-level resistance in VEEV against NHC, which makes it a very promising compound that might substitute RBV. These findings are very encouraging. Nevertheless, further studies with more relevant human cell lines, animal models as well as other viruses are needed to confirm whether this compound has a future as a broad-spectrum antiviral.

Favipiravir (T-705) and its defluorinated analog (T-1105). Favipiravir (T-705, 6-fluoro-3-hydroxy-2-pyrazinecarboxamide) is an approved drug in Japan for the treatment of influenza virus infections (121, 122). The drug is a purine analog and functions as a broad-spectrum antiviral agent which has also been reported to inhibit (*in vitro* and *in vivo*) the replication of a number of RNA viruses such as arenaviruses, bunyaviruses (123) and alphaviruses (124–126). During the 2014/2015 Ebola epidemic in western Africa, T-705 proved beneficial for infected patients (127).

Favipiravir is a prodrug, which is phosphoribosylated in the cell into its active form, a ribofuranosyl 5′-triphosphate metabolite (favipiravir-RTP). It acts as a pseudo purine and inhibits the viral replication of influenza. Two modes of action have been suggested: There is evidence that favirpiravir-RTP specifically blocks the influenza virus RNA-dependent RNA polymerase (RdRp) by binding at certain domains of the enzyme (122). Others suggested that favipiravir-RTP is incorporated into the nascent viral RNA, thus leading to lethal mutagenesis or preventing further extension of the RNA strand entirely by chain termination (128, 129).

As favipiravir is relatively novel, the information on its *in vitro* efficacy is limited. Values vary depending on the assay, cell line and virus strain used (**Tables 1, 2**). Apart from favipiravir itself, the defluorinated analog T-1105 has worked as an antiviral drug against CHIKV in *in vivo* experiments with mice (31). The drug prevented mice from developing severe neurological disease and reduced the mortality rate of the CHIKV infected animals. A dosage of 300 mg/kg T-705 daily and orally proved especially beneficial for CHIKV infected mice during the acute phase of the disease (125). Delang also identified T-705 resistant CHIKV variants *in vitro*. The mutant had acquired a mutation in the motif F1 of the RdRp, which seems to be important in the nucleoside triphosphate binding during and in the initiation of the viral RNA synthesis of +ssRNA viruses (130). Yet, Abdelnabi et al. (126) suggest that favipiravir has a high barrier of resistance. Abdelnabi made experiments in which he tried to create T-705-resistant coxsackievirus B3 (CVB3) (another +ssRNA virus), by

point-mutating the same F1 motif. These efforts resulted in either low-fidelity RdRp or unviable virus. Since NTP binding is a major fidelity checkpoint, point mutations in this F1 motif could destroy the activity of the polymerase or reduce catalysis (131).

The fact that resistant mutants develop, demonstrates how quickly RNA viruses can adapt to selective pressure via mutations. Understanding the role of conserved motifs like F1 is of great importance in order to understand the mode of action of certain drugs and possibly design more potent compounds.

Sofosbuvir. Sofosbuvir (β-D-2′-deoxy-2′-α-fluoro-2′-β-C-methyluridine, formerly known as PS-7977 or GS-7977) is a RdRp inhibitor approved by the FDA for the treatment of HCV infections (132). The drug is a nucleotide analog that is orally available and functions as a prodrug. In hepatocytes, sofosbuvir is metabolized to 2′-F-2′-C-methyluridine monophosphate (UMP) and further phosphorylated into its active triphosphate form (UTP). During the viral genome synthesis, UTP functions as a chain terminator, thus inhibiting HCV replication and production at the site of infection, in this case the liver (133). Sofosbuvir has recently been reported to inhibit YFV and ZIKV replication *in vitro* and *in vivo* (134–136).

Sofosbuvir has been tested against CHIKV *in vitro* (Huh-7 cells and astrocytes) and *in vivo* (mice) (24). The drug inhibited CHIKV replication and was three times more potent in inhibiting CHIKV in human hepatoma cells than RBV (**Table 2**). In human induced pluripotent stem cell-derived astrocytes, sofosbuvir did impair virus production and cell death in a MOI-dependent manner, yet not to such a degree as in the Huh-7 cells. This may be due to the fact that hepatocytes have the most effective system of turning the prodrug sofosbuvir into its active form (UTP), whereas astrocytes show less metabolic activity in this respect and thus have less of the active UTP form of the drug available (133). Furthermore, sofosbuvir prevented CHIKV-induced arthralgia-related paw oedema in adult mice as well as mortality in neonate mice (24). Since CHIKF can lead to chronic arthralgia, further studies are needed to evaluate if sofosbuvir in a combination therapy alongside anti-inflammatory drugs is beneficial to patients suffering from chronic CHIKV associated arthritis.

Interestingly, humans tolerate the drug better than mice. A 400 mg daily dose over a period of 12–24 weeks is the standard therapy for HCV patients (133), while doses of >33 mg/kg/day in a 7 day regime proved to be toxic to mice (136). The reason for this observation might be the decreased stability of sofosbuvir in rodent serum. This raises the question of how significant rodent models are for the evaluation of sofosbuvir or whether other (animal) models might be more representative.

Similar to favipiravir, sofosbuvir resistant HCV strains have been reported (137). Yet, the development of sofosbuvir resistant mutants seems to be slower compared to HCV inhibitors targeting other proteins. Researchers hold the high degree of amino acid conservation within the RdRp domain as well as the lack of fitness in mutated viruses responsible for this phenomenon (136).

Nevertheless, the fact that sofosbuvir blocks the viral replication of CHIKV as well as several flaviviruses is strong evidence for the presence of conserved motifs among RNA polymerases from +ssRNA viruses. The recent advances in elucidating the nsP4 structure and core domain function of CHIKV highlight these observations and may confirm that the RdRp is a feasible target for pan-antiviral molecules (91).

Other Viral Genome Replication Inhibitors

Mycophenolic acid (MPA). Mycophenolic acid (MPA) had already been discovered in 1893 and was isolated in 1896 as an antibacterial molecule produced by *Penicillium brevicompactum* (138). MPA is licensed by the FDA as a drug for transplantation rejection (139). The drug inhibits cellular inosine monophosphate dehydrogenase (IMPDH) and thus decreases the intracellular pools of guanosine triphosphate (GTP) and 2′-deoxyguanosine triphosphate (dGTP). This causes a disruption of viral and cellular RNA, DNA, and protein synthesis (140). Two derivatives of MPA are available for clinical use: mycophenolate mofetil (MMF, CellCept) and mycophenolate sodium (MPS, Myfortic). Mycophenolate mofetil is the orally bioavailable prodrug form of MPA. MPA has shown antiviral activity against DENV and Orthopoxvirus (141, 142).

Although MPA was reported to inhibit CHIKV *in vitro* in 2011, tests done in 2018 could not confirm these findings (143, 144). However, Ferreira tested MPA as a control alongside his compounds and indeed received good EC_{50} values, with MPA even performing slightly better than sofosbuvir and with a much better selectivity index ($SI = CC_{50}/IC_{50}$) than RBV (24). Likewise, other research groups used MPA as a reference against CHIKV and evaluated the efficacy against CHIKV (**Table 2**) (16, 32).

There are various studies confirming the antiviral, antibacterial, antifungal, immunosuppressive, and anticancer properties of MPA or its derivates (145). Yet it is important to deliberate whether the benefits of MPA as an antiviral outweigh its adverse effects as an immunosuppressant.

NsP3 and Possible Inhibitors

The nsP3 consists of three domains. The N-terminus has a macrodomain, while the C-terminus holds a hypervariable domain (HVD). The central part of the protein contains a zinc-binding domain which is sometimes referred to as the alphavirus-unique domain (AUD), a region that shares a strong sequence homology across the alphaviruses. The role of the AUD is so far undefined but the domain seems to be important in RNA replication and in the synthesis of negative sense and sub-genomic RNA (146).

There are hints indicating that the nsP3 is involved in inhibiting the assembly of the host cells stress granules (SG) which are essential for the degradation of viral mRNA (147). NsP3 is usually found in complex with other nsPs during infection. It also interacts with host factors. Saul et al. (148) discovered that the amount of nsP4 increased in a recombinant SFV with a duplicated nsP3-encoding sequence. Saul concluded that nsP3 is involved in the stabilization of nsP4. He could furthermore back other studies' findings that nsP3 is important for the (neuro-) virulence of old-world alphaviruses (148). In New-World alphaviruses, neurovirulence is mainly determined by structural proteins, particularly E2 (149).

So far, the complete function of the nsP3 macrodomain has not been fully unraveled although its crystal structure has been known since 2009 (PDB id: 3GPG and 3GPO) (150). The N-terminal macrodomain is highly conserved among alphaviruses but also occurs in other positive-strand RNA viruses such as coronaviruses and hepatitis E virus (151). There is evidence that the viral macrodomains bind ADP-ribose, dephosphorylate ADP-ribose-1"-phosphate and act as de-ADP-ribosylating enzymes thus counteracting antiviral ADP-ribosylation (152). Other studies indicated that the most likely biochemical function of viral macrodomains is de-ADP-ribosylation. By enzymatically removing mono- and poly-ADP-ribose from proteins, macrodomains might oppose the host cells' antiviral response (153). Furthermore, the mono(ADP-ribosyl)hydrolase activity of the nsP3 is critical for CHIKV replication in vertebrate hosts and insect vectors, and determines virulence in mice (154). These findings suggest that the macrodomain plays an important part in the host-pathogen conflict.

Nguyen et al. virtually screened a database of 1,541 compounds for possible hits that might block the nsP3 macrodomain of CHIKV (155). The group combined molecular docking, virtual screening, and molecular dynamics simulations to identify potential inhibitors. They ended up with three ligands that might have potential as nsP3 inhibitors. However, these findings were achieved *in silico* and still need to be verified by experimental studies *in vivo*.

Until Varjak et al. discovered a degradation signal at its C-terminus, nsP3 was thought to be a rather stable protein. Varjak could demonstrate that the nsP3 of SFV and Sinbis Virus (SINV) was degraded rapidly when the protein was expressed individually. On the other hand, nsP3 was significantly stabilized when it was expressed in the nsP123 polyprotein form (156). The role of this C-terminal degradation signal is still unknown but there are various hints that it may contribute to granting the optimal stoichiometry of the nsPs.

Especially the HVD at the C-terminal region of the nsP3 seems to be a center for interactions with host cell proteins, including stress granule (SG) components which might help the virus adapt to distinct cellular environments. Data suggests that the HVD interacts with several host factors through a conserved proline (P)-rich and duplicate FGDF motif. The letters of the motif correspond to the according amino acids, two phenylalanine residues which are separated from each other by a glycine and an aspartate residue (157). These interactions are needed for the assembly of virus genome replication complexes (158, 159). The FGDF motif seems particularly important for the successful replication of alphaviruses in mammalian cells. Experiments with CHIKV revealed that the virus' nsP3 has two FGDF motifs that bind to certain domains of the SG components in mammalian cells (160). SGs usually block host and viral translation. The interactions between the CHIKV nsP3 and the SG domains impede the organization of the SGs and thus may allow virus replication (147, 161, 162). When the alphavirus nsP3 HVD is mutated in a way that both FGDF motifs are disrupted, CHIKV is inactivated and SFV as well as SINV are attenuated in mammalian cells. If only one FGDF motif is present in CHIKV

or SFV nsP3, the affinity for the SG domains is reduced and the virus is attenuated as well. This leads to the conclusion that alphaviruses need two FGDF motifs for a successful viral replication in mammalian cells (146, 160, 161).

The HVD seems also to be a determinant for virulence in some viruses. There is evidence that the conserved FGDF motifs in the HVD of chikungunya virus nsP3 are required for the effective transmission of the virus from *Aedes aegypti* mosquito saliva to a vertebrate host (163).

The nsP3 seems to be an important protein in determining vector specificity. ONNV, which is closely related to CHIKV, is the only alphavirus known to be transmitted by *Anopheline* mosquito species. CHIKV on the other hand, is mainly transmitted by *Aedes* mosquitoes. Experiments with chimeric CHIKV expressing ONNV nsP3 revealed that *Anopheles gambiae* mosquitoes become susceptible for CHIKV although being naturally immune to WT CHIKV (164). This observation is in line with previous findings suggesting that nsP3 might be involved in specific protein-protein interactions and thus carries out host cell-dependent functions (165). A recent study revealed that nsP3 suppresses RNAi alongside nsP2 in CHIKV infected insect cells (84). As RNAi is an antiviral defense mechanism in various organisms that leads to a degradation of viral RNA, the suppression of RNAi by viral proteins enhances infection.

The impact of these interactions on biological and biochemical processes of the host cell at early stages of the infection are still under heavy investigation. There is hope that the interacting regions might prove valuable targets for intervention and opens new possibilities for vaccine development and antiviral drug discovery.

Kaur et al. (29) reported the discovery of the anti-CHIKV properties of **harringtonine**, a cephalotoxin alkaloid from the *Cephalotaxus harrintonica* trees. It was suggested that the compound inhibits the early stages of CHIKV infection after cellular endocytosis (29). Harringtonine was proposed to interfere with the protein translation of CHIKV since it seemed to inhibit the production of nsP3, E2 proteins, and CHIKV RNA (29, 166). Harringtonine was approved in 2012 by the FDA as a drug for the treatment of chronic myeloid leukemia (167). **Homoharringtonine**, an analog of harringtonine with an additional methyl group, was reported to have anti-CHIKV properties as well. According to Kaur, both compounds display minimal cytotoxicity on BHK-21 cells and primary human skeletal myoblasts at the dosage needed for inhibiting CHIKV. However, the drug itself is labeled as a cytotoxic agent and according to the Globally Harmonized System (GHS) harringtonine is fatal if swallowed (H300), in contact with skin (H310) or if inhaled (330) (168). This may be the reason that although Kaur's original article has been cited repeatedly, no studies on the anti-alphavirus properties of harringtonine have been published in the past 7 years.

Host-Targeting Antivirals

Many viruses depend on host factors to ensure their replication or are inhibited by such. Host factors present a valuable target for drugs to interfere in the virus' life cycle either by inhibiting host factors on which the virus relies on or by promoting host

factors that curb virus infection. Since host factors also play vital roles in normal physiology, their inhibition or promotion can lead to abnormal physiological function and toxicity. The impact such interference may have on the host organism must thus be critically elucidated. Ideally therapeutics would target interactions between host and viral factors without disrupting essential cellular processes. For the interested reader we refer to the review of Wong and Chu (169) that summarizes the current knowledge on the interplay of viral and host factors in CHIKV infection as well as potential targets for antivirals.

Viperin, Hsp90 Inhibitors, and Interferons
Viperin
Viperin (virus inhibitory protein, endoplasmic reticulum-associated, interferon-inducible) is an interferon (IFN)-induced host cell protein that has come into focus because it is responsible for inhibiting viral replication via multiple pathways. It thus represents an interesting target for antiviral drugs (170). Viperin has been reported to inhibit a broad spectrum of DNA and RNA viruses, including members of the herpesvirus, flavivirus, alphavirus, orthomyxovirus, paramyxovirus, rhabdovirus, and retrovirus family (170). CHIKV infection is also curbed via IFN-induction of viperin and compounds leading to the up-regulation of viperin may present a strategy to manage CHIKV infections. Studies could demonstrate that CHIKV infection is controlled via type I IFNs that induce the interferon-stimulated gene (ISG) RSAD2 (radical SAM domain-containing 2) which encodes viperin (171). Teng et al. showed that mice lacking RSAD2/viperin had a higher rate of CHIKV replication and more severe inflammatory symptoms in the joints. A recent study tried to elucidate the role of viperin in shaping the pathogenic CHIKV-specific CD4 T-cell adaptive immune response during late acute disease phase (172). The group used viperin deficient mice in which CD4 T-cell had been depleted. They could demonstrate that increased late acute joint inflammation was exclusively mediated by CD4 T cells and that Th1-IFNγ-producing T cells played a pivotal role in the joint pathology. Further experiments showed that viperin expression contributes to reducing disease severity in both haematopoietic and non-haematopoietic cells (172).

Hsp90 Inhibitors
Chaperones help in the folding, assembly and maturation of host- and viral proteins. Almost all viruses depend on the chaperone Hsp90 (heat shock protein 90) especially during replication to ensure their life cycle (173). This causes viruses to be hypersensitive to Hsp90 inhibition and provides a way to curb virus replication. Compounds interfering in Hsp90 function have a potential as broad-spectrum antiviral drugs, especially since experiments with picornaviruses demonstrated that Hsp90 inhibitors are refractory to the development of drug resistance (174). As mentioned before, Hsp90 also plays an important role during CHIKV replication due to its interaction with the nsP3 and nsP4 of CHIKV. The chaperone furthermore stabilizes CHIKV nsP2 and thus promotes virus replication (65). Studies demonstrated that the Hsp90 inhibitor **geldanamycin** (GA) reduce CHIKV replication, particle formation and infection

in vitro (65, 66). Yet, inhibiting Hsp90 very often results in toxicity, especially for the liver, presumably because Hsp90 is very abundant in liver cells and interacts with multiple proteins at crucial points in the cellular function. A lot of clinical trials with anti-Hsp90 drugs have been abandoned due to the *in vivo* toxicity (175). This also holds true for GA which is hepatotoxic as well as structurally instable, and thus has so far not been approved for clinical usage (176). Research is currently focussing on developing Hsp90 inhibitors with better pharmacological profile, such as **ganetespib**, which is relatively hydrophobic and less toxic (177). Ganetespib is currently under investigation in phase 1-3 clinical trials for the treatment of breast cancer, small cell lung cancer, acute myeloid leukemia, and myelodysplastic syndrome. However, its potential as an antiviral is not known but might be worth investigating once the drug is approved by the FDA.

Lillsunde et al. (178) investigated the antiviral activity of a number of **marine alkaloid-oroidin analogs** that are synthetic compounds and target the Hsp90. Lillsunde tested the compounds in replicon models against HCV and CHIKV. While 4 compounds selectively inhibited the HCV replicon, the compounds exhibited only moderate selectivity and efficacy against the CHIKV replicon in dose-response and cytotoxicity studies.

Interferons
Interferons (IFNs) play a vital role in the innate immune response to counter virus infections and thus have been the subjects of multiple studies. IFNs have been tested widely for their potential use as antivirals against a variety of viruses including HIV, Hepatitis C and B, and Influenza A (179). Type I IFNs [alpha/beta interferon (IFN-α/β)] are produced by the host cell upon sensing virus invasion. IFNs upregulate a variety of interferon-stimulated genes (ISGs). The protein products of the ISGs contribute to countering viral infections by suppressing viral spread and supporting the initiation of adaptive immunity [reviewed in (180)]. IFNs Type I are considered a "standard of care" in suppressing chronic HCV and HBV infections, while Type III IFNs have generated encouraging results as a treatment for HCV infection in phase III clinical trials (181). Various studies have confirmed that alphaviruses are also highly sensitive to the antiviral activity of Type-I IFNs (IFN-α/β) (182, 183).

Briolant et al. (27) compared the antiviral efficacy of IFN-α, glycyrrhizin, 6-azauridine, and RBV of inhibiting CHIKV and SFV infection *in vitro*. When combined with RBV, IFN-α2b had a sub-synergistic antiviral effect on both alphaviruses (27). A more recent study by Gallegos et al. (28) confirmed the highly synergistic effect of RBV and IFN α when administered as combination therapy *in vitro*.

In vivo studies with IFN-α/β receptor-deficient mice also demonstrated the importance of IFNs against CHIKV infection. The deficient mice lacked adequate IFN-α/β responses to the viral infection and CHIKV caused haemorrhagic fever, shock, and finally resulted in death (184).

Brehin et al. (185) investigated the role of IFN-induced 2′,5′-Oligoadenylate Synthetase (OAS) protein family in innate immunity to CHIKV. OAS proteins are critical components

of innate immunity and the group was able to show that the antiviral actions of IFN-α/β in HeLa cells are mediated due to the induction of these proteins. Various ISGs that affect alphavirus replication have been identified, including ISG15, ISG20, P56, ZAP, and Viperin (185).

Tetherin

Tetherin [also known as bone marrow stromal antigen 2 (BST-2)] is a host transmembrane protein with antiviral activity that is induced by IFN. Tetherin binds budded viral particles directly to the plasma membrane (PM) and thus restricts the release of enveloped viruses. The virus particles which are thus bound to the PM can then be endocytosed and degraded (186). Two isoforms of tetherin that differ in length are known. They are referred to as L- (long) and S- (short) tetherin and each has distinct biological properties (187). Tetherin showed antiviral activity against alphavirus release and studies demonstrated that tetherin does not affect viral entry or protein expression. L-tetherin is significantly more efficient in inhibiting the SFV release than the short isoform (186).

In response to this antiviral countermeasure, many viruses have evolved tetherin antagonists. Jones (80) postulated that CHIKV nsP1 is such a BST-2/tetherin antagonist. However, Wan et al. (81) could not confirm Jones' findings and suggested that the sole physical tethering of virus particles to the PM is not sufficient to restrict alphaviruses and that the subsequent virus endocytosis is a requirement for efficient inhibition of alphavirus release.

Silvestrol

The natural compound silvestrol (a cyclopenta[b]benzofuran flavagline) is an isolate from plants of the genus *Aglaia* and has been the focus of various antiviral studies over the past 5 years. Flavaglines have been the interest of anticancer research for more than two decades because they display antitumor activity (188). Silvestrol is a highly efficient, non-toxic and specific inhibitor of the host RNA helicase eIF4A (eukaryotic initiation factor-4A), which is part of the heterotrimeric translation initiation complex in eukaryotes (189). The host cell needs the RNA helicase eIF4A to unwind structured 5′-untranslated regions (UTRs) of mRNAs to allow translation. Since 5′-capped viral mRNAs often contain structured 5′-UTRs as well, it has been suggested that RNA viruses which have these structures might depend on eIF4A for their translation. Silvestrol proved to be a successful antiviral in multiple *in vitro* studies against a variety of RNA viruses, such as Ebola, Corona-, Picornaviruses and CHIKV (189–191).

Henß et al. (191) demonstrated that by delaying the protein synthesis of CHIKV nsPs and structural proteins, silvestrol also retarded the innate response to CHIKV infection. By curbing the amount of nsPs, silvestrol reduced CHIKV RNA replication. The compound also decreased the host protein shut-off which was induced by CHIKV infection, probably because of the lower total amount of nsP2. In accordance with this, silvestrol seemed not to impair the IFN-induced STAT1 phosphorylation and eIF2 did not become phosphorylated. All these *in vitro* findings suggest that inhibition of the host helicase eIF4A with silvestrol might be a therapeutic strategy to treat CHIKV infections. Further research is needed to find out how and if silvestrol can actually be of benefit against CHIKV infection *in vivo*.

Protein Kinase C Modulators and Plant Extracts

Plants have always been an important source of active substances and to date about 50% of the licensed drugs are natural products or were inspired by them (192). Natural compounds quite frequently have striking differences compared to chemical molecules, which often result in better pharmacological properties (193). The introduction of today's modern drug discovery process has led to a certain neglect of considering plants as a resource for bioactive compounds. But with the technological improvement in the field of natural product isolation, synthesis and screening, the interest in plants as a source for anti-infective natural compounds has been renewed (194).

After the massive CHIKV outbreak in the Indian Ocean region in 2005–2006, a large-scale quest for novel and selective antiviral compounds was initiated. A project called "Biodiversity and emerging viruses in the Indian Ocean: selection of drug candidates targeting the Chikungunya virus" was financially supported by the Center for Research and Monitoring of Emerging Diseases in the Indian Ocean (CRVOI) and carried out from March 2009 to December 2011 (195). Its goal was to find new selective antiviral compounds derived from plants from the Indian Ocean Region, an area with a vast botanical biodiversity. Soon after the program started, virologists, and natural product chemists discovered that the plant family with the most promising components was the *Euphorbiaceae*.

Especially **polycyclic** and **macrocyclic diterpenoids** as well as molecules derived from them came into focus of antiviral research. Within the family of *Eurphorbia* more than several hundred different macrocyclic diterpenoids of interest have been discovered. These molecules possess various types of carbon skeletons (e.g., jatrophane, lathyrane, myrsinane, ingenane, tigliane, daphnane, etc.). More than 20 skeletal types can only be found in this particular plant family (196). These molecules possess a broad structural diversity due to their different macrocyclic skeletons and the various aliphatic and aromatic ester groups.

Macrocyclic diterpenoids have the ability to modulate protein kinase C (PKC) activity (196). Particularly the **phorbol esters** or **phorboids** have a tendency to bind to phospholipid membrane receptors and activate the PKC (197). PKCs are a multigene family of related serine/threonine kinases that are involved in many signal transduction pathways and cellular responses. PKCs play a role in a multitude of cellular functions such as cell mitogenesis, differentiation and apoptosis, smooth muscle contraction, platelet aggregation, tumor-modulation, and anti-HIV activity (198). PKCs are classified into three sub-families with different isoforms depending on the way of their activation. The classical PKC (cPKC) isoforms (α, β, and γ) require calcium (Ca^{2+}) and the membrane-embedded ligand diacylglycerol (DAG) for activation, while the novel PKC (nPKC δ, ε, θ, η) are activated by DAG alone. The atypical PKC (aPKC Mζ-ι/λ) are not dependent on either ligand, but on proteins for activation (199).

All PKCs have an N-terminal regulatory moiety with a C1A domain and a C-terminal catalytic moiety for phosphorylation. Conventional and novel PKC isozymes have a second C1 domain (C1B) to which DAG binds (199). Phorbol esters have a two-order higher affinity to the C1B domain of conventional and novel PKC isoforms than DAG. This leads to the activation of the PKCs.

Recently a study reviewed the anti-CHIKV activity of about 80 naturally occurring macrocyclic diterpenes originating from the *Euphorbiaceae* plant family and about 30 commercially available natural diterpenoids (198) (**Table 1**). Some of these compounds have also been tested against other alphaviruses, like SFV or SINV. Other studies evaluated the antiviral properties of different plant compounds *in vitro* and found out that the phorbol esters **prostratin (12-deoxyphorbol 13-acetate)** and **12-O-tetradecanoylphorbol 13-acetate (TPA)** are potent inhibitors of CHIKV (11, 200). Allard et al. published on the anti-CHIKV properties of **trigocherrierin A**, an unusual chlorinated daphnane diterpenoid orthoester (DDO) from the plant *Trigonostemon cherrieri* (*Euphorbiaceae*), and analog compounds from the same plant (17, 45). Likewise, Nothias-Scaglia et al. found **Phorbol-12,13-didecanoate** to be the most potent inhibitor of CHIKV replication among 29 commercially available natural diterpenoids (201). Phorbol-12,13-didecanoate is structurally related to TPA. Corlay et al. tested **12-O-decanoylphorbol 13-acetate (DPA)**, a molecule that differs from TPA only by the length of the side chain that is attached at C-12 (10 carbons for DPA vs. 14 carbons for TPA) (34). DPA had anti-CHIKV properties but a small SI of 2.0 reflecting a narrow therapeutic window making this compound a poor choice as a future antiviral drug. A novel DDO called **neoguillauminin A** and four **12-deoxyphorbols** from *Euphorbiaceae* plants were recently found to have significant *in vitro* anti-CHIKV properties, three with an SI above 50 (**Table 1**) (15).

Yet despite the promising results of resent studies, the question of how said compounds manage to curb CHIKV replication has not been fully answered. Most studies assume that PKCs modulation is the key mechanism, but specifics are still outstanding. At the same time, the manner of how PKCs isoforms regulate intracellular signal transduction pathways and influence biological responses is still under heavy investigation and not completely understood. There are hints indicating that different translocation patters of the PKCs might lead to different intracellular signal transduction and cellular functions (202, 203). The cell type in which the PKCs are activated play a role as to how the response affects the organism. Additionally, the chemical properties (e.g., hydrophobicity) of different phorbol esters seem to play a critical role as well, since they induce different translocation patterns of PKCs in the cell. As conventional PKCs depend on plasma membrane bound Ca^{2+} and DAG as ligands, phorbol esters translocate them primarily to the PM, while the novel PKCs only depend on DAG and translocate to the more abundant and diacylglycerol-rich Golgi membrane (199). Studies showed that the stimulation of PKC δ by different phorbol esters induced distinct patterns of enzyme translocation. This indicates that lipophilicity of phorbol esters may contribute to differential PKC δ localization and thus to potentially different biological

activities (203). Nothias-Scaglia et al. demonstrated that the HIV-1 and HIV-2 inhibitory effects of phorbol esters were strongly correlated with those of CHIKV (13). This observation is even more interesting since CHIKV and HIV belong to two different virus genera (alphavirus and lentivirus). Thus, the most probable explanation would be a common PKC-based mechanism of action. Yet a broad and potent PKC modulator with very good anti-HIV activity showed no anti-CHIKV activity, which might indicate that different PKC isoforms are involved in the two different virus life cycles. Abdelnabi et al. (33) tried to shed light on the role of PKCs in the cellular antiviral response to CHIKV infection by studying the mechanism of how **prostratin** works as an antiviral against CHIKV. The group found out that different cell lines express varied levels of diverse PKC isoform. Abdelnabi used four different cell lines [buffalo green monkey kidney (BGM) cells, African green monkey kidney cells (Vero cells), human embryonic lung fibroblasts (HEL), and human skin fibroblast cells] and four different CHIKV strains. Prostratin curbed CHIKV RNA synthesis and the production of infectious virus progeny at a post-entry step during virus replication. The antiviral action of the compound was dose- and cell- dependent. The most potent antiviral effect was observed in human skin fibroblast cells which also showed the highest gene expression levels of the classical PKC isoforms (**Table 1**). The antiviral activity of prostratin was significantly reduced when PKC inhibitors were present. These results suggest that the activation of mostly classical PKCs is the reason for the antiviral effect of prostratin (33).

Multiple or Unidentified Targets

Many other molecules have been tested against CHIKV and other alphaviruses in the past 5 years, with a special focus on plant extracts or drugs originally licensed for other diseases. Some seemed promising at first but then, upon closer investigation and with different assay methods, turned out to have a narrow SI or bad chemical properties. For some, the mode of action is still unknown. Here only the most recent or promising will be mentioned if they have been subject to repeated studies. For details on their efficacy (see **Table 1**).

Micafungin

Various researchers successfully tested the antifungal drug micafungin against viruses such as CHIKV, SFV, and SINV *in vitro* (35, 159). Micafungin has been licensed for the treatment of invasive candidiasis in 2005 (204, 205). According to Ho et al., micafungin significantly reduced CHIKV infection, cytopathic effects, and progeny yield (35). The question of how micafungin inhibits viral infection is still not answered. It was observed that the drug proved to be more effective in inhibiting CHIKV progeny yield than in reducing RNA replication (35, 159). The researchers thus deducted that micafungin might have a major influence on the later stages of CHIKV infection. On the other hand, the inhibitory effects of micafungin were stronger in the full-time treatment group than in the post-treatment group. This finding allows the speculation that micafungin might target different intracellular events during virus infection, such as viral replication, intracellular and extracellular transmission, and

virus stability. The antifungal action of micafungin comes from the non-reversible inhibition of the β-1,3-D-glucan synthase of fungi, thus blocking the cell wall synthesis (206). Since neither mammalian cells nor viruses contain 1,3-beta-D-glucan polymers, the mechanism of action of micafungin still has to be elucidated. On the other hand, the absence of these polymers in mammal cells indicates a lack of mechanism-based toxicity of the drug that might partially account for the good tolerability in patients.

Abamectin, Ivermectin, and Berberine

Varghese et al. (36) conducted HTS of about 3000 compounds for their ability to inhibit CHIKV infection. Some of the substances were already licensed drugs or under investigation in clinical trials. With the help of a *Renilla reniformis* luciferase (Rluc) reporter system in baby hamster kidney (BHK-21) cells, Varghese could evaluate the compounds' impact on viral replication. After a second validation with WT and reporter CHIKV infection essays of 25 initial hits, Varghese identified five compounds with the capacity to curb CHIKV replication (36). Among these secondary hit compounds, **abamectin**, **ivermectin**, and **berberine** performed best with an inhibition activity against CHIKV of over 85%. Toxicity evaluations of these three compounds were done in BHK-21 and human hepatocellular (Huh-7.5) cells (**Table 1**). All three compounds also exhibited antiviral action against other alphaviruses, including SFV and SINV (39).

Abamectin and ivermectin are macrocyclic lactones which originate from the fungus *Streptomyces avemitilis* and are the most commonly used compounds of the avermectin family. Both drugs are potent endo- and ectoparasitic agents with a broad spectrum of activity. Especially ivermectin has been used as an insecticide for vector control and it seems that apart from its insecticide properties against *Aedes* and *Anopheles* species, it also displays antiviral activity against some arboviruses (207). The fact that ivermectin has both mosquitocidal and antiviral action may come in handy for vector control and limiting virus spread as well as infection at the same time. The drug is currently under investigation in a phase 2 clinical trial as a therapeutic for Dengue haemorrhagic fever (ClinicalTrials.gov identifier: NCT03432442). In flaviviruses (DENV, YFV, TBEV) ivermectin inhibits the NS3 helicase activity and thus curbs viral replication (208). The mode of action of abamectin and ivermectin against CHIKV is not clear, but it is being speculated that the drugs inhibit the RNA synthesis and down-regulate the viral protein expression of the nsP1 and nsP3 (36).

Berberine is a plant-derived isoquinoline alkaloid that is also able to inhibit CHIKV replication in a dose-dependent manner. It is believed to curb RNA synthesis and interfere with the viral protein expression (39). However, berberine has a wide range of bioactivities and it is also possible that the alkaloid interferes with host factors which promote CHIKV replication (209). Berberine reduced the virus-induced activation of cellular mitogen-activated protein kinase signaling, a pathway which is relevant for maintaining the viral life cycle. Inhibiting this kinase cascade with specific drugs resulted in a decreased production of CHIKV progeny virions. Varghese tested berberine *in vivo* in a mouse model where it significantly reduced CHIKV-induced

inflammatory disease (210). Berberine is currently under clinical investigation in a variety of trials; however, none of them test its use as an antiviral.

Coumarin Conjugates

Coumarins can be found in plants as well as certain microorganisms and animals. The (natural and/or synthetic) coumarins have a wide range of biological activities and they are in focus for the therapy of various conditions. A number of coumarins have been found to display antiviral, anticoagulant, anti-inflammatory, antimutagenic, antitumor, antitubercular, central nervous system stimulant, fungicidal or vasodilator activities (211).

Hwu designed and developed 22 compounds that were made up of uracil, arene, and coumarin derivatives (212). He tried to combine the antiviral properties previously described for uracil derivatives and coumarin compounds. Hwu tested the newly designed compounds against CHIKV *in vitro*. Five molecules displayed significant potency against CHIKV (212). In 2019, the same research group published a study after testing 21 new coumarin derivatives against CHIKV *in vitro*. This time coumarin derivatives had been conjugated with guanosine. Hwu had modified the design of the molecules and after HTS, three of these new conjugates were found to inhibit CHIKV in Vero cells with significant potency but with a better SI than the ones tested before (**Table 1**) (37). From the structure-activity relationship Hwu deduced that the coumarin moiety was essential and the presence of a –OMe group enhanced the antiviral activity. Still, Hwu did not try to elucidate the work mechanism of the antiviral activity of his compounds.

DISCUSSION

As CHIKV transmission depends on arthropod vectors in a complex interaction between virus host and the environment, a thorough understanding of these interactions is essential for the development of strategies to curb infections and the geographical spread of vectors. Especially climate change is one factor that may help arboviruses manifest in new areas that were formerly unsuitable for their vectors. International travel might further contribute to importing newly emerging arboviral diseases (like CHIK, Zika, or Dengue Fever virus). With autochthonous infections of CHIKV in France and Italy and established populations of *Aedes albopictus* in southern Germany, it is only a question of time until CHIKV manifests in moderate regions (3).

Thus, antiviral research remains of utmost importance to counter CHIKV infection. The different antiviral modes of action (MoAs), direct (by inhibiting the virus themselves), and indirect (by inhibiting host factors), have different merits, but both need to be considered and possibly combined for synergic effects of different MoAs.

A number of directly inhibiting antivirals against CHIKV that were tested *in vitro* were either discovered via *in silico* approach, high throughput screening of libraries or classical pharmacology. Especially plants have been rediscovered as a source for possible antivirals and yielded promising compounds like prostratin. Other drug candidates have been repurposed

and are already licensed for the treatment of different viral diseases, e.g., sofosbuvir, ribavirin, and favipiravir. As these molecules have already been intensely evaluated in patients, trials for them against CHIKV in humans may possibly be fast-tracked. Unfortunately, some failed to maintain their efficacy in *in vivo* experiments (e.g., chloroquine and ribavirin), while others (like favipiravir and sofosbuvir) look more promising in animal experiments but still have to be tested against CHIKV in humans.

Despite multiple efforts in antiviral research, there is no standardized protocol for determining efficacy and toxicity. This makes comparison of the different hits impossible. As demonstrated in **Tables 1**, **2**, efficacy and toxicity values vary considerably depending on the assay method, virus strain, and cell line. Some cell lines are refractory to the toxic effects of the molecules, possibly whitewashing the SI of the potential hit. The same applies for the assay methods, where each has its merits and its flaws. The lack of standardization as well as polypharmacology *in vivo* might be reasons why multiple drugs, although having achieved promising results *in vitro*, failed to be of benefit *in vivo*. Standardized efficacy and toxicity assays would help in calculating the SI which in turn is important for selecting molecules to test *in vivo*. So far, there is no defined cut-off for the SI, but a value of ≥ 10 is usually considered for animal models (39). A more thorough validation of potential hits in pre-clinical studies (e.g., multiple assay methods of selected hits *in vitro*) might help to avoid disappointment in *in vivo* assays.

Furthermore, as CHIKV infection often go hand in hand with other arboviral infections that are transmitted by the same *Aedes* species (e.g., DENV and ZIKV), a panantiviral which shows efficacy against these other viruses would be ideal. Apart from displaying anti-CHIKV activity, sofosbuvir, suramin, favipiravir, ribavirin, 6-azauridine, and ECGC also display antiviral activity against DENV or ZIKV or both *in vitro* (50, 136, 213–215).

Indirect antivirals targeting host factors yielded some promising results *in vitro*, but *in vivo* tests are still outstanding. This approach bears the risk of disrupting the physiological balance of the host factors which might lead to serious adverse effects.

Although research has brought forth a number of promising compounds, most of them still have to be validated *in vivo* and in clinical trials. The past epidemics caused by CHIKV demonstrated the impact a neglected or (re)emerging disease may have on a naïve population. Agents that have the potential to disable a population for a longer period with possible long-term sequelae, pose a vast threat to health and the economy. With no licensed vaccine and no specific antiviral treatment against CHIKF, research in the area of antiviral therapy is of utmost importance and the effort to find a specific treatment should be continued.

AUTHOR CONTRIBUTIONS

Both authors contributed to the article and approved the submitted version.

FUNDING

ACKNOWLEDGMENTS

REFERENCES

1. Silva LA, Dermody TS. Chikungunya virus: epidemiology, replication, disease mechanisms, and prospective intervention strategies. *J Clin Invest.* (2017) 127:737–49. doi: 10.1172/JCI84417
2. Robinson MC. An epidemic of virus disease in Southern province, tanganyika territory, in 1952-53. I. clinical features. *Trans Roy Soc Trop Med Hygiene.* (1955) 49:28–32. doi: 10.1016/0035-9203(55)90080-8
3. Control) EECfDPa. *Autochthonous Transmission of Chikungunya Virus in EU/EEA, 2007–2020.* (2020). Available online at: https://www.ecdc.europa.eu/en/all-topics-z/chikungunya-virus-disease/surveillance-and-disease-data/autochthonous-transmission (accessed August 17, 2020).
4. Control EuCfDPa. *Chikungunya Worldwide Overview: Geographical Distribution of Chikungunya Cases Reported Worldwide.* (2020). Available online at: https://www.ecdc.europa.eu/en/chikungunya-monthly (accessed July 17 2020).
5. Renault P, Balleydier E, D'Ortenzio E, Baville M, Filleul L. Epidemiology of Chikungunya infection on Reunion Island, Mayotte, and neighboring countries. *Med Mal Infect.* (2012) 42:93–101. doi: 10.1016/j.medmal.2011.12.002
6. Ruiz Silva M, van der Ende-Metselaar H, Mulder HL, Smit JM, Rodenhuis-Zybert IA. Mechanism and role of MCP-1 upregulation upon chikungunya

virus infection in human peripheral blood mononuclear cells. *Sci Rep.* (2016) 6:32288. doi: 10.1038/srep32288
7. Matusali G, Colavita F, Bordi L, Lalle E, Ippolito G, Capobianchi MR, et al. Tropism of the Chikungunya virus. *Viruses.* (2019) 11:175. doi: 10.3390/v11020175
8. CDC. *Chikungunya Virus: CDC Centres for Disease Control and Prevention.* (2020). Available online at: https://www.cdc.gov/chikungunya/geo/index.html (accessed September 19, 2019).
9. Pietila MK, Hellstrom K, Ahola T. Alphavirus polymerase and RNA replication. *Virus Res.* (2017) 234:44–57. doi: 10.1016/j.virusres.2017.01.007
10. Hucke FIL, Bestehorn-Willmann M, Bugert JJ. Prophylactic strategies to control Chikungunya virus infection. *Virus Genes.* (2020).
11. Bourjot M, Delang L, Nguyen VH, Neyts J, Gueritte F, Leyssen P, et al. Prostratin and 12-O-tetradecanoylphorbol 13-acetate are potent and selective inhibitors of Chikungunya virus replication. *J Nat Prod.* (2012) 75:2183–7. doi: 10.1021/np300637t
12. Bassetto M, De Burghgraeve T, Delang L, Massarotti A, Coluccia A, Zonta N, et al. Computer-aided identification, design and synthesis of a novel series of compounds with selective antiviral activity against chikungunya virus. *Antiviral Res.* (2013) 98:12–8. doi: 10.1016/j.antiviral.2013.01.002
13. Nothias-Scaglia LF, Pannecouque C, Renucci F, Delang L, Neyts J, Roussi F, et al. Antiviral activity of diterpene esters

on chikungunya virus and HIV replication. *J Nat Prod.* (2015) 78:1277–83. doi: 10.1021/acs.jnatprod.5b00073

14. Gigante A, Gomez-SanJuan A, Delang L, Li C, Bueno O, Gamo AM, et al. Antiviral activity of [1,2,3]triazolo[4,5-d]pyrimidin-7(6H)-ones against chikungunya virus targeting the viral capping nsP1. *Antiviral Res.* (2017) 144:216–22. doi: 10.1016/j.antiviral.2017.06.003

15. Olivon F, Allard PM, Koval A, Righi D, Genta-Jouve G, Neyts J, et al. Bioactive natural products prioritization using massive multi-informational molecular networks. *ACS Chem Biol.* (2017) 12:2644–51. doi: 10.1021/acschembio.7b00413

16. Scholte FE, Tas A, Martina BE, Cordioli P, Narayanan K, Makino S, et al. Characterization of synthetic Chikungunya viruses based on the consensus sequence of recent E1-226V isolates. *PLoS ONE.* (2013) 8:e71047. doi: 10.1371/journal.pone.0071047

17. Allard PM, Martin MT, Dau ME, Leyssen P, Gueritte F, Litaudon M. Trigocherrin A, the first natural chlorinated daphnane diterpene orthoester from Trigonostemon cherrieri. *Organ Lett.* (2012) 14:342–5. doi: 10.1021/ol2030907

18. Ho YJ, Wang YM, Lu JW, Wu TY, Lin LI, Kuo SC, et al. Suramin inhibits chikungunya virus entry and transmission. *PLoS ONE.* (2015) 10:e0133511. doi: 10.1371/journal.pone.0133511

19. Hwu JR, Gupta NK, Tsay SC, Huang WC, Albulescu IC, Kovacikova K, et al. Bis(benzofuran-thiazolidinone)s and bis(benzofuran-thiazinanone)s as inhibiting agents for chikungunya virus. *Antiviral Res.* (2017) 146:96–101. doi: 10.1016/j.antiviral.2017.08.008

20. Feibelman KM, Fuller BP, Li L, LaBarbera DV, Geiss BJ. Identification of small molecule inhibitors of the Chikungunya virus nsP1 RNA capping enzyme. *Antiviral Res.* (2018) 154:124–31. doi: 10.1016/j.antiviral.2018.03.013

21. Gigante A, Canela MD, Delang L, Priego EM, Camarasa MJ, Querat G, et al. Identification of [1,2,3]triazolo[4,5-d]pyrimidin-7(6H)-ones as novel inhibitors of Chikungunya virus replication. *J Med Chem.* (2014) 57:4000–8. doi: 10.1021/jm401844c

22. Das PK, Puusepp L, Varghese FS, Utt A, Ahola T, Kananovich DG, et al. Design and validation of novel chikungunya virus protease inhibitors. *Antimicrob Agents Chemother.* (2016) 60:7382–95. doi: 10.1128/AAC.01421-16

23. Lucas-Hourani M, Lupan A, Despres P, Thoret S, Pamlard O, Dubois J, et al. A phenotypic assay to identify Chikungunya virus inhibitors targeting the nonstructural protein nsP2. *J Biomol Screen.* (2013) 18:172–9. doi: 10.1177/1087057112460091

24. Ferreira AC, Reis PA, de Freitas CS, Sacramento CQ, Villas Boas Hoelz L, Bastos MM, et al. Beyond members of the flaviviridae family, sofosbuvir also inhibits chikungunya virus replication. *Antimicrob Agents Chemother.* (2019) 63:e01389–18. doi: 10.1101/360305

25. Franco EJ, Rodriquez JL, Pomeroy JJ, Hanrahan KC, Brown AN. The effectiveness of antiviral agents with broad-spectrum activity against chikungunya virus varies between host cell lines. *Antiviral Chem Chemother.* (2018) 26:2040206618807580. doi: 10.1177/2040206618807580

26. Rothan HA, Bahrani H, Mohamed Z, Teoh TC, Shankar EM, Rahman NA, et al. A combination of doxycycline and ribavirin alleviated chikungunya infection. *PLoS ONE.* (2015) 10:e0126360. doi: 10.1371/journal.pone.0126360

27. Briolant S, Garin D, Scaramozzino N, Jouan A, Crance JM. *In vitro* inhibition of Chikungunya and Semliki Forest viruses replication by antiviral compounds: synergistic effect of interferon-alpha and ribavirin combination. *Antiviral Res.* (2004) 61:111–7. doi: 10.1016/j.antiviral.2003.09.005

28. Gallegos KM, Drusano GL, DZ DA, Brown AN. Chikungunya virus: *in vitro* response to combination therapy with ribavirin and interferon Alfa 2a. *J Infect Dis.* (2016) 214:1192–7. doi: 10.1093/infdis/jiw358

29. Kaur P, Thiruchelvan M, Lee RC, Chen H, Chen KC, Ng ML, et al. Inhibition of chikungunya virus replication by harringtonine, a novel antiviral that suppresses viral protein expression. *Antimicrob Agents Chemother.* (2013) 57:155–67. doi: 10.1128/AAC.01467-12

30. Ehteshami M, Tao S, Zandi K, Hsiao HM, Jiang Y, Hammond E, et al. Characterization of β-d-N(4)-Hydroxycytidine as a novel inhibitor of chikungunya virus. *Antimicrob Agents Chemother.* (2017) 61:16. doi: 10.1128/AAC.02395-16

31. Delang L, Segura Guerrero N, Tas A, Querat G, Pastorino B, Froeyen M, et al. Mutations in the chikungunya virus non-structural proteins cause resistance to favipiravir (T-705), a broad-spectrum antiviral. *J Antimicrob Chemother.* (2014) 69:2770–84. doi: 10.1093/jac/dku209

32. Cruz DJ, Bonotto RM, Gomes RG, da Silva CT, Taniguchi JB, No JH, et al. Identification of novel compounds inhibiting chikungunya virus-induced cell death by high throughput screening of a kinase inhibitor library. *PLoS Negl Trop Dis.* (2013) 7:e2471. doi: 10.1371/journal.pntd.0002471

33. Abdelnabi R, Amrun SN, Ng LF, Leyssen P, Neyts J, Delang L. Protein kinases C as potential host targets for the inhibition of chikungunya virus replication. *Antiviral Res.* (2017) 139:79–87. doi: 10.1016/j.antiviral.2016.12.020

34. Corlay N, Delang L, Girard-Valenciennes E, Neyts J, Clerc P, Smadja J, et al. Tigliane diterpenes from Croton mauritianus as inhibitors of chikungunya virus replication. *Fitoterapia.* (2014) 97:87–91. doi: 10.1016/j.fitote.2014.05.015

35. Ho YJ, Liu FC, Yeh CT, Yang CM, Lin CC, Lin TY, et al. Micafungin is a novel anti-viral agent of chikungunya virus through multiple mechanisms. *Antiviral Res.* (2018) 159:134–42. doi: 10.1016/j.antiviral.2018.10.005

36. Varghese FS, Kaukinen P, Glasker S, Bespalov M, Hanski L, Wennerberg K, et al. Discovery of berberine, abamectin and ivermectin as antivirals against chikungunya and other alphaviruses. *Antiviral Res.* (2016) 126:117–24. doi: 10.1016/j.antiviral.2015.12.012

37. Hwu JR, Huang WC, Lin SY, Tan KT, Hu YC, Shieh FK, et al. Chikungunya virus inhibition by synthetic coumarin-guanosine conjugates. *Eur J Med Chem.* (2019) 166:136–43. doi: 10.1016/j.ejmech.2019.01.037

38. Abdelnabi R, Neyts J, Delang L. Chikungunya virus infections: time to act, time to treat. *Curr Opin Virol.* (2017) 24:25–30. doi: 10.1016/j.coviro.2017.03.016

39. Subudhi BB, Chattopadhyay S, Mishra P, Kumar A. Current strategies for inhibition of chikungunya infection. *Viruses.* (2018) 10:235. doi: 10.3390/v10050235

40. da Silva-Junior EF, Leoncini GO, Rodrigues EES, Aquino TM, Araujo-Junior JX. The medicinal chemistry of Chikungunya virus. *Bioorg Med Chem.* (2017) 25:4219–44. doi: 10.1016/j.bmc.2017.06.049

41. Bugert JJ, Hucke F, Zanetta P, Bassetto M, Brancale A. Antivirals in medical biodefense. *Virus Genes.* (2020) 56:150–67. doi: 10.1007/s11262-020-01737-5

42. Rainsford KD, Parke AL, Clifford-Rashotte M, Kean WF. Therapy and pharmacological properties of hydroxychloroquine and chloroquine in treatment of systemic lupus erythematosus, rheumatoid arthritis and related diseases. *Inflammopharmacology.* (2015) 23:231–69. doi: 10.1007/s10787-015-0239-y

43. Khan M, Santhosh SR, Tiwari M, Lakshmana Rao PV, Parida M. Assessment of *in vitro* prophylactic and therapeutic efficacy of chloroquine against Chikungunya virus in vero cells. *Med Virol.* (2010) 82:817–24. doi: 10.1002/jmv.21663

44. Bernard E, Solignat M, Gay B, Chazal N, Higgs S, Devaux C, et al. Endocytosis of chikungunya virus into mammalian cells: role of clathrin and early endosomal compartments. *PLoS ONE.* (2010) 5:e11479. doi: 10.1371/journal.pone.0011479

45. Allard PM, Leyssen P, Martin MT, Bourjot M, Dumontet V, Eydoux C, et al. Antiviral chlorinated daphnane diterpenoid orthoesters from the bark and wood of Trigonostemon cherrieri. *Phytochemistry.* (2012) 84:160–8. doi: 10.1016/j.phytochem.2012.07.023

46. Chopra A, Saluja M, Venugopalan A. Effectiveness of chloroquine and inflammatory cytokine response in patients with early persistent musculoskeletal pain and arthritis following chikungunya virus infection. *Arthritis Rheumatol.* (2014) 66:319–26. doi: 10.1002/art.38221

47. Roques P, Thiberville SD, Dupuis-Maguiraga L, Lum FM, Labadie K, Martinon F, et al. Paradoxical effect of chloroquine treatment in enhancing Chikungunya virus infection. *Viruses.* (2018) 10:268. doi: 10.3390/v10050268

48. Weber C, Sliva K, von Rhein C, Kummerer BM, Schnierle BS. The green tea catechin, epigallocatechin gallate inhibits chikungunya virus infection. *Antiviral Res.* (2015) 113:1–3. doi: 10.1016/j.antiviral.2014.11.001

49. Lu JW, Hsieh PS, Lin CC, Hu MK, Huang SM, Wang YM, et al. Synergistic effects of combination treatment using EGCG and suramin against the chikungunya virus. *Biochem Biophys Res Commun.* (2017) 491:595–602. doi: 10.1016/j.bbrc.2017.07.157

50. Basavannacharya C, Vasudevan SG. Suramin inhibits helicase activity of NS3 protein of dengue virus in a fluorescence-based high throughput assay format. *Biochem Biophys Res Commun.* (2014) 453:539–44. doi: 10.1016/j.bbrc.2014.09.113

51. Madsen C, Hooper I, Lundberg L, Shafagati N, Johnson A, Senina S, et al. Small molecule inhibitors of Ago2 decrease Venezuelan equine encephalitis virus replication. *Antiviral Res.* (2014) 112:26–37. doi: 10.1016/j.antiviral.2014.10.002

52. Albulescu IC, van Hoolwerff M, Wolters LA, Bottaro E, Nastruzzi C, Yang SC, et al. Suramin inhibits chikungunya virus replication through multiple mechanisms. *Antiviral Res.* (2015) 121:39–46. doi: 10.1016/j.antiviral.2015.06.013

53. Henß L, Beck S, Weidner T, Biedenkopf N, Sliva K, Weber C, et al. Suramin is a potent inhibitor of Chikungunya and Ebola virus cell entry. *Virol J.* (2016) 13:149. doi: 10.1186/s12985-016-0607-2

54. Chijioke CP, Umeh RE, Mbah AU, Nwonu P, Fleckenstein LL, Okonkwo PO. Clinical pharmacokinetics of suramin in patients with onchocerciasis. *Eur J Clin Pharmacol.* (1998) 54:249–51. doi: 10.1007/s002280050454

55. Fire A, Xu S, Montgomery MK, Kostas SA, Driver SE, Mello CC. Potent and specific genetic interference by double-stranded RNA in caenorhabditis elegans. *Nature.* (1998) 391:806–11. doi: 10.1038/35888

56. Bitko V, Barik S. Phenotypic silencing of cytoplasmic genes using sequence-specific double-stranded short interfering RNA and its application in the reverse genetics of wild type negative-strand RNA viruses. *BMC Microbiol.* (2001) 1:34. doi: 10.1186/1471-2180-1-34

57. Dana H, Chalbatani GM, Mahmoodzadeh H, Karimloo R, Rezaiean O, Moradzadeh A, et al. Molecular mechanisms and biological functions of siRNA. *Int J Biomed Sci.* (2017) 13:48–57.

58. Presloid JB, Novella IS. RNA viruses and RNAi: quasispecies implications for viral escape. *Viruses.* (2015) 7:3226–40. doi: 10.3390/v7062768

59. Lam JK, Chow MY, Zhang Y, Leung SW. siRNA versus miRNA as therapeutics for gene silencing. *Mol Ther Nucl Acids.* (2015) 4:e252. doi: 10.1038/mtna.2015.23

60. Dash PK, Tiwari M, Santhosh SR, Parida M, Lakshmana Rao PV. RNA interference mediated inhibition of Chikungunya virus replication in mammalian cells. *Biochem Biophys Res Commun.* (2008) 376:718–22. doi: 10.1016/j.bbrc.2008.09.040

61. Parashar D, Paingankar MS, Kumar S, Gokhale MD, Sudeep AB, Shinde SB, et al. Administration of E2 and NS1 siRNAs inhibit chikungunya virus replication *in vitro* and protects mice infected with the virus. *PLoS Negl Trop Dis.* (2013) 7:e2405. doi: 10.1371/journal.pntd.0002405

62. Lam S, Chen KC, Ng MM, Chu JJ. Expression of plasmid-based shRNA against the E1 and nsP1 genes effectively silenced Chikungunya virus replication. *PLoS ONE.* (2012) 7:e46396. doi: 10.1371/journal.pone.0046396

63. Bhomia M, Sharma A, Gayen M, Gupta P, Maheshwari RK. Artificial microRNAs can effectively inhibit replication of Venezuelan equine encephalitis virus. *Antiviral Res.* (2013) 100:429–34. doi: 10.1016/j.antiviral.2013.08.010

64. Saha A, Bhagyawant SS, Parida M, Dash PK. Vector-delivered artificial miRNA effectively inhibited replication of Chikungunya virus. *Antiviral Res.* (2016) 134:42–9. doi: 10.1016/j.antiviral.2016.08.019

65. Das I, Basantray I, Mamidi P, Nayak TK, Pratheek BM, Chattopadhyay S, et al. Heat shock protein 90 positively regulates Chikungunya virus replication by stabilizing viral non-structural protein nsP2 during infection. *PLoS ONE.* (2014) 9:e100531. doi: 10.1371/journal.pone.0100531

66. Rathore AP, Haystead T, Das PK, Merits A, Ng ML, Vasudevan SG. Chikungunya virus nsP3 & nsP4 interacts with HSP-90 to promote virus replication: HSP-90 inhibitors reduce CHIKV infection and inflammation *in vivo. Antiviral Res.* (2014) 103:7–16. doi: 10.1016/j.antiviral.2013.12.010

67. Kumar P, Wu H, McBride JL, Jung KE, Kim MH, Davidson BL, et al. Transvascular delivery of small interfering RNA to the central nervous system. *Nature.* (2007) 448:39–43. doi: 10.1038/nature05901

68. Brummelkamp TR, Bernards R, Agami R. A system for stable expression of short interfering RNAs in mammalian cells. *Science.* (2002) 296:550–3. doi: 10.1126/science.1068999

69. Jackson AL, Linsley PS. Recognizing and avoiding siRNA off-target effects for target identification and therapeutic application. *Nat Rev Drug Disc.* (2010) 9:57–67. doi: 10.1038/nrd3010

70. Judge AD, Sood V, Shaw JR, Fang D, McClintock K, MacLachlan I. Sequence-dependent stimulation of the mammalian innate immune response by synthetic siRNA. *Nat Biotechnol.* (2005) 23:457–62. doi: 10.1038/nbt1081

71. Lampio A, Kilpelainen I, Pesonen S, Karhi K, Auvinen P, Somerharju P, et al. Membrane binding mechanism of an RNA virus-capping enzyme. *J Biol Chem.* (2000) 275:37853–9. doi: 10.1074/jbc.M004865200

72. Ahola T, Kujala P, Tuittila M, Blom T, Laakkonen P, Hinkkanen A, et al. Effects of palmitoylation of replicase protein nsP1 on alphavirus infection. *J Virol.* (2000) 74:6725–33. doi: 10.1128/JVI.74.15.6725-6733.2000

73. Karo-Astover L, Sarova O, Merits A, Zusinaite E. The infection of mammalian and insect cells with SFV bearing nsP1 palmitoylation mutations. *Virus Res.* (2010) 153:277–87. doi: 10.1016/j.virusres.2010.08.019

74. Zhang N, Zhao H, Zhang L. Fatty acid synthase promotes the palmitoylation of chikungunya virus nsP1. *J Virol.* (2019) 93:e01747–18. doi: 10.1128/JVI.01747-18

75. Ahola T, Kaariainen L. Reaction in alphavirus mRNA capping: formation of a covalent complex of nonstructural protein nsP1 with 7-methyl-GMP. *Proc Natl Acad Sci USA.* (1995) 92:507–11. doi: 10.1073/pnas.92.2.507

76. Ghosh A, Lima CD. Enzymology of RNA cap synthesis. *Wiley Interdiscip Rev RNA.* (2010) 1:152–72. doi: 10.1002/wrna.19

77. Lampio A, Ahola T, Darzynkiewicz E, Stepinski J, Jankowska-Anyszka M, Kaariainen L. Guanosine nucleotide analogs as inhibitors of alphavirus mRNA capping enzyme. *Antiviral Res.* (1999) 42:35–46. doi: 10.1016/S0166-3542(99)00011-X

78. Bullard-Feibelman KM, Fuller BP, Geiss BJ. A sensitive and robust high-throughput screening assay for inhibitors of the chikungunya virus nsp1 capping enzyme. *PLoS ONE.* (2016) 11:e0158923. doi: 10.1371/journal.pone.0158923

79. Delang L, Li C, Tas A, Querat G, Albulescu IC, De Burghgraeve T, et al. The viral capping enzyme nsP1: a novel target for the inhibition of chikungunya virus infection. *Sci Rep.* (2016) 6:31819. doi: 10.1038/srep31819

80. Jones PH, Maric M, Madison MN, Maury W, Roller RJ, Okeoma CM. BST-2/tetherin-mediated restriction of chikungunya (CHIKV) VLP budding is counteracted by CHIKV non-structural protein 1 (nsP1). *Virology.* (2013) 438:37–49. doi: 10.1016/j.virol.2013.01.010

81. Wan JJ, Ooi YS, Kielian M. Mechanism of tetherin inhibition of alphavirus release. *J Virol.* (2019) 93(7). doi: 10.1128/JVI.02165-18

82. Fros JJ, van der Maten E, Vlak JM, Pijlman GP. The C-terminal domain of chikungunya virus nsP2 independently governs viral RNA replication, cytopathicity, and inhibition of interferon signaling. *J Virol.* (2013) 87:10394–400. doi: 10.1128/JVI.00884-13

83. Garmashova N, Gorchakov R, Volkova E, Paessler S, Frolova E, Frolov I. The old world and new world alphaviruses use different virus-specific proteins for induction of transcriptional shutoff. *J Virol.* (2007) 81:2472–84. doi: 10.1128/JVI.02073-06

84. Mathur K, Anand A, Dubey SK, Sanan-Mishra N, Bhatnagar RK, Sunil S. Analysis of chikungunya virus proteins reveals that non-structural proteins nsP2 and nsP3 exhibit RNA interference (RNAi) suppressor activity. *Sci Rep.* (2016) 6:38065. doi: 10.1038/srep38065

85. de Leuw P, Stephan C. Protease inhibitors for the treatment of hepatitis C virus infection. *GMS Infect Dis.* (2017) 5:34. doi: 10.3205/id000034

86. Jadav SS, Sinha BN, Hilgenfeld R, Pastorino B, de Lamballerie X, Jayaprakash V. Thiazolidone derivatives as inhibitors of chikungunya virus. *Eur J Med Chem.* (2015) 89:172–8. doi: 10.1016/j.ejmech.2014.10.042

87. Das PK, Merits A, Lulla A. Functional cross-talk between distant domains of chikungunya virus non-structural protein 2 is decisive for its RNA-modulating activity. *J Biol Chem.* (2014) 289:5635–53. doi: 10.1074/jbc.M113.503433

88. Matayoshi ED, Wang GT, Krafft GA, Erickson J. Novel fluorogenic substrates for assaying retroviral proteases by resonance energy transfer. *Science.* (1990) 247:954–8. doi: 10.1126/science.2106161

89. Rausalu K, Utt A, Quirin T, Varghese FS, Zusinaite E, Das PK, et al. Chikungunya virus infectivity, RNA replication and non-structural

polyprotein processing depend on the nsP2 protease's active site cysteine residue. *Sci Rep.* (2016) 6:37124. doi: 10.1038/srep37124

90. Rupp JC, Sokoloski KJ, Gebhart NN, Hardy RW. Alphavirus RNA synthesis and non-structural protein functions. *J Gen Virol.* (2015) 96:2483–500. doi: 10.1099/jgv.0.000249

91. Chen MW, Tan YB, Zheng J, Zhao Y, Lim BT, Cornvik T, et al. Chikungunya virus nsP4 RNA-dependent RNA polymerase core domain displays detergent-sensitive primer extension and terminal adenylyltransferase activities. *Antiviral Res.* (2017) 143:38–47. doi: 10.1016/j.antiviral.2017.04.001

92. Zou G, Chen YL, Dong H, Lim CC, Yap LJ, Yau YH, et al. Functional analysis of two cavities in flavivirus NS5 polymerase. *J Biol Chem.* (2011) 286:14362–72. doi: 10.1074/jbc.M110.214189

93. Eyer L, Nencka R, de Clercq E, Seley-Radtke K, Ruzek D. Nucleoside analogs as a rich source of antiviral agents active against arthropod-borne flaviviruses. *Antiviral Chem Chemother.* (2018) 26:2040206618761299. doi: 10.1177/2040206618761299

94. Slusarczyk M, Serpi M, Pertusati F. Phosphoramidates and phosphonamidates (ProTides) with antiviral activity. *Antiviral Chem Chemother.* (2018) 26:2040206618775243. doi: 10.1177/2040206618775243

95. Feng JY. Addressing the selectivity and toxicity of antiviral nucleosides. *Antiviral Chem Chemother.* (2018) 26:2040206618758524. doi: 10.1177/2040206618758524

96. Jordheim LP, Durantel D, Zoulim F, Dumontet C. Advances in the development of nucleoside and nucleotide analogues for cancer and viral diseases. *Nat Rev Drug Disc.* (2013) 12:447–64. doi: 10.1038/nrd4010

97. Varga A, Lionne C, Roy B. Intracellular metabolism of nucleoside/nucleotide analogues: a bottleneck to reach active drugs on HIV reverse transcriptase. *Curr Drug Metab.* (2016) 17:237–52. doi: 10.2174/1389200217666151210141903

98. De Clercq E. The clinical potential of the acyclic (and cyclic) nucleoside phosphonates: the magic of the phosphonate bond. *Biochem Pharmacol.* (2011) 82:99–109. doi: 10.1016/j.bcp.2011.03.027

99. Johnson AA, Ray AS, Hanes J, Suo Z, Colacino JM, Anderson KS, et al. Toxicity of antiviral nucleoside analogs and the human mitochondrial DNA polymerase. *J Biol Chem.* (2001) 276:40847–57. doi: 10.1074/jbc.M106743200

100. McGuigan C, Sutton PW, Cahard D, Turner K, O'Leary G, Wang Y, et al. Synthesis, anti-human immunodeficiency virus activity and esterase lability of some novel carboxylic ester-modified phosphoramidate derivatives of stavudine (d4T). *Antiviral Chem Chemother.* (1998) 9:473–9. doi: 10.1177/095632029800900603

101. McGuigan C, Tsang HW, Sutton PW, De Clercq E, Balzarini J. Synthesis and anti-HIV activity of some novel chain-extended phosphoramidate derivatives of d4T (stavudine): esterase hydrolysis as a rapid predictive test for antiviral potency. *Antiviral Chem Chemother.* (1998) 9:109–15. doi: 10.1177/095632029800900202

102. Sidwell RW, Huffman JH, Khare GP, Allen LB, Witkowski JT, Robins RK. Broad-spectrum antiviral activity of virazole: 1-beta-D-ribofuranosyl-1,2,4-triazole-3-carboxamide. *Science.* (1972) 177:705–6. doi: 10.1126/science.177.4050.705

103. Cooper AC, Banasiak NC, Allen PJ. Management and prevention strategies for respiratory syncytial virus (RSV) bronchiolitis in infants and young children: a review of evidence-based practice interventions. *Pediatr Nursing.* (2003) 29:452–6.

104. Mangia A, Santoro R, Minerva N, Ricci GL, Carretta V, Persico M, et al. Peginterferon alfa-2b and ribavirin for 12 vs. 24 weeks in HCV genotype 2 or 3. *N Engl J Med.* (2005). 352:2609–17. doi: 10.1056/NEJMoa042608

105. Huggins JW, Hsiang CM, Cosgriff TM, Guang MY, Smith JI, Wu ZO, et al. Prospective, double-blind, concurrent, placebo-controlled clinical trial of intravenous ribavirin therapy of hemorrhagic fever with renal syndrome. *J Infect Dis.* (1991) 164:1119–27. doi: 10.1093/infdis/164.6.1119

106. Ortac Ersoy E, Tanriover MD, Ocal S, Ozisik L, Inkaya C, Topeli A. Severe measles pneumonia in adults with respiratory failure: role of ribavirin and high-dose vitamin A. *Clin Respir J.* (2016) 10:673–5. doi: 10.1111/crj.12269

107. Huggins JW, Robins RK, Canonico PG. Synergistic antiviral effects of ribavirin and the C-nucleoside analogs tiazofurin and selenazofurin against togaviruses, bunyaviruses, and arenaviruses. *Antimicrob Agents Chemother.* (1984) 26:476–80. doi: 10.1128/AAC.26.4.476

108. Leyssen P, Balzarini J, De Clercq E, Neyts J. The predominant mechanism by which ribavirin exerts its antiviral activity *in vitro* against flaviviruses and paramyxoviruses is mediated by inhibition of IMP dehydrogenase. *J Virol.* (2005) 79:1943–7. doi: 10.1128/JVI.79.3.1943-1947.2005

109. Tam RC, Pai B, Bard J, Lim C, Averett DR, Phan UT, et al. Ribavirin polarizes human T cell responses towards a type 1 cytokine profile. *J Hepatol.* (1999) 30:376–82. doi: 10.1016/S0168-8278(99)80093-2

110. Scheidel LM, Stollar V. Mutations that confer resistance to mycophenolic acid and ribavirin on Sindbis virus map to the nonstructural protein nsP1. *Virology.* (1991) 181:490–9. doi: 10.1016/0042-6822(91)90881-B

111. Vo NV, Young KC, Lai MM. Mutagenic and inhibitory effects of ribavirin on hepatitis C virus RNA polymerase. *Biochemistry.* (2003) 42:10462–71. doi: 10.1021/bi0344681

112. Rozen-Gagnon K, Stapleford KA, Mongelli V, Blanc H, Failloux AB, Saleh MC, et al. Alphavirus mutator variants present host-specific defects and attenuation in mammalian and insect models. *PLoS Pathog.* (2014) 10:e1003877. doi: 10.1371/journal.ppat.1003877

113. Crotty S, Cameron CE, Andino R. RNA virus error catastrophe: direct molecular test by using ribavirin. *Proc Natl Acad Sci USA.* (2001) 98:6895–900. doi: 10.1073/pnas.111085598

114. Thomas E, Feld JJ, Li Q, Hu Z, Fried MW, Liang TJ. Ribavirin potentiates interferon action by augmenting interferon-stimulated gene induction in hepatitis C virus cell culture models. *Hepatology.* (2011) 53:32–41. doi: 10.1002/hep.23985

115. Ravichandran R, Manian M. Ribavirin therapy for Chikungunya arthritis. *J Infect Dev Countries.* (2008) 2:140–2. doi: 10.3855/T2.2.140

116. Mishra P, Kumar A, Mamidi P, Kumar S, Basantray I, Saswat T, et al. Inhibition of chikungunya virus replication by 1-[(2-Methylbenzimidazol-1-yl) methyl]-2-oxo-indolin-3-ylidene] amino] thiourea(MBZM-N-IBT). *Sci Rep.* (2016) 6:20122. doi: 10.1038/srep20122

117. Sung H, Chang M, Saab S. Management of hepatitis c antiviral therapy adverse effects. *Curr Hepatitis Rep.* (2011) 10:33–40. doi: 10.1007/s11901-010-0078-7

118. Pfeiffer JK, Kirkegaard K. Ribavirin resistance in hepatitis C virus replicon-containing cell lines conferred by changes in the cell line or mutations in the replicon RNA. *J Virol.* (2005) 79:2346–55. doi: 10.1128/JVI.79.4.2346-2355.2005

119. Urakova N, Kuznetsova V, Crossman DK, Sokratian A, Guthrie DB, Kolykhalov AA, et al. beta-d-N (4)-Hydroxycytidine is a potent anti-alphavirus compound that induces a high level of mutations in the viral genome. *J Virol.* (2018) 92:e01965–17. doi: 10.1128/JVI.01965-17

120. Tejero H, Montero F, Nuno JC. Theories of lethal mutagenesis: from error catastrophe to lethal defection. *Curr Topics Microbiol Immunol.* (2016) 392:161–79. doi: 10.1007/82_2015_463

121. Furuta Y, Gowen BB, Takahashi K, Shiraki K, Smee DF, Barnard DL. Favipiravir (T-705), a novel viral RNA polymerase inhibitor. *Antiviral Res.* (2013) 100:446–54. doi: 10.1016/j.antiviral.2013.09.015

122. Furuta Y, Takahashi K, Kuno-Maekawa M, Sangawa H, Uehara S, Kozaki K, et al. Mechanism of action of T-705 against influenza virus. *Antimicrob Agents Chemother.* (2005) 49:981–6. doi: 10.1128/AAC.49.3.981-986.2005

123. Gowen BB, Wong MH, Jung KH, Sanders AB, Mendenhall M, Bailey KW, et al. *In vitro* and *in vivo* activities of T-705 against arenavirus and bunyavirus infections. *Antimicrob Agents Chemother.* (2007) 51:3168–76. doi: 10.1128/AAC.00356-07

124. Julander JG, Smee DF, Morrey JD, Furuta Y. Effect of T-705 treatment on western equine encephalitis in a mouse model. *Antiviral Res.* (2009) 82:169–71. doi: 10.1016/j.antiviral.2009.02.201

125. Abdelnabi R, Jochmans D, Verbeken E, Neyts J, Delang L. Antiviral treatment efficiently inhibits chikungunya virus infection in the joints of mice during the acute but not during the chronic phase of the infection. *Antiviral Res.* (2018) 149:113–7. doi: 10.1016/j.antiviral.2017.09.016

126. Abdelnabi R, Morais ATS, Leyssen P, Imbert I, Beaucourt S, Blanc H, et al. Understanding the mechanism of the broad-spectrum antiviral activity of favipiravir (t-705): key role of the f1 motif of the viral polymerase. *J Virol.* (2017) 91:e00487–17. doi: 10.1128/JVI.00487-17

127. Mentre F, Taburet AM, Guedj J, Anglaret X, Keita S, de Lamballerie X, et al. Dose regimen of favipiravir for Ebola virus disease. *Lancet Infect Dis.* (2015) 15:150–1. doi: 10.1016/S1473-3099(14)71047-3

128. Arias A, Thorne L, Goodfellow I. Favipiravir elicits antiviral mutagenesis during virus replication *in vivo*. *eLife*. (2014) 3:e03679. doi: 10.7554/eLife.03679

129. Sangawa H, Komeno T, Nishikawa H, Yoshida A, Takahashi K, Nomura N, et al. Mechanism of action of T-705 ribosyl triphosphate against influenza virus RNA polymerase. *Antimicrob Agents Chemother.* (2013) 57:5202–8. doi: 10.1128/AAC.00649-13

130. Iglesias NG, Filomatori CV, Gamarnik AV. The F1 motif of dengue virus polymerase NS5 is involved in promoter-dependent RNA synthesis. *J Virol.* (2011) 85:5745–56. doi: 10.1128/JVI.02343-10

131. Peersen OB. Picornaviral polymerase structure, function, and fidelity modulation. *Virus Res.* (2017) 234:4–20. doi: 10.1016/j.virusres.2017.01.026

132. Keating GM, Vaidya A. Sofosbuvir: first global approval. *Drugs.* (2014) 74:273–82. doi: 10.1007/s40265-014-0179-7

133. Bhatia HK, Singh H, Grewal N, Natt NK. Sofosbuvir: A novel treatment option for chronic hepatitis C infection. *J Pharmacol Pharmacother.* (2014) 5:278–84. doi: 10.4103/0976-500X.142464

134. de Freitas CS, Higa LM, Sacramento CQ, Ferreira AC, Reis PA, Delvecchio R, et al. Yellow fever virus is susceptible to sofosbuvir both *in vitro* and *in vivo*. *PLoS Negl Trop Dis.* (2019) 13:e0007072. doi: 10.1371/journal.pntd.0007072

135. Ferreira AC, Zaverucha-do-Valle C, Reis PA, Barbosa-Lima G, Vieira YR, Mattos M, et al. Sofosbuvir protects Zika virus-infected mice from mortality, preventing short- and long-term sequelae. *Sci Rep.* (2017) 7:9409. doi: 10.1038/s41598-017-09797-8

136. Bullard-Feibelman KM, Govero J, Zhu Z, Salazar V, Veselinovic M, Diamond MS, et al. The FDA-approved drug sofosbuvir inhibits Zika virus infection. *Antiviral Res.* (2017) 137:134–40. doi: 10.1016/j.antiviral.2016.11.023

137. Lam AM, Espiritu C, Bansal S, Micolochick Steuer HM, Niu C, Zennou V, et al. Genotype and subtype profiling of PSI-7977 as a nucleotide inhibitor of hepatitis C virus. *Antimicrob Agents Chemother.* (2012) 56:3359–68. doi: 10.1128/AAC.00054-12

138. Gosio B. Ricerche batteriologiche e chimiche sulle alterazoni del mais. *Rivista d'Igiene e Sanita Publica Ann.* (1896) 7:825–68.

139. Allison AC, Eugui EM. Preferential suppression of lymphocyte proliferation by mycophenolic acid and predicted long-term effects of mycophenolate mofetil in transplantation. *Transpl Proc.* (1994) 26:3205–10.

140. Lowe JK, Brox L, Henderson JF. Consequences of inhibition of guanine nucleotide synthesis by mycophenolic acid and virazole. *Cancer Res.* (1977) 37:736–43.

141. Smee DF, Bray M, Huggins JW. Antiviral activity and mode of action studies of ribavirin and mycophenolic acid against orthopoxviruses *in vitro*. *Antiviral Chem Chemother.* (2001) 12:327–35. doi: 10.1177/095632020101200602

142. Diamond MS, Zachariah M, Harris E. Mycophenolic acid inhibits dengue virus infection by preventing replication of viral RNA. *Virology.* (2002) 304:211–21. doi: 10.1006/viro.2002.1685

143. Khan M, Dhanwani R, Patro IK, Rao PV, Parida MM. Cellular IMPDH enzyme activity is a potential target for the inhibition of Chikungunya virus replication and virus induced apoptosis in cultured mammalian cells. *Antiviral Res.* (2011) 89:1–8. doi: 10.1016/j.antiviral.2010.10.009

144. Rashad AA, Neyts J, Leyssen P, Keller PA. A reassessment of mycophenolic acid as a lead compound for the development of inhibitors of chikungunya virus replication. *Tetrahedron.* (2018) 74:1294–306. doi: 10.1016/j.tet.2017.12.053

145. Siebert A, Prejs M, Cholewinski G, Dzierzbicka K. New analogues of mycophenolic acid. *Mini Rev Med Chem.* (2017) 17:734–45. doi: 10.2174/1389557516666161129160001

146. LaStarza MW, Lemm JA, Rice CM. Genetic analysis of the nsP3 region of Sindbis virus: evidence for roles in minus-strand and subgenomic RNA synthesis. *J Virol.* (1994) 68:5781–91. doi: 10.1128/JVI.68.9.5781-5791.1994

147. Fros JJ, Domeradzka NE, Baggen J, Geertsema C, Flipse J, Vlak JM, et al. Chikungunya virus nsP3 blocks stress granule assembly by recruitment of G3BP into cytoplasmic foci. *J Virol.* (2012) 86:10873–9. doi: 10.1128/JVI.01506-12

148. Saul S, Ferguson M, Cordonin C, Fragkoudis R, Ool M, Tamberg N, et al. Differences in processing determinants of nonstructural polyprotein and in the sequence of nonstructural protein 3 affect neurovirulence of semliki forest virus. *J Virol.* (2015) 89:11030–45. doi: 10.1128/JVI.01186-15

149. Atkins GJ, Sheahan BJ. Molecular determinants of alphavirus neuropathogenesis in mice. *J Gen Virol.* (2016) 97:1283–96. doi: 10.1099/jgv.0.000467

150. Malet H, Coutard B, Jamal S, Dutartre H, Papageorgiou N, Neuvonen M, et al. The crystal structures of Chikungunya and Venezuelan equine encephalitis virus nsP3 macro domains define a conserved adenosine binding pocket. *J Virol.* (2009) 83:6534–45. doi: 10.1128/JVI.00189-09

151. Gorbalenya AE, Koonin EV, Lai MM. Putative papain-related thiol proteases of positive-strand RNA viruses. Identification of rubi- and aphthovirus proteases and delineation of a novel conserved domain associated with proteases of rubi-, alpha- and coronaviruses. *FEBS Lett.* (1991) 288:201–5. doi: 10.1016/0014-5793(91)81034-6

152. Fehr AR, Jankevicius G, Ahel I, Perlman S. Viral macrodomains: unique mediators of viral replication and pathogenesis. *Trends Microbiol.* (2018) 26:598–610. doi: 10.1016/j.tim.2017.11.011

153. Eckei L, Krieg S, Butepage M, Lehmann A, Gross A, Lippok B, et al. The conserved macrodomains of the non-structural proteins of Chikungunya virus and other pathogenic positive strand RNA viruses function as mono-ADP-ribosylhydrolases. *Sci Rep.* (2017) 7:41746. doi: 10.1038/srep41746

154. McPherson RL, Abraham R, Sreekumar E, Ong SE, Cheng SJ, Baxter VK, et al. ADP-ribosylhydrolase activity of Chikungunya virus macrodomain is critical for virus replication and virulence. *Proc Natl Acad Sci USA.* (2017) 114:1666–71. doi: 10.1073/pnas.1621485114

155. Nguyen PT, Yu H, Keller PA. Discovery of *in silico* hits targeting the nsP3 macro domain of chikungunya virus. *J Mol Model.* (2014) 20:2216. doi: 10.1007/s00894-014-2216-6

156. Varjak M, Zusinaite E, Merits A. Novel functions of the alphavirus nonstructural protein nsP3 C-terminal region. *J Virol.* (2010) 84:2352–64. doi: 10.1128/JVI.01540-09

157. Panas MD, Schulte T, Thaa B, Sandalova T, Kedersha N, Achour A, et al. Viral and cellular proteins containing FGDF motifs bind G3BP to block stress granule formation. *PLoS Pathog.* (2015) 11:e1004659. doi: 10.1371/journal.ppat.1004659

158. Gotte B, Liu L, McInerney GM. The enigmatic alphavirus non-structural protein 3 (nsp3) revealing its secrets at last. *Viruses.* (2018) 10:105. doi: 10.3390/v10030105

159. Kim C, Kang H, Kim DE, Song JH, Choi M, Kang M, et al. Antiviral activity of micafungin against enterovirus 71. *Virol J.* (2016) 13:99. doi: 10.1186/s12985-016-0557-8

160. Kim DY, Reynaud JM, Rasalouskaya A, Akhrymuk I, Mobley JA, Frolov I, et al. New world and old world alphaviruses have evolved to exploit different components of stress granules, fxr and g3bp proteins, for assembly of viral replication complexes. *PLoS Pathog.* (2016) 12:e1005810. doi: 10.1371/journal.ppat.1005810

161. Panas MD, Varjak M, Lulla A, Eng KE, Merits A, Karlsson Hedestam GB, et al. Sequestration of G3BP coupled with efficient translation inhibits stress granules in Semliki Forest virus infection. *Mol Biol Cell.* (2012) 23:4701–12. doi: 10.1091/mbc.e12-08-0619

162. Scholte FE, Tas A, Albulescu IC, Zusinaite E, Merits A, Snijder EJ, et al. Stress granule components G3BP1 and G3BP2 play a proviral role early in Chikungunya virus replication. *J Virol.* (2015) 89:4457–69. doi: 10.1128/JVI.03612-14

163. Goertz GP, Lingemann M, Geertsema C, Abma-Henkens MHC, Vogels CBF, Koenraadt CJM, et al. Conserved motifs in the hypervariable domain of chikungunya virus nsP3 required for transmission by aedes aegypti mosquitoes. *PLoS Negl Trop Dis.* (2018) 12:e0006958. doi: 10.1371/journal.pntd.0006958

164. Saxton-Shaw KD, Ledermann JP, Borland EM, Stovall JL, Mossel EC, Singh AJ, et al. O'nyong nyong virus molecular determinants of unique vector specificity reside in non-structural protein 3. *PLoS Negl Trop Dis.* (2013) 7:e1931. doi: 10.1371/journal.pntd.0001931

165. Lastarza MW, Grakoui A, Rice CM. Deletion and duplication mutations in the C-terminal nonconserved region of Sindbis virus nsP3: effects on

phosphorylation and on virus replication in vertebrate and invertebrate cells. *Virology.* (1994) 202:224–32. doi: 10.1006/viro.1994.1338

166. Jadav SS, Sinha BN, Hilgenfeld R, Jayaprakash V. Computer-aided structure based drug design approaches for the discovery of new anti-CHIKV agents. *Curr Comput Aid Drug Design.* (2017) 13:346–61. doi: 10.2174/1573409913666170309145308

167. Alvandi F, Kwitkowski VE, Ko CW, Rothmann MD, Ricci S, Saber H, et al. U.S. Food and drug administration approval summary: omacetaxine mepesuccinate as treatment for chronic myeloid leukemia. *Oncologist.* (2014) 19:94–9. doi: 10.1634/theoncologist.2013-0077

168. Abcam. *Abcam safety data sheet of harringtonine [Abcam safety data sheet of harringtonine].* Available online at: https://www.abcam.com/ps/Products/141/ab141941/Msds/ab141941_CLP1_EN.pdf (accessed October 22, 2019).

169. Wong KZ, Chu J. The Interplay of Viral and Host Factors in Chikungunya Virus Infection: Targets for Antiviral Strategies. *Viruses.* (2018) 10:294. doi: 10.3390/v10060294 (accessed August 13, 2019)

170. Seo JY, Yaneva R, Cresswell P. Viperin: a multifunctional, interferon-inducible protein that regulates virus replication. *Cell Host microbe.* (2011) 10:534–9. doi: 10.1016/j.chom.2011.11.004

171. Teng TS, Foo SS, Simamarta D, Lum FM, Teo TH, Lulla A, et al. Viperin restricts chikungunya virus replication and pathology. *J Clin Invest.* (2012) 122:4447–60. doi: 10.1172/JCI63120

172. Carissimo G, Teo T-H, Chan Y-H, Lee CY-P, Lee B, Torres-Ruesta A, et al. Viperin controls chikungunya virus-specific pathogenic T cell IFNγ Th1 stimulation in mice. *Life Sci Alliance.* (2019) 2:e201900298. doi: 10.26508/lsa.201900298

173. Geller R, Taguwa S, Frydman J. Broad action of Hsp90 as a host chaperone required for viral replication. *Biochim Biophys Acta.* (2012) 1823:698–706. doi: 10.1016/j.bbamcr.2011.11.007

174. Geller R, Vignuzzi M, Andino R, Frydman J. Evolutionary constraints on chaperone-mediated folding provide an antiviral approach refractory to development of drug resistance. *Genes Dev.* (2007) 21:195–205. doi: 10.1101/gad.1505307

175. Wang Y, Jin F, Wang R, Li F, Wu Y, Kitazato K, et al. HSP90: a promising broad-spectrum antiviral drug target. *Arch Virol.* (2017) 162:3269–82. doi: 10.1007/s00705-017-3511-1

176. Hoter A, El-Sabban ME, Naim HY. The HSP90 family: structure, regulation, function, and implications in health and disease. *Int J Mol Sci.* (2018) 19:2560. doi: 10.3390/ijms19092560

177. Jhaveri K, Modi S. Ganetespib: research and clinical development. *OncoTargets Ther.* (2015) 8:1849–58. doi: 10.2147/OTT.S65804

178. Lillsunde KE, Tomasic T, Kikelj D, Tammela P. Marine alkaloid oroidin analogues with antiviral potential: A novel class of synthetic compounds targeting the cellular chaperone Hsp90. *Chem Biol Drug Design.* (2017) 90:1147–54. doi: 10.1111/cbdd.13034

179. Li SF, Gong MJ, Zhao FR, Shao JJ, Xie YL, Zhang YG, et al. Type I interferons: distinct biological activities and current applications for viral infection. *Cell Physiol Biochem.* (2018) 51:2377–96. doi: 10.1159/000495897

180. Hoffmann HH, Schneider WM, Rice CM. Interferons and viruses: an evolutionary arms race of molecular interactions. *Trends Immunol.* (2015) 36:124–38. doi: 10.1016/j.it.2015.01.004

181. Lin FC, Young HA. Interferons: Success in anti-viral immunotherapy. *Cytokine Growth Factor Rev.* (2014) 25:369–76. doi: 10.1016/j.cytogfr.2014.07.015

182. Zhang Y, Burke CW, Ryman KD, Klimstra WB. Identification and characterization of interferon-induced proteins that inhibit alphavirus replication. *J Virol.* (2007) 81:11246–55. doi: 10.1128/JVI.01282-07

183. Couderc T, Chretien F, Schilte C, Disson O, Brigitte M, Guivel-Benhassine F, et al. A mouse model for Chikungunya: young age and inefficient type-I interferon signaling are risk factors for severe disease. *PLoS Pathog.* (2008) 4:e29. doi: 10.1371/journal.ppat.0040029

184. Rudd PA, Wilson J, Gardner J, Larcher T, Babarit C, Le TT, et al. Interferon response factors 3 and 7 protect against Chikungunya virus hemorrhagic fever and shock. *J Virol.* (2012) 86:9888–98. doi: 10.1128/JVI.00956-12

185. Brehin AC, Casademont I, Frenkiel MP, Julier C, Sakuntabhai A, Despres P. The large form of human 2′,5′-Oligoadenylate Synthetase (OAS3) exerts antiviral effect against Chikungunya virus. *Virology.* (2009) 384:216–22. doi: 10.1016/j.virol.2008.10.021

186. Ooi YS, Dube M, Kielian M. BST2/tetherin inhibition of alphavirus exit. *Viruses.* (2015) 7:2147–67. doi: 10.3390/v7042147

187. Cocka LJ, Bates P. Identification of alternatively translated Tetherin isoforms with differing antiviral and signaling activities. *PLoS Pathog.* (2012) 8:e1002931. doi: 10.1371/journal.ppat.1002931

188. Lee SK, Cui B, Mehta RR, Kinghorn AD, Pezzuto JM. Cytostatic mechanism and antitumor potential of novel 1H-cyclopenta[b]benzofuran lignans isolated from Aglaia elliptica. *Chem Biol Inter.* (1998) 115:215–28. doi: 10.1016/S0009-2797(98)00073-8

189. Biedenkopf N, Lange-Grunweller K, Schulte FW, Weisser A, Muller C, Becker D, et al. The natural compound silvestrol is a potent inhibitor of Ebola virus replication. *Antiviral Res.* (2017) 137:76–81. doi: 10.1016/j.antiviral.2016.11.011

190. Muller C, Schulte FW, Lange-Grunweller K, Obermann W, Madhugiri R, Pleschka S, et al. Broad-spectrum antiviral activity of the eIF4A inhibitor silvestrol against corona- and picornaviruses. *Antiviral Res.* (2018) 150:123–9. doi: 10.1016/j.antiviral.2017.12.010

191. Henß L, Scholz T, Grunweller A, Schnierle BS. Silvestrol inhibits chikungunya virus replication. *Viruses.* (2018) 10:592. doi: 10.3390/v10110592

192. Newman DJ, Cragg GM. Natural products as sources of new drugs from 1981 to (2014). *J Nat Prod.* (2016) 79:629–61. doi: 10.1021/acs.jnatprod.5b01055

193. Feher M, Schmidt JM. Property distributions: differences between drugs, natural products, and molecules from combinatorial chemistry. *J Chem Inform Comput Sci.* (2003) 43:218–27. doi: 10.1021/ci0200467

194. Mathur S, Hoskins C. Drug development: Lessons from nature. *Biomed Rep.* (2017) 6:612–4. doi: 10.3892/br.2017.909

195. Leyssen P, Smadja J, Rasoanaivo P, Gurib-Fakim A, Mahomoodally MF, Canard B, et al. Biodiversity as a source of potent and selective inhibitors of chikungunya virus replication. In: Gurib-Fakim A, editor. *Novel Plant Bioresources: Applications in Food, Medicine and Cosmetics.* 1 edition. Hoboken, NJ: John Wiley & Sons, Ltd. (2014). p. 151–61. doi: 10.1002/9781118460566.ch11

196. Vasas A, Hohmann J. Euphorbia diterpenes: isolation, structure, biological activity, and synthesis (2008-2012). *Chem Rev.* (2014) 114:8579–2. doi: 10.1021/cr400541j

197. Goel G, Makkar HP, Francis G, Becker K. Phorbol esters: structure, biological activity, and toxicity in animals. *Int J Toxicol.* (2007) 26:279–88. doi: 10.1080/10915810701464641

198. Remy S, Litaudon M. Macrocyclic diterpenoids from euphorbiaceae as a source of potent and selective inhibitors of chikungunya virus replication. *Molecules.* (2019) 24:e24122336. doi: 10.3390/molecules24122336

199. Newton AC. Protein kinase C as a tumor suppressor. *Semin Cancer Biol.* (2018) 48:18–26. doi: 10.1016/j.semcancer.2017.04.017

200. Bourjot M, Leyssen P, Neyts J, Dumontet V, Litaudon M. Trigocherrierin A, a potent inhibitor of chikungunya virus replication. *Molecules.* (2014) 19:3617–27. doi: 10.3390/molecules19033617

201. Nothias-Scaglia LF, Retailleau P, Paolini J, Pannecouque C, Neyts J, Dumontet V, et al. Jatrophane diterpenes as inhibitors of chikungunya virus replication: structure-activity relationship and discovery of a potent lead. *J Nat Prod.* (2014) 77:1505–12. doi: 10.1021/np500271u

202. Wang QJ, Bhattacharyya D, Garfield S, Nacro K, Marquez VE, Blumberg PM. Differential localization of protein kinase C delta by phorbol esters and related compounds using a fusion protein with green fluorescent protein. *J Biol Chem.* (1999) 274:37233–9. doi: 10.1074/jbc.274.52.37233

203. Wang QJ, Fang TW, Fenick D, Garfield S, Bienfait B, Marquez VE, et al. The lipophilicity of phorbol esters as a critical factor in determining the pattern of translocation of protein kinase C delta fused to green fluorescent protein. *J Biol Chem.* (2000) 275:12136–46. doi: 10.1074/jbc.275.16.12136

204. European Medicines Agency. *EPAR Summary for the Public; EMA/598388/2011: European Medicines Agency;* (2011). Available online at: https://www.ema.europa.eu/en/documents/overview/mycamine-epar-summary-public_en.pdf (accessed May 29, 2019).

205. European Medicines Agency. *Assessment Report for Mycamine: European Medicines Agency;.* (2008). Available online at: http://www.ema.europa.eu/docs/en_GB/document_library/EPAR_-_Public_assessment_report/human/000734/WC500031079.pdf (accessed June 2, 2019).

206. Douglas CM. Fungal beta(1,3)-D-glucan synthesis. *Med Mycol.* (2001) 39(Suppl 1):55–66. doi: 10.1080/mmy.39.1.55.66

207. Dong S, Kang S, Dimopoulos G. Identification of anti-flaviviral drugs with mosquitocidal and anti-Zika virus activity in Aedes aegypti. *PLoS Negl Trop Dis.* (2019) 13:e0007681. doi: 10.1371/journal.pntd.0007681

208. Mastrangelo E, Pezzullo M, De Burghgraeve T, Kaptein S, Pastorino B, Dallmeier K, et al. Ivermectin is a potent inhibitor of flavivirus replication specifically targeting NS3 helicase activity: new prospects for an old drug. *J Antimicrob Chemother.* (2012) 67:1884–94. doi: 10.1093/jac/dks147

209. Ortiz LM, Lombardi P, Tillhon M, Scovassi AI. Berberine, an epiphany against cancer. *Molecules.* (2014) 19:12349–67. doi: 10.3390/molecules190812349

210. Varghese FS, Thaa B, Amrun SN, Simarmata D, Rausalu K, Nyman TA, et al. The antiviral alkaloid berberine reduces chikungunya virus-induced mitogen-activated protein kinase signaling. *J. Virol.* (2016) 90:9743–57. doi: 10.1128/JVI.01382-16

211. Srikrishna D, Godugu C, Dubey PK. A review on pharmacological properties of coumarins. *Mini Rev Med Chem.* (2018) 18:113–41. doi: 10.2174/1389557516666160801094919

212. Hwu JR, Kapoor M, Tsay SC, Lin CC, Hwang KC, Horng JC, et al. Benzouracil-coumarin-arene conjugates as inhibiting agents for chikungunya virus. *Antiviral Res.* (2015) 118:103–9. doi: 10.1016/j.antiviral.2015.03.013

213. Qiu L, Patterson SE, Bonnac LF, Geraghty RJ. Nucleobases and corresponding nucleosides display potent antiviral activities against dengue virus possibly through viral lethal mutagenesis. *PLoS Negl Trop Dis.* (2018) 12:e0006421. doi: 10.1371/journal.pntd.0006421

214. Crance JM, Scaramozzino N, Jouan A, Garin D. Interferon, ribavirin, 6-azauridine and glycyrrhizin: antiviral compounds active against pathogenic flaviviruses. *Antiviral Res.* (2003) 58:73–9. doi: 10.1016/S0166-3542(02)00185-7

215. Raekiansyah M, Buerano CC, Luz MAD, Morita K. Inhibitory effect of the green tea molecule EGCG against dengue virus infection. *Arch Virol.* (2018) 163:1649–55. doi: 10.1007/s00705-018-3769-y

Conflict of Interest: The authors declare that the research was conducted in the absence of any commercial or financial relationships that could be construed as a potential conflict of interest.

IV.   OBJECTIVES

This thesis describes experiments with Chikungunya virus and has the focus on three different objectives.

Objective I: Evaluation of different human cell lines for their potential as *in vitro* cell models for infection with wild type (CHIKV^{Brazil}) and lab adapted (CHIKV^{Ross}) CHIKV strains, and for antiviral testing.

Most antiviral *in vitro* assays against CHIKV are conducted in Vero cells. This cell line neither represents the relevant species (human) nor the relevant clinical site of CHIKV infection (joints, muscles or CNS). Finding a suitable *in vitro* cell model to represent neurogenic CHIKV disease in humans was thus one objective of this thesis. Additionally, lab-adapted CHIKV strains may differ considerably from field isolates as far as cell affinity and antiviral sensitivity are concerned. This is why we compared the lab-adapted CHIKV strain Ross with a CHIKV field isolate from Brazil for their ability to infect different cell lines and how they are affected by different antiviral substances. Furthermore, we sequenced the genomes of both strains to identify possible mutations that might explain the observed differences.

Objective II: Test a panel of 34 selected compounds *in vitro* for their antiviral activity against wt CHIKV isolate from Brazil.

To date, there are no approved antiviral drugs available for the treatment of CHIKF (or other alphaviruses). By screening 34 potential antiviral candidates via cell viability assays for their efficacy against a CHIKV field isolate, one other objective was to identify a candidate with IC_{50} in the low micromolecular range and high CC_{50} and thus a wide selectivity index (SI = CC_{50}/IC_{50}).

Objective III: Compare different antiviral assay methods and evaluate their feasibility for investigating antivirals against CHIKV in U138 cells.

There are different assay methods to test antiviral activity against a virus (e.g., cell viability assays, virus yield assays) or the potential cytotoxicity of antiviral candidates in cells. As it was possible to identify a human glioblastoma cell line for antiviral assays against CHIKV, one objective was to asses if this cell line was equally well suited for different assay methods as Vero-B4 and yielded comparable results.

V.   MATERIALS AND METHODS

1.   Cell line experiments

All equipment and solutions that came into contact with cells were sterile. Cell related work was done under a Class-II-biosafety cabinet (Claire pro B3-190, Berner, Germany) in a BSL-2 lab. All cell culture incubations were performed in a > 95% humidified, 37 °C incubator with 5% CO_2. All solutions with direct contact to the cells had been warmed up to room temperature or 37 °C in advance. All cell lines portrayed below are adherent.

1.1.   Cell culture

Cells were cultured in sterile T75 cell culture flasks with vented caps, (NUNC™ EasY Flask™ 75 m^2 Nunclon™ Delta Surface, Thermo Fischer Scientific, Denmark) with 10 mL of Dulbecco's Modified Eagle Medium (DMEM(1X) + GlutaMAX™-I medium, Thermo Fisher Scientific Ltd, UK), depending on the cell line with either 1 g/L of D-glucose (in the following referred to as Low Glucose (LG)) or with 4.5 g/L of D-glucose (High Glucose (HG) and 5% heat inactivated Foetal Bovine Serum (FBS, Sigma-Aldrich, Hilden, Germany) in an incubator at 37 °C with a 5% CO_2 setting and humidified atmosphere (Heracell, Thermo Scientific). Cells requiring DMEM HG medium are U138, U251. Cells that grow on DMEM LG medium are Vero-B4, A549, DBTRG and Huh-7.

Cell confluence was controlled every other day with a microscope. The cells were split when they exceeded a confluence of 80%.

Cells were split using the following protocol (modified from Ammerman, Beier-Sexton [109]):

➢ Remove cell supernatant and place bottle vertically.

➢ Add 1.5 mL of trypsin (TrypLE™ Express, Gibco, Life Technologies Limited, UK) to each bottle, distribute it equally on the cell layer by gently canting the bottle.

➢ Remove trypsin and add another 0.5 mL of fresh trypsin.

➢ Place bottle into an incubator at 37 °C and 5% CO_2 for 5 min.

➢ Gently shake or tap the flask to detach cells.

➢ Add 10 mL DMEM with 5% FBS to inactivate trypsin and wash down cells in media, pipetting gently to break up clumps of cells.

➢ Prepare desired dilution of cells by removing superfluous amounts of cells and adding up the bottle with fresh medium to a total of 10-15 mL DMEM with 5% FBS. Depending on the cell line, dilutions of 1:5 to 1:10 were done.

Media were renewed depending on media pH.

Counting and seeding cells

Supernatant of an 80% confluent T75 flask was removed and 1.5 mL of trypsin added to the flask. After cells detached from the bottle, 10 mL of culture medium was added to the flask and gently mixed to ensure that the cells did not clump. The contents of the bottle were transferred into a 15 mL conical tube (Cellstar® Tubes, Greiner Bio-One, Germany); 10 µL of 0.4% trypan blue (Gibco) was added into a 1.5 mL Eppendorf tube and mixed with 10 µL of the cell suspension. After 5 minutes 10 µL of the dye-cell-mixture was put on a Neubauer improved cell counting camber (NanoEnTek Inc. South Korea). The cells were counted using a LeicaDM3000 microscope (Leica, Wetzlar, Germany) according to the generally used formula:

$$\frac{\text{Cells}}{\text{mL}} = \left(\frac{(\text{number of cells counted}) \times (\text{dilution factor})}{(\text{number of large squares counted}) \times (\text{volume of 1 large square})}\right) \times 1000$$

Depending on the number of cells, adequate dilutions were made with the cell specific growth media to achieve the required cell concentrations.

Cells were seeded into the various plates using an Eppendorf Multipette® plus pipet with 10 mL Combitips advanced® (Eppendorf, Germany).

Contamination:

Cells were checked for mycoplasma contamination every other month. A PCR for mycoplasma was performed with the cell supernatant in which the cells had grown for at least 30 hours. Cells were deliberately kept in antibiotics-free medium to be able to spot contaminations immediately. In case of contamination, the flasks were destroyed or the running experiment was aborted and redone.

1.1.1.   A549

The A549 cell line (ATCC® CCL-185™) originates from a human lung carcinoma [110]. Its morphology is epithelial-like (Figure 5A) and doubling time is 24 hours. For maintenance bottles were split in a ration of 1:10 twice a week. To have a full bottle within the next day, split ratio was 2-3:10. Cells were kept in DMEM LG with 5% FBS.
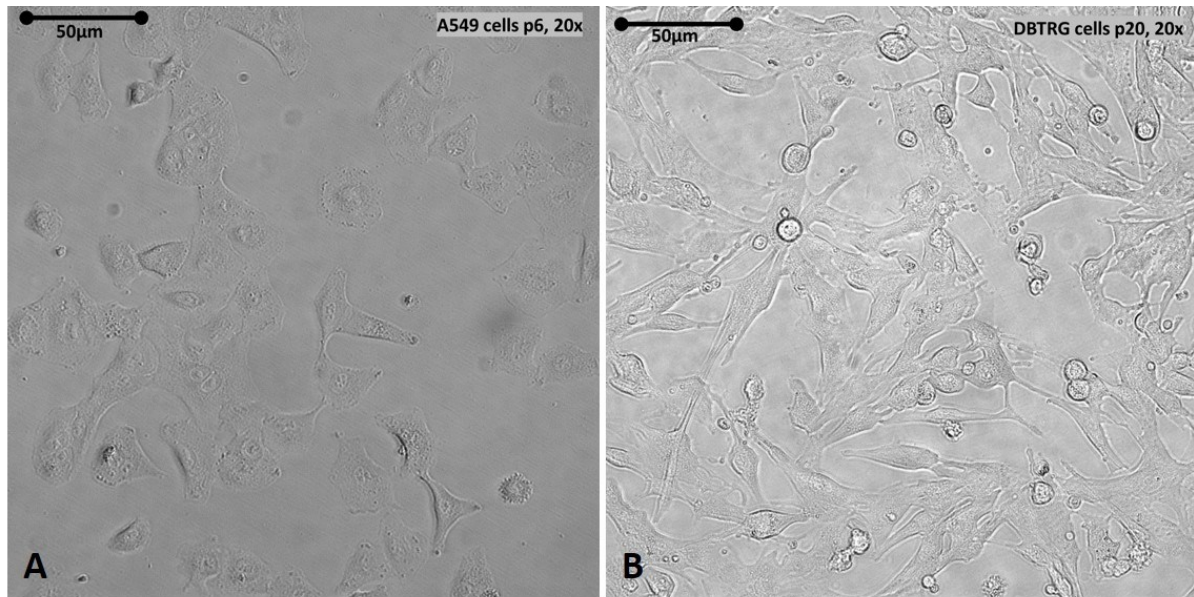
Figure 5: Microscopic pictures of A549 and DBTRG cells
A) A549 cells at about 50% confluency, B) 70% confluent DBTRG cells. Pictures were taken with the Leica DM3000 microscope and the Leica Application Suite Version 4.1.0. Magnification and the passage (p) of the cells are stated on the top right corner of the photos.

1.1.2.   DBTRG

The glioblastoma cell line DBTRG-05MG (ATCC® CRL-2020™) was established out of tissue from a patient with glioblastoma multiforme who had been treated with local brain irradiation and multidrug chemotherapy [111]. The cells have a spindle, fibroblast-like morphology (see Figure 5B). Doubling time is around 48 hours. The cells were kept in DMEM LG with 5% FSB and split in a ratio of 2:10 twice a week.

1.1.3.   Huh-7

The Huh-7 cell line (JCRB0403) (Figure 6A) has been initiated out of a human hepatocellular carcinoma by Nakabayashi, Taketa [112]. The cells grow in an epithelial way and double every 24 hours. Cells were kept in DMEM LG with 5% FBS and were split twice a week in a ratio of 1:10.
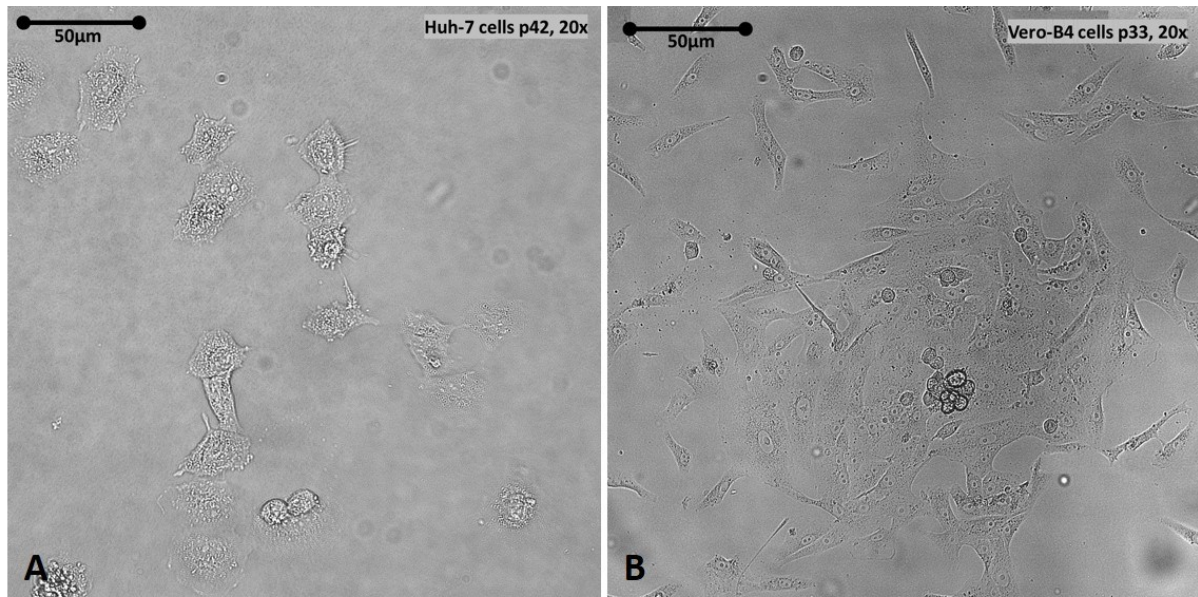
Figure 6: Microscopic photo of Huh-7 and Vero-B4 cells
A) Huh-7 cells at a confluency of about 20%, B) 60% confluent Vero-B4 cells. Pictures were taken with the Leica DM3000 microscope and the Leica Application Suite Version 4.1.0. Magnification and the passage (p) of the cells are stated on the top right corner of the photos.

1.1.4. Vero-B4

The Vero cell line (ATCC® CCL-81™) comes from the kidney of a normal, adult, African green monkey (*Cercopithecus aethiops*) [11]. The cells grow in an epithelial way (Figure 6B). Split ratios for maintaining bottles were 1:10 twice a week. The cells double in about 24 hours. Vero-B4 cells were kept in DMEM LG with 5% of FBS.

1.1.5. U138 and U251

The human glioblastoma cell lines U138 (ATCC® HTB-16™) and U251 (ATCC® HTB-17™; formerly known as U-373 MG) are adherent [113, 114], show different proliferation rates and morphologies. While U251 (Figure 7B) double in about 23 hours and grow in an epithelial and pleomorphic way, U138 (also epithelial) take up to 70 hours to double (Figure 7A). This was taken into consideration when maintaining and using the cells in the various assays. Both cell lines were kept in DMEM HG medium with 5% of FBS.
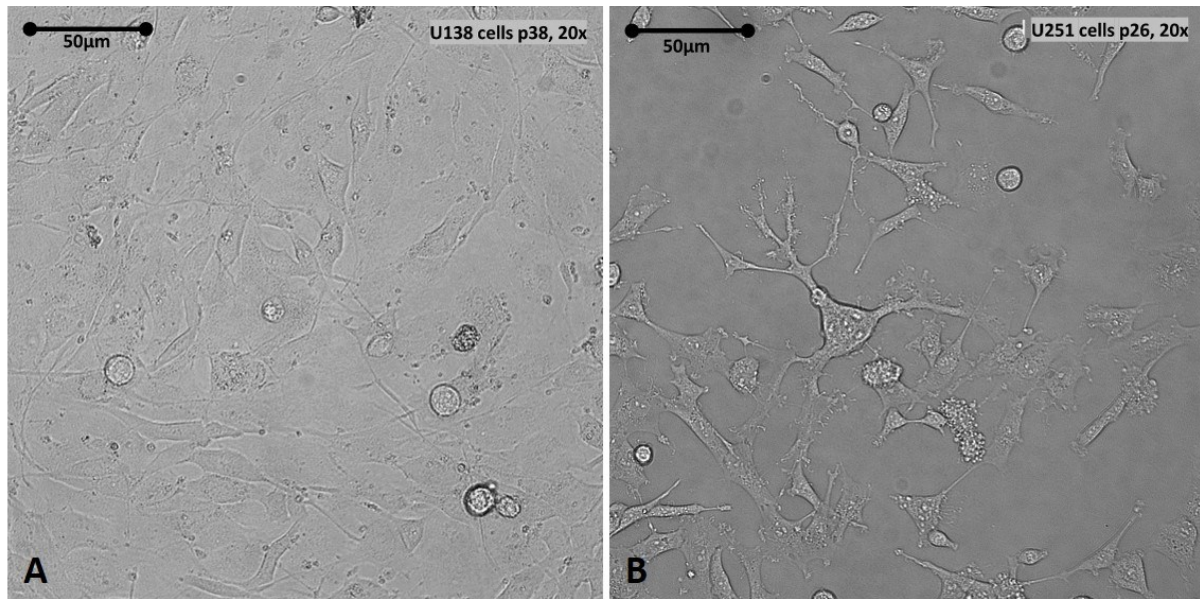
Figure 7: Microscopic photo of U138 and U251 cells
A) U138 cells at about 60% confluency, B) 45% confluent U251 cells. Pictures were taken with the Leica DM3000 microscope and the Leica Application Suite Version 4.1.0. Magnification and the passage (p) of the cells are stated on the top right corner of the photos.

U138 need cell-to-cell contract to proliferate. The cells were split in a ratio of 3:10 when maintaining the bottles and 5:10 when preparing for an 80-90% confluent bottle in 1-2 days' time. Due to long doubling time, infection experiments with U138 cells were run for 5 days instead of 4 days.

U251 were split twice a week in a ratio of 1:10. The cells were kept in DMEM HG with 5% of FBS. U251 turned out especially sensitive to overgrowing.

1.2.   Evaluation of seeding density of Huh-7 cells with MTS

100 µL Huh-7 cells per well were plated in a 96-well plate in various cell densities (5×10^2, 1×10^3, 5×10^3 and 1×10^4 cells/well) in DMEM LG 5% FBS the previous day. The following day, 100 µL of DMEM LG without supplementation of FBS was added to mimic the future toxicity experiments and the plate was then incubated for 5 days at 37 °C and 5% CO_2 and humified atmosphere. After 5 days, 20, 30 or 40 µL of MTS/PMS (CellTiter 96®AQ$_{ueous}$ Non-Radioactive Cell Proliferation Assay (MTS) (Promega, USA)) solution were added (Table 2). The plate was then incubated again at 37 °C and 5% CO_2. Absorbance was measured at 490 nm in the VictorX5 Reader after 1 and 2 hours of incubation. Each set of parameters was repeated at least 3 times.

1.3. **Kill curves**

See VI.1 CHIKV strains Brazil (wt) and Ross (lab-adapted) differ with regard to cell host range and antiviral sensitivity and show CPE in human glioblastoma cell lines U138 and U251

1.4. **Evaluation of CHIKV binding on different cell lines via immunofluorescence test (IFT)**

Two 12-well multiwell plates (Greiner Bio-one, Frickenhausen, Germany) were prepared with sterile round glass cover slips (16 mm diameter) for each well and 5×10^4 cells/mL/well were seeded with each cell line infection being repeated 3 times and one well holding non-infected cells (Mock). DMEM LG with 5% FBS was used as medium for Vero-B4, A549, Huh-7, U251 and DBTRG cells, while U138 were kept in high glucose medium. The cells were allowed to settle overnight and the next day the supernatant was removed. 500 µL of virus dilution with a MOI of 0.065 were added to each infection well. The plates were incubated for 1 hour at 37 °C with 5% CO_2 and > 95% humidified atmosphere. After incubation, the supernatant was removed and replaced with 1 mL of DMEM HG with 2.5% FBS. Plates were then put back in the incubator.

Two days after infection, the supernatant of the cells was removed and cells were fixed with ice cold methanol-acetone (1:1) and put in the -80 °C freezer for 30 minutes. Then, the coverslips (CS) were removed from the wells, washed twice with PBS and allowed to dry. Then each CS was covered with 1% BSA in PBST (blocking buffer) for 30 min to block unspecific binding of the antibodies. Then, 100 µL of the primary antibody (anti-CHIKV (IgG) antibody by Euroimmun F160129BF diluted 1:100 in blocking buffer) were added and the CS were incubated in a humidified chamber for 1 hour RT. Then the CS were washed 3 times with PBS. The CS were then covered with 100 µL of a 1:1000 dilution of secondary antibody (Alexa Fluor 488 goat α-human IgG by Invitrogen in 1% BSA in PBST) and incubated in a humidified chamber for 1 hour at RT without light. Then CS were washed with PBS three times. For counterstaining of nucleoli, 100 µL of 0.1-1 µg/mL DAPI (DNA stain) was mounted on the CS and incubated for 1 min, then washed off again with PBS. After drying, mounting medium was applied to each CS which were then transferred on glass slides (2 cover slips each) and sealed with nail polish. Finished slides were stored in the dark at -20 °C or 4 °C.

For microscopy, the Confocal Laser Scanning Microscope LSM 710 by Zeiss or the Leica DMI 3000 B microscopes, a 40x or 63x object lens and immersion oil was used.

1.4.1.   Microscopes

Leica DMI 3000 B microscope

Leica DMI 3000 B is a manual inverted research microscope provided by Leica Microsystems. This microscope is suitable for fluorescence and many other uses like live cell, time-lapse imaging, high-speed multi-fluorescence optical sectioning, micromanipulation and more. The microscope was used for routine investigations in infected and backup cells and for simple fluorescence imaging.

LSM 710 - Confocal laser scanning microscope

The LSM 710 is a fully motorised upright confocal microscope constructed by Carl Zeiss. It is an instrument capable of creating detailed, high-contrast images. It has an excitation laser light suppression. This kind of microscope is generally used with fluorescence optics. While conventional fluorescence microscopes illuminate the whole specimen, the confocal laser scanning microscope (CLSM) captures the light that is emitted by a single plane of the sample. A laser beam (LASOS RMC 7812 Z1 Argon laser) scans the specimen pixel by pixel and line by line. The fluorescence emitted from the illuminated material is collected and brought to an image at a suitable light detector. A pinhole aperture is placed in front of the detector, at a position that is conjugated to the plane in focus. This pinhole obstructs the light that comes from objects outside that plane. Thus, only light from objects that are in focus can reach the detector. Pictures were taken using the ZEN 2.1 Software by Zeiss.

1.5.   Investigating CHIKV yield in different cell lines via RT-PCR

1.5.1.   Infection of cells and sample taking

A549, Huh-7, Vero-B4, DBTRG and U138 cells were plated in a 24-well plate at a cell density of 1×10^5 Cells/mL/well. Cells were kept in DMEM LG with 5% FBS, the brain derived cells (DBTRG and U138) were kept in DMEM HG medium. Cells were incubated and allowed to settle overnight. Virus dilutions were made with DMEM to get MOIs of 0.1, 0.01 and 0.001. For infection, the supernatant was removed and 100 µL of the virus dilution was put on the corresponding wells (non-infected Mock controls were treated with 100 µL of DMEM) and incubated for 10 minutes. Then 1000 µL of DMEM LG/HG with 5% FBS were added to the wells. A 50 µL sample of the supernatant was collected (0*dpi*) and diluted in 450 µL of DMEM. 140 µL of this 1:10 diluted sample was put in 560 µL AVL buffer with 5.6 µL cRNA and stored at -80 °C until RNA purification for PCR. Samples were taken every day at the same time. Before taking samples, 50 µL of growth medium were added to each well to keep the volumes in the wells adjusted. Experiments ran for 5 days and were repeated 3 times independently.

1.5.2.   **Purification of CHIKV RNA**

Purification of CHIKV specific RNA was either done manually with the QIAmp® RNA Mini Kit (Qiagen) or automatically with the QIACube (Qiagen, Hilden, Deutschland) with the corresponding RNA purification Kit according to the user manual. Purifications were done in a separate lab with no CHIKV related work, to prevent contamination of the samples. Purified samples were stored at -80 °C until PCR was done. With each purification run, a control (RNase free water) was purified as well. A 10-fold dilution of the CHIKV stock was purified to create a standard curve in the reverse transcriptase (RT) -PCR.

Denaturing of CHIKV was done by lysing the sample under highly denaturing conditions to inactivate RNases and to ensure isolation of intact viral RNA. The principle of the kit lies in the binding of the RNA to a QIAamp silica membrane while contaminants are efficiently washed away by using different wash buffers.

1.5.3.   **Chikungunya virus RT-PCR**

RealStar® Chikungunya RT-PCR Kit 2.0 (Altona, Hamburg, Germany) was used for the *in vitro* qualitative detection of CHIKV specific RNA. The test was conducted according to the manufacturer's protocol. With the alteration that sample size was 12.5 µL instead of 25 µL. The composition of the master mix, the thermoprofile, as well as the measured colours are displayed in Table 1.

The master mix was done in a spatially separated area to prevent contamination. The reagents were added into a 1.5 mL Eppendorf tube, mixed by pulse-vortexing it and centrifuged briefly. Per sample 20 µL were pipetted into a PCR tube (Eppendorf, Germany), and 10 µL of sample were added. Measurements of fluorescence were done using a RotorGeneQ thermocycler (Quiagen, (Hilden, Germany)) or the Light Cycler® 480 (Roche) during the amplification cycle.

Table 1: Master Mix, temperature profile and colour channels for Chikungunya-real time-PCR 2.0 according to Altona.

Master Mix		
Master A		5 µL
Master B		15 µL
Internal Control IC		1 µL
Reaction:	20 µL Master Mix + 10 µL sample	
Thermological profile		
Hold (reverse transcription)	1x	20 min at 55 °C
Denaturing	1x	15 sec at 95 °C
Amplification (Cycling)	45x	15 sec at 95 °C 45 sec at 55 °C 15 sec at 15 °C
Reading		
CHIKV Quantification		FAM
Reference internal control		JOE

1.5.4. Data Evaluation

Evaluation of the PCR was done using the Rotor-Gene Q – Pure Detection Software Version 2.3.1 (Quiagen)/ Light Cycler® 480 Software (Roche) Excel (Microsoft) and GraphPad Prism 6. Samples with cycle threshold (Ct) values of < 35 and with sigmoid curves were considered positive. With each PCR a negative and a positive control were run along as well as a 10-fold dilution of virus stock RNA to create a standard curve to be able to estimate the amount of viral RNA. Calculations, trendline, equation and coefficient of determination (R^2) were done using Microsoft Excel and the graph of the standard curve was done with GraphPad Prism 6 programme. For yield curves means and standard deviations were calculated from three independent experiments with Microsoft Excel. Curves were then created using GraphPad Prism 6.

2. Chikungunya virus propagation and evaluation

All live CHIKV related work was done in a BSL-3(**) lab under a Class II biosafety cabinet (Berner Claire® pro, Berner International GmbH, Germany). Once the virus had been deactivated, work was continued under BSL-2 lab conditions. The CHIKV strain (L3-4497 DH 150827) originates from a patient isolate from Brazil (2015) (in this thesis further referred to as CHIKV[Brazil]; GenBank accession number Banklt2561907 Chikungunya_Brazil_4497 ON009842.). CHIKV had been diagnosed via IFT by the diagnostic laboratory (ZBD) of the Institute of Microbiology of the German Armed Forces when the sample had arrived. Serum of the patient had been used to infect Vero-B4 and C6/36 cells to grow and multiply the virus for the reference stocks.

2.1.   **Virus stock production**

For the production of a working CHIKV stock, the wildtype (wt) CHIKV^{Brazil} isolate L3-4497 that had previously been cultivated on Vero-B4 (Stock #6) and C6/36 (Stock #7) cells by the ZBD were used. CHIKV stock production was done as described in VI.1

2.2.   **Plaque assay for CHIKV stock titre**

Plaque assays were done using Vero-B4 and U138 cells as described in VI.1

2.3.   **Electron microscopy**

After cultivating CHIKV^{Brazil} in Vero-B4 cells for 4 days, 80 µL of supernatant was inactivated with 10 µL of 25% glutaraldehyde and 10 µL of 20% paraformaldehyde (both Merck, Germany). Hydrophilisation of the grids was done with 1% alcian-blue (according to the recipe of the RKI); negative contrast staining was done with phosphotungstic acid (1%; Merck, Germany).

For verification, the VirusExplorer20151127 of the Robert Koch Institute (RKI) [115] was taken into consideration as well as the publication of Noranate, Takeda [116]. Electron microscopy was done with the Zeiss Libra 120 TEM using Image SP Software and the TEMCon32 Programme (Zeiss, Germany). Magnification was 80 000x.

3.   **Antiviral compounds and reference substance testing**

A total number of 34 antiviral compounds were provided from medical chemists Andrea Brancale and Marcella Bassetto in Cardiff [117]. All compounds were sent to us as solid powders and dissolved in DMSO (Dimethyl sulfoxide HyBRI-MAX®, Sigma-Aldrich®, UK). Stock solutions with concentrations of 10 mM were created and frozen until needed at -20 °C. For further delusions assay medium was used (DMEM LG). The wells of the screening and plaque reduction assay contained compounds at a concentration of 10 µM and 0.1% of DMSO.

3.1.   **1st Series: *in silico* nsP2 protease inhibitors**

The first series encompassed 19 compounds (#1-19) which were all modelled *in silico* after the hit of Bassettos study in 2013 (Figure 8). The general idea behind the constructs can be seen in Figure 8. For the complete list of the series-1 compounds see Appendix XII.1.1.1. These compounds were designed as nsP2 protease inhibitors and were constructed to match the nsP2 CHIKV protease active site with the binding amino acid residues His1083, Cys1013, Asn1082, and Trp1084 forming the docking pose.
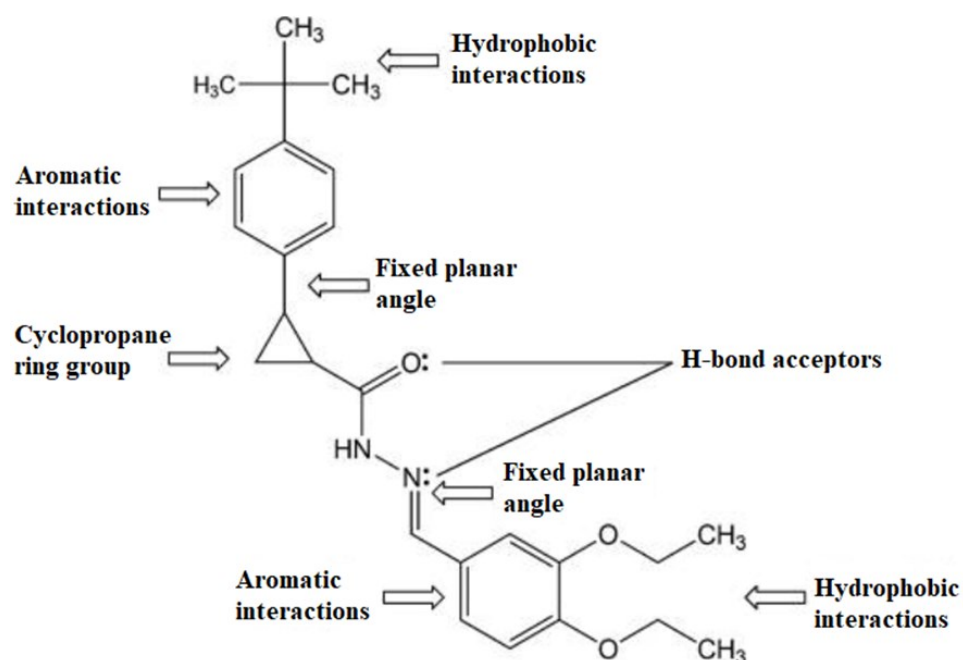
Figure 8: Pharmacophoric characterisation of the compounds from our first Bassetto series.
The molecule features two terminal aromatic/hydrophobic groups, a hydrogen bonding donor and acceptor centres in the bridge structure. All nsP2 inhibitors crudely follow this scheme, with differences either in the terminal aromatic/hydrophobic groups and/or the H-bond accepting middle part. Only three of the 19 protease inhibitors contained the cyclopropane ring group at the upper fixed planar angle. In other constructs, the ring was replaced by various forms of $-CH_2-$ links. (Picture altered from Das, Puusepp [118])

3.2. 2nd Series: Nucleoside analogues and ProTides of defluorinated favipiravir (T-1105)

The second series consists of 15 analogues of the defluorinated favipiravir (T-1105). These compounds are either direct nucleoside (purine) analogues (#20-26) or ProTides (meaning, they are pronucleotides that consist of a 5'-nucleoside monophosphate/phosphonate in which the two hydroxyl groups are masked with an amino acid ester and an aryloxy moiety) (#27-34). Either way, they are meant to interfere with the nsP4 polymerase and the viral DNA/RNA synthesis (usually by causing termination of the nascent DNA/RNA chain) or by inhibition of cellular or viral enzymes that are involved in the nucleoside/tide metabolism. For the complete list of the series 2 compounds see Appendix XII.1.1.2.

3.3. Reference substances

Ribavirin (RBV) was used at a concentration of 410 µM as a control, since Briolant, Garin [119] and Gallegos, Drusano [120] had previously published IC_{50} values for RBV in similar *in vitro* assays of 341 µM and 419 µM respectively. Franco, Rodriquez [121] confirmed an IC_{50} of 408.2 µM in Vero cells. RBV was dissolved in sterile water and held in stocks of 100 mg/mL (= 410 mM).

Since the 34 compounds were dissolved in DMSO and wells held final DMSO concentrations of 0.1% in the screening and the plaque reduction assay, Mock controls as well as CHIKV infected cells without compound also contained 0.1% of DMSO.

3.4. Screening assays for selecting working compounds

3.4.1. Screening of the compounds via viability assay (MTS)

The viability of the infected cells was evaluated with the CellTiter 96®AQ$_{ueous}$ Non-Radioactive Cell Proliferation Assay (MTS) (Promega, USA) according to the manufacturer protocol with the difference that 20 µL (not 40 µL) of the combined MTS/PMS solution was use per 200 µL/well in all MTS assays.

Cells were seeded in a clear 96-well plate at a density of 1×10^4 cells/100 µL per well (Vero-B4, U138) or 1×10^3 cells/100 µL per well (Huh-7, toxicity only) the previous day in DMEM with 5% FBS and allowed to settle overnight. The next day, 50 µL of compound was added to a final concentration of 10 µM in the well, 1 hour prior to adding 50 µL of CHIKV at a MOI of 0.64. Chemotoxicity was run parallelly in the same way, but by adding 50 µL of DMEM instead of the virus solution. The plates were incubated at 37 °C and 5% CO_2 with > 95% relative humidity for 4 days (Vero-B4 and Huh-7) or 5 days (U138). Then 20 µL of MTS/PMS solution were added to each well and the plates were incubated for 1 and 2 hours. Absorbance was measured using either the iMark™ Mikroplate Reader or the VictorX5 (toxicity only) at a wavelength of 490 nm. Experiments were repeated three times independently with each well having three technical replicates. Raw data were converted to percentages of controls with Microsoft Excel and statistical analysis as well as graphs were done with GraphPad Prism 6 software.

3.4.2. Plaque reduction assay

Vero-B4 cells were plated at 1.2×10^5 cells/mL/well in DMEM LG with 5% FBS in a clear 24-well plate (Cellstar®, Greiner, Germany). After settling overnight, supernatant was removed and 500 µL of compound in DMEM LG with 2.5% of FBS was added (final drug concentration per well: 10 µM). After 1 hour of incubation at 37 °C and 5% CO_2, 100 µL of a CHIKV dilution that was calculated to produce about 20-40 plaques per well, was added. After 30 minutes, 400 µL methylcellulose (Sigma-Aldrich, Germany) overlay (3 parts 2.5% methylcelluloses in H_2O and one part of DMEM LG and 2.5% FBS) was added, (final methylcellulose concentration: 0.875%; final FBS concentration: 1.5% per well). As a control RBV was used (410 µM). The plates were checked for CPE daily with a microscope. Three to four days *pi* 1 mL of crystal violet solution (0.2% crystal violet and 20% formaldehyde (both Merck, Germany)) was added directly on the overlay of each well. The plate was then sealed and put

into the fridge overnight. The following day, the plates were gently washed with ddH_2O (using a serological pipet) 3 times. The plates were dried and plaques were evaluated. Each compound was repeated twice per plate and compounds which displayed interesting results were repeated in multiple independent experiments.

3.5.   Assays with selected compounds against CHIKV

3.5.1.   Virus yield assay with selected compounds in U138 cells

U138 cells were plated in a 24-well plate with 1.5×10^5 cells/well in DMEM HG with 5% FBS. Cells were allowed to settle overnight and incubated at 37 °C with 5% CO_2 and > 95% humidified atmosphere.

Treatment: The next day, supernatant was removed and 1 mL of the compound dilutions added to the corresponding wells and incubated for 30 minutes (37 °C, 5% CO_2). Cells were treated with either of compound #13 or T-1105 (both at 10 µM), 410 µM of RBV or 0.1% of DMSO. Mock control corresponds to non-infected, untreated cells while positive control are infected, untreated cells (both with 0.1% DMSO).

Infection and sampling: Supernatants were removed and 100 µL of CHIKV[Brazil] at a MOI of 0.001 was put on the cells, distributed evenly and the plate incubated for 10 minutes. Virus had previously been diluted in DMEM. Mock controls were treated likewise but with 100 µL of DMEM. Then 1000 µL of the corresponding compound dilution (in DMEM with 5% FBS) were added to the cells and gently mixed. Supernatant samples of 50 µL was collected every day. Before taking samples, 50 µL of growth medium including the corresponding compound were added to the well so to keep the volumes in the wells adjusted.

The samples were diluted 1:10 with DMEM and 140 µL of the dilution was mixed with 560 µL of AVL buffer with 5.6 µL cRNA and stored at -80 °C until further processing. Experiments ran for 5 days and were repeated 3 times independently. For **purification of the CHIKV RNA and Chikungunya RT-PCR** see IV. 1.5.2 and VI. 1.5.3.

Evaluation

All samples with Ct levels of < 35 and with sigmoid curves were considered positive. Means and standard error of mean (SEM) were calculated from three independent experiments with Graph pad Prism 6. Curves were created with the same programme. Statistical significance was calculated with a two-way ANOVA test, comparing infected but untreated cells with the treated cells at different time points (day 0 to day 5 *post* infection).

3.5.2.   IC$_{50}$/CC$_{50}$ of selected compounds

Cells were seeded in a clear 96-well plate at a density of 1×10^4 cells/100 µL per well (Vero-B4, U138) or 1×10^3 cells/100 µL per well (Huh-7, toxicity only) the previous day in DMEM LG

(U138 in HG) with 5% FBS and allowed to settle overnight. Serial dilutions of the compounds were prepared in (DMEM LG). One hour before infection, 50 µL of the compound dilution was added and the cells were incubated for 1 hour. Upon infection 50 µL of a virus dilution (MOI 0.325 or 0.355) (efficacy) or 50 µL of medium (toxicity) was added. The plates were incubated at 37 °C with 5% CO_2 and > 95% relative humidity for 4 (Vero-B4 and U138 efficacy) to 5 (toxicity in Huh-7 and U138) days. After incubation, each well was treated with 20 µL of MTS/PMS solution (Promega), then incubated for 1 to 2 hours. Absorbance was measured using either the iMark™ Mikroplate Reader or the VictorX5 (toxicity only) at a wavelength of 490 nm.

The serial dilution of the compounds had a final well concentration as follows:

-   Compound #13 had 0.5 to 30 µM in efficacy and toxicity assays.
-   T-1105 had 1 to 100 µM efficacy and toxicity assays.
-   RBV had between 10 and 700 µM in the assays.

Mock and untreated infected cells contained 0.3% of DMSO.

Each compound concentration was done in triplets and each plate was repeated at least in three different independent experiments. Raw data were converted to percentages of controls with Microsoft Excel and a t-test was done to analyse the probability. Raw data were then transferred to GraphPad Prism 6 and IC_{50} and CC_{50} values were derived from the dose-response curves that was analysed by the programme. IC_{50} value were calculated in relation to the raw data values of the most efficient compound concentration (= relative IC_{50}). CC_{50} was calculated in relation to non-infected untreated cells (Mock control). Goodness of fit and plausible range are given by R^2 and 95% Confidence Interval (95%CI). If a raw data value deviated more than 20% from the mean of the repeats, this particular value was omitted.

3.6.   Real-time cell analysis (RTCA) with xCELLigence

Real-time cell analysis (RTCA) monitors cell viability in a dynamic and non-offensive way. The xCELLigence (ACEA Biosciences, San Diego, CA USA) is a microelectronic biosensor technology that measures electronic impedance based on the cell adherence to the plate. The impedance is defined as CI (Cell Index) and gives information on the cell status (differences in cell number, adhesion degree, cellular morphology and viability) [122].

The xCELLigence RTCA system encompasses an electronic sensor analyser, a device station, a control unit, and E-Plate 96. In this study the provided software was RTCA Software 2.0 (Roche). Voltage for the analyser was between 100 V and 240 V with a frequency of 50 Hz to 60 Hz. The device station was placed in the incubator at least 4 hours before the beginning of the experiment.

3.6.1. Cell growth and proliferation assay with RTCA

The growth, proliferation and adhesion kinetics of Vero-B4, Huh-7, U138 and U251 cells were determined using RTCA technology to find the ideal cell amount for seeding. A volume of 50 µL of DMEM LG (U138 wells with HG) with 5% FBS was put in each well of the 96-well E-plate (gold-microelectrode array integrated E-plate; ACEA Biosciences, San Diego, CA USA). The plate was installed in the device station for background impedance reading and checking the connections of the electrodes. Serial dilutions of 2.5×10^3, 5×10^3, 7.5×10^3, 1×10^4, 1.5×10^4 and 2×10^4 cells in 50 µL DMEM HG were prepared. Then 50 µL of cell suspension was added to each well (total volume of 100 µM/well). The E-plates were incubated at RT for 30 min in a laminar flow cabinet and then placed on the RTCA SP Station in the incubator at 37 °C. CI values were measured every 15 minutes. After 20 hours, 100 µL of DMEM LG/HG without FBS was added to mimic the conditions of the planned infection experiment. Experiments ran for 5 days. Measurements, raw data evaluation and graphs were done by RTCA Software 2.0 (Roche). Data points represent means ± standard deviation from 2 independent experiments with 4 or 6 technical replicates each.

3.6.2. Efficacy and toxicity of antivirals against CHIKV using RTCA

A volume of 50 µL of DMEM LG (HG for U138) with 5% FBS were added to each well of a 96-well E-plate. The plate was installed in the device station for background impedance reading and connections check. Then, Vero-B4, U138 and Huh-7 cells (toxicity only) were seeded in the 96-well E-plate at a concentration of 1×10^4 cells/50 µL, incubated at RT for 30 min under the laminar flow cabinet and then placed on the RTCA station and incubated at 37 °C until the next day. Nineteen to 24 hours after seeding the plate was detached from the device station and 50 µL of the compound (diluted in DMEM LG/HG) was added to the corresponding wells. The plate was replaced in the RTCA station and incubated for 1 hour.

Cells were then either infected with CHIKV[Brazil] (by adding 50 µL of virus dilution, MOI 0.4) for efficacy testing or not (addition of 50 µL DMEM) for toxicity evaluation. Final FBS concentration/well was 2.5%. Final compound concentrations were: #13 at 10 µM, T-1105 at 10 and 50 µM, RBV at 410 µM. Non-infected and untreated Mock and positive control contained 0.1% of DMSO, which corresponds to the DMSO in the #13 and T-1105 treated cells. All wells were done in triplets. The plate was replaced in the RTCA station and monitored for close to 6 days. Impedance was measured every 15 min. The experiment was repeated three times independently. Measurements and raw data were done by RTCA Software 2.0 (Roche). Raw data was transferred to Microsoft Excel and mean ± standard deviation from significant time points (9 data sets (3 independent experiments each with 3 technical replicates)) were

calculated. Then graphs and statistical analysis were done with GraphPad Prism 6 software. A one-way ANOVA Sidiak's multiple comparison test was done comparing compound treated cells with the positive control (infected but not treated cells; efficacy evaluation) or non-infected, untreated Mock (toxicity evaluation).

4.   Controls

Control compounds:

Ribavirin (RBV): All compound assays contained a RBV control with 410 µM of RBV. At this concentration, RBV showed antiviral activity with statistical significance against CHIKV in all our assays.

Defluorinated favipiravir (T-1105): Compound #25 corresponds to T-1105, defluorinated favipiravir. It was included in all experiments for selected compounds at a concentration of either 10 µM or 50 µM as previous IC_{50} values published by Delang, Segura Guerrero [123] ranged were 7.0 ± 1 µM and 47 ± 12 µM (depending on the protocol).

Other controls:

Cell culture was checked for mycoplasma contamination every 4 months via PCR from supernatant. Contaminated cells were eliminated.

PCR

Preparation of PCR samles and preparation of master mix were done in a spacially separated area to avoid cross contamination.

Purification control: To exclude CHIKV RNA cross contamination of samples and/or reagents, a purification control was made. In every RT-PCR a sample with RNase free water (Qiagen) was purified and treated the same way as the experimental samples.

Negative control: Likewise, one sample containing RNase free water was mixed with the PCR reagents and added in every RT-PCR alongside the other samples to see if there was a contamination either of the PCR regents or by pipetting.

Positive control: A sample which was known to contain viral RNA and was provided by the manufacturer of the RT-PCR Kit was put in every PCR as a positive control.

5.   Statistical data analysis

Screening assay with MTS: Mean values and standard deviation (SD) were calculated using Microsoft Excel and analysed with GraphPad Prism 6 using a One-Way ANOVA (analysis of variance) with a multiple comparisons test. The means of treated and infected cells were compared either to CHIKV infected, untreated cells (to determine efficacy) or Mock (non-

infected untreated cells) (to determine toxicity). P-values < 0.05 indicated by asterisks show differences among the means which are statistically significant.

Yield assay: All samples with Ct levels of < 35 and with sigmoid curves were considered positive. Means and standard error of mean (SEM) were calculated from three independent experiments with GraphPad Prism 6. Curves were created with the same programme. Statistical significance was calculated with a two-way ANOVA test, comparing infected but untreated cells with the treated cells at different time points (day 0 to day 5 *pi*).

IC$_{50}$/CC$_{50}$ evaluation with MTS: Raw data were converted to percentages of controls with Microsoft Excel and a t-test was done to analyse the probability. Data were then transferred to GraphPad Prism 6 programme and IC$_{50}$ or CC$_{50}$ values were calculated via dose-response curves (equation: log(inhibitor) *vs*. normalised response with variable slope). R^2 and 95% confidence interval (95%CI) was also calculated by the programme.

xCELLigence analysis: For RTCA data analysis, the normalised CI value was calculated for each well. This was done automatically by the RTCA Software 2.0 (Roche). Curves, means and standard deviation of cell growth and proliferation assays were done with the RTCA Software. Means and standard deviations of efficacy and toxicity RTCA assays were calculated with Microsoft Excel (data points are the mean ± standard deviation from nine data sets (3 independent experiments with 3 identical wells each)). Graphs and statistics were done with GraphPad Prism 6. An ordinary one-way ANOVA Sidiak's multiple comparison test was done comparing either untreated infected cells (positive control; efficacy evaluation) or untreated Mock (toxicity evaluation) with the treated groups. P-values were calculated and are given in the graphs indicated with asterisks as p-value * < 0.05; ** < 0.01; *** < 0.005; **** < 0.0001.

VI. RESULTS

1. CHIKV strains Brazil (wt) and Ross (lab-adapted) differ with regard to cell host range and antiviral sensitivity and show CPE in human glioblastoma cell lines U138 and U251

Friederike I. L. Hucke[1],*, Malena Bestehorn-Willmann[1], Marcella Bassetto[2], Andrea Brancale[3], Paola Zanetta[4], Joachim J. Bugert[1]

[1]Bundeswehr Institute of Microbiology, Neuherbergstraße 11, 80937 München, Germany

[2]Department of Chemistry, Faculty of Science and Engineering, Swansea University, United Kingdom

[3]Cardiff School of Pharmacy and Pharmaceutical Sciences, Cardiff University, United Kingdom

[4]Laboratory of Applied Microbiology, Center for Translational Research on Allergic and Autoimmune Diseases (CAAD), Department of Health Sciences (DISS), School of Medicine, Università del Piemonte Orientale (UPO), 28100 Novara, Italy

The manuscript is presented in its published form and has therefore its own reference section formatted in the style of the journal. References and abbreviations from the manuscript are not included in the relevant sections at the beginning and the end of this document. Figures and tables are numbered individually within the manuscript. The corresponding supplementary material has been added directly following the reference section of this publication.

ORIGINAL PAPER

CHIKV strains Brazil (wt) and Ross (lab-adapted) differ with regard to cell host range and antiviral sensitivity and show CPE in human glioblastoma cell lines U138 and U251

Friederike I. L. Hucke[1] · Malena Bestehorn-Willmann[1] · Marcella Bassetto[2] · Andrea Brancale[3] · Paola Zanetta[4] · Joachim J. Bugert[1]

Abstract

Chikungunya virus (CHIKV), a (re)emerging arbovirus, is the causative agent of chikungunya fever. To date, no approved vaccine or specific antiviral therapy are available. CHIKV has repeatedly been responsible for serious economic and public health impacts in countries where CHIKV epidemics occurred. Antiviral tests in vitro are generally performed in Vero-B4 cells, a well characterised cell line derived from the kidney of an African green monkey. In this work we characterised a CHIKV patient isolate from Brazil (CHIKV[Brazil]) with regard to cell affinity, infectivity, propagation and cell damage and compared it with a high-passage lab strain (CHIKV[Ross]). Infecting various cell lines (Vero-B4, A549, Huh-7, DBTRG, U251, and U138) with both virus strains, we found distinct differences between the two viruses. CHIKV[Brazil] does not cause cytopathic effects (CPE) in the human hepatocarcinoma cell line Huh-7. Neither CHIKV[Brazil] nor CHIKV[Ross] caused CPE on A549 human lung epithelial cells. The human astrocyte derived glioblastoma cell lines U138 and U251 were found to be effective models for lytic infection with both virus strains and we discuss their predictive potential for neurogenic CHIKV disease. We also detected significant differences in antiviral efficacies regarding the two CHIKV strains. Generally, the antivirals ribavirin, hydroxychloroquine (HCQ) and T-1105 seem to work better against CHIKV[Brazil] in glioblastoma cells than in Vero-B4. Finally, full genome analyses of the CHIKV isolates were done in order to determine their lineage and possibly explain differences in tissue range and antiviral compound efficacies.

Edited by A. Lorena Passarelli.

✉ Friederike I. L. Hucke
  fr_hucke@freenet.de

[1] Bundeswehr Institute of Microbiology, Neuherbergstraße 11, 80937 Munich, Germany

[2] Department of Chemistry, Faculty of Science and Engineering, Swansea University, Swansea, UK

[3] Cardiff School of Pharmacy and Pharmaceutical Sciences, Cardiff University, Cardiff, UK

[4] Laboratory of Applied Microbiology, Center for Translational Research on Allergic and Autoimmune Diseases (CAAD), Department of Health Sciences (DISS), School of Medicine, Università del Piemonte Orientale (UPO), 28100 Novara, Italy

Abbreviations

95% CI	95% Confidence interval
Abs	Absorption
CC_{50}	Half maximal cytotoxic concentration
CHIKF	Chikungunya fever
CHIKV	Chikungunya virus
Cp	Capsid protein
CPE	Cytopathic effect
CQ	Chloroquine
DENV	Dengue virus
dpi	Days post infection
ECSA	East-Central-South African
FBS	Foetal bovine serum
FDA	U.S. Food and Drug Administration
GAG	Glycosaminoglycans
HCQ	Hydroxychloroquine
HG	"High glucose"; medium supplemented with 4.5 g/L of D-glucose

IC$_{50}$	Half maximal inhibitory concentration
IOL	Indian Ocean Lineage
LG	"Low glucose"; medium supplemented with 1 g/L of D-glucose
MOI	Multiplicity of infection
n	Number of independent repetitions
NC	Nucleocapsid
nsp	Non-structural protein
RBV	Ribavirin
RdRp	RNA-dependent RNA polymerase
SD	Standard deviation
SFV	Semliki Forest virus
SI	Selectivity index
SINV	Sindbis virus
WA	West African
wt	Wild type
ZIKV	Zika virus

Introduction

Taxonomy, structure, genome organisation, ecology, and epidemiology

Chikungunya virus (CHIKV) is an arthropod borne (arbo-) virus of the *alphavirus* genus. Belonging to the "Old World" viruses, CHIKV is categorised as an arthritogenic alphavirus due to the primary site of disease manifestation, the joints [1].

To date three CHIKV phylogroups and one distinct sub-lineage are known. The phylogroups consist of the West African (WA), East-Central-South African (ECSA) and Asian genotype [2]. The Indian Ocean Outbreak, which started in Kenya in 2004, was caused by a mutated sublineage that is referred to as the Indian Ocean Lineage (IOL) and originated from of the ECSA isolates [3].

CHIKV is an enveloped virus and the virion contains single-standed, positive-sense RNA of about 11,800 nucleotides [4]. The virus has the general structure of all alphaviruses (for details on structure, epidemiology, and pathogenesis see Hucke, Bestehorn-Willmann [5] and Hucke and Bugert [6]).

CHIKV is generally transmitted to humans by the bite of an infected mosquito from the *Aedes* family, mainly *Aedes aegypti* and *Aedes albopictus* [7]. After entering the skin, viral replication and amplification seem to occur mainly in dermal fibroblasts [8]. Dendritic cells capture virus particles, transport them to the nearest lymph nodes where blood monocytes and macrophages are infected. At this point viremia sets in [9]. Via blood stream CHIKV then reaches the muscles and joints. Infection of these sites causes the main symptoms of CHIKF—myalgia and arthralgia. Infection of the joints often results in cartilage degradation and bone loss [10], which explains the severe and debilitating arthralgia that are the hallmark of the disease and gave the virus its name. After the acute phase of the illness has passed, myalgia and arthralgia can go into a chronic state and last for months or even years, leaving the patient with a severely deteriorated quality of life.

Apart from these well-known sites of infection, CHIKV has been known to infect a wide range of secondary organs which may cause severe complications in patients [7]. Although CHIKV has originally not been classified as a neurotropic virus, the La Reunion outbreak recorded an increased number of neurological complications (*e.g.* meningitis, encephalitis, febrile seizures, Guillain Barré syndrome, neuro-ocular diseases), especially in the elderly and the very young [11, 12]. It was demonstrated that CHIKV is able to replicate in neurons, astrocytes, oligodendrocytes, and microglia cells [13].

To date, no approved vaccine or specific antiviral therapies are available. Considering the time it takes to fully recover from CHIKV disease, an effective antiviral is of utmost importance. A variety of antivirals curb CHIKV infection in vitro but lack efficacy in vivo [6]. Well established antivirals for in vitro assays are chloroquine/hydroxychloroquine, ribavirin, and favipiravir, although they show significant differences in their efficacy depending on the virus strain and cell line [6].

So far, little focus has been given on which human cell lines are suitable for in vitro studies with CHIKV. Also the question on whether different virus strains show different cell affinities in relevant human cell lines has not been addressed properly. Furthermore, antivirals might have different efficacies depending on the cell line and the virus strain. There is the possibility that high-passage, laboratory-adapted strains (such as CHIKV^{Ross}) are able to replicate in cell lines which are not affected by wt CHIKV infection. This raises the question to which extent such high-passage reference strains are still comparable to field strains in regard of antiviral efficacies.

To shed light on these questions, two different CHIKV strains, the high-passage Ross strain, isolated in 1953 (CHIKV^{Ross}), and a field isolate from Brazil, isolated in 2015 (CHIKV^{Brazil}) were compared with regard to cell affinity and drug sensitivity towards well established antiviral substances. Finally, a whole genome sequence comparison of both strains was performed to try to explain differences in cell affinity or drug sensitivities on a genomic level.

Materials and methods

Cells and cell culture

Vero-B4 cells (ATCC® CCL-81™) [14], A549 cells (ATCC® CCL-185™) [15], Huh-7 cells (JCRB0403) [16],

the glioblastoma cell line DBTRG-05MG (ATCC® CRL-2020™) [17], were obtained from ATCC whilst the human glioblastoma cell lines U138 (aka U-138 MG, ATCC® HTB-16™) and U251 (aka U-251 MG, ATCC® HTB-17™; formerly known as U-373 MG) were a gift of R. Brack-Werner, Institute of Virology, German Research Center for Environmental Health (GmbH).

Dulbecco's Modified Eagle Medium (DMEM(1X) + GlutaMAX™-I medium, Thermo Fisher Scientific Ltd, UK), with either 1 g/L of D-glucose (in the following referred to as "Low Glucose" (LG)) or with 4.5 g/L of D-glucose ("High Glucose" (HG)) were used. 5% heat inactivated foetal bovine serum (FBS; Sigma-Aldrich, Hilden, Germany) was added. U138 and U251 cells were kept on DMEM HG medium whilst Vero-B4, A549, DBTRG, and Huh-7 were kept on DMEM LG.

Antiviral substances

The antiviral compound T-1105 was provided by the School of Pharmacy and Pharmaceutical Sciences of the Cardiff University, UK. T-1105 is a direct nucleoside (purine) analogue and the defluorinated analogue of favipiravir (T-705). The compound was provided as a solid powder and was dissolved in DMSO to create a 10 mM solution.

Other antiviral substances used as controls were ribavirin (RBV), and hydroxychloroquine (HCQ) (both from Sigma-Aldrich). RBV and HCQ were dissolved in purified water to create stock solutions of 100 mM and 10 mM, respectively. For further dilutions DMEM LG was used.

Virus

Viruses used in this study are part of the BSL3 reference collection of the Bundeswehr Institute of Microbiology (IMB), Munich. The wildtype CHIKV strain L3-4497 originates from a patient isolate from Brazil (CHIKV^{Brazil}; 2015). Sub-passaged samples of the initial cultivation (Vero-B4) were used to establish a working stock of CHIKV (also grown on Vero-B4). In this study the wildtype CHIKV strain used had previously been passaged twice on Vero-B4 cells after its isolation. GenBank accession number: Banklt2561907 Chikungunya_Brazil_4497 ON009842.

The lab attenuated CHIKV Ross strain L3-3950 (CHIKV^{Ross}; NH177) has been isolated from an outbreak in Tanzania in 1953 [18–20]. GenBank accession number: Banklt2561907 Chikungunya_Ross_NH177 ON009843.

Both virus strains belong to the ESCA genotype.

Virus stock production

Vero-B4 cells were cultivated in a T75 flask in DMEM LG with 5% FBS until they reached 80% confluence. After removal of supernatant and a one-time washing with DMEM LG, 500 μL of the original virus stock suspension from the L3 reference stocks were added to the T75 cell culture flask and canted gently to ensure the virus reached the entire cell layer. After one minute, 20 mL of DMEM LG with 5% FBS were added to the bottle and subsequently flasks were incubated at 37 °C and 5% CO_2 until maximal cytopathic effect (CPE) was observed via microscope (Zeiss Axiovert25, Germany).

Two to three days post infection the supernatant of the bottle was collected, FBS was added to a final concentration of 20%, and the virus solution was aliquoted into 1 mL cryotubes with 500 μL of CHIKV suspension each and stored at -70 °C. Virus stock titres were evaluated via plaque assay.

Virus tittering via plaque assay

One mL of Vero-B4 and U138 cells (1.2×10^5 cells/mL) were seeded into a 24-well plate and allowed to settle overnight. The next day, the supernatant of the cells was removed and cells were infected with 200 μL of a tenfold serial dilution (DMEM LG) of CHIKV^{Brazil} or CHIKV^{Ross} (Vero-B4 cells only).

The plate was gently swayed and incubated for 30 min at 37 °C and 5% CO_2.

Then, 800 μL of 0.8–1% carboxymethylcellulose (CMC) (Sigma-Aldrich, Schnelldorf, Germany) dissolved in Milli-Q water, sterilised by autoclaving, mixed with DMEM and 2.5% FBS, was carefully added to each well using a multi-pette (Eppendorf, Germany). The plate was then incubated at 37 °C with 5% CO_2 and observed daily for CPE with a microscope. Three to four days pi the cells were fixed and dyed by adding 1 mL of crystal violet (aqueous solution with 0.2% certified crystal violet and 20% formaldehyde (both from Merck, Darmstadt, Germany)) directly to each well. The plate was then incubated in the fridge at 4 °C overnight. Plates were then gently washed with distilled water until all the CMC and superfluous dye had been removed. Plaque assays with Vero-B4 cells were repeated at least 3 times independently. Assays with U138 cells were repeated twice.

Cell viability assay with MTS and data evaluation

Unless stated otherwise, cells were seeded at a density of 1×10^4 cells/100 μL/well in DMEM with 5% FBS in clear 96-well plates and allowed to settle overnight. The plates were incubated at 37 °C with 5% CO_2 and 95–99% relative humidity. For treatment 50 μL of compound dilution were added to the corresponding wells. Virus infection was done with 50 μL of CHIKV dilution one hour after treatment. Toxicity assays and untreated non-infected (Mock) control were done adding 50 μL of medium instead of virus dilution.

Final FBS concentration in the treated/infected wells was 2.5%. The plates were then incubated for 4 days.

All cell viability assays were done using the CellTiter 96®AQ$_{ueous}$ Non-Radioactive Cell Proliferation Assay (MTS) (Promega, USA) according to the manufacturer's protocol with the difference that 20 µL MTS solution were used per 200 µL of experimental volume. Absorbance was measured at 490 nm with a reference wavelength of 620 nm using an ELISA plate reader (iMark™ Mikroplate Reader).

Apart from IC$_{50}$/CC$_{50}$ evaluation, the Optical Density (OD) values obtained were put into relation to Mock control with Microsoft Excel. Mock thus represents 100% viable cells in the column graphs. All graphs were prepared using GraphPad Prism 6 Software.

For comparisons of the different virus strains, ordinary one-way ANOVA tests were done (GraphPad). Probabilities of the test results are given with *p*-values.

Raw data values were put into relation with Mock control (Mock = 100%) and the positive control (untreated infected cells = 0%) in Excel. For calculation of IC$_{50}$ and CC$_{50}$ values, a dose–response curves equation (using raw data) of Graph-Pad Prism 6 was applied. The programme then calculated the relative IC$_{50}$ value in relation to the raw data values of the most efficient compound concentration. Goodness of fit and plausible range are given by R^2 and 95% Confidence Interval (95% CI). If a raw data value deviated more than 20% from the mean of the repeats, this particular value was omitted.

Kill curves

Apart from Huh-7 cells, all cells were seeded at a density of 1×10^4 cells/100 µl/well in DMEM with 5% FBS in 96-well plates. Huh-7 cells were seeded with only 5×10^3 cells/100 µl/well, due non-linear readout with CellTiter 96®AQ$_{ueous}$ Non-Radioactive Cell Proliferation Assay at higher concentration. After settling overnight, the cells were infected with 50 µL of virus dilutions ranging from 0 to 10^{-5} and incubated for 30 min. Then 50 µL of DMEM were added. Kill curve infection experiments were repeated at least thrice independently, with three technical replicates. Cell viability was evaluated using MTS.

Comparison of compound efficacy

RBV, HCQ, and T-1105 were used in concentrations previously published to inhibit wt CHIKV in Vero cells [21, 22]. The concentration used in our experiments were thus: RBV at 410 µM, HCQ at 10 µM, T-1105 at 10 µM and 50 µM.

As T-1105 was dissolved in DMSO, final DMSO concentration in all wells of the assay was uniformly 0.1% (Mock and positive control as well) to make sure the controls were unbiased by the solvent.

Treatment and infection of the cells were done as described in the IC$_{50}$/CC$_{50}$ experiments with the difference that multiplicity of infection (MOI) was 0.64. Each compound concentration had three or six technical replicates and the experiments were repeated at least thrice independently.

IC$_{50}$/CC$_{50}$ evaluation of RDV, HCQ, and T-1105 in Vero-B4 and U138 cells

For IC$_{50}$/CC$_{50}$ evaluation Vero-B4 and U138 cells were used. Serial dilutions of the compounds (RBV, HCQ, and T-1105) were prepared in assay medium (DMEM LG). To avoid precipitation of T-1105, a final concentration of 0.3% DMSO was kept in all wells containing this compound (and in the corresponding control wells). Serial dilutions of RBV ranged from 10 to 500 µM in U138 cells and 200 µM to 1000 µM in Vero-B4 and the toxicity assays. Serial dilutions of HCQ and T-1105 ranged from 1 to 100 µM. A volume of 50 µL of the compound dilution was added to the cells. Infection was done at a MOI of 0.355 with the CHIKV strain Brazil. As T-1105 had DMSO as a supplement to ensure solubility, two different kind of Mock and positive control (untreated infected cells) were run along, one with 0.3% of DMSO and the other without. Each compound was repeated at least thrice independently with three technical replicates.

Whole genome sequencing of chikungunya virus L3-4497 strain Brazil and Ross L3-3950 from InstMikroBio BW

For sequencing one vial of the respective stock solutions of CHIKV$^{Brazil/Ross}$ was used and the total RNA was purified using the Viral RNA Mini Kit (Qiagen, Hilden, Germany) according to the manual. For Library preparation the NEB-Next® Ultra™ II RNA Library Prep Kit for Illumina® was used according to the manufacturer's protocol. Paired-end sSequencing of the generated libraries was performed on an Illumina MiSeq platform using a Miseq Reagent Kit V2 500 cycles chemistry.

De novo assemblies were generated for the two samples using the tool SPAdes version: 3.14.1. Pairwise alignments of the two generated whole genomes were generated using the ClustalW algorithm.

Results

Genome differences between the two virus strains

The CHIKV virus strains CHIKV^{Ross} and CHIKV^{Brazil} belong to the ECSA genotype. Genome analysis revealed

57 amino acid differences in the structural and non-structural polyproteins between our Brazilian field isolate and the Ross strain as shown in Fig. 1. For complete genome sequences of both virus strains see GenBank accession numbers Banklt2561907 Chikungunya_Ross_NH177 ON009843 and Banklt2561907 Chikungunya_Brazil_4497 ON009842.

Kill curve experiments

Vero-B4 cells are very sensitive to CHIKV infection. Even at an MOI of 0.000645 CHIKV Ross still killed more than 60% of Vero-B4 4 days post infection (*4dpi*) in the MTS cell viability test. In a one-way ANOVA comparison of both CHIKV strains, no statistically significant difference could be detected with regard to cell infectivity and cell death between CHIKV^{Brazil} and CHIKV^{Ross} in Vero-B4 cells (Fig. 2A).

A549 did not show any cytopathogenic effects (CPE) when infected with either CHIKV strain (Fig. 2B). Only at the highest MOI (6.45) with CHIKV^{Ross}, limited cell death could be observed (65.96% ± 11.74% viable cells). Infection with a MOI of 63.5 and 6.35 of wt CHIKV even indicated proliferating cells (> 100% viable cells).

The human hepatoma cell line Huh-7 only showed cell death when infected with wt CHIKV^{Brazil} at a very high MOI of 127 (Fig. 2C). Infection with MOI of 12.7 and lower did not result in a statistically different cell viability than non-infected Huh-7 cells. Infection with CHIKV^{Ross} resulted in extensive cell death *4dpi* when a MOI was between 0.0129 and 12.9 (80% dead Huh-7 cells). CHIKV^{Ross} infection at a MOI 0.00129 still killed 45% of Huh-7 cells *4dpi*. The comparison of the two CHIKV strains at corresponding MOI displayed a highly significant difference with $p < 0.0001$ between 0.0129 and 12.9 (Fig. 2C).

The brain derived cell line DBTRG was susceptible to CHIKV infection in a dose-dependent manner. At MOI ≥ 0.064, both virus strains showed diminished cell viability that was statistically significant ($p < 0.0001$) from non-infected cells (Fig. 2D). The wt CHIKV^{Brazil} had similar significance at MOI 0.00064. High MOI (≥ 6.4) of both virus strains were needed to achieve extensive cell death > 50%.

The U138 cell line was susceptible to CHIKV infection and the cells showed extensive CPE *4dpi* with either CHIKV strain. CHIKV^{Ross} showed significantly more dead cells at a MOI 0.064 than CHIKV^{Brazil} (35.5% vs. 56.2% surviving cells; $p < 0.001$). Likewise at a MOI of 0.64, 32% of the U138 cells survived CHIKV^{Brazil} whilst 21% survived CHIKV^{Ross} (Fig. 2E).

U138 did not show plaques when infected with CHIKV^{Brazil}, although the plaque assays with U138 were conducted the same way as with Vero-B4.

U251 cells were more sensitive to CHIKV infection than U138 cells. At a MOI of 0.00064 of CHIKV Ross only 30.69 ± 18.46% of U251 cells survived after 4 days. There is however, no MOI dependent linear progression of the curve but rather an undulated one as far as CHIKV^{Ross} on U251 is concerned (Fig. 2F). Four days after infection of U251 cells with CHIKV^{Brazil} at MOI 0.00064, 56.32 ± 25.64% of the cells had survived. CHIKV^{Brazil} at MOI ≥ 0.0064 kills > 65–70% of the U251 cells.
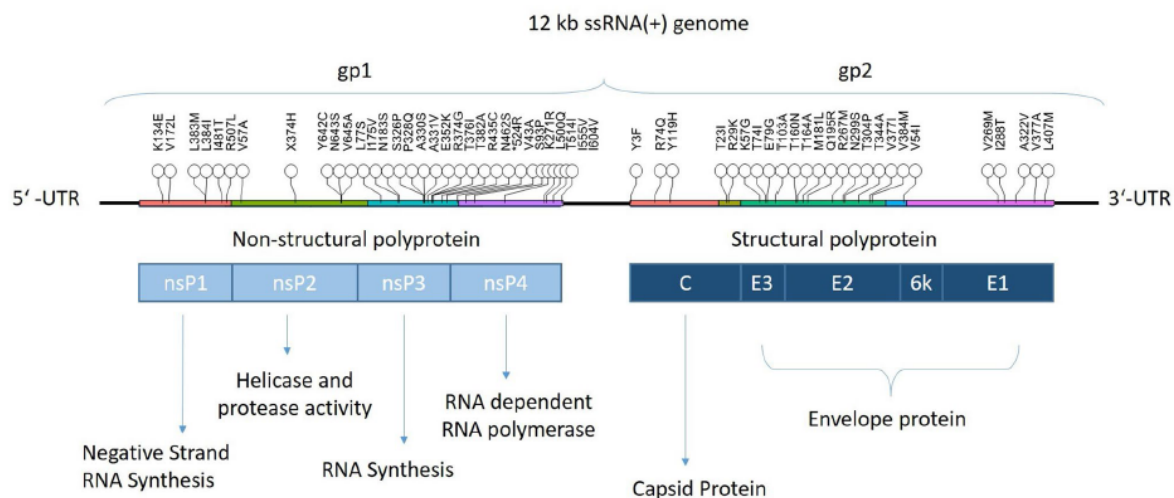
Fig. 1 Genome structure and amino acid differences between CHIKV^{Brazil} and CHIKV^{Ross}. Differences in amino acids (single letter code) as Brazil-position-Ross
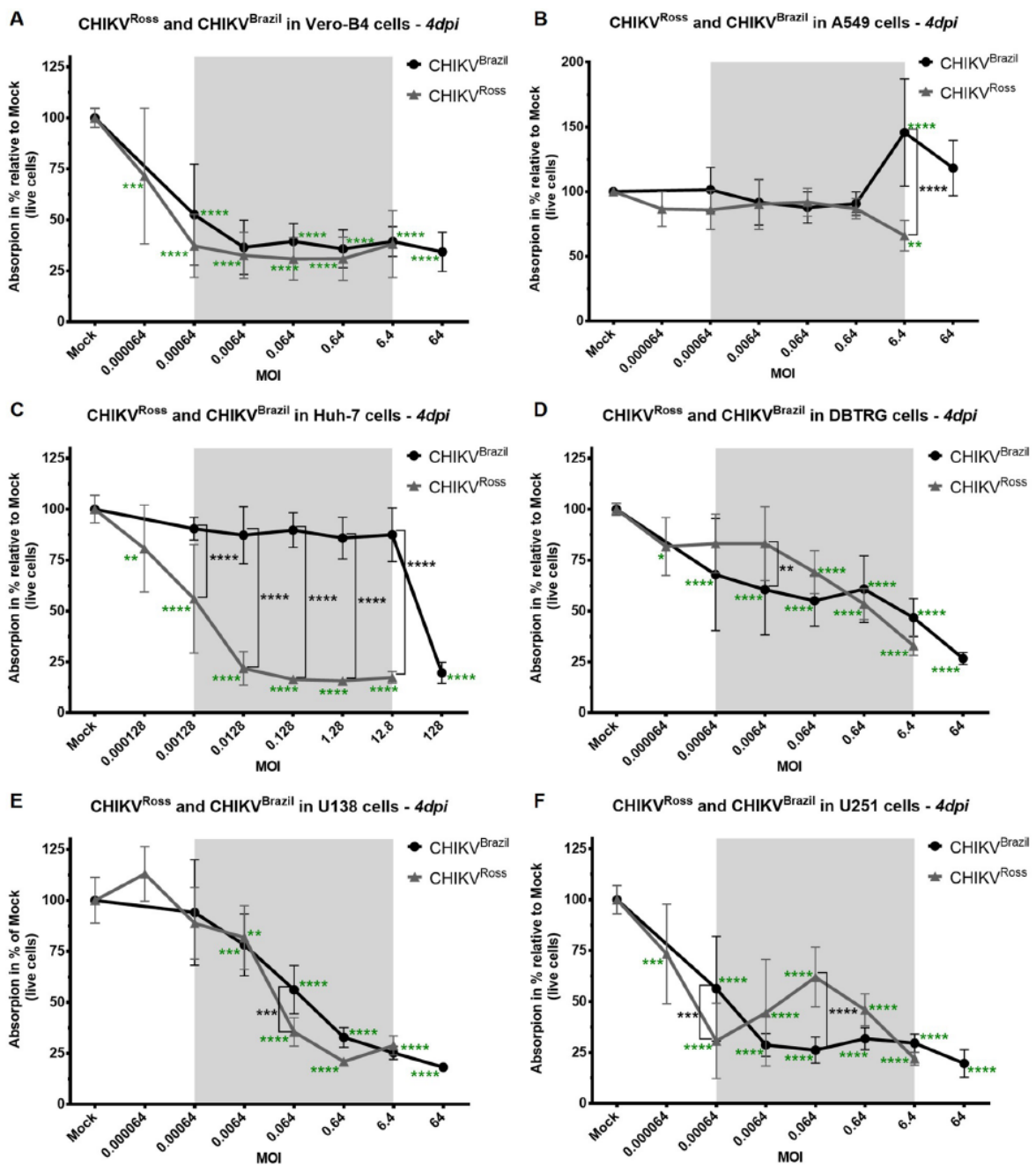
Fig. 2 Effect of CHIKV[Ross] and CHIKV[Brazil] on different cell lines. Comparison of the infectivity/cell damage caused by two CHIKV strains CHIKV[Brazil/Ross] at increasing MOI. Cell viability was measured in a colorimetric assay (MTS cell viability test) *4dpi*. Data are means±SD of at least three independent experiments with three technical replicates, with 100% corresponding to non-infected cells (Mock). Asterisks indicating the *p*-values generated in a one-way ANOVA test comparison of non-infected cells with infected cells (green asterisks), and of the different virus strains at the same MOI (grey area and black asterisks). *p*-values are indicated as follows: *$p < 0.05$; **$p < 0.01$; ***$p < 0.001$; ****$p < 0.0001$. **A** Vero-B4 cells (1×10^4 cells/well); **B** A549 cells (1×10^4 cells/well); **C** Huh-7 cells (5×10^3 cells/well); **D** DBTRG cells (1×10^4 cells/well); **E** U138 cells (1×10^4 cells/well); **F** U251 cells (1×10^4 cells/well)

Comparison antiviral compounds vs virus/cell line

In Vero-B4 cells none of the administered compounds displayed any efficacy against either CHIKV strain (MOI: 0.64) at the applied concentrations (Fig. 3A). In U138 cells, RBV (410 µM), T-1105 (50 µM), and HCQ (10 µM) showed statistically significant efficacy against both CHIKV strains ($p < 0.0001$) (Fig. 3C). RBV and HCQ protected U138 cells significantly better from CPE caused by wt CHIKV[Brazil] than from the lab strain CHIKV[Ross] ($p < 0.001$ and < 0.0001, respectively).

In the toxicity testing Vero-B4 cells treated with T-1105, and HCQ showed a low toxic effect of the compound with 80–90% ($\pm$ 5.31–9.45%) of the cells surviving (Fig. 3C). HCQ showed a highly significant difference to untreated cells with a cell survival of $81.44 \pm 5.31\%$ and $p < 0.0001$. RBV treatment resulted in more viable Vero-B4 cells than the untreated control ($121.82 \pm 15.57\%$ viable cells), whilst in U138, RBV lead to statistically significant toxicity ($70.43 \pm 13.14\%$ viable cells) (Fig. 3B, D). The difference in RBV toxicity between the two cell lines was statistically significant with $p < 0.0001$. Neither T-1105 nor HCQ led to significant cell damage in U138 cells (Fig. 3D).
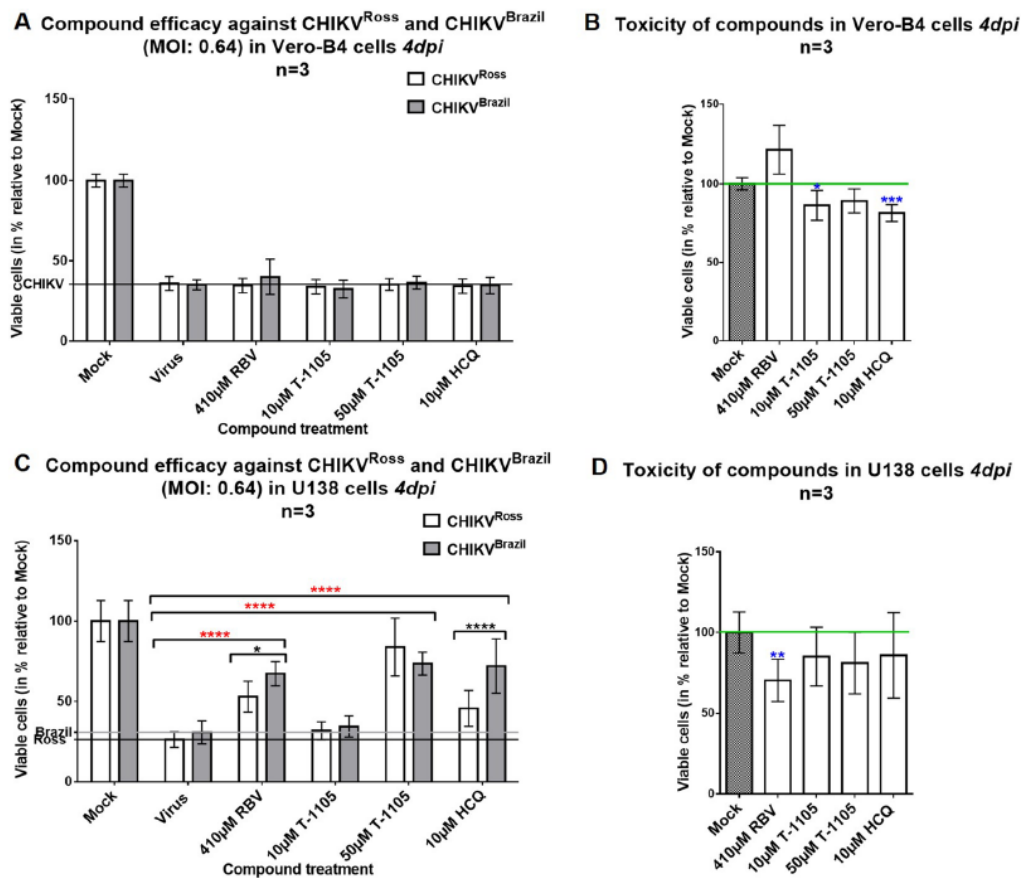
Fig. 3 Comparison of compound efficacy and toxicity against CHIKV[Ross] and CHIKV[Brazil] in the cell lines Vero-B4 and U138. Cells were treated with certain concentrations of HCQ, RBV, or T-1105 and were either infected with CHIKV (efficacy test **A** and **C**) or not (toxicity test **B** and **D**). Four days after infection/treatment, cell survival was determined with MTS. Values are given as percentages in relation to Mock control and are means of three independent experiments each with at least three technical replicates. **A** Vero-B4 and **C** U138 cells were infected with CHIKV[Ross] (white columns) or CHIKV[Brazil] (grey columns). Statistically significant differences of the compound efficacies between the different virus strains CHIKV[Ross] and wt CHIKV[Brazil] in the same cell line were evaluated in a one-way ANOVA test and are indicated by black asterisks. Red asterisks indicate significant (positive) differences between the positive control (black and grey line) and treated, infected cells (same corresponding virus strain and cell line). **B** and **D** Compound toxicity in Vero-B4 (**B**) and U138 (**D**) cells. Statistically significant (negative) differences between Mock control (grey bar and green line) and the treated cells (white bars), are indicated by blue asterisks. The number of asterisks indicate p-values as follows: $*p < 0.05$; $**p < 0.01$; $***p < 0.001$; $****p < 0.0001$

IC₅₀/CC₅₀ evaluation of RDV, HCQ, and T-1105 in Vero-B4 and U138 cells

A dose-dependent inhibition of CPE in both cell lines could be observed with HCQ and RBV. However, only in U138 cells was a dose-dependent effect for T-1105 detectable. Efficacies of HCQ and RBV differed considerably in the two cell lines (Table 1).

Of the four tested potential CHIKV antiviral substances (RBV, HCQ, and T-1105) only HCQ and RBV showed dose-dependent efficacies in Vero-B4 cells. However, even at 1000 µM concentration of RBV, only $37.55 \pm 6.15\%$ (at MOI 0.325) surviving cells were detectable and thus no IC₅₀ value could be generated (data not shown). Efficacy of HCQ was observable between the concentrations of 1 µM and 30 µM. At concentrations > 30 µM HCQ was considerably toxic. An IC₅₀ value of 18.29 µM and a CC₅₀ of 49.63 µM could be generated for HCQ in Vero-B4 cells at MOI 0.355 (Fig. 4A and B) leading to an SI of 2.7. For T-1105 no dose-dependent efficacy against CHIKV in Vero-B4 could be observed (concentration range 5–100 µM).

All tested compounds showed a dose-dependent antiviral effect against wt CHIKV[Brazil] in U138 cells. Efficacy of HCQ in U138 was observed using the compound at concentrations between 1 and 15 µM, as concentrations above 15 µM were toxic to the cells. An IC₅₀ value of 4.136 µM and a CC₅₀ of 35.45 µM was observed (Fig. 4C, D), leading to an SI of 8.57 for HCQ in U138.

RBV was effective against CHIKV[Brazil] in U138 cells with an IC₅₀ of 165.8 µM (See Fig. 3A and B in Supplemental materials). No maximal toxic effect was observable at the highest concentration of 500 µM (data not shown). Consequently it was not possible to generate an exact CC₅₀ value. As CC₅₀ is > 500 µM, the SI would therefore be > 3.

The compound T-1105 (the defluorinated analogue of favipiravir) was effective against wt CHIKV in U138 cells with an IC₅₀ of 34.21 µM (see supplemental materials). At the highest concentration (100 µM), no significant CPE was observable. The SI can thus be assumed to be > 3.

Taken together, these data demonstrate that HCQ, RBV, and T-1105 inhibit CHIKV-induced cell death of U138 cells in a dose-dependent manner. With the exception of HCQ the compounds had no significant toxic effect on this particular cell line at the tested concentrations.

Discussion

Kill curve experiments

CHIKV in vitro experiments are usually conducted in Vero cells as they propagate the virus well and show extensive CPE [23]. However, Vero cells originate from the kidney of an African green monkey and do not represent the usual site of infection in humans. As the latest CHIKV outbreaks reported an increase in neurological complications following CHIKF, it was one of our objectives to find a human derived neurological (immortalised) cell line to establish an in vitro model for neurogenic CHIKV (and possibly other neurogenetic alphavirus) infection.

There is a report of another glioblastoma cell line (U-87 MG (ATCC HTB-14)) being tested in CHIKV experiments [24, 25]. The study of Abraham et al. evaluated the glioblastoma cell line (U87-MG) with wt CHIKV isolate (RGCB355/KL08 CHIKV strain) with regard to susceptibility to infection, visible CPE, autophagy, apoptosis, and innate immune response. However, there are indications that this cell line is not the original cell line published by Ponten in 1968 [26, 27]. The DNA profile of the U87MG is different from that of the original and thus the origin of this cell line is unknown [25].

For these reasons, we tested different human glioblastoma cell lines (DBTRG, U138, and U251) for the susceptibility of infection with CHIKV and their suitability for cell viability assays with this virus. Furthermore, Huh-7 and A549, for which controversial data with regard to CHIKV infectivity have been published, were evaluated with the same objectives. As these differences might be due to the fact that different CHIKV strains have been used in the aforementioned studies, we compared the lab-adapted CHIKV strain Ross and the field isolate from Brazil in in vitro cell cultures and by full genome analysis.

In our study, all tested glioblastoma cell lines were susceptible to CHIKV infection. However, in DBTRG cells, extensive CPE with > 50% nonviable cells could only

Table 1 IC₅₀ and CC₅₀ values of different compounds against wt CHIKV[Brazil] (MOI: 0.355) in Vero-B4 and U138 cells

Compound	IC₅₀ (µM)		CC50(µM)		SI	
	Vero-B4	U138	Vero-B4	U138	Vero-B4	U138
Ribavirin	n.d	165.8	> 1000	> 500	> 1.5	> 3
Hydroxychloroquine	18.29	4.136	49.63	35.45	2.7	8.57
T-1105	n.d	34.21	> 100	> 100	n.d	> 3

CC₅₀ half maximal cytotoxic concentration, IC₅₀ half maximal inhibitory concentration, n.d. not determined, SI selectivity index;

A Efficacy of HCQ in Vero-B4 cells (1×10^4 cells/well) vs CHIKV^{Brazil} (MOI: 0.355)
IC$_{50}$: 18.29 µM

R^2= 0.9733; 95%CI[4.630 to 72.24] µM
n=3
Number of analyzed datapoints: 53

B Toxicity of HCQ in Vero-B4 cells (1×10^4 cells/well)
CC$_{50}$: 49.63 µM

R^2= 0.7930; 95%CI[43.51 to 56.60] µM
n=3
Number of analyzed datapoints: 57

C Efficacy of HCQ in U138 cells (1×10^4 cells/well) vs CHIKV^{Brazil} (MOI: 0.355)
IC$_{50}$: 4.136 µM

R^2= 0.7973; 95%CI[3.152 to 5.428] µM
n=4
Number of analyzed datapoints: 53

D Toxicity of HCQ in U138 cells (1×10^4 cells/well)
CC$_{50}$: 35.45 µM

R^2: 0.8023; 95%CI[30.91 to 40.65] µM
n=3
Number of analyzed datapoints: 72

Fig. 4 IC$_{50}$ and CC$_{50}$ of HCQ in Vero-B4 and U138 cells. Hydroxychloroquine inhibits CHIKV^{Brazil}-induced cell death in Vero-B4 (**A**) and U138 (**C**) cells in a dose-dependent manner. Cells (1×10^4 cells/well) were infected at an MOI of 0.355 and treated with a serial dilution of HCQ. After 4 days, cell death was determined via a colorimetric cell viability assay (MTS). Toxicity assays in Vero-B4 (**B**) and U138 (**C**) cells were performed similarly without infection of the cells. The data represent means ± SD of raw data from at least 3 independent experiments performed with three technical replicates. Normalised fit of dose–response curves was calculated with GraphPad Prism 6 Software

be achieved at MOI ≥ 6.4. U138 and U251 cells showed extensive CPE *4dpi* with either CHIKV strain (Fig. 2E). U251 cells were more sensitive to wt CHIKV^{Brazil} infection than U138 cells. Yet, the kill curve of U251 infected with CHIKV^{Ross} strain was not a strictly dose-dependent linear progression but rather an undulated one (Fig. 2F). Furthermore, SD in U251 was also rather high (sometimes > 25%).

One important observation was that cell viability assay with MTS in U251 is not working reliably when the experiment duration exceeds 3 days and the initial cell concentration is ≥ 1×10^4 cells/well. The reason might be that the cells double in 23 h and are sensitive to overgrowing [26, 28]. Too many cells will cause U251 to stop proliferating, curb their metabolic rates, and reach a state of stasis. In this state, U251 cells no longer reduce MTS into its formazan product. Consequently, the absorbance of the plate appears to be the same as in dead cells although there are a multitude of alive U251 cells. This results in false interpretation of test results. Seeding too few cells, on the other hand, results in badly proliferating cells, since it was our observation that both U251 (and U138) cells need close cell-to-cell contacts in order to form a stable layer. For these reasons, U251 were not used in the other experiments, since those experiments were designed to run for 4 days. Still, U251 cells might be a useful cell line for CHIKV studies if the experimental parameters are adapted accordingly.

The human lung derived cell line A549 proved unsuitable experiments testing cell viability since it displayed no CPE after infection with wt CHIKV[Brazil] and only limited cell death at the highest MOI (6.45) of CHIKV[Ross] at *4dpi* (Fig. 2B). The kill curve in MTS assays of wt CHIKV[Brazil] on A549 cells even indicated more viable cells at the highest MOI (63.5 and 6.35) than in the non-infected control. This phenomenon might be explained with some of the cells dying at such high MOI (possibly due to apoptosis), which then leaves more space and substrate for the surviving cells. At lower MOI and in the control, the A549 cells were over-confluent and might have curbed down their metabolism, leading to a lower MTS reduction (which leads to lower OD values). Apart from a bad or unreliable CPE, the amount of virus needed to conduct viability experiments on A549 is very high. The A549 cell line has been described in CHIKV experiments before, but reports are contradictory. Sourisseau, Schilte [29] state that wt CHIKV virions bind to A549 cells without replicating within the cell, and Solignat, Gay [30] did not observe any CPE on wt CHIKV infected A549. Other studies do not recommend this cell line claiming that CHIKV does not reproduce in A549 [31]. Franco, Rodriquez [32], however, used this cell line to test RBV and favipiravir against an attenuated CHIKV strain (vaccine strain 181/clone25) at MOI 0.1 in a yield assay, looking at virus in the supernatant. This would indicate that this particular CHIKV strain does replicate in A549 cells and is secreted into the supernatant. It is possible that the laboratory-generated, attenuated vaccine strain (181/clone25) has some affinity to this cell line, yet, for cell viability experiments with our clinical isolate of CHIKV[Brazil] and the Ross strain, A549 cell cannot be recommended.

The Huh-7 human hepatocarcinoma cell line is often used to evaluate hepatocellular toxicity of compounds in vitro [33]. Huh-7 cells only showed cell death after infection with wt CHIKV[Brazil] at a very high MOI of 127. Data showed that an increased initial MOI of CHIKV promotes the effect of CHIKV-induced cellular transcriptional shutoff in cells and thus leads to apoptosis [34]. This effect could be observed in cells infected with higher MOI [34], and it could explain the CPE in A549 and Huh-7 at very high MOI. We observed the biggest difference in CPE between the two virus strains in Huh-7 cells. Whilst the wt CHIKV was not able to significantly damage Huh-7 cells at MOI ≤ 12.7, the Ross strain showed a dose-dependent CPE (Fig. 2C).

Solignat, Gay [30] has successfully used Huh-7 cells in CHIKV experiments before. In his work, Huh-7 cells were infected at higher MOI with the West African CHIKV strain 5′CHIKV-EGFP that encodes a GFP protein. According to the study, there was detectable viral replication and CPE [30]. Antiviral efficacy assays measuring virus yield were conducted using Huh-7 cells by Franco, Rodriquez [32] (vaccine strain of CHIKV (181/clone 25)) and Ferreira, Reis

[35] (CHIKV (Asian strain), not further specified). Additionally, a study from Roberts, Zothner [36] evaluated a variety of cell lines for their use in experiments with a sub-genomic replicon (SGR) system CHIKV SGR (CHIKV-D-Luc-SGR), derived from the ECSA strain (ICRES). To test infectious virus, the group used a full-length infectious cDNA clone of CHIKV-LR2006 OPY1. According to the group, Huh-7 cells could be infected by said CHIKV construct and did yield infectious virus in moderate amounts. A549 cells on the other hand were less suited. No observations were done in regard of CPE in the two cell lines in this particular study. Thus, the results of the research cannot be transferred to cell viability assays with wt CHIKV.

The fact that other studies have successfully used the Huh-7 cell line in CHIKV cell viability assays might be due to the use of different, lab-adapted, or modified CHIKV strains. Interestingly, the field isolate tested in this study showed no CPE on Huh-7 cells whilst the Ross strain displayed extended cell kill. This might be due to cell culture adaption of CHIKV[Ross]. Genome analysis of both strains revealed that both CHIKV strains (CHIKV[Ross] and CHIKV[Brazil]) belong to the ESCA clade.

For other arboviruses like Dengue Virus (DENV) or Zika Virus (ZIKV), A549, and Huh-7 are very useful cell lines, as these viruses replicate well and show CPE [31, 37–39]. Since coinfections of CHIKV, DENV, and ZIKV occur due to geographical overlapping in tropical regions, cell lines in which all these viruses may be propagated might have been one objective as to why A549 and Huh-7 cells have repeatedly been tried in CHIKV experiments. Especially DENV and CHIKV cause similar fever-like symptoms, and are difficult to diagnose [31].

To our knowledge a comparison of lab-adapted CHIKV strain with wt CHIKV isolates with regard to cell affinity in different cell lines has only been done by Wikan, Sakoon-watanyoo [40]. The group tested a panel of cell lines with different CHIKV strains (two field isolates and the original Ross strain). Still, their cell line panel did not encompass Huh-7 and A549 cells.

The reasons for the different CPE of CHIKV[Brazil] and CHIKV[Ross] on various cell lines are currently unknown. One possible explanation might be the presence or absence of specific cell surface receptors and/or host proteins which are necessary for an efficient infection, replication, and virus production with cell lysis. Even if certain cell lines have already been described as susceptible, different CHIKV strains might still not work.

Various studies observed strain differences in CHIKV tropism and virulence [41]. The cell culture adapted CHIKV strain 181/25, which had been investigated as a possible vaccine strain after being passaged various times in vitro, displays increased glycosaminoglycan (GAG) binding due to a specific mutation in the E2 glycoprotein (G82R) [41–45].

GAGs serve as attachment factors for many pathogenic viruses and are amongst the central factors which trigger CHIKV attachment [44]. The viral spike glycoproteins E2 and E1 play an important role for the infection of target cells. Whilst the E2 protein is thought to be responsible for receptor binding, the E1 protein contains a hydrophobic fusion peptide and is necessary for viral and cellular membrane fusion [46].

da Silva and colleagues could demonstrate by reciprocal amino acid substitutions at residue 82 of the E2 glycoprotein that the exchange G82R resulted in a phenotype switch in CHIKV [44]. Their data suggest that an Arginine at position 82 of E2 increases the affinity of the glycoprotein for GAGs [44]. These findings also support the hypothesis that the G82R substitution in E2 of CHIKV strain 181/25 contributes to attenuation of the vaccine strain due to GAG binding [45]. Further research in vitro and in vivo conclude that an arginine at residue 82 lead to a greater dependence on GAGs for infection of mammalian cells [41]. These results indicate that GAG utilisation plays a role in regulating CHIKV tropism and host responses that contribute to arthritis, a cardinal symptom of CHIKV disease [41].

Other point mutations in the E2 protein (e.g. E79K, E266K, and E166K) affecting GAG binding were observed in cell culture adapted CHIKV strains [43, 47, 48]. These strains were more dependent on GAGs for infection and showed reduced in vivo replication. By increasing the positive charge in domain A of the E2 protein, these point mutations affected the binding affinity of the virus. The positive charge acquisition is a phenomenon commonly observed in cell culture adapted alphaviruses and often correlates with an attenuated phenotype in vivo [45, 49, 50].

Mutation at critical points of the envelope surface proteins may introduce changes in charge and hydrophobicity of the CHIKV E1 and E2 glycoprotein [51]. Such changes in the E1/E2 proteins can influence pH sensitivity and dramatically affect virus structure and production [52, 53]. Furthermore, mutations in specific regions of the E2 protein may directly influence interactions with a specific cell surface receptor thus influencing virulence and adaption [48, 54].

Whole genome sequencing revealed 5 differences in the E1 glycoprotein (Fig. 1). One difference was at the E1 protein position 322. Whilst CHIKV[Ross] has a valine in this position, CHIKV[Brazil] has an alanine. Studies showed that membrane fusion of endosomes containing CHIKV is triggered by E1 glycoproteins and that this process is pH dependent. Mutations in the E1 protein at position 226 can lead to phenotypes which require lower pH compared to the parent strains to trigger fusion [55, 56].

Differences in the E1 protein between the two strains may be responsible for the differences in HCQ response, as HCQ (and the more toxic base substance chloroquine (CQ)) is known to raise the endosomal pH and thus intervene with CHIKV membrane fusion [57]. It is therefore possible that some of these changes have an impact on the acid pH-triggered conformational changes in alphavirus E1 during membrane fusion [58].

Furthermore, whole genome sequencing of the strains used in this study revealed differences at four positions in the nsP2, a protein known to be connected with cytopathogenicity especially of old-world alphaviruses. Apart from other functions, the nsP2 inhibits host transcription which eventually induces cell death [59].

Whether the discovered genome differences between CHIKV[Ross] and CHIKV[Brazil] are responsible for the differences in cell affinity (especially concerning Huh-7 cells) need to be further investigated using mutagenesis of the respective sites and observation on the effects on cell tropism in reverse genetics experiments.

Comparison of compound efficacy in different cell lines against two different CHIKV strains

Despite being treated with compounds that should potentially confer some protection at the concentrations used, Vero-B4 cells showed no significant cell survival after 4 days of CHIKV challenge. A possible reason for the inefficacy of the compounds might be the higher MOI of 0.64 with which the cells were infected (compared to an MOI of 0.355 in the IC_{50}/CC_{50} experiments and considerably lower MOIs of 0.005–0.01 in previous studies with the same setup [21].

Previously published data states that RBV was efficient against wt CHIKV (MOI: 0.005) with an IC_{50} of 423.6 μM and a CC50 > 500 μM [21]. The same study states CQ's IC_{50} as 5–10.6 μM with a CC_{50} of > 36 μM. Delang, Segura Guerrero [22] however tested CQ against CHIKV Indian Ocean strain 899 (lab) at MOI 0.01 in Vero cells and generated IC_{50} values of 11 and 28 μM. Delang also tested T-1105 against this lab CHIKV strain at MOI 0.01 and IC_{50} values were 7–47 μM, with a CC_{50} value of 571 μM [22]. HCQ is a less toxic derivative of CQ and its efficacy is comparable to CQ.

U138 cells on the other hand benefited considerably from RBV, T-1105 (50 μM), and HCQ treatment, despite the higher MOI. The reason for the difference in compound efficacy between the two cell lines might be due to the different ability of the respective cells to process the compounds into their active analogues.

Furthermore, there was a significant difference in RBV toxicity between the two cell lines. Whilst RBV lead to an increase of the MTS signal in Vero-B4 cells, U138 cells showed diminished signals which can be interpreted as fewer viable cells. There might be different reasons for this observation:

i. The compounds kill some cells, leave space for the remaining cells which then have spare room and medium and become highly metabolically active, hence they are able to reduce MTS into the signal yielding formazan product more effectively.

ii. Vero-B4 have a higher proliferation rate (doubling time 24 h) than U138 cells (doubling time 47–72 h) [28, 60]. It is thus possible that Vero-B4 cells also have a higher metabolism and are able to process RBV quicker into a less toxic compound.

iii. Additionally, there is the chance that RBV actually causes cell proliferation or an activation of metabolism in Vero-B4 cells, whilst U138 cells are hampered/damaged by the compound.

When comparing efficacies of the compounds between the two strains, RBV and HCQ protected U138 cells significantly better from wt CHIKV than from CHIKV Ross.

CQ/HCQ are effective at early stages of viral infection [61]. The drugs seem to impair cell-virus surface interactions. Pre-treatment of Vero cells with CQ impairs terminal glycosylation of ACE2, a cell surface receptor used by severe acute respiratory syndrome corona virus (SARS-CoV) for cell attachment [62]. Khan et al. suggested a similar mechanism to be responsible for the inhibition of CHIKV infection by CQ in vitro [61]. In the case of other alphaviruses like Sindbis virus (SINV) and Semliki Forest virus (SFV), viral fusion with the host cell membrane is achieved via conformational changes in the viral envelope glycoprotein. These changes are triggered by clathrin-mediated endocytosis by the target cell and the low pH of the endosomal compartment [63]. This low endosomal pH is said to be required for CHIKV entry into cells as well [29]. Bernard and colleagues could demonstrate that the base CQ raises the endosomal pH by interfering with the protonation of the endocytic vesicles. This prevents the E1 fusion step needed for the release of CHIKV RNA into the cell cytoplasm [64].

In our comparative experiments, HCQ showed a statistically significant higher efficacy against the wt CHIKV^{Brazil} than against the CHIKV^{Ross} strain. The CHIKV^{Brazil} strain may rely on a lower pH to grant membrane fusion (possibly due to mutations in the E1 glycoprotein as mentioned above), or the strain CHIKV^{Ross} has gained a more efficient way to grant fusion with the host cell membrane during its repeated passage in Vero cells (possibly due to mutations in the E2 protein). It should be mentioned that HCQ is only used as a control for measuring efficacy in vitro, as patients do not benefit from HCQ treatment during acute CHIKV disease and the drug has no suppressive effect on peripheral viral load in patients [65].

Differences of IC$_{50}$/CC$_{50}$ values in different cell lines

Both, IC$_{50}$ and CC$_{50}$ of HCQ observed in this study are higher than previously published data of chloroquine in Vero cells. This might be due to a different MOI.

RBV did show a dose-dependent efficacy, however, the maximal protection of Vero-B4 cells at the highest drug concentrations did not outnumber $37.55 \pm 6.15\%$ (at MOI 0.325) surviving cells and thus no IC$_{50}$ value could be generated. Published data from comparable experiments give IC$_{50}$ values for RBV of 423.6–765.8 μM in Vero-E6 cells [6, 21]. One possible explanation for not exceeding 37.55% surviving Vero-B4 cells might be the fact that the aforementioned publication used different CHIKV strains, VeroE6 cells, and infected with a lower MOI (0.005). At the highest concentration (1000 μM) RBV showed no toxic effect on Vero-B4 cells. The other compounds neither displayed a positive effect against CHIKV^{Brazil} nor negative effects on Vero-B4 cells at the used concentrations. Altogether, the experiments showed that HCQ and RBV inhibit CHIKV^{Brazil}-induced cell death of Vero-B4 cells in a dose-dependent manner and that HCQ was considerably more effective in preventing CHIKV-related CPE in Vero-B4 than RBV (Table 1).

Vero-B4 cells could not be protected from CHIKV infection with T-1105 at the concentrations used. This was unexpected, since Delang reported IC$_{50}$ values of 7–47 μM for T-1105 in Vero cells in his study [22]. The concentrations used in the experiments for T-1105 in this study ranged from 5 to 100 μM, well in the range to detect an efficacy of the compound against CHIKV^{Brazil}. However, Delang used VeroA cells, different CHIKV strains and infected the cells with an MOI of 0.1. It is possible that the difference in CHIKV strain, cell line, and MOI contributed to the discrepancy between our results and previously published data. Since the compound did show efficacy against CHIKV^{Brazil} in U138 cells, issues related to the compound itself (e.g. degradation due to repeated thaw-freeze-cycles) can be ruled out.

Both RBV and T-1105 are antivirals that interfere with the viral genome replication by inhibiting the nsP4 polymerase. Both are synthetic purine nucleoside analogues [6], and act as broad-spectrum antivirals, with multiple mechanisms of action ascribed to them. Both might either block the RNA-dependent RNA polymerase (RdRp) function of the nsP4 by binding at certain domains of the enzyme and/or they might be incorporated into the viral genome and thus lead to lethal mutagenesis [32]. Others suggest that RBV interferes with the nsP1 guanylyl transferase and/or methyltransferase activity and thus leads to a production of untranslatable mRNAs [66]. RBV and T-1105 (as well as the fluorinated form favipiravir T-705) have to be phosphorylated by host cell kinases into their mono-, di-, and triphosphate metabolites. The triphosphate form is the active

metabolite which is eventually incorporated into the viral genome, thus leading to error catastrophe [67].

Resistance against RBV and favipiravir (T-705) has been reported and is explained by mutations in nsP4. RBV resistance was put down to a mutation from K291R in nsP4 whilst favipiravir resistance was explained by a C483Y mutation [22, 66]. Whole genome sequencing of our strains revealed that neither CHIKV Ross nor Brazil have these mutations. Our experiments confirmed the findings of Franco and colleagues that compound efficacy varies between host cell lines. While Vero-B4 cells were refractory to the treatment of RDV, T-1105, and to a lesser extend HCQ, U138 cells could be protected by all three compounds considerably better. A study demonstrated that the accumulation of RBV is host cell dependent due to the presence or absence of specific nucleoside transporters [68]. This could also hold true for other nucleoside analogues like T-1105. Furthermore, pro-drugs like RBV and T-1105 depend on host kinases for phosphorylation into their active metabolite. The resistance of some cell types to RBV may thus depend on the intracellular RBV metabolism [69]. A study on the cell line-dependent activation and antiviral activity of T-1105 revealed that T-1105 activation in Vero cells was hindered by inefficient conversion of the ribonucleoside monophosphate to the ribonucleoside diphosphate en route to forming the active triphosphate [70]. This might be one reason, why T-1105 is less potent in Vero-B4 than in U138 cells. It is likely that the distribution of host cell kinases differs between species and tissues and thus lead to a varying intracellular concentration of the triphosphate forms of RBV and possibly T-1105 [32].

Conclusion

Two glioblastoma cell lines (U138 and U251) were identified as potentially useful in vitro cell culture models for CHIKV infection and evaluation of antiviral activity. To our knowledge, this is the first time these two cell lines have been described in connection with CHIKV antiviral tests. Furthermore, A549 and Huh-7 cells cannot be recommended for cell viability assays with wt CHIKV, as these cell lines do not show CPE. Furthermore, our experiments proved that there are differences in cytopathological effects and antiviral efficacies between wt and laboratory-adapted CHIKV strains.

Author contributions JJB and FH conceived the layout of the project. FH performed all experiments with CHIKV. MB-W was responsible for all work connected with sequencing and genome analysis. FH, MB-W and PZ performed statistical analysis and generated the figures and tables. FH and MB-W wrote the first draft of the manuscript. MB-W, MB, AB, and JJB contributed providing additional information as well as reviewing the manuscript. JJB supervised and funded the project as well as oversaw data analysis, manuscript drafting, and revision.

Declarations

References

1. Singh SK (2015) Overview on chikungunya virus pathogenesis. In: Singh SK (ed) Human emerging and re-emerging infections: viral & parasitic infections. Wiley, New Jersey, pp 177–188
2. Powers AM et al (2000) Re-emergence of Chikungunya and O'nyong-nyong viruses: evidence for distinct geographical lineages and distant evolutionary relationships. J Gen Virol 81(Pt 2):471–479
3. Schuffenecker I et al (2006) Genome microevolution of chikungunya viruses causing the Indian Ocean outbreak. PLoS Med 3(7):e263
4. Brown RS, Wan JJ, Kielian M (2018) The alphavirus exit pathway: what we know and what we wish we knew. Viruses 10(2):89
5. Hucke FIL, Bestehorn-Willmann M, Bugert JJ (2020) Prophylactic strategies to control Chikungunya virus infection. Virus Genes 57:133
6. Hucke FIL, Bugert JJ (2020) Current and promising antivirals against chikungunya virus. Front Public Health 8:916
7. Matusali G et al (2019) Tropism of the Chikungunya virus. Viruses 11(2):175
8. Zhang R et al (2018) Mxra8 is a receptor for multiple arthritogenic alphaviruses. Nature 557(7706):570–574
9. Ruiz Silva M et al (2016) Mechanism and role of MCP-1 upregulation upon chikungunya virus infection in human peripheral blood mononuclear cells. Sci Rep 6:32288
10. Lokireddy S, Vemula S, Vadde R (2008) Connective tissue metabolism in chikungunya patients. Virol J 5:31
11. Mehta R et al (2018) The neurological complications of chikungunya virus: a systematic review. Rev Med Virol 28(3):e1978

12. Cerny T et al (2017) The range of neurological complications in Chikungunya fever. Neurocrit Care 27(3):447–457

13. Das T et al (2015) Multifaceted innate immune responses engaged by astrocytes, microglia and resident dendritic cells against Chikungunya neuroinfection. J Gen Virol 96(Pt 2):294–310

14. Yasumura YK (1963) Studies on SV40 in tissue culture-preliminary step for cancer research in vitro. Nihon Rinsho 21:1201–1215

15. Lieber M et al (1976) A continuous tumor-cell line from a human lung carcinoma with properties of type II alveolar epithelial cells. Int J Cancer 17(1):62–70

16. Nakabayashi H et al (1982) Growth of human hepatoma cells lines with differentiated functions in chemically defined medium. Cancer Res 42(9):3858–3863

17. Kruse CA et al (1992) Characterization of a continuous human glioma cell line DBTRG-05MG: growth kinetics, karyotype, receptor expression, and tumor suppressor gene analyses. In Vitro Cell Dev Biol 28(9–10):609–614

18. Ross RW (1956) The Newala epidemic. III. The virus: isolation, pathogenic properties and relationship to the epidemic. J Hyg (Lond) 54(2):177–191

19. Arankalle VA et al (2007) Genetic divergence of Chikungunya viruses in India (1963–2006) with special reference to the 2005–2006 explosive epidemic. J Gen Virol 88(Pt 7):1967–1976

20. Volk SM et al (2010) Genome-scale phylogenetic analyses of chikungunya virus reveal independent emergences of recent epidemics and various evolutionary rates. J Virol 84(13):6497–6504

21. Scholte FE et al (2013) Characterization of synthetic Chikungunya viruses based on the consensus sequence of recent E1–226V isolates. PLoS ONE 8(8):e71047

22. Delang L et al (2014) Mutations in the chikungunya virus non-structural proteins cause resistance to favipiravir (T-705), a broad-spectrum antiviral. J Antimicrob Chemother 69(10):2770–2784

23. Sudeep AB et al (2019) Differential susceptibility & replication potential of Vero E6, BHK-21, RD, A-549, C6/36 cells & Aedes aegypti mosquitoes to three strains of chikungunya virus. Indian J Med Res 149(6):771–777

24. Abraham R et al (2013) Induction of cytopathogenicity in human glioblastoma cells by chikungunya virus. PLoS ONE 8(9):e75854

25. Allen M et al (2016) Origin of the U87MG glioma cell line: good news and bad news. Sci Transl Med 8(354):35re43

26. Pontén J, Macintyre EH (1968) Long term culture of normal and neoplastic human glia. Acta Pathol Microbiol Scand 74(4):465–486

27. Pontén J, Westermark B (1978) Properties of human malignant glioma cells in vitro. Med Biol 56(4):184–193

28. Weller M et al (1998) Predicting chemoresistance in human malignant glioma cells: the role of molecular genetic analyses. Int J Cancer 79(6):640–644

29. Sourisseau M et al (2007) Characterization of reemerging chikungunya virus. PLoS Pathog 3(6):e89

30. Solignat M et al (2009) Replication cycle of chikungunya: a re-emerging arbovirus. Virology 393(2):183–197

31. Olagnier D et al (2014) Inhibition of dengue and chikungunya virus infections by RIG-I-mediated type I interferon-independent stimulation of the innate antiviral response. J Virol 88(8):4180–4194

32. Franco EJ et al (2018) The effectiveness of antiviral agents with broad-spectrum activity against chikungunya virus varies between host cell lines. Antivir Chem Chemother 26:2040206618807580

33. Lin J et al (2012) Comparative analysis of phase I and II enzyme activities in 5 hepatic cell lines identifies Huh-7 and HCC-T cells with the highest potential to study drug metabolism. Arch Toxicol 86(1):87–95

34. Li YG et al (2013) Chikungunya virus induces a more moderate cytopathic effect in mosquito cells than in mammalian cells. Intervirology 56(1):6–12

35. Ferreira AC et al (2019) Beyond members of the flaviviridae family, sofosbuvir also inhibits chikungunya virus replication. Antimicrob Agents Chemother 63(2):e01389

36. Roberts GC et al (2017) Evaluation of a range of mammalian and mosquito cell lines for use in Chikungunya virus research. Sci Rep 7(1):14641–14641

37. Chan JF et al (2016) Differential cell line susceptibility to the emerging Zika virus: implications for disease pathogenesis, non-vector-borne human transmission and animal reservoirs. Emerg Microbes Infect 5(8):e93

38. Vicenti I et al (2018) Comparative analysis of different cell systems for Zika virus (ZIKV) propagation and evaluation of anti-ZIKV compounds in vitro. Virus Res 244:64–70

39. Franco EJ, Pires de Mello CP, Brown AN (2021) Antiviral evaluation of UV-4B and interferon-alpha combination regimens against dengue virus. Viruses 13(5):771

40. Wikan N et al (2012) Chikungunya virus infection of cell lines: analysis of the East, Central and South African lineage. PLoS ONE 7(1):e31102

41. Ashbrook AW et al (2014) Residue 82 of the Chikungunya virus E2 attachment protein modulates viral dissemination and arthritis in mice. J Virol 88(21):12180–12192

42. Levitt NH et al (1986) Development of an attenuated strain of chikungunya virus for use in vaccine production. Vaccine 4(3):157–162

43. Gardner CL et al (2014) Deliberate attenuation of chikungunya virus by adaptation to heparan sulfate-dependent infectivity: a model for rational arboviral vaccine design. PLoS Negl Trop Dis 8(2):e2719

44. Silva LA et al (2014) A single-amino-acid polymorphism in Chikungunya virus E2 glycoprotein influences glycosaminoglycan utilization. J Virol 88(5):2385–2397

45. Gorchakov R et al (2012) Attenuation of Chikungunya virus vaccine strain 181/clone 25 is determined by two amino acid substitutions in the E2 envelope glycoprotein. J Virol 86(11):6084–6096

46. Schnierle BS (2019) Cellular attachment and entry factors for chikungunya virus. Viruses 11(11):1078

47. Henrik Gad H et al (2012) The E2–E166K substitution restores Chikungunya virus growth in OAS3 expressing cells by acting on viral entry. Virology 434(1):27–37

48. Coffey LL et al (2011) Arbovirus high fidelity variant loses fitness in mosquitoes and mice. Proc Natl Acad Sci USA 108(38):16038–16043

49. Davis NL et al (1991) Attenuating mutations in the E2 glycoprotein gene of Venezuelan equine encephalitis virus: construction of single and multiple mutants in a full-length cDNA clone. Virology 183(1):20–31

50. Klimstra WB, Ryman KD, Johnston RE (1998) Adaptation of Sindbis virus to BHK cells selects for use of heparan sulfate as an attachment receptor. J Virol 72(9):7357–7366

51. Maljkovic Berry I et al (2019) Global outbreaks and origins of a chikungunya virus variant carrying mutations which may increase fitness for Aedes aegypti: revelations from the 2016 Mandera, Kenya Outbreak. Am J Trop Med Hyg 100(5):1249–1257

52. Akahata W, Nabel GJ (2012) A specific domain of the Chikungunya virus E2 protein regulates particle formation in human cells: implications for alphavirus vaccine design. J Virol 86(16):8879–8883

53. Lu YE et al (2001) In vivo generation and characterization of a soluble form of the Semliki forest virus fusion protein. J Virol 75(17):8329–8339

54. Tsetsarkin KA, Weaver SC (2011) Sequential adaptive mutations enhance efficient vector switching by Chikungunya virus and its epidemic emergence. PLoS Pathog 7(12):e1002412–e1002412
55. Tsetsarkin KA, McGee CE, Higgs S (2011) Chikungunya virus adaptation to Aedes albopictus mosquitoes does not correlate with acquisition of cholesterol dependence or decreased pH threshold for fusion reaction. Virol J 8:376
56. Gay B et al (2012) pH-dependent entry of chikungunya virus into Aedes albopictus cells. Infect Genet Evol 12(6):1275–1281
57. Askarian F et al (2021) A review on the pharmacokinetic properties and toxicity considerations for chloroquine and hydroxychloroquine to potentially treat coronavirus patients. Toxicol Res. https://doi.org/10.1007/s43188-021-00101-5
58. Sahoo B, Gudigamolla NK, Chowdary TK (2020) Acidic pH-induced conformational changes in chikungunya virus fusion protein E1: a spring-twisted region in the domain I-III linker acts as a hinge point for swiveling motion of domains. J Virol 94(23):e01561-e1620
59. Akhrymuk I et al (2019) Novel mutations in nsP2 abolish chikungunya virus-induced transcriptional shutoff and make the virus less cytopathic without affecting its replication rates. J Virol 93(4):e02062-e2118
60. Ammerman NC, Beier-Sexton M, Azad AF (2008) Growth and maintenance of Vero cell lines. Curr Protoc Microbiol 4:4E
61. Khan M et al (2010) Assessment of in vitro prophylactic and therapeutic efficacy of chloroquine against Chikungunya virus in vero cells. J Med Virol 82(5):817–824
62. Vincent MJ et al (2005) Chloroquine is a potent inhibitor of SARS coronavirus infection and spread. Virol J 2:69
63. DeTulleo L, Kirchhausen T (1998) The clathrin endocytic pathway in viral infection. Embo J 17(16):4585–4593
64. Bernard E et al (2010) Endocytosis of chikungunya virus into mammalian cells: role of clathrin and early endosomal compartments. PLoS ONE 5(7):e11479
65. Roques P et al (2018) Paradoxical effect of chloroquine treatment in enhancing chikungunya virus infection. Viruses 10(5):268
66. Beaucourt S, Vignuzzi M (2014) Ribavirin: a drug active against many viruses with multiple effects on virus replication and propagation. Molecular basis of ribavirin resistance. Curr Opin Virol 8:10–15
67. Crotty S, Cameron CE, Andino R (2001) RNA virus error catastrophe: direct molecular test by using ribavirin. Proc Natl Acad Sci USA 98(12):6895–6900
68. Ibarra KD, Pfeiffer JK (2009) Reduced ribavirin antiviral efficacy via nucleoside transporter-mediated drug resistance. J Virol 83(9):4538–4547
69. Shah NR, Sunderland A, Grdzelishvili VZ (2010) Cell type mediated resistance of vesicular stomatitis virus and Sendai virus to ribavirin. PLoS ONE 5(6):e11265
70. Huchting J et al (2019) Cell line-dependent activation and antiviral activity of T-1105, the non-fluorinated analogue of T-705 (favipiravir). Antiviral Res 167:1–5

1   Supplementary material:

1.1 IC_{50}/CC_{50} of DMSO on Vero-B4 and U138 cells

DMSO has cytotoxic properties at higher concentrations. It depends to a great deal on the cell line, at which concentration DMSO cubs cell proliferation. As no published data could be found for U138 cells, experiments were run to generate CC_{50} (and possible IC_{50}) values to rule out any cytotoxic or antiviral effect of DMSO in the actual experiment at the DMSO concentration used. Serial dilutions of DMSO (final concentration of compound in the wells were 4%, 3%, 2%, 1%, 0.75%, 0.5%, 0.25%, 0.1%) were prepared in assay medium (DMEM).

The experiments were run and evaluated as described in the kill curve section. Each experiment was repeated at least 3 times independently with three technical replicates.

Results:

DMSO has no antiviral effect on CHIKV in Vero-B4 or U138 cells. The cytotoxic effect of DMSO was significant in Vero-B4 cells at concentrations $\geq 3\%$ (Supp. Fig. 1). The CC_{50} in Vero-B4 cells calculated as 2.395% (Supp. Fig. 2A).
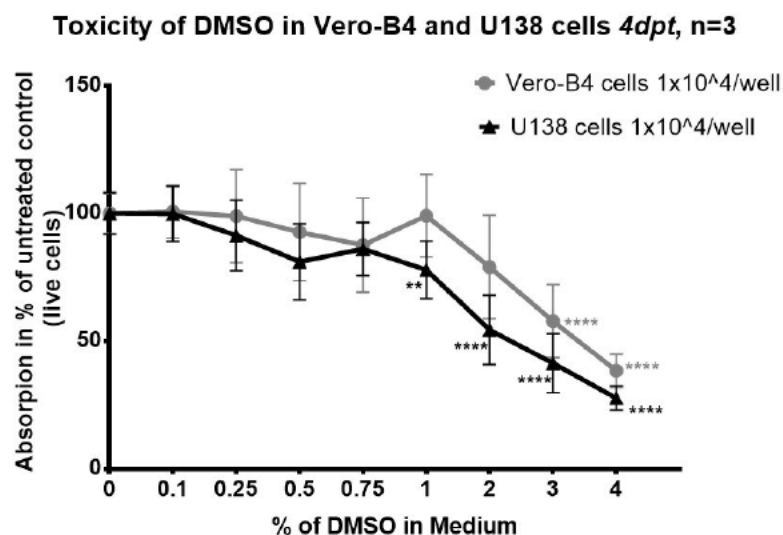
Supp. Fig. 1. Cytotoxic effect of DMSO on Vero-B4 and U138 cells

Vero-B4 (grey graph) and U138 (black graph) cells were treated with different concentrations of DMSO (0.1-4%) for four days (*4dpt*). Cell survival was determined with a colorimetric cell viability endpoint assay (MTS). Statistically significant differences between the untreated Mock control (=100% viable cells) and the treated cells were evaluated in a one-way ANOVA test (GraphPad Prism6) and are indicated by asterisks. The number of asterisks indicate p-values as follows: * $p < 0.05$; ** $p < 0.01$; *** $p < 0.001$; **** $p < 0.0001$. In Vero-B4 cells (grey graph and round symbols), DMSO showed a statistically significant cytotoxic effect at concentrations $\geq 3\%$. In U138 cells (black graph and triangle symbol), DMSO concentrations $\geq 1\%$ showed statistically significant cytotoxicity. Abbreviations: dpt, days post treatment; DMSO, dimethyl sulfoxide; n, number of independent repetitions.

In U138 cells, DMSO concentrations $\geq 1\%$ showed significant cytotoxicity (Supp. Fig. 1) and the CC_{50} calculated to 1.383% (Supp. Fig. 2B). Thus concentrations $\leq 0.6\%$ DMSO during cell assay experiments were considered as acceptable to Vero-B4 and U138 cells.
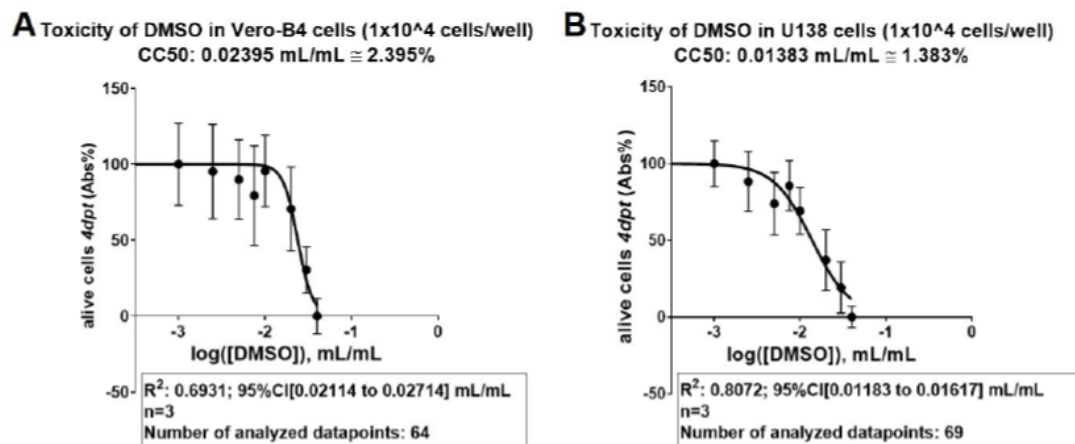
Supp. Fig. 2. CC$_{50}$ values of DMSO in Vero-B4 (A) and U138 (B) cells

Vero-B4 (A) and U138 (B) cells (1×10^4 cells/well) were treated with different concentrations of DMSO for 4 days. Cell death was then determined via a colorimetric cell viability assay (MTS). The data represent means ± SD of raw data from 3 independent experiments performed with three technical replicates. Normalized fit of dose-response curve was done with GraphPad Prism 6 Software. Abbreviations: 95%CI, 95% confidence interval; Abs, absorption; CC$_{50}$, half maximal cytotoxic concentration; dpt, days post treatment; DMSO, dimethyl sulfoxide; n, number of independent repetitions.

1.2   IC$_{50}$ of RBV and T-1105 in U138
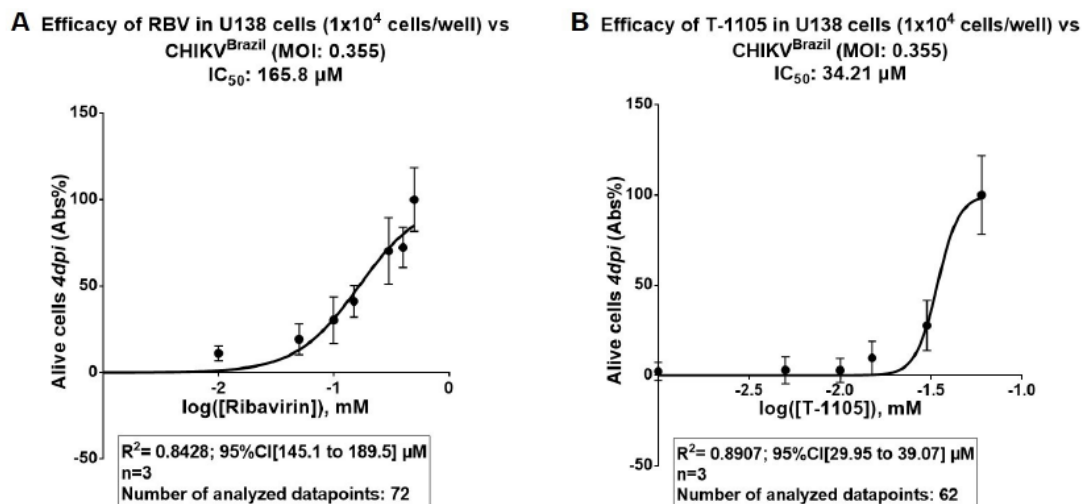
Supp. Fig. 3. IC$_{50}$ of Ribavirin and T-1105 in U138 glioblastoma cells

Ribavirin (A) and T-1105 (B) inhibit CHIKV-induced cell death in U138 cells in a dose-dependent manner. U138 (1×10^4 cells/well) were infected at an MOI of 0.355 and treated with RBV or T-1105 at the indicated concentrations. After 4 days, cell death was determined via a colorimetric cell viability assay (MTS). Toxicity assays were performed similarly without infection of the cells. The highest concentration of Ribavirin (500 µM) used on U138 cells did not result in a maximal toxic effect on the cells, thus no CC$_{50}$ could be calculated with (data not shown). T-1105 had no significant toxic effect at the highest concentration (100 µM; data not shown). Data represent means ±SD of raw data from 3 independent experiments performed with three technical replicates. Normalized fit of dose-response curve was done with GraphPad Prism 6 Software. Abbreviations: 95%CI, 95% confidence interval; Abs, absorption; CC$_{50}$, half maximal cytotoxic concentration; IC$_{50}$, half maximal inhibitory concentration; n, number of independent repetitions; RBV, ribavirin; wt, wild type.

2.   Characterisation of cell lines

2.1.   Evaluation of seeding density of Huh-7 cells for MTS assays

As Huh-7 are able to metabolise MTS very efficiently, cell numers had to be adjusted to the reagent in order to get comparable results with the other cell lines and OD values that were in the linear range of the reader (0.0 to 2.0). Initial cell numbers of 1×10^3 cells/well and 5×10^3 cells/well of Huh-7 cells and 20 µL of MTS reagent yielded acceptable OD values after 1- and 2-hours incubation (Table 2). However, at 1×10^4 cells/well the conversion of MTS into formazan is reduced, suggesting that the cells are too dense and are curbing their metabolic activity. For the other cell lines (Vero-B4, U138 and U251) a 10-fold higher number (1×10^4 /cells/well) yielded OD values in the desired range (data not shown).

Table 2: OD values of different Huh-7 cell densities and amounts of MTS/PMS solution.
Viability assays ran for 5 days and MTS/PMS incubation was 1 to 2 hours.

Cell density	OD values after 1 h incubation at Different amounts of MTS			2 h incubation Amount of MTS		
	20 µL	**30 µL**	**40 µL**	**20 µL**	**30 µL**	**40 µL**
5×10^2 cells	0.543 ± 0.035	0.600 ± 0.018	0.630 ± 0.031	0.750 ± 0.072	0.870 ± 0.053	0.863 ± 0.031
1×10^3 cells	0.705 ± 0.004	0.820 ± 0.015	0.856 ± 0.082	1.094 ± 0.021	1.332 ± 0.011	1.278 ± 0.122
5×10^3 cells	0.979 ± 0.069	1.066 ± 0.058	1.133 ± 0.099	1.727 ± 0.226	2.104 ± 0.166	2.283 ± 0.315
1×10^4 cells	0.941 ± 0.075	1.094 ± 0.064	1.268 ± 0.093	1.300 ± 0.053	1.456 ± 0.019	1.764 ± 0.100

2.2.   CHIKV effect on different cell lines

2.2.1.   CHIKV kill curves on different cell lines

see VI.1

2.2.2.   IFT

The reference cell line Vero-B4 showed the best IFT signal among the tested cell lines (bright green signal in Figure 9A & B) while nuclei are stained light blue with DAPI. U251 and U138 cells also displayed a very well detectable immunofluorescence (Figure 10A-C). A strong immunofluorescence signal indicates CHIKV particles in the cell membrane. Cells are interconnected with neighbouring cells via cellular protrusions or membrane extensions (Figure 9A-C and Figure 10A-C).
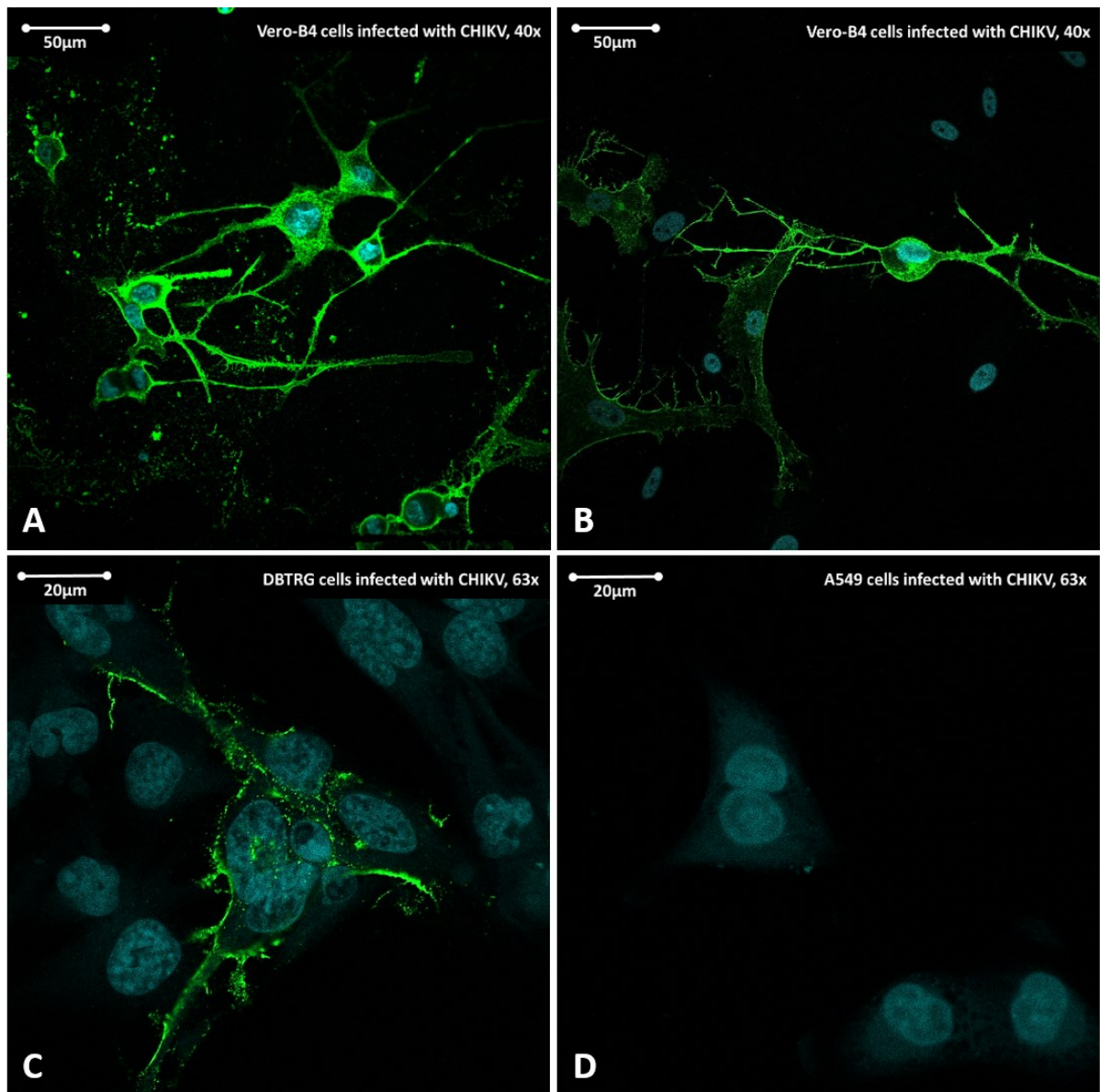
Figure 9: Immunofluorescence staining against CHIKV in Vero-B4, DBTRG and A549 cells.
Cells infected with CHIKV[Brazil] (MOI: 0.065) and immunostained with anti-CHIKV (IgG) antibody (AB) (primary AB) by Euroimmun F160129BF and Alexa Fluor 488 goat α-human IgG (secondary AB) by Invitrogen. Nucleoli are stained with DAPI (light blue). Microscopy was done with the Confocal Laser Scanning Microscope LSM 710 by Zeiss. Pictures were edited with the ZEN 2.1 Software by Zeiss. Bars indicate either 50 µm or 20 µm. Magnification and cell line are stated in the top right corner of each indicidual photo. **A)** & **B)** Vero-B4 cells infected with CHIKV (bright green signal). A strong immunofluorescence signal indicates CHIKV particles in the cell membrane. Cells are interconnected with neighbouring cells via cellular protrusions or membrane extensions. **C)** DBTRG cells infected with CHIKV. **D)** A549 cells infected with CHIKV. Each cell line was repeated 3 times per plate and the setup was repeated at least twice in independent experiments.
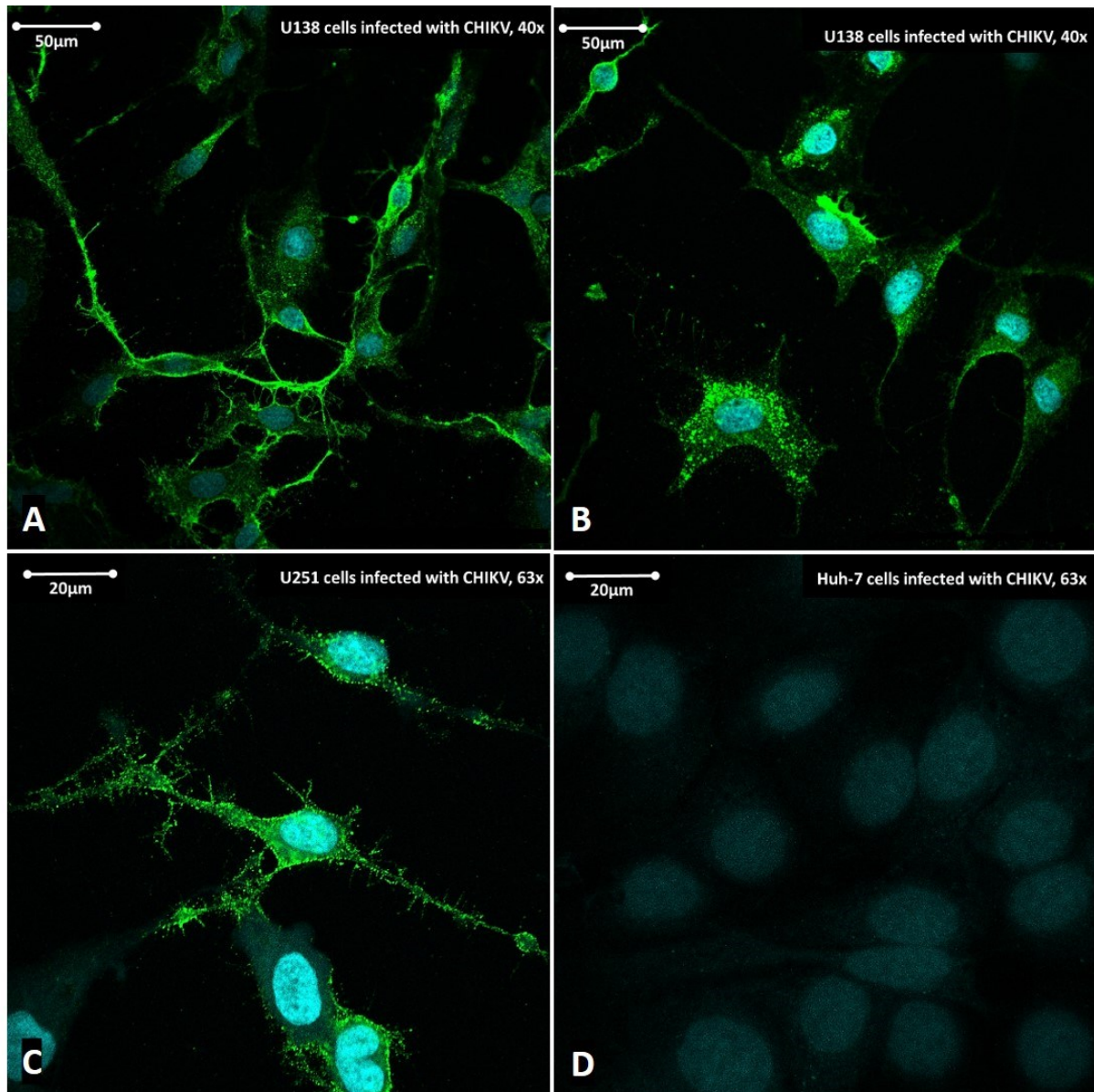
Figure 10: Immunofluorescence staining against CHIKV in U138, U251 and Huh-7 cells.
Cells infected with CHIKV[Brazil] (MOI: 0.065) and immunostained with anti-CHIKV (IgG) antibody
(AB) (primary AB) by Euroimmun F160129BF and Alexa Fluor 488 goat α-human IgG (secondary AB)
by Invitrogen. Nucleoli are stained with DAPI (light blue). Microscopy was done with the Confocal
Laser Scanning Microscope LSM 710 by Zeiss. Pictures were edited with the ZEN 2.1 Software by
Zeiss. Bars indicate either 50 µm or 20 µm. Magnification and cell line are stated in the top right corner
of each indicidual photo. **A)** & **B)** U138 cells infected with CHIKV (bright green signal indicates
CHIKV virions in the cell membrane). A strong immunofluorescence signal indicates CHIKV particles
in the cell membrane. Cells are interconnected with neighbouring cells via cellular protrusions or
membrane extensions. **C)** U251 cells infected with CHIKV. **D)** Huh-7 cells infected with CHIKV. Each
cell line was repeated 3 times per plate and the setup was repeated at least twice in independent
experiments.

DBTRG cells had very weak IFT signals, probably due to too low MOI, but some virus particles

still seemed to bind to this cell line (Figure 9C). Compared to Vero-B4 cells, fewer DBTRG

cells were infected with CHIKV. CHIKV infection of Huh-7 and A549 cells at a MOI of 0.065

did not result in a detectable IFT signal (Figure 10D and Figure 9D). Both cell lines appeared

like non-infected controls (Mock), which all showed no CHIKV IFT signals only DAPI blue stained nuclei (data not shown).

2.2.3. Yield assay RT-PCR

The RT-PCR in this thesis underwent 45 cycles of amplification. All samples with Ct levels of < 35 and with sigmoid curves were considered positive.

The standard curve from the PCR of a 10-fold dilution (1:10 to $1:10^5$) of a viral stock with known titre can be seen in Figure 11. From these standard curves as well as the different MOI (0.001, 0.01 and 0.1) it could be deducted that 3 Ct value points correspond to a 10-fold RNA amount (Figure 11). For analysis, the means of three independent experiments were created with standard deviation (SD). Maximal SD of the curves was ± 4.10, thus any difference between the maximal and minimal Ct points of > 5 Ct points was considered significant.
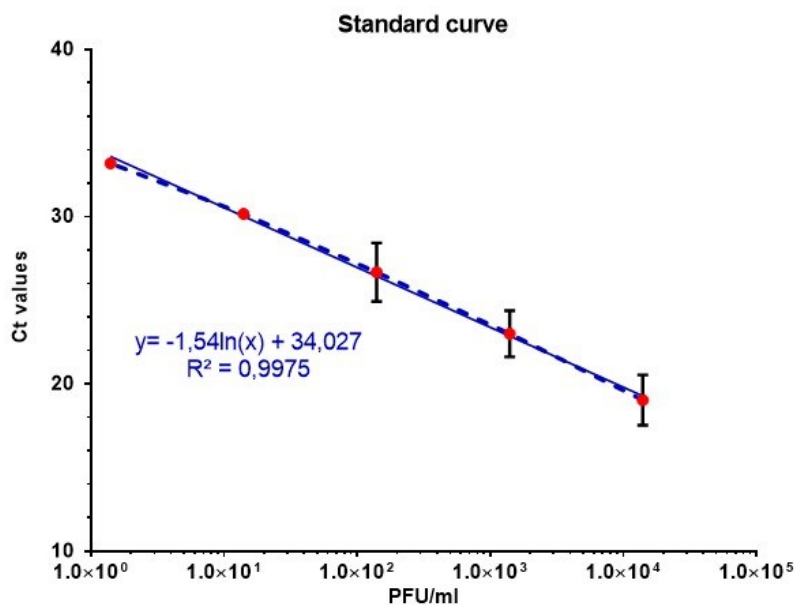
Figure 11: Standard curve created with 10-fold dilution series of CHIKV^{Brazil} stock.
A 10-fold dilution series from 10^{-2} to 10^{-6} of a CHIKV^{Brazil} stock with known titre was purified and the amount of viral RNA was quantified indirectly via CHIKV RT-PCR. Calculations, trendline, equation and coefficient of determination (R^2) were done using Microsoft Excel and the graph was established with GraphPad Prism programme. Ct, cycle threshold; PFU, plaque forming units.

MOI of 0.001 resulted initial Ct values of 28.16 ± 1.99, while MOI 0.01 had 25.21 ± 1.68 and MOI of 0.1 had 21.26 ± 1.34 Ct values.

Three days *pi* with MOI 0.001, the Ct values of Vero-B4 and U138 cells had dropped to 16.30 ± 2.32 (Vero-B4) and 16.82 ± 1.6 (U138) which calculates to a mean difference (ΔCt) of 11.58 ± 0.23 compared to the initial level upon infection (0*dpi*) (Figure 12). This corresponds to a nearly 4-log increase ($1×10^4$) in virus amount. None of the other tested cell lines (DBTRG, Huh-7 and A549) showed any similar increase in viral RNA.
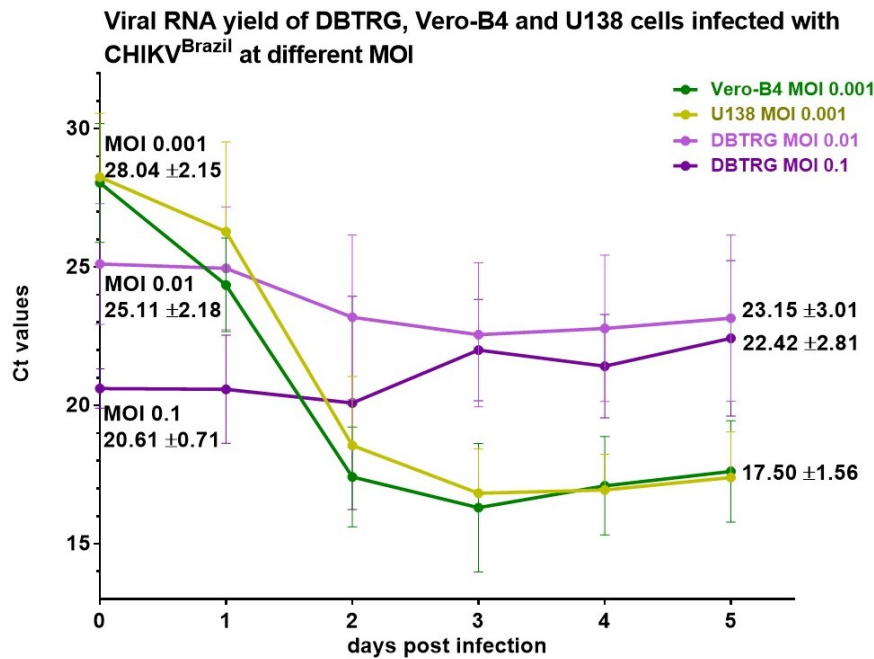
Figure 12: Viral RNA yield of Vero-B4, U138 and DBTRG cells infected with CHIKV^Brazil over the course of 5 days.

Cells were infected with CHIKV^Brazil at different MOIs and supernatant was collected every day for 5 days *pi.* Supernatant was diluted 1:10 with AVL-buffer and RNA was purified using the QIACube (Qiagen). PCR was done with RealStar® Chikungunya RT-PCR (Kit 2.0; Altona). Means and standard deviations were calculated from three independent experiments with Microsoft Excel. All samples with Ct levels of < 35 and with sigmoid curves were considered positive. Curves were created using GraphPad Prism. Vero-B4 (green graph) and U138 (yellow graph) cells were infected with a MOI of 0.001. Infection of DBTRG cells (purple graphs) with CHIKV were at MOI of 0.01 (light purple graph) and 0.1 (dark purple graph). Ct, cycle threshold; MOI, multiplicity of infection.

DBTRG cells infected with CHIKV at a MOI of 0.01 did show some changes in the Ct values over time, but the increase in viral RNA was not as significant as in the Vero-B4 and the U138 cells. ΔCt between the highest and the lowest Ct value was 2.55 Ct point and thus was in the range of the SD (Figure 12). At a 10-fold higher MOI (MOI 0.1) DBTRG did not show any increase in viral RNA.

A549 cells had some increase in viral RNA at the lowest MOI (0.001) with ΔCt being 5.77 ± 2.56 points (Figure 13A). At higher MOI however, no significant change in the Ct values could be observed between the first day of infection and the following 5 days in A549 cells (Figure 13A).

Huh-7 cells showed no change in Ct levels in the course of a 5-days infection (Figure 13B). The MOI had no influence on the virus production in Huh-7 cells. At the lowest MOI (0.001) Ct value at the day of infection was 28.18 ± 1.79, while *3dpi* it was 27.90 ± 2.07 and 28.62 ± 1.58 at the end of the experiment after 5 days (Figure 13B).

Figure 13: Viral RNA yield of A549 (A), Huh-7 (B) and Vero-B4 cells infected with CHIKV[Brazil] over the course of 5 days.
Cells were infected with CHIKV[Brazil] at different MOIs and supernatant was collected every day for 5 days *pi.* Supernatant was diluted 1:10 with AVL-buffer and RNA was purified using the QIACube (Qiagen). PCR was done with RealStar® Chikungunya RT-PCR (Kit 2.0; Altona). Means and standard deviations were calculated from three independent experiments with Microsoft Excel. Curves were created using GraphPad Prism. Vero-B4 cells (green graphs) were infected with a MOI of 0.001. **A)** Infection of A549 cells (blue graphs) with CHIKV were at different MOI. **B)** Huh-7 Characterisation of Chikungunya virus.

The Ct values at MOI 0.01 and MOI 0.1 also showed no significant difference during the course of infection, with initial Ct values of 25.24 ± 1.78 and 21.65 ± 1.69 respectively and final values of 25.13 ± 1.10 for MOI 0.01 and 21.41 ± 1.10 for MOI 0.1 *5dpi.*

2.2.4.   **Titre of CHIKV stocks**

Two days *post* infection all the Vero-B4 cells had detached and the virus was harvested. Two different stocks (labelled as #6 (first virus isolation from the patient's serum on Vero-B4 cells) and #7 (first cultivation on arthropod C6/36 cells)) were created. Differences in the titre between the two stocks could be observed which is interesting given the fact that they originate from the same serum and the only difference was their initial cultivation (either on Vero-B4 or on C6/36 cells). Stock #6 had an about 10-fold higher titre than stock #7. We tried tittering $CHIKV^{Brazil}$ on Vero-B4 and U138 cells (Figure 14B).

One plaque assay plate for both stocks can be seen in Figure 14. For stock #6 the dilutions $1:10^5$ and $1:10^6$ produced countable plaques (exemplary plate in Figure 14A has a plaque count of $((11+11+10+20)/4) \times 5 \times 10^5 = 65 \times 10^5 = 6.5 \times 10^6$ PFU/mL for Stock #6. Assays were repeated at least four times independently for Stock #6 and produced titres between 6.5×10^6 and 18.2×10^6 PFU/mL. Calculations were thus done with a mean titre of 1.27×10^7 PFU/mL. Stock #7 ended up with a titre of 7.25×10^5 PFU/mL. Stock #6 or progeny of this stock was mainly used for infection experiments.

No plaques formed on the U138 cell layer even though the plates were processed the same way as the ones that held Vero-B4 cells (Figure 14B). Even after 5 days of incubation no clearly separated plaques could be observed on U138 cells. It is possible that immunostaining might be a more suitable way to determine virus titre in U138 cells. In this thesis, we thus calculated MOI with the Vero-B4 titres for all experiments (even those that were done with different cell lines) to have comparable virus amounts in all infection experiments.
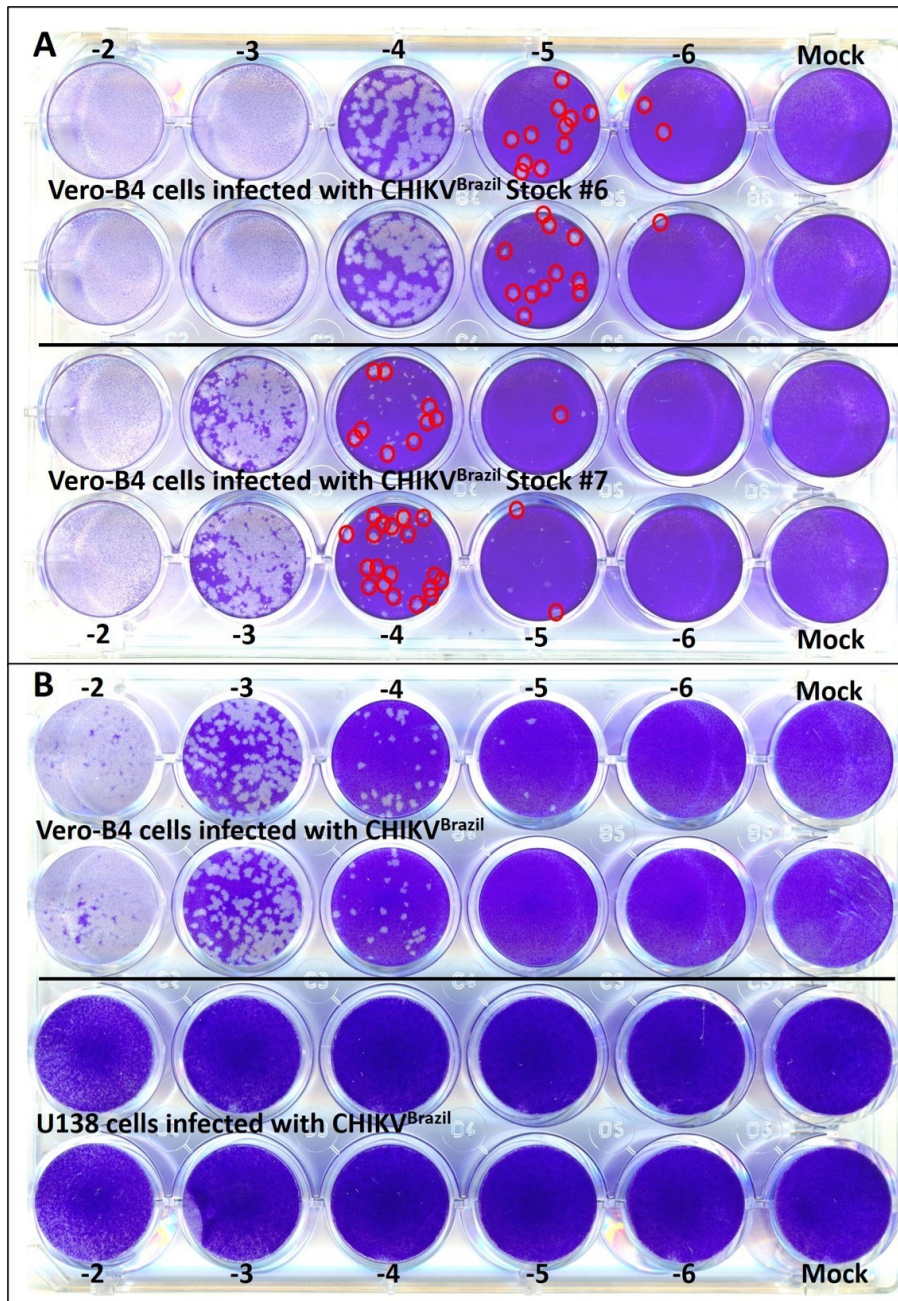
Figure 14 A & B: CHIKV titration with plaque assay.
Cells (Vero-B4 or U138) were seeded at 1.2×10^5 cells/mL/well in a 24-well plate and allowed to settle overnight. A 10-fold dilution of each virus stock added. Overlay consisted of 800 µL of 0.8 - 1% methyl cellulose mixed with DMEM and 2.5% FBS. The plates were incubated at 37 °C with 5% CO_2 for 4 days, then the cells were fixed and dyed with 1 mL of crystal violet per well. Mock represents non-infected cells. The numbers above and below the wells indicate the exponent of the virus dilution. **A)** Titration of CHIKV[Brazil] stock #6 and #7 on Vero-B4 cells. Stock #6 is derived from CHIKV[Brazil] that had initially been cultivated on Vero-B4 cells while stock #7 was firstly grown on C6/36 cells. Counted plaques are marked with a red circle to distinguish them from dye and wash artefacts. **B)** Titration of a CHIKV[Brazil] stock on Vero-B4 and U138 cells. The CHIKV[Brazil] stock on U138 had once been subpassaged on U138 cells. While on Vero-B4 cells, countable plaques form in dilution -4 and -5, no distinguishable plaques can be observed in U138 cells.

2.2.5. Electron microscopy

Electron microscopic pictures of CHIKV were taken using the ZEISS Libra 120 TEM

Electronic Microscope. Pictures of particles were compared to pictures of Noranate *et al*. (2014)

from his publication on the 'Characterization of Chikungunya Virus-Like Particles' (Figure 16) and the VirusExplorer20151127 of the Robert Koch Institute (RKI) [115].
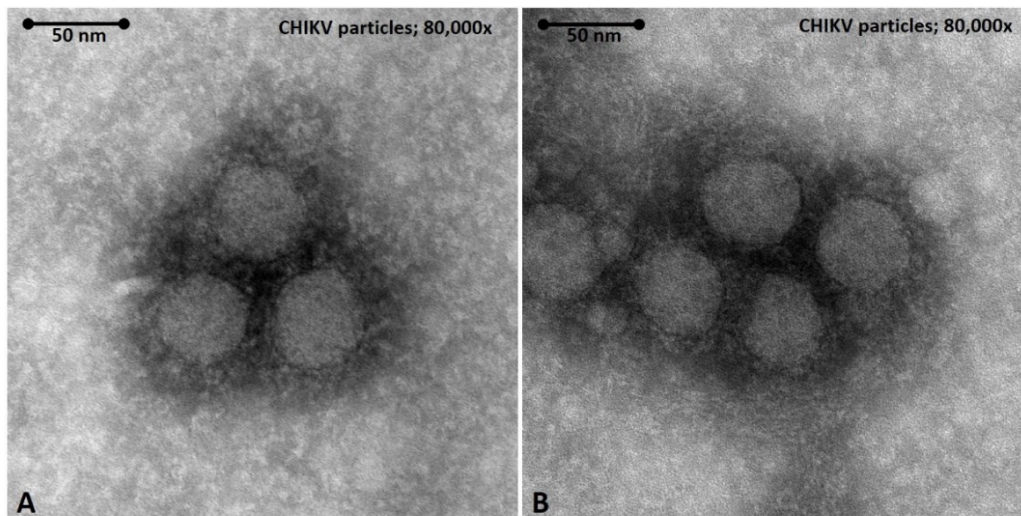
Figure 15: Transmission electron microscopic images of CHIKV.
CHIKV was cultivated in Vero-B4 cells for 4 days, then 80 µL of supernatant was inactivated with 10 µL of 25% glutaraldehyde and 10 µL of 20% paraformaldehyde. Hydrophilisation of the grids was done with 1% alcian-blue; negative contrast staining was done with phosphotungstic acid (1%). Microscopy was done with the ZEISS Libra 120 TEM Electronic Microscope. The bars indicate 50 nm. Magnification is 80,000x. Enveloped virions with icosahedral nucleocapsid symmetry with a diameter of 50-60 nm can be seen as would correspond to virions of the *Togaviridae*.

We were able to visualise virus particles that fit the description of togaviruses: enveloped virions with icosahedral nucleocapsid symmetry, spherical particles, 50-60 nm in diameter (Figure 15).
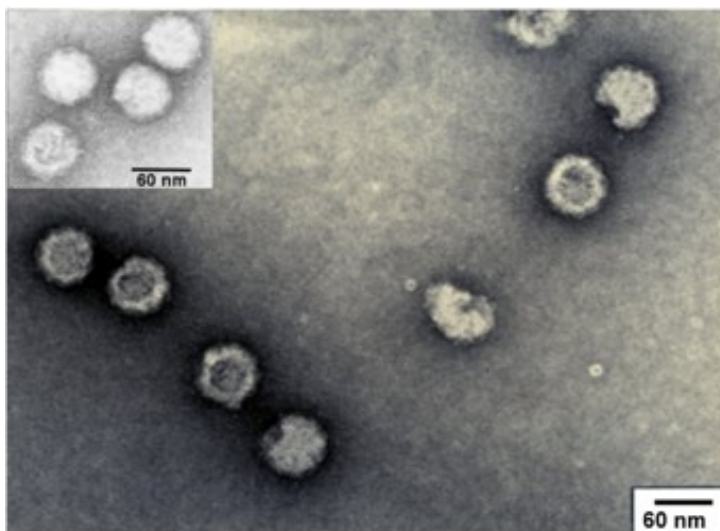
Figure 16: TEM pictures of CHIKV VLPs and CHIKV virions.
TEM analysis of purified virus like particles (VLPs) and CHIKV virion (top, left corner) done by Noranate and colleagues. Bars indicate 60 nm, magnification is 150,000x. Virions show great morphological similarity to our findings as well as the same size. (Picture retrieved from Noranate, Takeda [116])

3. Characterisation of compounds

3.1. Compound screening via viability assays

3.1.1. MTS screening results

Antiviral activity of 34 compounds (#1-34) at a concentration of 10 µM varied between Vero-B4 and U138 cells in the efficacy assays. Apart from the RBV control, seven compounds (#7, 10, 13, 14, 16-18) had values which were statistically significant with a p-value < 0.05 in the brain derived U138 cell line (Figure 17). More than 50% of U138 cells survived CHIKV challenge when treated with 10 µM of #13 (57.79% ± 13.47% viable cells), #14 (64.92% ± 16.65%) or #17 (53.75% ± 2.85%) (Figure 17). The RBV control (410 µM) showed a good antiviral activity of the compound with constantly between 71% to 81% of viable U138 cells. About 28% of the U138 cells survived CHIKV infection *5dpi* (Figure 17). The toxicity assays in U138 cells revealed statistically significant (p-value < 0.05) toxicity for compounds #16-18 and RBV in U138 cells (data not shown). Still more than 75% of the U138 cells survived treatment with these four compounds (data not shown).

In Vero-B4 cells, compounds #14, 16 and 17 showed statistically significant differences to untreated infected cells (Figure 18A). Apart from RBV (55-66% viable Vero-B4 cells) compound #14 worked best ensuring 37.48% ± 2.82% cells to survive CHIKV infection (Figure 18A). In untreated, infected controls about 24% of the Vero-B4 cells survived CHIKV challenge for 4 days at an initial MOI of 0.64.

The toxicity screen in Vero-B4 showed a statistically significant negative difference to Mock control for compound #14 (39.73% ± 8.85% viable Vero-B4 cells) (Figure 18B). No other compound had cytotoxic effects on Vero-B4 cells (data not shown). Huh-7 cells did not show any CPE when infected with CHIKV[Brazil] even at MOI 6.4 (see colums with black square pattern in Figure 19A & B). Thus, this cell line was only used for toxicity evaluation. Statistically significant (negative) differences to Mock control could be observed for compounds #9, 13, 14, 27 and RBV (Figure 19).
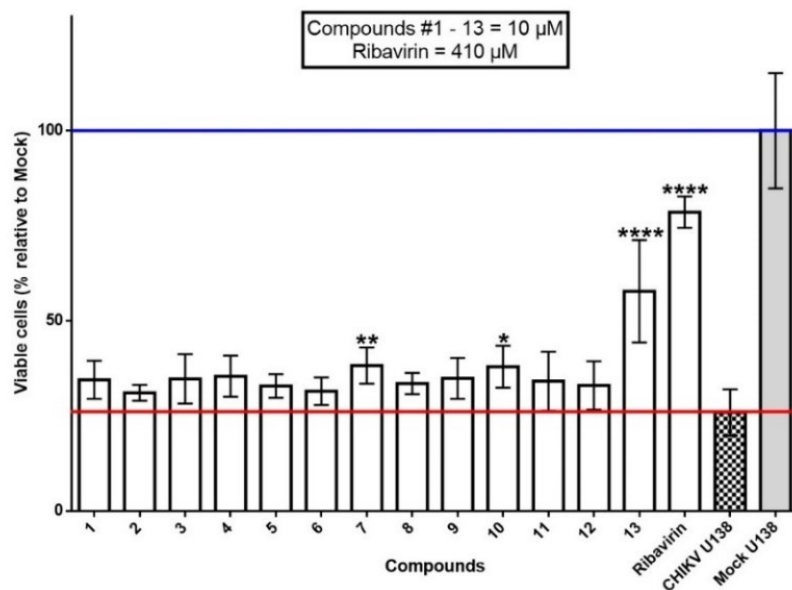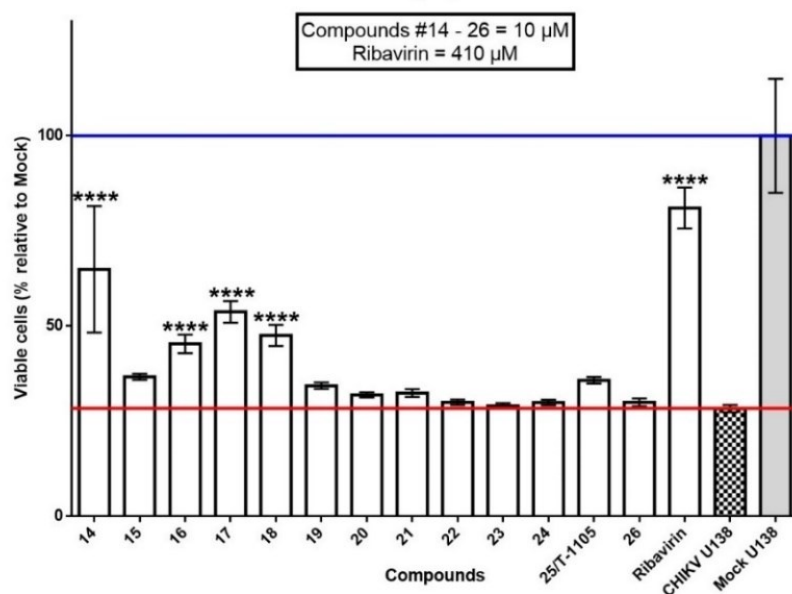
Figure 17: Efficacy of some compounds in U138 cells challenged with CHIKV[Brazil] (MOI of 0.64).

Human glioblastoma cells U138 were infected with CHIKV and treated with the compounds at 10 µM or RBV at 410 µM. Five days after infection, cell survival was determined with MTS. Values are given as percentages in relation to Mock control (grey columns and blue line) and are means of three independent experiments each with at least three technical replicates. Error bars indicate SD of the relative values. **(A)** Efficacy of of compounds #1-14 against CHIKV. **(B)** Efficacy of the compounds #14-26 against CHIKV. Statistically significant (positive) differences between cells treated with compounds (white columns) and the positive control (virus only, columns with black square pattern and red line) were evaluated in a one-way ANOVA test and are indicated by black asterisks (p-values). P-values are given as follows: * $p < 0.05$; ** $p < 0.01$; **** $p < 0.0001$. MOI, multiplicity of infection; *dpi*, days post infection; MOI, multiplicity of infection; n, number of independent repeats.
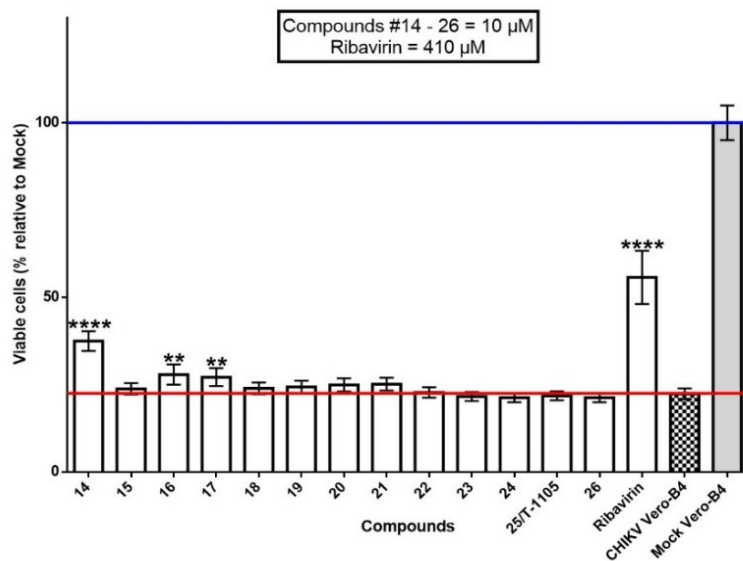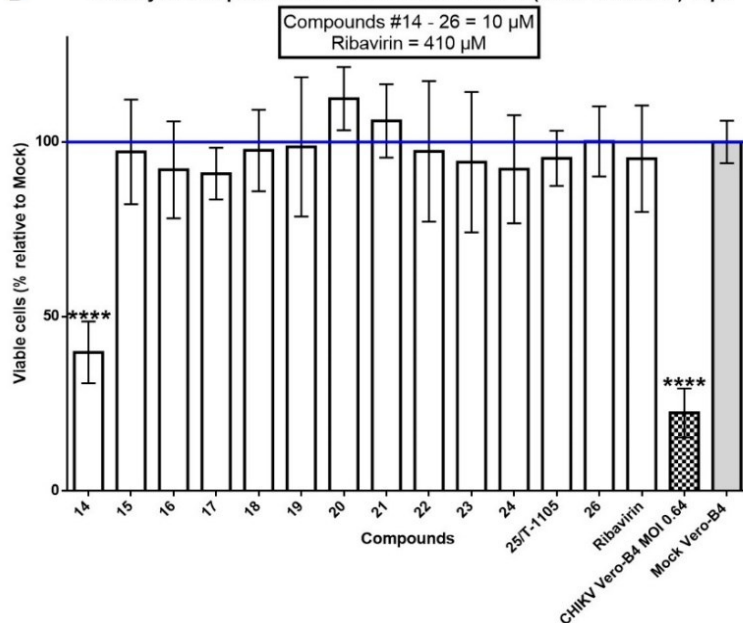
Figure 18: Efficacy against CHIKV^{Brazil} and toxicity of compounds at 10 µM in Vero-B4 cells.

Vero-B4 cells were infected at the indicated MOI (A) efficacy test) or not (B) toxicity test) and treated with various compounds. Four days after infection/treatment, cell survival was determined with MTS. Values are given as percentages in relation to Mock control and are means of three independent experiments each with at least three technical replicates. Error bars indicate SD of the relative values. **(A)** Vero-B4 were infected with CHIKV^{Brazil} and treated with different compounds (white columns). Statistically significant (positive) differences between cells treated with compounds and the positive control (virus only, columns with black square pattern and red line) were evaluated in a one-way ANOVA test and are indicated by black asterisks. **(B)** Compound toxicity in Vero-B4 cells. Statistically significant (negative) differences between Mock control (100% live cells; grey bar and blue line) and the treated cells (white bars), are indicated by black asterisks. The number of asterisks indicate p-values as follows: ** $p < 0.01$; **** $p < 0.0001$. Graphs were done and analysed with GraphPad Prism in a One-Way ANOVA multiple comparisons test. MOI, multiplicity of infection; n, number of independent repeats; *dpi*, days post infection; *dpt*, days post treatment.
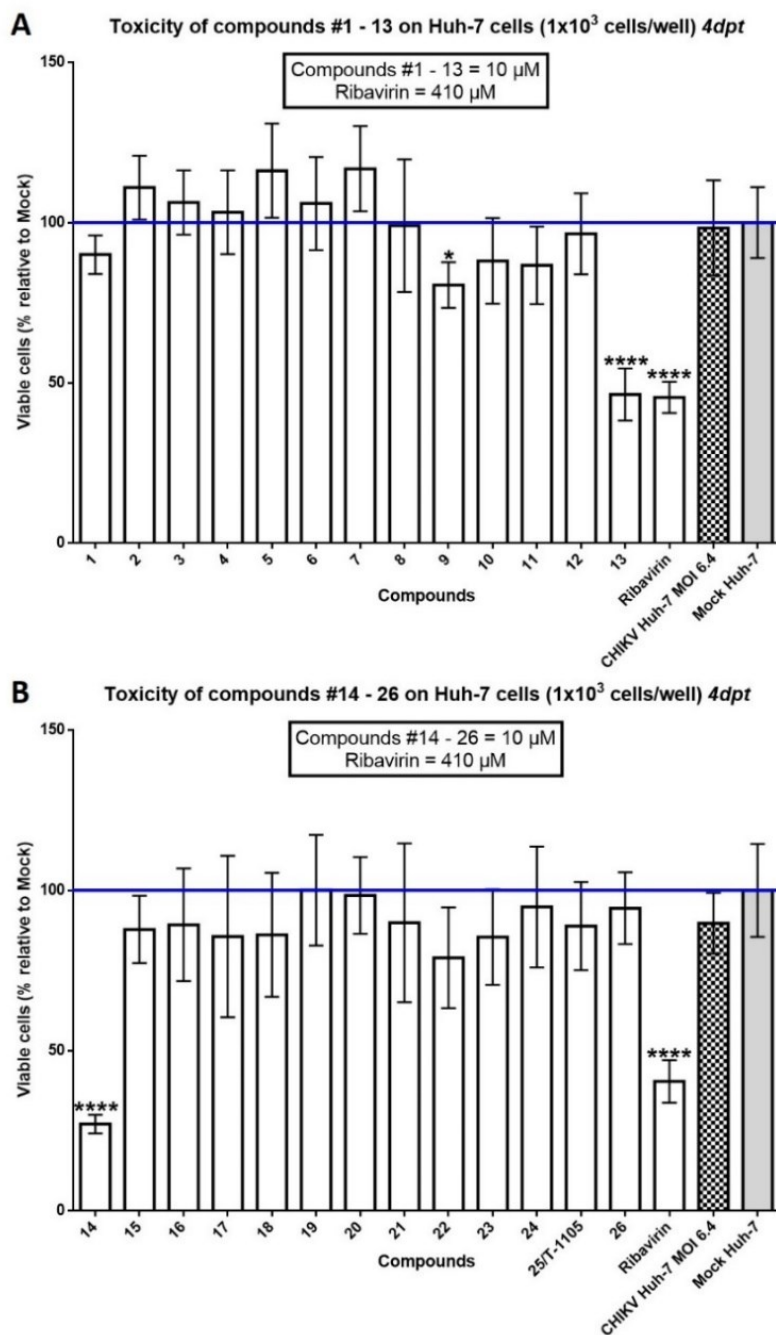
Figure 19: Toxicity of compounds at 10 µM in Huh-7 cells 4 days after treatment.
Human hepatoma (Huh-7) cells were incubated with a selection of compounds for 4 days. Four days after infection/treatment, cell survival was determined with MTS. Values are given as percentages in relation to Mock control and are means of three independent experiments each with at least three technical replicates. Error bars indicate SD of the relative values. The white colums show toxicity of compounds #1-13 **(A)** and #14-26 **(B)** in Huh-7 cells. Statistically significant (negative) differences between Mock control (100% live cells; grey bar and blue line) and the treated cells (white bars), are indicated by black asterisks. The number of asterisks indicate p-values as follows: * $p < 0.05$; **** $p < 0.0001$. *dpt*, days post treatment.

While > 80% of the Huh-7 survived 4 days of treatment with compounds #9 and 27, compounds #13 (46.40% ± 8.14% viable Huh-7 cells), #14 (27.09% ± 2.93%) and RBV (40-45%) were more toxic (Figure 19).

3.2.   Plaque reduction assay

Some compounds that showed activity in the individual assays of the screening were parallelly investigated with a plaque reduction assay. The antiviral effects of the compounds on the plaques were diverse, some produced less plaques, some produced smaller plaques and some had intermediate results (small plaques and 'normal' sized plaques and decreased or unaltered number). For statistical analyses only the plaques that matched the size of the virus infected, untreated control were counted. If the plaque size was considerably smaller, it was noted accordingly. An example of the different plaque features can be seen in Figure 20.
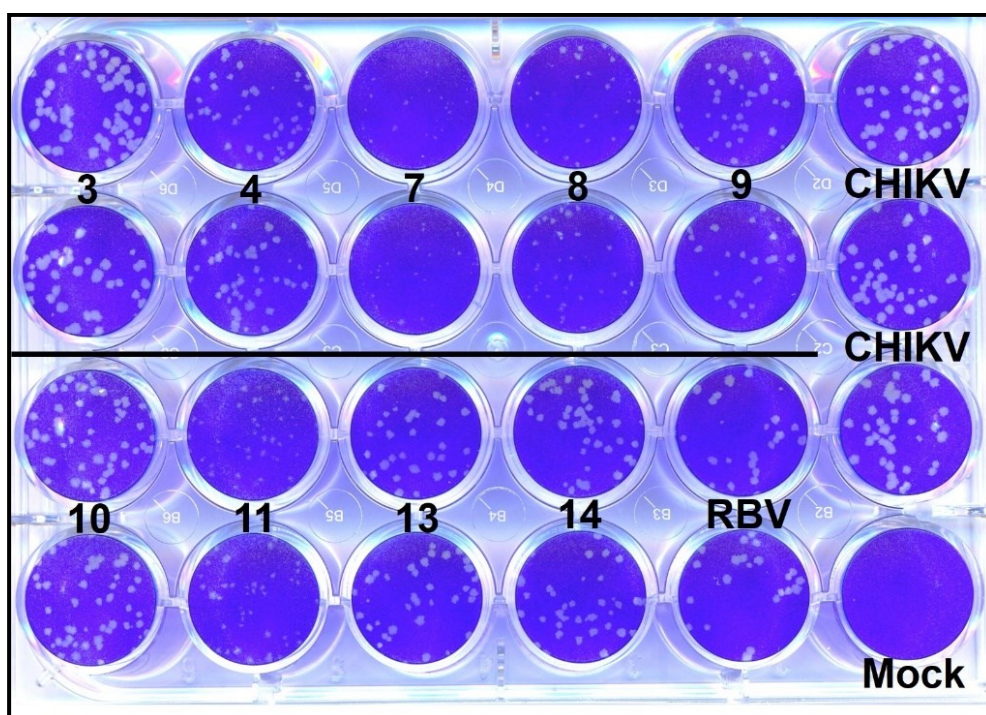
Figure 20: Plaque reduction assay (PRA) on Vero-B4 cells.
Vero-B4 cells were seeded at 1.2×10^5 cells/mL/well in a 24-well plate and allowed to settle overnight. After removal of the supernatant 500 µL of compound dilution (DMEM LG, 2.5% FBS) were added one hour prior infection with CHIKV[Brazil]. Overlay consisted of 400 µL of 1.875% methyl cellulose mixed with DMEM and 0.6% FBS. The plates were incubated at 37 °C with 5% CO_2 for 4 days, then the cells were fixed and dyed with 1 mL of crystal violet per well. Mock represents non-infected cells. All the compounds were used at a final concentration of 10 µM, RBV at 410 µM. Mock represents untreated non-infected cells. The numbers on the plate indicate the different compounds. 'CHIKV' indicates infected but untreated controls (mean in this plate is 38 ± 5.6 PFU). For the statistical evaluation, only plaques matching the size of the CHIKV controls were counted. PFU, plaque forming units; RBV, ribavirin.

RBV decreased the number as well as the size of plaques. Compounds #3 and #10 had no significant effect on plaque number, but the size of the plaques in the wells treated with #10 are smaller. Plaque size is considerably smaller in the wells treated with compounds #7, 8, and 11. Compounds #4, 9, 13, and 14 also displayed smaller plaques, yet not to such an extent as the previously mentioned compounds. A full analysis of all performed plaque reduction assays can be seen in Figure 21.
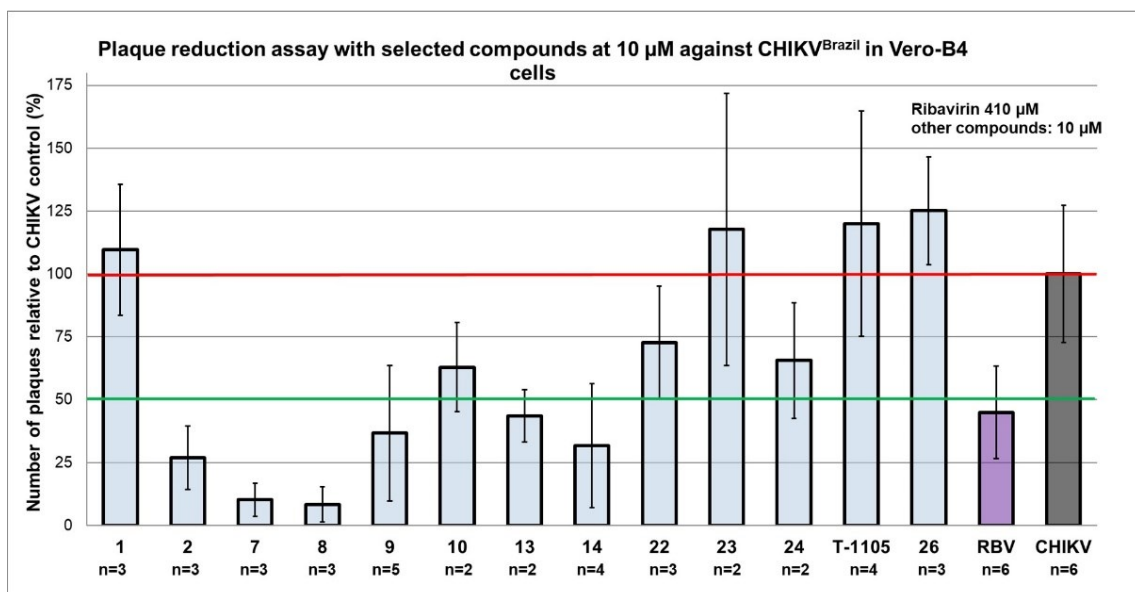
Figure 21: Evaluation of plaque reduction assays performed in Vero-B4 cells infected with CHIKV and selected compounds at 10 µM.

Values are given as means in relation to infected, untreated controls (grey bar CHIKV = 100%). SD is in percent relative to the mean number of plaques of the infected, untreated controls. 'n' gives the number of repetitions of independent experiments each with two technical replicates. The red line indicates 100% of virus activity/infectivity and the green line 50% PFU reduction. Analysis was done with Microsoft Excel.

3.3.   Virus yield assay with selected compounds in U138 cells

All non-infected and untreated Mock controls (contamination control) had no detectable Ct level at 5*dpi* (data not shown). Coinciding with the findings in chapter V.2.2.3 (Yield assay RT-PCR), the peak of yielded viral RNA in U138 cells was detected 3*dpi* (Figure 22A). The amount of viral RNA in the positive control increased $1 \times 10^{3.2}$-fold (ΔCt of 9.62) two days and $1 \times 10^{3.8}$-fold (ΔCt of 11.38) three days after infection (Figure 22).
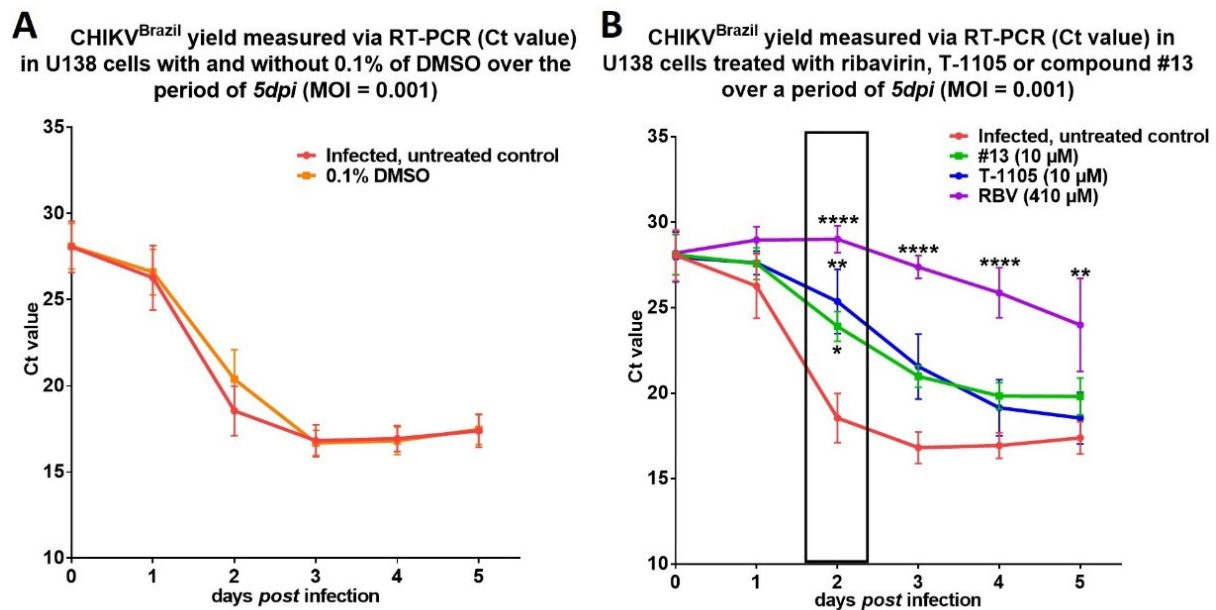
Figure 22: Viral RNA yield in U138 cells infected with CHIKV (MOI 0.001) treated with various compounds.
A) Infected and untreated control (red graph) and infected U138 cells supplied with 0.1% of DMSO (yellow graph). **B)** U138 cells infected with CHIKV^{Brazil} at MOI 0.001 and treated with compound #13 (green graph), T-1105 (blue graph) or RBV (purple graph). A two-way ANOVA test was applied to analyse differences between infected and not treated control (red graph) and the differently treated cells at the indicated time points. The black rectangle is placed over the values measured at day two after infection. Statistically significant differences are indicated with asterisks and give p-values as follows: * $p < 0.05$; ** $p < 0.01$; **** $p < 0.0001$. Abbreviations: Ct, cycle threshold; *dpi*, days post infection; MOI, multiplicity of infection; RBV, ribavirin.

There was no significant difference between the infected, untreated control (positive control) and cells treated with 0.1% of DMSO (Figure 22A).

The decrease in viral RNA yield in the cells treated with 10 µM of compounds #13 and T-1105 compared to the positive control was only statistically significant two days after infection (Figure 22B). Compound #13 diminished viral RNA yield in treated cells by 5.35 Ct points (= ΔCt) compared to untreated cells (this corresponds to a 55-fold ($1\times10^{1.74}$) reduction of viral RNA). T-1105 performed equally well two days after infection, ΔCt between treated and untreated cells was 5.55. This corresponds to a 70-fold ($1\times10^{1.85}$) lower amount of viral RNA in the supernatant of treated cells. Cells treated with 410 µM of RBV had a statistically highly significant (p-value < 0.0001) reduction of viral RNA yield compared to the positive control. The Ct levels of RBV treated U138 cells (purple graph in Figure 22B) stayed at the initial RNA level until day 3 *pi* and stayed significantly low throughout the whole experiment. ΔCt of RBV treated cells and the positive control at day 2 *pi* was 11.47. During the first two days after

infection, the Ct calues of RBV treated cell thus correspond to the initial infectious virus amount.

3.4.   IC$_{50}$/CC$_{50}$ of selected compounds

Table 3: IC$_{50}$ and CC$_{50}$ values of different compounds against wt CHIKV^{Brazil} (MOI: 0.355) in Vero-B4 and U138 cells.

Compound	IC$_{50}$ (µM)		CC$_{50}$ (µM)		SI	
	Vero-B4	U138	Vero-B4	U138	Vero-B4	U138
Ribavirin	479.6	139	> 700	> 500	> 1.46	> 3.6
T-1105	n.d.	35.74	> 100	> 100	n.d.	> 2.8
#13	n.d.	4.3	> 30	> 30	n.d.	> 7

Abbreviations: CC$_{50}$, half maximal cytotoxic concentration; IC$_{50}$, half maximal inhibitory concentration; n.d., not determined; SI, selectivity index.

Ribavirin:

RBV showed a dose-dependent efficacy against CHIKV^{Brazil} (MOI 0.325) in Vero-B4 cells (1×10^4 cells/well). An IC$_{50}$ of 480 µM was determined in 4 different, independent experiments each with three technical replicates (Figure 23A).
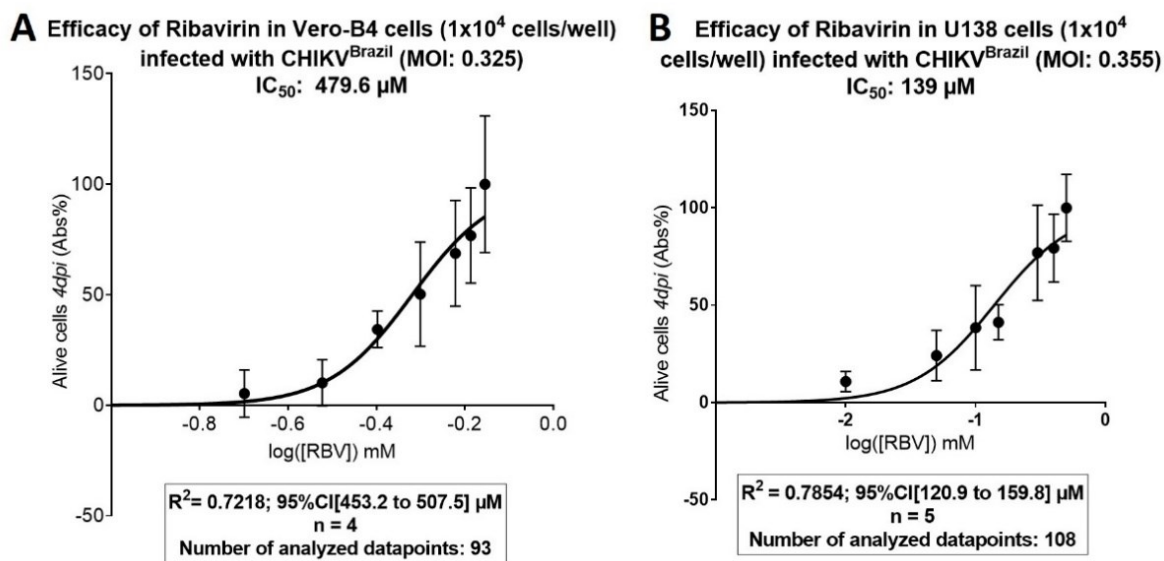
Figure 23: IC$_{50}$ value of ribavirin in Vero-B4 and U138 cells infected with CHIKV^{Brazil}. RBV inhibits CHIKV^{Brazil}-induced cell death in Vero-B4 **(A)** and U138 **(C)** cells in a dose-dependent manner. Cells (1×10^4 cells/well) were infected with CHIKV at an indicated MOI and treated with a serial dilution of RBV. After 4 days, cell death was determined via a colorimetric cell viability assay (MTS). The data represent means ± SD of raw data from at least 4 independent experiments performed with three technical replicates. Normalised fit of dose-response curves was calculated with GraphPad Prism 6 Software. Abbreviations: Abs, absorption; IC$_{50}$, half maximal inhibitory concentration; RBV, ribavirin; MOI, multiplicity of infection; n, number of independent repetitions.

CC_{50} value for RBV in Vero-B4 cells could not be determined due to bad curve fit (R^2). Analysis showed no toxicity at the highest concentrations (700 µM; data not shown). Selectivity index (SI) can be assumed to be > 1.46 (Table 3).

IC_{50} value for RBV in U138 cells (1×10^4 cells/well) infected with CHIKV[Brazil] (MOI 0.355) was 139 µM (Figure 23B). CC_{50} could not be determined as U138 cells were not negatively affected by the highest RBV concentration (500 µM). SI can thus be assumed to be > 3.6 (Table 3).

T-1105

A dose-dependent effect of T-1105 could only be detected in U138 cells but not in Vero-B4 cells (Figure 24A). No toxic effect was observed at the highest concentration (100 µM) in all cell lines (Vero-B4, U138 and Huh-7) (data not shown). SI can thus be assumed to be > 2.8 for U138 cells (Table 3).
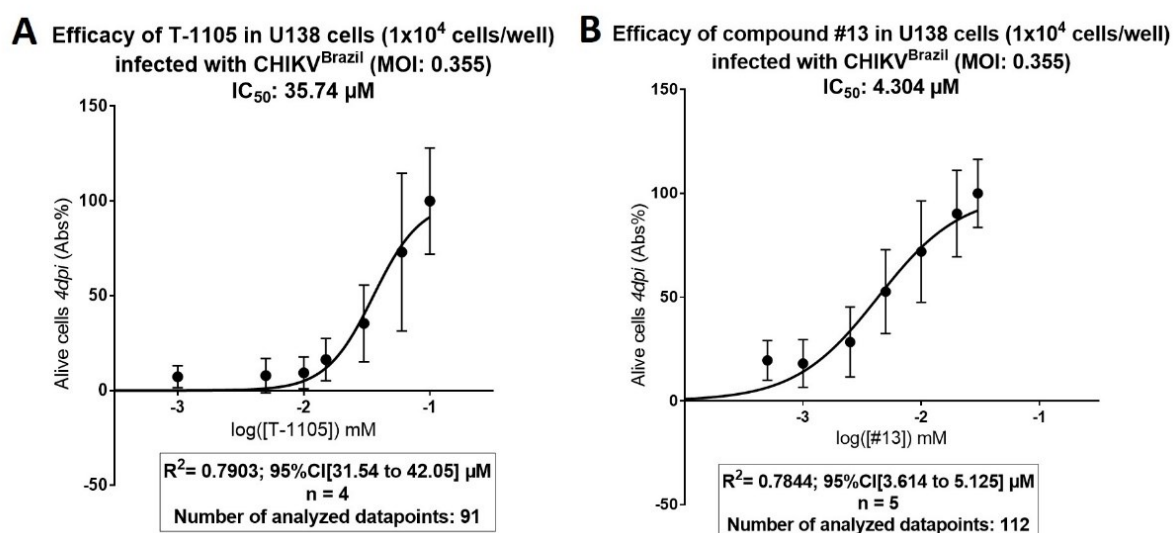
Figure 24: IC_{50} value of compounds T-1105 and #13 in U138 cells infected with CHIKV[Brazil].
T-1105 **(A)** and #13 **(B)** inhibit CHIKV-induced cell death in U138 cells in a dose-dependent manner. U138 (1×10^4 cells/well) were infected at an MOI of 0.355 and treated with the compounds at the indicated concentrations. After 4 days, cell death was determined via a colorimetric cell viability assay (MTS). Data represent means ± SD of raw data from at least 4 independent experiments each with three technical replicates. Normalised fit of dose-response curve was done with GraphPad Prism 6 Software. Abbreviations: 95%CI, 95% confidence interval; Abs, absorption; IC_{50}, half maximal inhibitory concentration; n, number of independent repetitions.

Compound #13

A dose-dependent effect of compound #13 could only be observed in U138 cells (not in Vero-B4). In U138 an IC_{50} of 4.3 µM could be observed (Figure 24B). Repeated tests to determine a CC_{50} in various cell lines (Vero-B4, U138) failed because of irregular response of the cells to increasing compound dose. In Vero-B4 and U138 cells, concentrations up to 30 µM

showed no dose-dependent toxic effect on the cells (SI in U138 cells > 7). It could be observed that with increasing concentration (> 10 µM), the compound precipitated in the (aqueous) dilution. Microscopic analysis revealed that #13 formed crystals at concentrations > 10 µM.

3.5. Real-time cell analysis with xCELLigence

3.5.1. Monitoring of cell growth and proliferation

The ideal number of cells for a RTCA assay was determined by monitoring cell growth and proliferation of each cell line at different densities. RTCA software was used to evaluate CI values through the measured impedance recordings. Cell densities in the graphs increase with the darker shade of each corresponding colour. The lightest shade thus represents 2.5×10^3 cells/well, and continues to increase in the following steps: 5×10^3, 7.5×10^3, 1×10^4, 1.5×10^4 and 2×10^4 cell/well (darkest shaded colour). As shown in Figure 25 and Figure 26, cell lines displayed different ranges of CI values.

Huh-7 and Vero-B4 cells had a similar CI range during the preliminary phase of cell adhesion and proliferation (first 20 hours of the experiment) (Figure 25A and B). Maximum CI values for Vero-B4 cells were between 4.0 and 6.0, while for Huh-7 cells CI values ranged around 5.0. U138 and U251 had lower CI values (Figure 26A and B). U138 reached between 1.0 and 2.5 CI (depending on the cell density) while U251 was between 0.3 and 2.0 CI. There was a definite variety in the curves of the different cell densities and cell lines. When Huh-7 cells were seeded lower than 7.5×10^3 cells/well the cells did not grow exponentially but linearly in the initial 20 hours. The two lowest cell densities in Huh-7 (2.5×10^3 and 5×10^3) had CI values below 3.0 (Figure 25A).
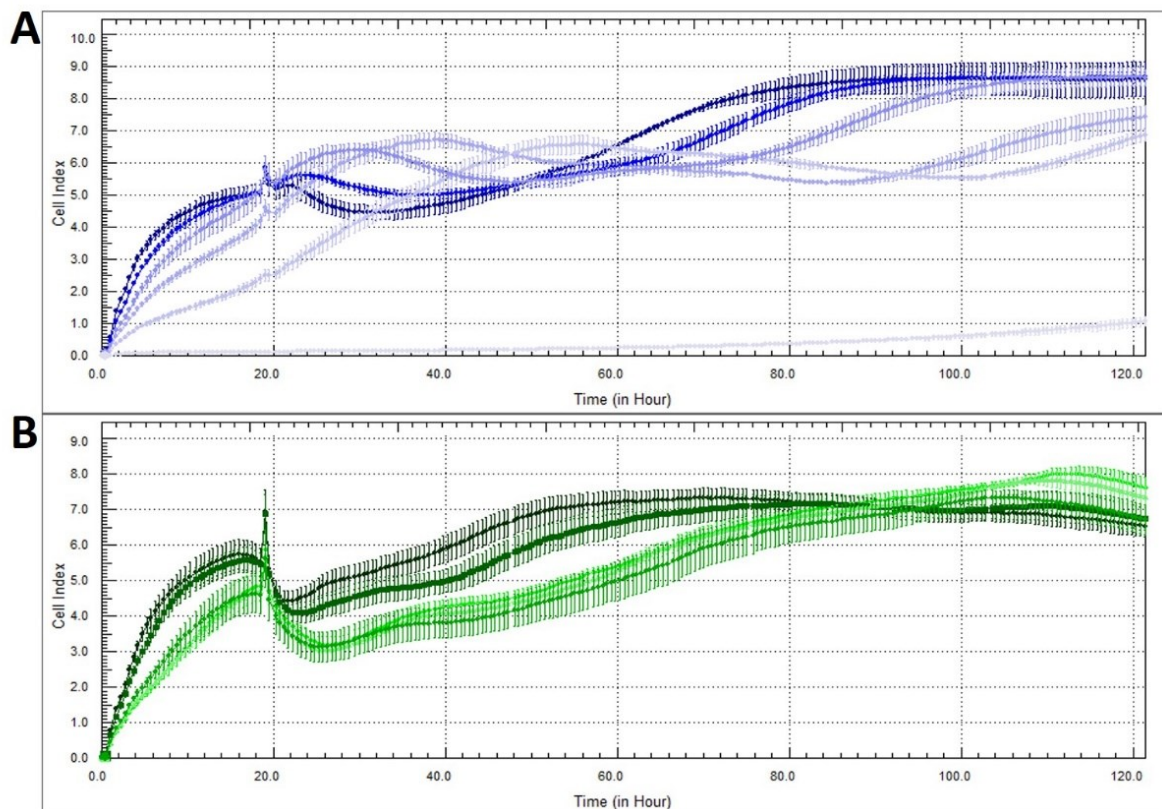
Figure 25: Proliferation curves of Huh-7 (A) and Vero-B4 (B) cells.
Different cell densities (2.5×10^3, 5×10^3, 7.5×10^3, 1×10^4, 1.5×10^4 and 2×10^4 cells/well) were seeded in a 96-well E-plate and monitored via RTCA over 5 days. CI (cell index) indicates the adherence of the cells to the plate and is measured through electronic impedance in intervals of 15 minutes. The peak at 19 hours timepoint comes from adding 100 µL of medium. The curves normalise at 20 hours. **A)** Huh-7 cells at different cell densities (blue graphs, increasing cell numbers are indicated by darker shades of the colour; lightest shade: 2.5×10^3; darkest shade: 2.0×10^4 cells/well). **B)** Vero-B4 cells at different cell densities (green graphs, increasing cell numbers are indicated by darker shades of the colour; lightest shade: 5×10^3; darkest shade: 2.0×10^4 cells/well). Data points are means from quadruplicates with standard deviation. Analysis was done with RTCA Software 2.0 (Roche).

Vero-B4, U138 and U251 cells seeded $\geq 7.5\times10^4$ cells/well showed exponential growth (Figure 25B and Figure 26). For these three cell lines, higher cell densities (1.5×10^4 and 2.0×10^4) displayed better exponential curves during the initial 24 hours, however, in the course of the experiment (> 60 hours post seeding) the cells turned static or detached from the plate, which was detectable through decreasing CI values (Figure 25 & Figure 26). As a result, 1×10^4 cells/well was selected as the optimum seeding concentration for the four cell lines.
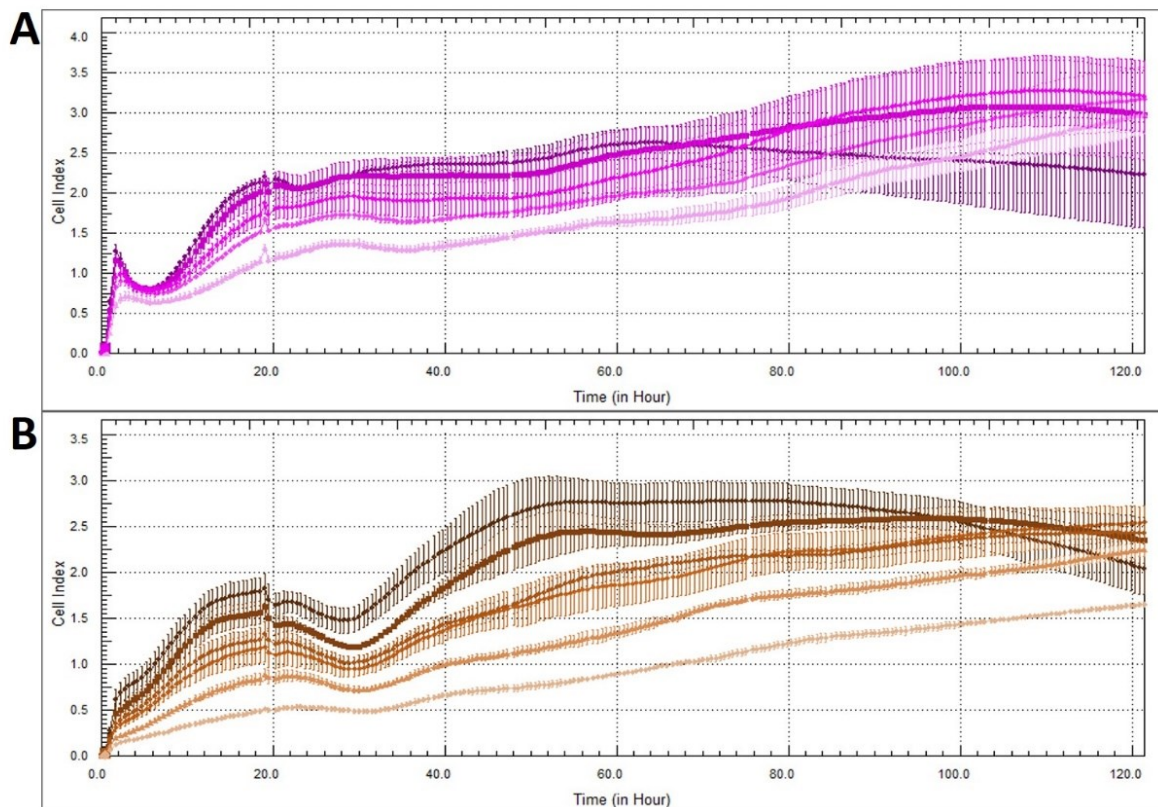
Figure 26: Proliferation curves of U138 (A) and U251 (B) cells.
Different cell densities (2.5×10^3, 5×10^3, 7.5×10^3, 1×10^4, 1.5×10^4 and 2×10^4 cells/well) were seeded in a 96-well E-plate and monitored via RTCA over 5 days. CI (cell index) indicates the adherence of the cells to the plate and is measured through electronic impedance in intervals of 15 minutes. The peak at 19 hours timepoint comes from adding 100 µL of medium. The curves normalise at 20 hours. **A)** U138 cells at different cell densities (purple graphs, increasing cell numbers are indicated by darker shades of the colour; lightest shade: 5×10^3; darkest shade: 2.0×10^4 cells/well). **B)** U251 cells at different cell densities (brown graphs, increasing cell numbers are indicated by darker shades of the colour; lightest shade: 2.5×10^3; darkest shade: 2.0×10^4 cells/well). Data points are means from quadruplicates with standard deviation. Analysis was done with RTCA Software 2.0 (Roche).

3.5.2. Efficacy and toxicity of antivirals against CHIKV monitored with RTCA

Efficacy (Vero-B4 and U138 cells):

In Vero-B4 cells detectable CPE (declining CI) sets in about 18 hours *pi.* CI values dropped rapidly below 6.0 in infected, untreated Vero-B4 cells and reached 0.08 CI 80 hours after the experiment started (Figure 27A). In Mock control, the CI increased continuously to a maximal CI of 7.49 ± 0.16 at 90 hours timepoint and declined gradually thereafter (CI at 5.95 ± 0.14 when experiment was terminated after nearly 6 days). Vero-B4 cells treated with 410 µM of RBV had delayed onset of CPE compared to the positive control (Figure 27A, black dashed vertical line). CI values started to decline about 30 hours later than in the untreated infected cells. At the 80 hours timepoint, RBV treated cells still had a CI of 5.0 ± 0.62. The graphs of Vero-B4 cells treated with 10 µM of compound #13 or T-1105 did not deviate significantly from the curve of the infected, untreated control. Vero-B4 cells treated with 50 µM of T-1105

had a significant shift of the curve (Figure 27A, dark blue graph). CI values declined 16 hours later than the positive control. At 80 hours timepoint, 50 μM T-1105 treated cells still had a CI of 1.4 ± 0.5.

U138 growth curves differed from those of Vero-B4 (Figure 27B). The CI values of U138 were lower and the non-infected Mock control with 0.1% DMSO reached maximum CI values between 1.8 and 2.3 and continuously stayed on that level throughout the experiment (Figure 27B). CPE set in 22 hours *pi* in U138 cells. CI values declined slower than in Vero-B4 cells. U138 positive control had a CI of 0.98 ± 0.34 at 80 hours timepoint and 0.09 ± 0.13 when the experiment was terminated after 140 hours.
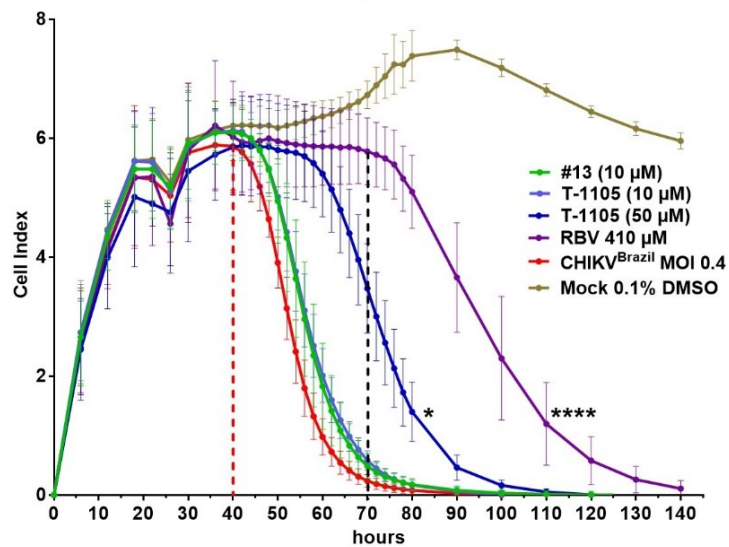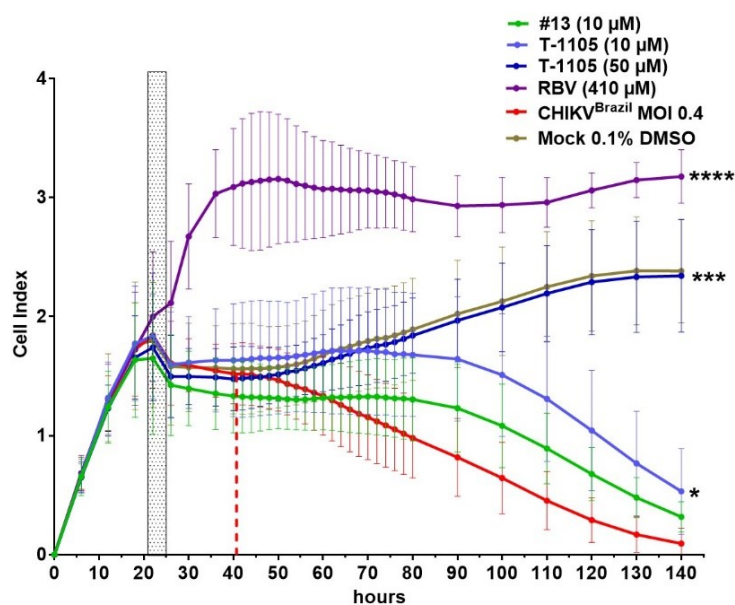
Figure 27: Monitoring cell status and efficacy of #13, T-1105 and ribavirin in CHIKV infected Vero-B4 (A) and U138 (B) cells for 6 days via RTCA.
Cells (1×10^4 cells/well) were treated with either compound #13 (green graphs), T-1105 (blue graphs) or RBV (purple graphs) and infected with CHIKV[Brazil] (MOI of 0.4). The cells were monitored via RTCA for 6 days. Impedance was measured every 15 minutes. A one-way ANOVA Sidiak's multiple comparison test was done comparing compound treated cells with the positive control (red curves). P values are indicated with asterisks as follows: * $p < 0.05$; *** $p < 0.005$; **** $p < 0.0001$. Measurements and raw data were done by RTCA Software 2.0 (Roche), graphs and statistical analysis with GraphPad Prism 6 software. Data points are the mean ± standard deviation from nine data sets (three independent experiments each with three technical replicates) of significant time points and were calculated with Microsoft Excel. Treatment and infection caused the spike in the graphs at ~25 hours. The vertical, dashed red line marks onset of declining CI values due to CPE in the positive control (red graphs). Brown curves show non-infected, untreated Mock control with 0.1% DMSO. **A)** Vero-B4 cells; the black dashed vertical line indicates the onset of CPE in the RBV treated cells (about 30 hours delayed from the untreated control). **B)** U138 cells; the grey colums indicates the time the cells needed to normalise after treatment and infection. Abbreviations: MOI, multiplicity of infection; RBV, ribavirin.

U138 treated with 410 µM of RBV reached significantly higher CI values (3.03 ± 0.37 CI compared to 1.57 ± 0.35 in Mock after 36 hours). Additionally, there was no detectable onset of CPE in RBV treated U138 cells (Figure 27B, purple graph). These cells stayed on CI levels of over 3.0 until the termination of the experiment.

Although differences in the curves between compound #13 treated U138 cells and the positive control were observable, compound #13 treatment (10 µM) had no statistically significant influence on infected U138 cells (Figure 27B, green graph *vs.* red graph). U138 cells treated with 10 µM of T-1105 (Figure 27B, light blue graph) had a delayed onset of CPE compared to the positive control. CI values started to decline about 68 hours *pi*, which is about 56 hours later than the positive control. At the 80 hours timepoint, these cells had a CI of 1.67 ± 0.52 and 0.53 ± 0.36 at the end of the experiment. U138 cells treated with 50 µM of T-1105 had a growth curve similar to non-infected Mock control and no detectable onset of CPE (Figure 27B, dark blue graph).

Toxicity (Vero-B4, U138 and Huh-7 cells)

In Vero-B4 cells (Figure 28A), Mock control reached maximal CI values of 7.49 ± 0.16 at 90 hours timepoint and gradually declined thereafter to reach a CI of 5.95 ± 0.14 after 140 hours. Cells treated with 10 µM of compound #13 (Figure 28A) had curves close to Mock control, reaching a top CI value of 7.05 ± 0.30 at 90 hours timepoint. The CI at the last measuring point of 140 hours was 6.08 ± 0.39. RBV (410 µM) treated cells reached a maximum CI of 6.51 ± 0.27 at 90 hours and 6.08 ± 0.17 when the experiment was terminated after 140 hours. The CI values of #13 and RBV had no statistically significant difference from the Mock control. Similarly, no onset of CPE could be detected in the T-1105 treated Vero-B4 cells; the curves had no statistically different course than the Mock control (Figure 28A).

In U138 cells (Figure 28B), Mock control reached CI values of 1.57 ± 0.37 after 30 hours and increased continuously to a maximum of 2.39 ± 0.45 at 130 hours timepoint. Cells treated with 10 µM of compound #13 (Figure 28B) had a curve with the same course like the Mock control, but lower CI values. After 30 hours of monitoring, #13 treated cells had a CI value of 1.38 ± 0.34. The CI at 130 hours was 2.11 ± 0.31 and had no statistically significant difference from the Mock control (Figure 28B).
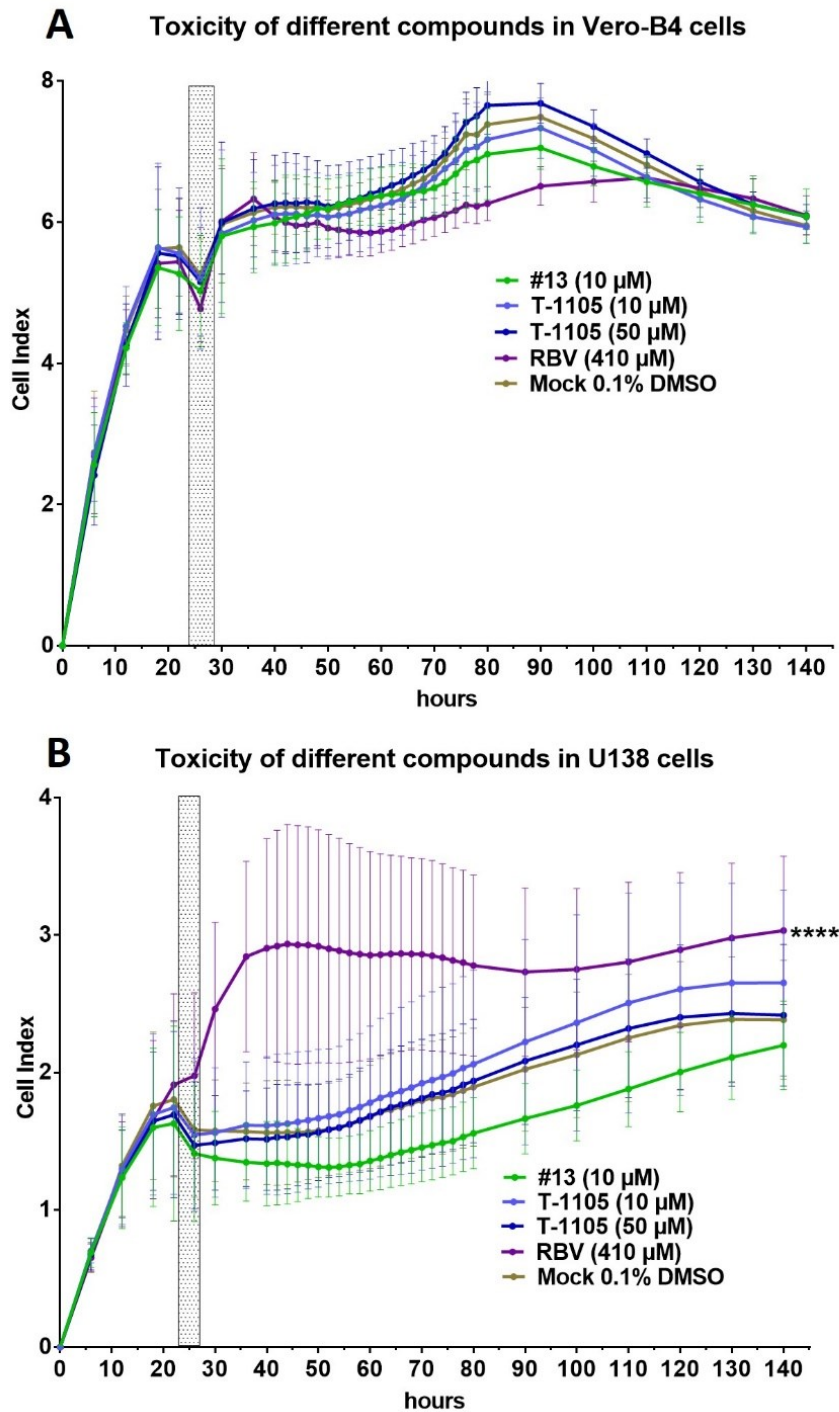
Figure 28: Monitoring cell status and toxicity of #13, T-1105 and ribavirin in Vero-B4 (A) and U138 (B) cells for 6 days via RTCA.
Cells (1×10^4 cells/well) were treated with either compound #13 (green graphs), T-1105 (blue graphs) or RBV (purple graphs) monitored via RTCA for nearly 6 days (140 hours). Impedance was measured every 15 minutes. A one-way ANOVA Sidiak's multiple comparison test was done comparing compound treated cells with untreated Mock control (brown curves). P values are indicated with asterisks as follows: **** $p < 0.0001$. Measurements and raw data were done by RTCA Software 2.0 (Roche), graphs and statistical analysis with GraphPad Prism 6 software. Data points are the mean ± standard deviation from nine data sets (three independent experiments each with three technical replicates) of significant time points and were calculated with Microsoft Excel. Treatment and infection caused the spike in the graphs at ~25 hours (grey rectangle). Brown curves show non-infected, untreated Mock control with 0.1% DMSO. **A)** Vero-B4 cells. **B)** U138 cells. Abbreviations: MOI, multiplicity of infection; RBV, ribavirin.

RBV (410 µM) treated U138 cells (Figure 28B, purple graph) reached significantly higher CI values than the Mock control and continued to have CI values of over 2.74 until the termination of the experiment. Interestingly, the impedance in RBV treated cells was very similar to RBV treated and CHIKV infected U138 cells (see Figure 27B). The RBV (410 µM) treated U138 cells had the same graph course as the CHIKV infected and RBV treated U138 cells. The RBV challenged U138 cells reached significantly higher CI values than the Mock control (e.g., CI of 2.84 ± 0.69 compared to 1.57 ± 0.35 in Mock at 36 hours timepoint). U138 cells treated with either concentration (10 µM and 50 µM) of T-1105 had no statistically different graph courses than the Mock control (Figure 28B). At 36 hours timepoint, T-1105 treated cells had CI values of 1.62 ± 0.46 (10 µM) and 1.52 ± 0.35 (50 µM). After 130 hours, CI values were at 2.65 ± 0.73 (10 µM) and 2.43 ± 0.53 (50 µM).

The Mock control of Huh-7 cells reached a peak at 30 hours timepoint of 10.21 ± 1.22 CI after which the curve had a downward course with a minimum of 6.69 ± 0.75 CI at 60 hours timepoint, then rising continuously to a final CI of 10.89 ± 0.87 at 140 hours (Figure 29, brown graph). Huh-7 cells treated with compound #13 had CI values of 11.01 ± 1.55 at 30 hours, a minimal CI of 8.29 ± 1.06 after 60 hours and a CI of 10.15 ± 0.70 at the termination of the experiment. According to the one-way ANOVA test, 10 µM of #13 did not lead to a statistically significant difference compared to Mock, although the course is slightly altered (Figure 29, green curve). Treatment of Huh-7 cells with 410 µM of RBV resulted in a significant graph difference (p-value < 0.05) between treated cells and Mock control. The RBV group reached maximal CI values of 10.89 ± 1.16 after 36 hours of monitoring. The graph had a continuous downward course until the end of the experiment, where the minimal CI of 8.35 ± 0.42 was registered (140 hours). T-1105 treatment of Huh-7 cells did not lead to statistically different graph courses from the Mock control (Figure 29, blue graphs). The CI values were in the same range as the Mock control at both T-1105 concentrations.
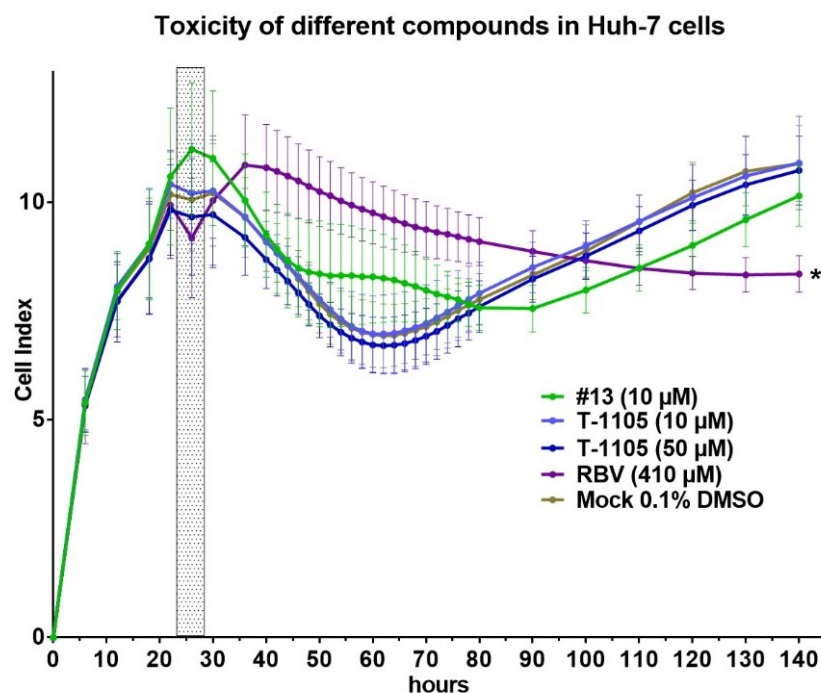
Figure 29: Monitoring cell status and toxicity of #13, T-1105 and ribavirin in Huh-7 cells for 6 days via RTCA.

Huh-7 cells (1×10^3 cells/well) were treated with either compound #13 (green graphs), T-1105 (blue graphs) or RBV (purple graphs) monitored via RTCA for nearly 6 days (140 hours). Impedance was measured every 15 minutes. A one-way ANOVA Sidiak's multiple comparison test was done comparing compound treated cells with untreated Mock control (brown curves). P values are indicated with asterisks as follows: * $p < 0.05$. Measurements and raw data were done by RTCA Software 2.0 (Roche), graphs and statistical analysis with GraphPad Prism 6 software. Data points are the mean ± standard deviation from nine data sets (three independent experiments each with three technical replicates) of significant time points and were calculated with Microsoft Excel. Treatment and infection caused the spike in the graphs at ~25 hours (grey rectangle). The brown curve shows non-infected, untreated Mock control with 0.1% DMSO. Abbreviations: RBV, ribavirin.

VII.   DISCUSSION

In the line of this thesis, 34 antiviral compounds were tested against a clinical isolate of CHIKV. In addition, different assay methods as well as different cell lines were evaluated for their usefulness in antiviral tests against different strains of Chikungunya virus (CHIKV[Brazil] *vs.* CHIKV[Ross]).

Because of its homology in the nsP2 to VEEV, CHIKV was used as a surrogate and prototypic alphavirus. CHIKV can be handled under BSL-3(**) conditions while the equine encephalitis viruses have to be strictly kept under BSL-3 conditions [124]. The neurotropic New World alphaviruses can all be transmitted via aerosols, causing severe disease [7]. So far, no lab-acquired CHIKV infections attributed to aerosols have been known, although non-human primates (NHP) do develop mild symptoms of CHIKF when exposed to CHIKV aerosols [24]. According to the 'Biostoffverordnung of the Bundesministerium für Justiz und Verbraucherschutz' (2013), BSL-2 agents are biological agents which can cause a human disease and pose a threat to people working with them. A public spread is unlikely and there is an effective prophylaxis or treatment available. BSL-3 agents are biological agents which can cause a severe disease in humans and pose a serious threat to people working with them. The public spread of these agents is possible (e.g., via aerosols), but usually there is an effective prophylaxis or treatment. Certain BSL-3 agents which are generally not transmitted by air are BSL-3(**) classified [125]. BSL-3(**) (internationally also referred to as BSL-2+) conditions are in between BSL-2 and BSL-3 and can roughly be seen as BSL-2 labs with enhanced precautions ([124, 125]). For further details and information on BSL-3(**) conditions and agents I refer to the technical rules for biological agents (TRBA 100) published by the committee on biological agents (German 'Ausschuss für Biologische Arbeitsstoffe' – ABAS, 2013 [125]).

1.   Discussion on cell lines

In order to find suitable cell lines for CHIKV infection experiments, various cell lines were tested accordingly (MTS, IFT, plaque and viral RNA yield assay). For discussion on kill curves of the different cell lines see VI.1

A549

This cell line has been described in CHIKV experiments before, but reports are contradictory. Sourisseau, Schilte [126] and stated that wt CHIKV virions bind to A549 cells without proliferating within the cell. Lack of replication of CHIKV in A549 was also observed by Olagnier, Scholte [127]. Solignat, Gay [128] did not detect any CPE on wt CHIKV infected

A549. Franco, Rodriquez [121] however, used this cell line to test RBV and favipiravir against an attenuated CHIKV strain (vaccine strain (181/clone25) at MOI 0.1) in a yield assay. According to Franco, CHIKV proliferated in A549 cells. It is possible that the lab generated attenuated vaccine strain (181/clone25) has some affinity to this cell line. Others report that A549 yield low virus titres, but still propagate CHIKV [129].

Our own observations proved this cell line as unsuitable for wt CHIKV^{Brazil} experiments since it displays no CPE, no CHIKV binding on the cells surface in the IFT and no viral RNA yield.

DBTRG

This brain derived cell line was tried as an infection model as CHIKV has been known to cause CNS disease. Although DBTRG was susceptible to CHIKV infection, the MOI needed to achieve a 'noticeable' kill was high. CHIKV did bind to the DBTRG cell surface, as IFT visualisation showed, the signal was however considerably weaker than in Vero-B4. Furthermore, infection of DBTRG with wt CHIKV at MOI 0.1 did not result in a yield of viral RNA, suggesting that a higher viral load is needed. This makes DBTRG unsuitable for our kind of experiments because high virus titres are needed and the results may be unreliable. It is possible that a different CHIKV strain (presumably an IOL isolate) might show better infectivity on this cell line.

Huh-7

The cell line is very sensitive to toxic effects and thus presents an ideal model for testing compound toxicity [130]. The human hepatoma cell line (Huh-7) showed different susceptibility depending on the CHIKV strain (see VI.1).

Viral RNA yield of CHIKV^{Brazil} could not be detected at neither MOI tested and in IFT the cell line had no detectable signal, suggesting that CHIKV^{Brazil} did not bind on the cell surface. This made this cell line unsuitable for antiviral assays with our CHIKV^{Brazil} isolate. Huh-7 cells were still used to critically elucidate the toxic properties of our compounds.

Vero-B4

Vero cells have been extensively used for CHIKV replication studies and plaque assays. The Vero-B4 cell line which derived from the original Vero cell line, is one of the most commonly used aneuploid mammalian cell lines in CHIKV research as it propagates CHIKV in high titres and shows extensive CPE [129]. In this thesis it was used as a reference cell line in viability screening assays, IC_{50}/CC_{50} assays, plaque reduction assays and in plaque assays to determine CHIKV titre. However, especially when looking for antivirals that eventually are destined for use in human patients, a human derived cell line (preferably from a site with clinical relevance)

to test antivirals in, is more desirable. Cell difference between species may affect virus affinity, compound efficacy and toxicity and might lead to misleading or inconclusive data.

U138 and U251

The human glioblastoma cell lines U138 and U251 were tested excessively for their susceptibility for CHIKV infection. U138 cells had a strong IFT signal, and viral RNA yield in the corresponding experiments were equal to Vero-B4 cells. U138 were well suited for CHIKV infection experiments with some limitation: experiments to establish U138 and U251 as human cell lines for CHIKV plaque assays did not result in detectable plaques. As CPEs are detectable through MTS, a different overlay or a different staining method, e.g., immunostaining, may work better.

U251 double in 23 hours and are sensitive to overgrowing. IFT showed strong signals, thus CHIKV seemed to bind to the U251 cell surface. One important observation was that cell viability assay with MTS in U251 was not working reliably when the experiment duration exceeded 3 days and when the initial cell concentration was $\geq 1 \times 10^4$ cells/well (96-well plate). Seeding too few cells resulted in badly proliferating cells (both U138 and U251), since the cells need close cell-to-cell contacts in order to form a layer. Too many cells will cause U251 to stop proliferating, curb their metabolism and reach a mode of stasis. In this state, U251 cells no longer reduced MTS into its formazan product. Consequently, the absorbance of the plate was so low that it would suggest no U251 cells were left alive, despite the fact that they were overconfluent. For these reasons, we carried our experiments on with U138 cells.

2.   Chikungunya virus from patient isolate

As previously described, two stocks of the same CHIKV isolate were created, the difference being that in Stock #6 the first virus isolation from the patient's serum was done on Vero-B4 cells and in #7 the first cultivation happened on arthropod C6/36 cells (mosquito). To create our stock titres both 'first cultivation stocks' were handled the same and two similar Vero-B4 cell bottles were infected. Still, differences in the titre between the two stocks could be observed. The titre from #7 was more than 10-fold lower than the titre of #6. This concurs with the findings Acharya, Paul [131] that CHIKV has a lower replication rate in C6/36 cells than in mammalian cells, produces less CPE and has a reduced antiviral response when tested in human and murine cell lines. According to Acharya, the impairment comes from reduced binding ability to glycosaminoglycan (GAG) receptors on mammalian cells. Since enveloped viruses acquire parts of the host cell membrane to generate the viral envelope membrane, the envelopes of these viruses have a variable carbohydrate and lipid composition, depending on the cell type

they originate from [131]. Furthermore, mosquito and mammalian cells enzymatically modify the viral glycoproteins after translation in different ways which leads to the formation of different kinds of oligosaccharides [131, 132]. Arachya demonstrated that a loss of GAG receptor binding is responsible for the reduced infectivity in CHIKV after mosquito cell passage and that after a successive passage in mammalian cells, CHIKV regained the binding capability. This may also explain why some lab-adapted CHIKV strains show different cell affinities than field isolated CHIKV. This fact should be kept in mind when creating stocks destined for infection experiments in mammalian cells. Viral stocks from two different cell lines (mammalian *vs*. mosquito) should not be used alternatively in the same line of infection experiments unless the stocks are to be compared in this respect.

The CHIKV used in this thesis is a patient isolate originating from Brazil. CHIKV has been verified through IFT and PCR. Genome sequencing revealed that the isolate belongs to the ECSA genotype. This is in conclusion with the fact that phylogenetical analysis of CHIKV cases in Brazil revealed 41 importations of CHIKV and also the presence of the ECSA genotype [133].

3.   Discussion on compound experiments

Starting from the structure of the initial hit published by Bassetto, De Burghgraeve [117], a series of novel analogues (designed and synthesised by Bassetto to inhibit the nsP2 of CHIKV) were tested against wt CHIKV along with a series of favipiravir analogues (nucleoside analogues and ProTides). Since Bassetto's first hit had anti-CHIKV IC_{50} values in the low micromolar range, an initial compound concentration of 10 µM was chosen for the screening assays. Any compound showing efficacy in this range, was to be investigated further. Among these were #13, 14, 16, 17 and 18 when tested in U138 cells. All these compounds are nsP2 inhibitors and showed no statistically significant toxic effect in U138 cells. In Vero-B4 cells only #14 showed efficacy. The compound was toxic to such an extent that only 37.92% of Vero-B4 cells survived, though. It is thus possible that the toxic properties of the compound led to a stress induced shut-down in the Vero-B4 cells that eventually also prevented the virus from replicating [134]. In Huh-7 cells the cytopathic effect of #13 (46.7% viable cells) was less than RBV (40-45% viable cells) but #14 was considerably toxic with only 26.84% of Huh-7 cells staying alive. As compound #14 was considerably more toxic than #13 at 10 µM in all tested cell lines, this compound was dropped from further IC_{50}/CC_{50} investigations.

Apart from RBV (HCQ) and T-1105 as controls, compound #13 was thus chosen for further investigation.

Bassettos lead compound from her previous study of 2013 was not among the tested *in silico* drugs. Her lead molecule inhibited CHIKV in a virus-cell-based CPE reduction assay with an IC_{50} value of 5.0 µM and IC_{50} values of 3.3 and 4.9 µM in a virus yield assay on Vero cells [117]. This is in line with the IC_{50} values we generated for our selected compound #13. Structurally closer analogues of this Bassetto's lead did show minor efficacy in our screening assays (compounds #14, 16, and 17), but were not selected further.

Comparing the efficacy of the control compounds and the selected #13 in different assays led to interesting results. While RBV worked well in all assays and in both cell lines (statistically highly significant differences toward positive control in the virus yield assay in U138 and in the RTCA monitoring in Vero-B4 and in U138), compound #13 did only show statistically significant efficacy in U138 cells. Also, T-1105 worked significantly better in U138 than in Vero-B4 cells (in the RTCA). It is likely that differences in the cell's metabolisms of the two cell lines are one reason for the different compound efficacies. Vero-B4 cells e.g., have a doubling time of 24 hours while U138 take twice that long [109, 135]. See also discussion in VI.1.

It was possible to demonstrate that the compounds #13, T-1105 and RBV actually curb virus replication in U138 cells (Figure 22B). While compound #13 and T-1105 treated cells had a reduced viral RNA production, CHIKV production in the RBV treated U138 cells was stalled completely during the first two days after infection.

As to why the majority of analogues tested in this thesis (and #13 in Vero-B4 cells) did not perform equally well as her original hit of Bassetto's lead might have (apart from their different chemical structure) various causes. Bassetto used a different CHIKV strain (CHIKV Indian Ocean strain 889 *vs.* CHIKV^{Brazil}) with a different infectious dose ($100CCID_{50}$ *vs.* MOI 0.64), in different cell densities (2.5×10^4 *vs.* 1×10^4 cells/well) over a different time *post i*nfection (6 days *vs.* 4 days) [117].

Monitoring Vero-B4 and U138 cells treated with selected compounds with and without CHIKV infection over a period of 6 days via RTCA led to interesting observations. While Vero-B4 cells display a 30-hours delayed onset of CPE under RBV (410 µM) treatment and CHIKV challenge compared to positive control, U138 seem to proliferate under RBV influence. CI values of RBV treated U138 cells nearly double in the first 30 hours compared to Mock control and there is no significant difference between the values of cells in the efficacy or in the toxicity assay. Not only does the virus not affect the cells, but the viability of the cells is considerably higher in the RBV treated U138 cells unrelated to virus addition. This phenomenon could at least be partly attributed to the different metabolic rates of the two cell lines. As mentioned before, Vero-B4

cells double in half the time than U138 and thus the time it takes for the cell to react to certain stresses might also be different.

Different modes of action are attributed to RBV. The drug is a nucleoside analogue and cells need to convert RBV to ribavirin monophosphate (RMP) [136]. This is done by the adenosine kinase. Depending on the cell type, cells have different amounts of this enzyme available. Consequently, cells with less adenosine kinase can accumulate only small amounts of RMP [137]. RMP is then further phosphorylated into RDP (the diphosphate form) and RTP (triphosphate), the latter being the predominant active metabolite in cells. This further processing varies according to the amount of RMP available [136, 137]. The major antiviral action of RBV is that RTP inhibits the inosine monophosphate dehydrogenase (IMPDH) and thus curbs cellular GTP pools. GTP is very important for viral and cellular RNA-, DNA- and (glycol)protein synthesis, in energy storage, intracellular signalling and translation by ribosomes [136]. Another mechanism attributed to RBV is its ability to interact with enzymes that cap cellular mRNAs and viral genomic RNAs. RBV inhibits capping of RNA genomes either by interfering with guanosyltransferase or methyltransferase activities of the nsP1 [138]. This leads to mRNAs that are not fit for translation. RBV also directly inhibits nsP4 RdRp and thus stops viral genome replication. While these mechanisms could explain inhibition of CHIKV replication and a later onset of CPE in Vero-B4 cells (when RBV pool is used up, CHIKV can replicate again), it does not explain the proliferation of the U138 cell line in the non-infected but RBV treated cells. Further investigations might be justified to shed light on this observation.

The cell curves of Vero-B4 cells treated with 50 µM of T-1105 show a delayed onset of CPE which is half way in between positive control and RBV. In U138 cells, 50 µM of T-1105 lead to a cell profile similar to Mock control. 10 µM of T-1105 result in a delayed onset of CPE compared to the positive control. CI values start to decline about 56 hours later than in the positive control.

T-1105 is a nucleoside analogue like RBV and the active metabolite works as a pseudo purine. There are two suggested modes of action: (1) specifically blocking RNA-dependent RNA polymerase (RdRp) by binding at certain domains of the enzyme [139, 140]; (2) incorporation of favipiravir-RTP into the nascent viral RNA thus leading to lethal mutagenesis [141, 142] or chain termination [143, 144]. In order to work, T-1105 has to be phosphoribosylated in the cell into its active form, a ribofuranosyl 5'-triphosphate metabolite (favipiravir-RTP). Delang and colleagues have identified a favipiravir resistant CHIKV variant which had a mutation in the

motif F1 of the RdRp [123]. This would suggest that blocking the RdRp is the probable mode of antiviral action of T-1105 against CHIKV.

Vero-B4 cells seem to be able to phosphorylate T-1105, but higher doses are needed and at 50 µM, the antiviral effect only lasts for 16 hours. The reasons might be that either the phosphorylation capacity does not allow the cells to be more efficient, or the nucleoside pool is used up and there is no more substrate (RBV) for the Vero- B4 cells to metabolise.

U138 cells also seem to be able to phosphorylate T-1105 and thus block CHIKV replication entirely at the concentration of 50 µM. At 10 µM CHIKV replication is at least delayed. Either this cell line metabolises the compound more efficiently than Vero-B4 or at a rate that grants CHIKV inhibition for the entire time at higher doses (5 days).

#13 did have some effect on the cells when compared to the untreated, infected cells in the RTCA, however the difference was not statistically significant. Possibly the concentration was too low or the compound's poor solubility did prevent its cellular uptake. As already discussed early, either some vehicle is found that enables the delivery of the drug to the site of action or the drug has to be chemically modified to adjust the pharmacological properties. The issue has been discussed with the medical chemists who designed the compounds and it seems to be a common problem with these kinds of compounds.

3.1. IC_{50}/CC_{50} in Vero-B4 and U138 cells

The 50% inhibitory concentration (IC_{50}) is defined as the compound concentration that is able to inhibit the virus-induced cell death by 50% compared to infected but untreated control. The IC_{50} is thus the half maximal inhibitory concentration of a compound that is able to inhibit a certain agent (in this case CHIKV). The 50% cytotoxic/cytostatic concentration is defined as the compound concentration that reduces the overall metabolic activity of non-infected but treated cells by 50% compared to non-infected and untreated cells (Mock). In this thesis, relative IC_{50} values are given. As the IC_{50} is calculated by putting compound concentration in relation with untreated infected control (positive control), 100% does not correlated with non-infected healthy cells (this would then correspond to the absolute IC_{50}), but with the highest concentration at which the compound was administered. This has to be kept in mind as the IC_{50} does not mean that 50% of the cells actually survived. Especially for RBV in Vero-B4 cells, the IC_{50} value can thus be misleading, as at the highest concentration used (700 µM) only 40-50% of the cells survived compared to non-infected and not treated Mock control. The same is the case with compound #13 in U138 cells. Even at the highest concentration of 30 µM only about 40-60% (in relation to Mock control) of the U138 cells survived CHIKV[Brazil] challenge.

Higher concentrations of the compound did not result in an increase in cell survival, but rather stalled cell viability (possibly due to cytotoxic effects).

Interestingly T-1105 did not result in a dose-response curve against CHIKV[Brazil] in Vero-B4 cells despite the fact that Delang and colleagues had published a study in 2014 stating that T-1105 had IC_{50} values of 7 and 47 µM (depending on the protocol he used) in Vero cells [123]. Delang however, had used a lab strain for his T-1105 tests. Thus, it is possible that our field isolate CHIKV strain may not show drug sensitivity at the concentrations between 5 and 100 µM. Furthermore, a more recent study tested favipiravir against CHIKV in Vero cells and had IC_{50} values of 184.53 µM (MOI 0.0001 of CHIKV vaccine strain (181/clone 25)) [121]. Interestingly, the group conducting the study used Huh-7 and A549 cells (MOI 0.1) to generate IC_{50} values (measuring virus yield). Both cell lines could not be infected with our wt CHIKV[Brazil] strain. The study generated IC_{50} values of 127.3 µM in Huh-7 cells and 245.13 µM in A549. Such data is very interesting but, on the same hand, raises questions on the comparability of the results. Delang, Segura Guerrero [123] had used a similar MTS assay from Promega like the one used in this thesis, while Franco generated his IC_{50} values measuring virus yield via plaque assays in Vero cells [121, 123]. Since further investigations with the xCELLigence proved T-1105 to be very effective at 50 µM, the IC_{50} generated in this thesis for T-1105 seem plausible and rather comparable with Delang's findings. These comparisons show how important it is to test a compound in different cell lines, against different virus stains and in different assay systems.

For #13 on the other hand, the IC_{50} of 4.3 µM is in accordance with the IC_{50} values of Bassetto's first hit and subsequent analogues that were tested against CHIKV Indian Ocean strain 889 (isolated in 2006 but now used as a 'lab' strain). Compound #13 is an analogue to Bassettos lead compound and her related compounds had values in the similar low micromolecular range in Vero cells [117, 145]. Compound #13 did not dissolve well in aqueous medium and precipitated at concentrations > 10µM. Microscopy revealed aggregated crystals of #13 at the bottom of the wells. The fact that compound concentration >30 µM did not result in higher compound efficacy might be rooted in the precipitation. It is also possible that the crystallisation of the compound at higher concentrations might be a reason for inconsistent cell viability curves especially in toxicity assays. An increase of soluble compound could not be achieved without raising the DMSO concentration in the supernatant of the cells. DMSO increase might however also impair cell viability as especially U138 cells were more sensitive to DMSO toxicity [146]. To improve solubility, either the chemical properties of the compounds need to be altered (e.g., the molecule is made more hydrophilic, which also bears the risk of losing the pharmacological

properties) or the drug has to be delivered via carriers. Drug delivery is a common problem in pharmacology and a great deal of research is focussing on new ways to deliver drugs to the site of action, e.g., by nanoparticles or nano micelles [147, 148].

The generated IC_{50} values of RBV in Vero-B4 cells are in conclusion with previous studies (for details and references see [149]). In this thesis mean IC_{50} value was 480 µM in Vero-B4 cells. RBV had a 3.5-fold higher efficacy in U138 cells. No CC_{50} could be generated in both U138 and Vero-B4 cells, RBV showed some toxicity at 410 µM in U138 cells (85% live cells) and none in Vero-B4. RBV is a commonly used positive control in CHIKV antiviral cell viability assays. However, the dosages needed to have a CHIKV antiviral effect *in vivo* fall outside of the therapeutic window for RBV and are considered toxic in humans. To achieve an effective dose for RBV against CHIKV, an adult human patient would have to take a 71-fold higher amount of the drug than the standard clinical dosage regimen for Hepatitis C virus (HCV) infection [120, 150]. This dosage would result in serious adverse effects such as haemolytic anaemia, pulmonary, dermatologic, and teratogenic effects [151, 152]. Thus, RBV is not a suitable treatment regimen for CHIKV infection in humans and there is a great need for new therapeutic strategies for the treatment of CHIKF.

4.   Discussion on different assay methods

Depending on the assay method, the focus lies either on the cell viabily or virus production. Consequently, different questions may be answered and it is not wise to rely on one of these assays alone.

Cytopathic effect (CPE) inhibition assays evaluate morphological changes in cells caused by cytopathogenic virus (or compounds). The MTS cell viability assay, RTCA or plaque reduction assays work with registering CPE. Cell viability assays such as MTS, RTCA and PRA focus on the cell status without giving information on virus proliferation. These systems monitor the well-being of the cell and the cell layer. RTCA is limited to adherent cells. Both MTS and RTCA are feasible for evaluating compound toxicity. As a result, the efficacy and toxicity of compounds can be investigated at the same time. PRA however is not capable of monitoring compound toxcitiy.

Virus yield quantification assays on the other hand, focus on the virus production. Either virus egress is measured via quantitative PCR methods (viral RNA/DNA in the supernatant is detected regardless if intact virions are present or not) or via a follow-up plaque assay (collected supernatant is used to infect a plaque assay plate). In the latter, only infectious virions are registered. Virus yield assay don't register compound toxicity either.

4.1.   Cell viability and compound screening assays with MTS

The viability of the infected cells was evaluated with the CellTiter 96®AQ~ueous~ Non-Radioactive Cell Proliferation Assay (MTS) (Promega, USA). This assay is a colorimetric method to determine the number of viable cells in proliferation and chemosensitivity assays. The assay consists of a tetrazolium compound (3-(4,5-dimethylthiazol-2-yl)-5-(3-carboxymethoxyphenyl)-2-(4-sulfophenyl)-2H-tetrazolium; MTS) and an electron coupling reagent (phenazine methosulfate; PMS). Live cells are able to reduce MTS into a formazan product that is soluble in cell culture medium and its' absorbance can be measured at 490 nm. Metabolically active cells achieve this conversion of MTS into formazan by dehydrogenase enzymes.

According to the manufacturer, a ratio of 20 µL combined MTS/PMS solution per 100 µL culture medium should be used. However, if sensitivity of the assay is not a limiting factor, Promega states that 20 µL of the combined MTS/PMS solution may be adequate for use with volumes as large as 200 µL/well. This relation was used in all our MTS assays.

The MTS assay method is suited for HTS and it is possible to evaluate efficacy and toxicity of compounds. Nevertheless, it has some limits. If cells grow too dense the optical density (OD) values might exceed those that are in the linear range of the reading instrument. For the iMark™ Microplate Reader form BioRad (Germany) a photometric range from 0.0 to 3.5 OD is given. For the Victor™X5 by PerkinElmer (USA) the photometric range is 0.0 to 4.0 with linearity granted between 0.0 and 2.0 and a precision in this range of 0.01. To achieve values within this range it is necessary discover the cell concentration that is enough to yield good result, yet not too many so that the cells are overconfluent at the end of the experiment.

It must be noted that different cell lines are able to metabolise the MTS agent at different rates [153]. It is thus important to evaluate each cell line individually in this respect to find an appropriate seeding density. Huh-7 cells turned out to proliferate at a very high rate and were used in the toxicity assays. Attempts with initial cell densities of 1×10^4 cells/well did not work out well, because Huh-7 were able to metabolise MTS very efficiently and OD values repeatedly went beyond 2.0 after less than 2 hours of incubation. For toxicity assays 1×10^3 Huh-7 cells/100 µL/well are sufficient to yield satisfying results 4 to 5 days after treatment, while all the other cell lines were seeded at 1×10^4 cells/100 µL/well.

Apart from absorption values that are too high (and thus outside the linear range), too many cells may also cause irritating results. Initial MTS screening assays with U251 cells led to readings with extremely low OD values, suggesting that all the cells were dead. Microscopical observation however revealed confluent cell layers. The cells were so dense (and overconfluent)

that they had gone into a static state and curbed their metabolic activity. As the mode of action of MTS assays relies on metabolically active cells [153], the MTS reaction did not take place which gave the impression destructed cells.

Consequently, viability assay results gained with MTS reagent should be interpreted critically especially in cell lines with short doubling times (like Huh-7 and U251 cells). Cell morphology should be checked under a microscope when the assay results are doubtful (e.g., readout suggests no viable cells in Mock control).

Furthermore, phenol red medium has an absorption between 0.2 and 0.26 OD itself. These absorption values suggested that more cells might be alive than actually are. Microscopic observation of the plates would verify that this is not the case. To avoid this background absorption, it is either possible to use phenol red free media in the experiments or measure the plates before addition of MTS reagent (T_0) and subtract the corresponding OD values from the ones measured after MTS addition and incubation (T_1) (T_1-T_0 = ΔOD). Since we used phenol red media in all experiments, the background interference was the same in all experiments. A similar problem may arise from compounds that are of yellow colour. These compounds have their own OD values and could suggest cell viability although the cells might have died (due to cytotoxicity). For yellow-coloured compounds, MTS cannot be recommended and another cell viability assay method should to be used (e.g., CellTiter-Glo® Luminescent Cell Viability Assay (Promega) which works with luminescence, not absorption).

The MTS/PMS assay method is easy, quick, objective, relatively cheap and suitable for large screenings as well as IC_{50}/CC_{50} evaluation. Only metabolic active cells are detected, though [153]. Moreover, it is an endpoint assay and the ideal time for stopping and evaluating the experiment is not detectable, but depends on experience, or publications with similar tests.

In this thesis, screening 34 compounds for their antiviral activity against CHIKV with MTS led to the discovery to a potential candidate. Still, it is reasonable to test discovered hits in more than just one test system to independently verify their antiviral potential.

4.2. Plaque reduction assay (PRA)

The only cell line that worked in plaque assays was Vero-B4. Repeated attempts to use any of the other human cell lines (A549, Huh-7, U138, and U251) failed. A549 and Huh-7 could not be infected by wt CHIKV[Brazil] and U138 and U251 did not form plaques. This shows one of the flaws of PRA as it is limited to viruses (and cells) that cause cell lysis or death [154]. PRA is a well-established way to test antivirals, as it is cheap and worked at with Vero, still it would be preferable to have a human cell line with clinical relevance for antiviral assays. Possibly other ways of detecting infected cells, (e.g., immunostaining) might work with U138 cells.

The PRA partly verified the results of the initial MTS screening (e.g., RBV and #14). Yet, some compounds that did not strike out in the screening MTS assay repeatedly had antiviral effects in the PRA at the same concentration. Compounds #4, 7 and 8 had notably decreased plaque sizes and #9 had a reduced plaque number which is not consistent with the screening assay where no antiviral effect could be observed in all four compounds. Compound #13 did show plaque reduction on Vero-B4, however, in the screening on Vero-B4 this compound did not strike out.

A plaque is formed when cells are lysed or killed by a virus. Since the overlay prevents the virus from spreading, the neighbouring cells are re-infected either from newly set free virus particles or via cell-to-cell transmission by intercellular extensions [108]. The neigbouring cells are killed as well, gradually forming a whole or plaque in the cell layer [155]. It is assumed that one plaque was originally started from one infectious virus particle [155].

Fewer plaques could indicate that the virus is hindered to enter the host cell. Some virus particles manage to enter the cell, replicate and are transmitted from cell to cell, thus destroying the cell layer. Smaller plaque size may indicate that the virus is able to infect the cell, but replication is blocked or slowed down because of some enzyme inhibition or curbed down host cell metabolism. In addition to that, compounds might block the cell-to-cell transmission or the lysis on the cell. Smaller plaques may also indicate that the virus is not able to exit the host cell or that lysis or cell death are delayed. The compounds (notably #13 and #14) leading to smaller plaques are all potential nsP2 inhibitors. The nsP2 is a protein with C-terminal cysteine (auto)protease activity that cleaves initial polyprotein into individual non-structural proteins thus enabling viral replication [8]. It would be reasonable that not virus entry, but virus proliferation is inhibited.

The PRA is easy and relatively cheap method. Still, it has limits for large screenings as it is labour intensive. It is not capable of evaluating compound toxicity. It allows limited interpretation of the results on virus entry, proliferation and exit due to plaque size and amount. Nevertheless, the endpoint evaluation (counting plaques) is very subjective which becomes less acurate if plaque morphology is indistinct [156]. Moreover, it is an endpoint assay and the time for stopping the assay should be determined microscopically (for Vero-B4 cells minimum 3 days *pi.*).

4.3. Viral RNA yield in treated U138 cells

The selective antiviral effect on compounds that are believed to inhibit virus replication can be evaluated with the help of a virus yield assay. Yield assays allow quantification of dose-response effects of a compound against a virus in two ways: (i) by the help of a quantitative

RT-PCR it is possible to detect the amount of viral nucleic acids (RNA or DNA) that is released in the supernatant; (ii) with a follow-up plaque titration assay it is possible to quantify the infectious virus particles that were released in supernatant [117]. While the first method detects all nucleic acids, no matter if they are released in intact capsids, defective viral particles or free RNA /DNA unless the sample is pretreated with nucleases, the second only registers infectious virions [157].

In this thesis, increase in viral RNA in the supernatant of the cells was measured by quantitative RT-PCR and it was thus possible to demonstrate that compound #13, T-1105 and RBV treated U138 cells had a reduced viral RNA production.

Yield assays with quantitative RT-PCR are an accurate way of determining nucleic acid production. If the focus lies on infective virions, a plaque assay has to follow for quantification (which is more time consuming than a PCR). But yield assays are labour intensive, time consuming and if a commercial PCR Kit is used for RNA detection, also quite expensive. Besides, viral yield assays give no information on compound toxicity. It is possible that a compound has severe cytotoxic effects and therefore shows no viral RNA increase, due to the fact that no cells are left alive to replicate the virus. It is therefore crucial to check on compound toxicity separately. For these reasons this assay method is not recommendable for HTS. To complement other assays, it is however a valuable method to monitor compound efficacy on virus replication.

4.4.   xCELLigence/RTCA monitoring

Real-time cell analysis (RTCA) monitors cell viability in a dynamic and non-offensive way by measuring electronic impedance based on the adherence of the cells to the plate [122]. CI (Cell Index) defines the impedance and gives information on the cell status. It is an arbitrary unit and is defined as $(Rn-Rb)/15$ where Rn is the cell–electrode impedance of the well with the cells and Rb is the background impedance of the well with the medium alone. The cell index value directly correlates with the number of viable cells [158]. It is thus possible to measure cellular features, including viral cytopathic effect (CPE). Without adherent cells, CI value is zero. The values increase consistently when more cells attach to the electrodes at the well bottom. CI values of 1 to 4 is defined as weak, 5 to 10 moderate and 10 to 15 a strong degree of cell adherence [159]. Nonetheless, different cell lines display different CI values even when the cell numbers are the same. It is thus important to empirically determine optimal cell numbers for each cell type.

As to antiviral testings against CHIKV via RTCA, the method is able to detect changes in cell morphology at precise timepoints, which is not the case with classical end point assays like MTS.

One major advantage of RTCA over the aforementioned methods is the continuous evaluation of the cells during the entire assay time. With the xCELLigence it is possible to detect differences between various cell lines and the reaction of the different cell lines on virus or compound challenge. The ideal treatment and infection time can be determined, as well as effects between treatment and the termination of the experiment. While the aforementioned CPE assay methods (MTS, PRA) did not detect an efficacy of of T-1105 at 10 µM in U138 cells, the RTCA monitoring clearly registered an antiviral action against CHIKV. At the same time, #13 did not yield a significant antiviral action in the RTCA monitoring while it showed efficacy in the MTS screening and at the RNA Yield assay at day 2 *pi*. RTCA has its advantages over "classical" assay methods, it is very accurate, easy and objective and requires not more handling of the plates than MTS assays. Additionally, IC_{50}/CC_{50} evaluations are possible as well. Regardless, it is only possible to evaluate one 96-well plate per RTCA device at a time, which makes it unsuitable for HTS and since one 96-well plate costs around 120 euros, it is by far the most expensive method. Hence, it does have its limits and cannot be seen as a panacea but should be applied as a complementary method for gaining supplemental information.

VIII. CONCLUSION AND FUTURE PROSPECTS / SCHLUSSFOLGERUNG UND AUSBLICK

This work demonstrates the successful application of various methods to test a series of *in silico* generated antiviral compounds against wt CHIKV. Besides, this thesis is the first record of successfully using the human glioblastoma cell line U138 as model for neurogenic CHIKV infection. Moreover, we were able to show that also the glioblastoma cell line U251 is susceptible to CHIKV infection and might be a used in infection assays. The cell lines A549 and Huh-7 proved unsuitable for CHIKV infection tests with our Brazilian clinical isolate since the virus does not replicate in these cell lines. At least Huh-7 might work with lab-adapted CHIKV[Ross] strain. Our experiments also proved that there are differences in cytopathological effects and antiviral efficacies between wt and laboratory-adapted CHIKV strains and in different cell lines.

As many drugs inhibit CHIKV replication at different potencies based on factors like MOI, cell type, viral strain/genotype and assay readouts, care must be taken when choosing an assay method, virus strain or cell line. Objective readouts should be given preference over empirical readouts which are based on the experience of a human reader (e.g., quantifying cytopathic effects under a light microscope) and might thus vary considerably. The use of different assay methods is certainly a good concept to evaluate and verify antiviral tests. The pros and cons of the different methods have to be known and ideally should complement one another so to receive the most meaningful results.

Compared to previously published data obtained by similar assays, the data and values of the compounds and the controls in this thesis vary within an acceptable range for each cell type. The calculated IC_{50} values are consistent and within the order of magnitude of published data. Especially the IC_{50} value determined for T-1105 in U138 cells ($IC_{50} = 35.74$ µM; R^2 of 0.790) seems reasonable given the fact that in the RTCA monitoring 50 µM of T-1105 fully protected the cells against CHIKV[Brazil] infection. It must be noted that despite the molecular modelling of the *in silico* designed potential nsP2 inhibitors (like #13), it still needs to be validated if the retardation of virus replication is actually grounded on nsP2 inhibition. This might be some project for future research, as assay methods on how to specifically test for nsP2 inhibitors have been published [118, 160].

The initial screenings for efficacy and toxicity in this thesis were done at 10 µM compound concentration due to previous publications on IC_{50} values of *in silico* nsP2 inhibitors [117, 145]. Various studies showed that some compounds and especially nucleoside analogues display different IC_{50} values depending on the cell line and their ability to metabolise (pro)drugs [137].

For future screening of drug series, I would recommend efficacy and toxicity screens at 10 µM, after which all compounds that show cytotoxicity and no or little efficacy at that dosage are being dismissed. The remaining compounds should then be screened again at 50 or even 100 µM. With this approach, all compounds that show toxicity at a low µM range can be rejected and the compounds which might display an antiviral effect at a higher concentration are not missed.

Future experiments might investigate if the discovered antiviral property of compound #13 also works in other alphaviruses. Especially an antiviral efficacy against the new world *Alphavirus* VEEV would be of interest, since the compound had originally been designed to inhibit the nsP2 of VEEV.

Schlussfolgerung und Ausblick

In dieser Arbeit wurden verschiedene Methoden zur Testung einer Reihe von *in silico* generierten antiviralen Substanzen gegen ein klinisches CHIKV Isolat erfolgreich eingesetzt. Dies ist zugleich die erste Veröffentlichung über den erfolgreichen Einsatz der humanen Glioblastom-Zelllinie U138 als neuronales Infektionsmodell für CHIKV. Zudem konnte gezeigt werden, dass sich CHIKV auch in der humanen Glioblastoma-Zelllinie U251 repliziert und dass diese Zelllinie ebenfalls für verschiedene Infektionsexperimente einsetzbar ist. Die Zelllinien A549 und Huh-7 stellten sich als unbrauchbar für Infektionsexperimente mit dem hier verwendeten CHIKV Isolat aus Brasilien heraus, da sich das Virus nicht in diesen Zellen vermehren konnte. Huh-7 Zellen scheinen zumindest mit dem Labor-adaptierten CHIKV[Ross] Stamm infizierbar zu sein. Zudem bewiesen unsere Experimente, dass es zwischen feldisolierten und labor-adaptierten CHIKV Stämmen, sowie zwischen verschiedenen Zelllinien, unterschiedliche zytopathologische Effekte und antivirale Wirkungen gibt.

Viele Substanzen hemmen die Replikation von CHIKV in unterschiedlichen Konzentrationen, abhängig von MOI, Zelltyp, Virusstamm und Assay Methode. Daher muss darauf geachtet werden, welche Methode, welcher Virusstamm und welche Zelllinie benutzt werden sollen. Objektiven Messmethoden sollten empirischen Methoden vorgezogen werden, da letztere von der Erfahrung und dem Geschick einer Person abhängen (etwa der Quantifizierung von zytopathischen Effekten mithilfe eines Lichtmikroskopes) und somit größeren Schwankungen unterliegen. Die Verwendung unterschiedlicher Methoden kann ein gutes Konzept für die Evaluierung und Bestätigung von antiviralen Tests sein. Die Vor- und Nachteile jeder Methode müssen bekannt sein. Idealerweise ergänzen sich die Tests, so dass die bestmöglichen Aussagen über die Ergebnisse gemacht werden können.

Verglichen mit zuvor veröffentlichten Daten ähnlicher Tests, bewegen sich die Daten und Werte der (Referenz-) Substanzen welche in dieser Arbeit getestet wurden, in einem für die unterschiedlichen Zelllinien akzeptablen Bereich. Die ermittelten IC_{50}- Werte sind stetig und in der Größenordnung von vorangegangenen Publikationen. Vor allem der IC_{50}-Wert für T-1105 in U138 Zellen (IC_{50} = 35.74 µM; R^2 von 0.790) erscheinen glaubwürdig in Anbetracht der Tatsache, dass in der RTCA-Messung eine Konzentration von 50 µM von T-1105 die Zellen vollständig vor einer Infektion mit CHIKV[Brazil] schützt. Es muss jedoch erwähnt werden, dass obgleich die *in silico* designten Substanzen potentielle nsP2 Inhibitoren sind (wie #13), es noch zu beweisen gilt, ob die Verringerung der CHIKV Replikation tatsächlich auf eine nsP2 Inhibition zurückzuführen ist. Dies zu ergründen könnte ein zukünftiges Projekt sein, da Methoden mit denen man speziell nsP2 Inhibition testen kann, bereits publiziert wurden [118, 160].

Das Screening der Substanzen für Effektivität und Toxizität wurde bei einer Konzentration von 10 µM durchgeführt, da vorangegangene Publikationen über ähnliche Substanzen (*in silico* nsP2 Inhibitoren) IC_{50}-Werte in diesem Bereich beschrieben [117, 145]. Verschiedene Veröffentlichungen belegen, dass einige Substanzen (allen voran Nukleosidanaloga) in unterschiedlichen Zelllinien auch unterschiedliche IC_{50}-Werte besitzen, abhängig von der Fähigkeit des Zelltyps die Substanzen (oder deren Vorstufe) zu metabolisieren [137]. Für zukünftige Screenings antiviraler Substanzen würde ich daher folgendes Vorgehen vorschlagen: Zunächst wird ein Screening Assay bei 10 µM durchgeführt und alle Substanzen welche bei dieser Konzentration eine Zytotoxizität bei fehlender oder mangelhafter Effektivität vorweisen, werden aussortiert. Die übrigen Substanzen werden bei einer höheren Konzentration (50 oder sogar 100 µM) erneut gescreent. Mit diesem Ansatz können alle Substanzen welche im unteren mikromolaren Bereich zytotoxisch sind ausgesondert werden und die Substanzen welche eventuell eine antivirale Effektivität bei einer höheren Konzentration besitzen, werden nicht übersehen.

Zukünftige Experimente könnten untersuchen ob die gefundenen antiviralen Eigenschaften von Substanz #13 auch bei anderen Alphaviren funktionieren. Insbesonders wäre es von Interesse ob eine antivirale Wikung gegen die Alphaviren der Neuen Welt wie etwa VEEV bei #13 vorhanden ist, da die Substanz urspünglich als ein Inhibitor für das nsP2 von VEEV designt wurde.

IX. SUMMARY

Alphaviruses belong to the RNA viruses and are globally distributed with a broad host range. They are zoonotic arboviruses and although they usually maintain their common cycle between mosquito vectors and avian or mammal hosts, they can nevertheless cause frequent infections in humans and livestock. This makes alphaviruses an economic and public health concern. While infections in the arthropod vector are persistent and asymptomatic, humans develop disease symptoms ranging from fever, rash, nausea and polyarthritis to fatal encephalitis. Although mortality in humans for many alphaviruses is considered low, the acute disease can be incapacitating and clinical sequelae may last for months to years, leaving some patients with chronic morbidities [161]. Climate change as well as vector range change can contribute to the spread of a formerly neglected tropical disease and turn it into an emerging (or re-emerging) disease with vast impact, especially when a naïve population is affected. Such emergence events are exemplified by the Chikungunya virus (CHIKV) outbreaks in the Indian Ocean (especially La Réunion Island) in 2005/2006 and the epidemic in the Caribbean which started with the first autochthonous cases in 2013 after CHIKV had been (re)introduced to the Americas [161-163]. To date, no specific antiviral therapies or safe, effective vaccines against alphaviruses are available for public use [164]. It is thus important to identify possible targets for antiviral intervention and find antivirals that block these targets.

The goal of this study was to test a number of antiviral compounds for their efficacy against a wildtype Chikungunya virus strain in cell viability assays. Some of the compounds have been developed *in silico* as potential inhibitors of the CHIKV/VEEV non-structural protein 2 (nsP2), while others are nucleoside analogues. CHIKV was used, firstly as a primary target for the antiviral compounds and secondly as a surrogate virus for those alphaviruses which require higher biosafety levels (such as Venezuelan, Western and Eastern Equine Encephalitis virus (VEE, WEE and EEEV)). In order to establish the cell viability assays, various cell lines were tested for their susceptibility to CHIKV infection with the goal to find a human cell line that would mimic CHIKV infection in the central nervous system. It was possible to identify the human glioblastoma cell lines U138 and U251 as being susceptible to CHIKV infection. Besides, different assay methods were compared (MTS/PMS viability assay, plaque reduction assay, viral RNA yield and electrical impedance monitoring (xCELLigence RTCA system)) to find a procedural method that would give the best information on dose-response effects of a compound against Chikungunya virus. After an initial screening of 34 antiviral compounds, it was possible to select a promising candidate which was further evaluated in IC_{50}/CC_{50} assays and compared to ribavirin (RBV) and T-1105 as reference compounds. The goal was to find a

substance with a good selective index (SI= CC_{50}/IC_{50}). The selected antiviral compound (#13) had efficacy in the low micromolecular range (4 µM) with no observable cytotoxicity in Vero-B4 and U138 cells at 30 µM.

X.   ZUSAMMENFASSUNG

Alphaviren sind RNA Viren mit einer weltweiten Verbreitung und einem breiten Wirtsspektrum. Sie sind zoonotische Arboviren, die meist in ihrem üblichen Infektionskreislauf mit Moskitos als Vektoren und Vögeln oder Wildsäugern als Wirt zirkulieren. Dennoch kommt es regelmäßig zu Infektionen bei Menschen und Nutztieren, wodurch Alphaviren von Interesse für Wirtschaft und öffentliche Gesundheit sind. Während beim Vektor die Infektion persistierend und symptomlos von statten geht, entwickeln Menschen Krankheitserscheinungen wie Fieber, Hautausschlag, Übelkeit, Polyarthritis bis hin zu tödlichen Encephalitiden. Obgleich die Mortalität im Menschen bei vielen Alphaviren als gering eingeschätzt wird, kann der akute Krankheitsverlauf den Patienten für sehr lange Zeit außer Gefecht setzen mit klinischen Rückfällen die Monate bis Jahre nach der akuten Krankheit andauern können und zu chronischen Beschwerden führen können [161]. Der Klimawandel und Wechsel zu anderen Vektoren können die Ausbreitung einer einst vernachlässigten tropischen Krankheit fördern und dazu führen, dass sie zu einer neu (oder wieder) auftretenden Erkrankung mit großen Auswirkungen wird, v.a. wenn eine naïve Bevölkerung betroffen ist. Dies wurde deutlich in den CHIKV Ausbrüchen im Indischen Ozean (v.a. auf La Réunion) 2005/2006 sowie der Epidemie in der Karibik welche 2013 die ersten autochthonen Fälle hatte, nachdem CHIKV (wieder) in Amerika eingeführt wurde [161-163]. Bis heute gibt es noch keine spezifische antivirale Therapie oder effektive für die breite Bevölkerung zugelassene Impfung gegen Alphaviren [164]. Es ist daher von größter Wichtigkeit, mögliche Ziele für antivirale Substanzen zu identifizieren und geeignete Substanzen für diese Ziele zu finden.

Im Rahmen dieser Arbeit sollten diverse antiviral Substanzen in Zellviabilitätstests auf ihre Wirksamkeit gegen ein klinisches Chikungunya Virus-Isolat getestet werden. Ein Teil der Substanzen gehören zu *in silico* hergestellten potentiellen Inhibitoren des nicht-struktur Proteins 2 (nsP2), der Rest sind Nukleosid Analoga. Das Chikungunya Virus (CHIKV) dient hier zum einen als primäres Ziel der antiviralen Substanzen als auch als Surrogat-Organismus für jene Alphaviren, welche eine höhere Sicherheitsstufe erfordern (etwa neurotrope Alphaviren, die unter BSL3 Bedingungen untersucht werden müssen). Zur Etablierung der Assays wurden zunächst unterschiedliche Zelllinien auf ihre Empfänglichkeit für Chikungunya Infektion getestet. Ziel war es zudem, eine humane Zelllinie zu finden, die ein Infektionsmodell für den neuronalen Krankheitsverlauf des Chikungunya Fiebers ermöglicht. Es gelang zwei humane Glioblastom-Zelllinien U138 und U251 zu identifizieren welche sich für Versuche mit CHIKV eignen.

Zudem wurden unterschiedliche Testsysteme (MTS/PMS Viabilitätsassay, Plaque Reduktionstest, Yield assay und Impedanzmessung (xCELLigence)) miteinander verglichen, um eine Vorgehensweise zu finden, welches die aussagekräftigsten Ergebnisse bezüglich der Dosis-Wirkungsrelation eines Stoffes gegen Chikungunya Virus liefert. Nach einem initialen Screening von 34 antiviralen Substanzen, konnte eine vielverstprechende Verbindung selektiert werden welche in IC_{50}/CC_{50} Versuchen weiter evaluiert wurde und mit zwei Referenzsubstanzen (Ribavirin und T-1105) verglichen wurde. Ziel war es, eine Substanz mit einem guten selektiven Index ($SI = CC_{50}/IC_{50}$) zu identifizieren. Die selektierte antivirale Verbindung #13 hatte eine Effektivität im unteren mikromolekularen Bereich (4 µM) und bei Konzentration von 30 µM keine zellschädigende Wirkung in Vero-B4 und U138 Zellen.

XI.   REFERENCES

1.   Kuhn, R.J., *Togaviridae*, in *Fields Virology*, D.M.H. Knipe, P. M.;, Editor. 2007, Lippincott, Williams, and Wilkins: Philadelphia, Pennsylvania, USA. p. 1001-1067.

2.   Rupp, J.C., et al., *Alphavirus RNA synthesis and non-structural protein functions*. J Gen Virol, 2015. **96**(9): p. 2483-2500.

3.   Reed, D.S., et al., *Aerosol infection of cynomolgus macaques with enzootic strains of venezuelan equine encephalitis viruses*. J Infect Dis, 2004. **189**(6): p. 1013-7.

4.   Reed, D.S., et al., *Aerosol exposure to western equine encephalitis virus causes fever and encephalitis in cynomolgus macaques*. J Infect Dis, 2005. **192**(7): p. 1173-82.

5.   Reed, D.S., et al., *Severe encephalitis in cynomolgus macaques exposed to aerosolized Eastern equine encephalitis virus*. J Infect Dis, 2007. **196**(3): p. 441-50.

6.   Rusnak, J.M., et al., *Comparison of Aerosol- and Percutaneous-acquired Venezuelan Equine Encephalitis in Humans and Nonhuman Primates for Suitability in Predicting Clinical Efficacy under the Animal Rule*. Comp Med, 2018. **68**(5): p. 380-395.

7.   Weaver, S.C., et al., *Alphaviruses: population genetics and determinants of emergence*. Antiviral Res, 2012. **94**(3): p. 242-57.

8.   Silva, L.A. and T.S. Dermody, *Chikungunya virus: epidemiology, replication, disease mechanisms, and prospective intervention strategies*. J Clin Invest, 2017. **127**(3): p. 737-749.

9.   Manimunda, S.P., et al., *Clinical progression of chikungunya fever during acute and chronic arthritic stages and the changes in joint morphology as revealed by imaging*. Trans R Soc Trop Med Hyg, 2010. **104**(6): p. 392-9.

10.   Mogi, M., et al., *The Climate Range Expansion of Aedes albopictus (Diptera: Culicidae) in Asia Inferred From the Distribution of Albopictus Subgroup Species of Aedes (Stegomyia)*. J Med Entomol, 2017. **54**(6): p. 1615-1625.

11.   Yasumura, Y.K., Y., *Studies on SV40 in tissue culture-preliminary step for cancer research in vitro*. Nihon rinsho, 1963. **21**: p. 1201–1215.

12.   Nii-Trebi, N.I., *Emerging and Neglected Infectious Diseases: Insights, Advances, and Challenges.* Biomed Res Int, 2017. **2017**: p. 5245021.

13.   Klohe, K., et al., *The 2017 Oslo conference report on neglected tropical diseases and emerging/re-emerging infectious diseases – focus on populations underserved.* Infectious Diseases of Poverty, 2019. **8**(1): p. 40.

14.   Moloo, A. *Neglected tropical diseases*. 2019 [cited 2019 December 19th]; Available from: https://www.who.int/neglected_diseases/diseases/en/.

15.   WHO. *R&D Blueprint for Action to Prevent Epidemics*. [PDF] 2016; R&D Blueprint for Action to Prevent Epidemics; Action Plan; May 2016]. Available from: https://www.who.int/publications/m/item/an-r-d-blueprint-for-action-to-prevent-epidemics.

16.   Frickmann, H. and O. Herchenröder, *Chikungunya Virus Infections in Military Deployments in Tropical Settings-A Narrative Minireview.* Viruses, 2019. **11**(6).

17.   (AFHSC), A.F.H.S.C.-. *Images in health surveillance: dengue and chikungunya virus vectors and prevention.* Msmr, 2014. **21**(1): p. 16-7.

18.   WHO, *Public health response to biological and chemical weapons: WHO guidance (2004) Annex 3: Biological Agents*. 2004, World Health Organization: Geneva.

19.   Rotz, L.D., et al., *Public health assessment of potential biological terrorism agents.* Emerg Infect Dis, 2002. **8**(2): p. 225-30.

20.   Fleming, D., O.; Hunt, Debra;, *Biological Safety Principles and Practices* 4th ed. 2006, Washington: ASM Press.

21.   Croddy, E.H., J.; Perez-Armendariz, C.;, *Chemical and Biological Warfare.* 2002, New York, USA: Springer.

22.   Zacks, M.A. and S. Paessler, *Encephalitic alphaviruses.* Vet Microbiol, 2010. **140**(3-4): p. 281-6.

23.   Sharma, A. and B. Knollmann-Ritschel, *Current Understanding of the Molecular Basis of Venezuelan Equine Encephalitis Virus Pathogenesis and Vaccine Development.* Viruses, 2019. **11**(2).

24.   Cirimotich, C.M., et al., *Chikungunya virus infection in Cynomolgus macaques following Intradermal and aerosol exposure.* Virol J, 2017. **14**(1): p. 135.

25.   Suhrbier, A., M.C. Jaffar-Bandjee, and P. Gasque, *Arthritogenic alphaviruses--an overview.* Nat Rev Rheumatol, 2012. **8**(7): p. 420-9.

26.   Garmashova, N., et al., *The Old World and New World alphaviruses use different virus-specific proteins for induction of transcriptional shutoff.* J Virol, 2007. **81**(5): p. 2472-84.

27.   Singh, S.K., *Overview on Chikungunya Virus Pathogenesis*, in *Human Emerging and Re-emerging Infections: Viral & Parasitic Infections*, S.K. Singh, Editor. 2015, John Wiley & Sons, Inc. : New Jersey. p. 177-188.

28.   Kraemer, M.U., et al., *The global distribution of the arbovirus vectors Aedes aegypti and Ae. albopictus.* Elife, 2015. **4**: p. e08347.

29.   Tsetsarkin, K.A., et al., *A single mutation in chikungunya virus affects vector specificity and epidemic potential.* PLoS Pathog, 2007. **3**(12): p. e201.

30.   Schuffenecker, I., et al., *Genome microevolution of chikungunya viruses causing the Indian Ocean outbreak.* PLoS Med, 2006. **3**(7): p. e263.

31.   Hannaman, D., et al., *A Phase 1 clinical trial of a DNA vaccine for Venezuelan equine encephalitis delivered by intramuscular or intradermal electroporation.* Vaccine, 2016. **34**(31): p. 3607-12.

32.   Chang, L.J., et al., *Safety and tolerability of chikungunya virus-like particle vaccine in healthy adults: a phase 1 dose-escalation trial.* Lancet, 2014. **384**(9959): p. 2046-52.

33.   Erasmus, J.H., S.L. Rossi, and S.C. Weaver, *Development of Vaccines for Chikungunya Fever.* J Infect Dis, 2016. **214**(suppl 5): p. S488-s496.

34.   Reisinger, E.C., et al., *Immunogenicity, safety, and tolerability of the measles-vectored chikungunya virus vaccine MV-CHIK: a double-blind, randomised, placebo-controlled and active-controlled phase 2 trial.* Lancet, 2019. **392**(10165): p. 2718-2727.

35.   Guzmán-Terán, C., et al., *Venezuelan equine encephalitis virus: the problem is not over for tropical America.* Ann Clin Microbiol Antimicrob, 2020. **19**(1): p. 19.

36.   Brown, D.T.C., L. D.; , *Replication of alphaviruses in mosquito cells*, in *The Togaviridae and Flaviviridae*, S.S. Schlesinger, M. J.;, Editor. 1986, Plenum Press: New York, NY. p. 171-207.

37.   Strauss, J.H. and E.G. Strauss, *The alphaviruses: gene expression, replication, and evolution.* Microbiol Rev, 1994. **58**(3): p. 491-562.

38.   Schütz, S. and P. Sarnow, *Interaction of viruses with the mammalian RNA interference pathway.* Virology, 2006. **344**(1): p. 151-7.

39.   Kash, J.C., et al., *Global host immune response: pathogenesis and transcriptional profiling of type A influenza viruses expressing the hemagglutinin and neuraminidase genes from the 1918 pandemic virus.* J Virol, 2004. **78**(17): p. 9499-511.

40.   Brown, R.S., J.J. Wan, and M. Kielian, *The Alphavirus Exit Pathway: What We Know and What We Wish We Knew.* Viruses, 2018. **10**(2).

41.   Melancon, P. and H. Garoff, *Processing of the Semliki Forest virus structural polyprotein: role of the capsid protease.* J Virol, 1987. **61**(5): p. 1301-9.

42.   Khan, A.H., et al., *Complete nucleotide sequence of chikungunya virus and evidence for an internal polyadenylation site.* J Gen Virol, 2002. **83**(Pt 12): p. 3075-3084.

43.   Kielian, M., C. Chanel-Vos, and M. Liao, *Alphavirus Entry and Membrane Fusion.* Viruses, 2010. **2**(4): p. 796-825.

44.   Rose, P.P., et al., *Natural resistance-associated macrophage protein is a cellular receptor for sindbis virus in both insect and mammalian hosts.* Cell Host Microbe, 2011. **10**(2): p. 97-104.

45.   Panda, D., et al., *Genome-wide RNAi screen identifies SEC61A and VCP as conserved regulators of Sindbis virus entry.* Cell Rep, 2013. **5**(6): p. 1737-48.

46.   Bernard, E., et al., *Endocytosis of chikungunya virus into mammalian cells: role of clathrin and early endosomal compartments.* PLoS One, 2010. **5**(7): p. e11479.

47.   Klimstra, W.B., K.D. Ryman, and R.E. Johnston, *Adaptation of Sindbis virus to BHK cells selects for use of heparan sulfate as an attachment receptor.* J Virol, 1998. **72**(9): p. 7357-66.

48.   Klimstra, W.B., et al., *DC-SIGN and L-SIGN can act as attachment receptors for alphaviruses and distinguish between mosquito cell- and mammalian cell-derived viruses.* J Virol, 2003. **77**(22): p. 12022-32.

49.   Wengler, G. and G. Wengler, *Identification of a transfer of viral core protein to cellular ribosomes during the early stages of alphavirus infection.* Virology, 1984. **134**(2): p. 435-42.

50.   Singh, I. and A. Helenius, *Role of ribosomes in Semliki Forest virus nucleocapsid uncoating.* J Virol, 1992. **66**(12): p. 7049-58.

51.   Wengler, G., D. Würkner, and G. Wengler, *Identification of a sequence element in the alphavirus core protein which mediates interaction of cores with ribosomes and the disassembly of cores.* Virology, 1992. **191**(2): p. 880-8.

52.   Kääriäinen, L. and T. Ahola, *Functions of alphavirus nonstructural proteins in RNA replication.* Prog Nucleic Acid Res Mol Biol, 2002. **71**: p. 187-222.

53.   Laakkonen, P., et al., *Alphavirus replicase protein NSP1 induces filopodia and rearrangement of actin filaments.* J Virol, 1998. **72**(12): p. 10265-9.

54.   Spuul, P., et al., *Phosphatidylinositol 3-kinase-, actin-, and microtubule-dependent transport of Semliki Forest Virus replication complexes from the plasma membrane to modified lysosomes.* J Virol, 2010. **84**(15): p. 7543-57.

55.   Jose, J., A.B. Taylor, and R.J. Kuhn, *Spatial and Temporal Analysis of Alphavirus Replication and Assembly in Mammalian and Mosquito Cells.* mBio, 2017. **8**(1).

56.   Das, I., et al., *Heat shock protein 90 positively regulates Chikungunya virus replication by stabilizing viral non-structural protein nsP2 during infection.* PLoS One, 2014. **9**(6): p. e100531.

57.   LaStarza, M.W., J.A. Lemm, and C.M. Rice, *Genetic analysis of the nsP3 region of Sindbis virus: evidence for roles in minus-strand and subgenomic RNA synthesis.* J Virol, 1994. **68**(9): p. 5781-91.

58.   Cristea, I.M., et al., *Tracking and elucidating alphavirus-host protein interactions.* J Biol Chem, 2006. **281**(40): p. 30269-78.

59.   Fros, J.J., et al., *Chikungunya virus nsP3 blocks stress granule assembly by recruitment of G3BP into cytoplasmic foci.* J Virol, 2012. **86**(19): p. 10873-9.

60.   Kim, D.Y., et al., *New World and Old World Alphaviruses Have Evolved to Exploit Different Components of Stress Granules, FXR and G3BP Proteins, for Assembly of Viral Replication Complexes.* PLoS Pathog, 2016. **12**(8): p. e1005810.

61.   Salonen, A., et al., *Properly folded nonstructural polyprotein directs the semliki forest virus replication complex to the endosomal compartment.* J Virol, 2003. **77**(3): p. 1691-702.

62.   Froshauer, S., J. Kartenbeck, and A. Helenius, *Alphavirus RNA replicase is located on the cytoplasmic surface of endosomes and lysosomes.* J Cell Biol, 1988. **107**(6 Pt 1): p. 2075-86.

63.   Acheson, N.H. and I. Tamm, *Replication of Semliki Forest virus: an electron microscopic study.* Virology, 1967. **32**(1): p. 128-43.

64.   Grimley, P.M., I.K. Berezesky, and R.M. Friedman, *Cytoplasmic structures associated with an arbovirus infection: loci of viral ribonucleic acid synthesis.* J Virol, 1968. **2**(11): p. 1326-38.

65.   Friedman, R.M., et al., *Membrane-associated replication complex in arbovirus infection.* J Virol, 1972. **10**(3): p. 504-15.

66.   Grimley, P.M., et al., *Specific membranous structures associated with the replication of group A arboviruses.* J Virol, 1972. **10**(3): p. 492-503.

67.   Pietila, M.K., K. Hellstrom, and T. Ahola, *Alphavirus polymerase and RNA replication.* Virus Res, 2017. **234**: p. 44-57.

68.   Hardy, W.R., et al., *Synthesis and processing of the nonstructural polyproteins of several temperature-sensitive mutants of Sindbis virus.* Virology, 1990. **177**(1): p. 199-208.

69.   Lemm, J.A., et al., *Polypeptide requirements for assembly of functional Sindbis virus replication complexes: a model for the temporal regulation of minus- and plus-strand RNA synthesis.* Embo j, 1994. **13**(12): p. 2925-34.

70.   Shirako, Y. and J.H. Strauss, *Regulation of Sindbis virus RNA replication: uncleaved P123 and nsP4 function in minus-strand RNA synthesis, whereas cleaved products from P123 are required for efficient plus-strand RNA synthesis.* J Virol, 1994. **68**(3): p. 1874-85.

71.   Shirako, Y. and J.H. Strauss, *Cleavage between nsP1 and nsP2 initiates the processing pathway of Sindbis virus nonstructural polyprotein P123.* Virology, 1990. **177**(1): p. 54-64.

72.   Rubach, J.K., et al., *Characterization of purified Sindbis virus nsP4 RNA-dependent RNA polymerase activity in vitro.* Virology, 2009. **384**(1): p. 201-8.

73.   Tomar, S., et al., *Catalytic core of alphavirus nonstructural protein nsP4 possesses terminal adenylyltransferase activity.* J Virol, 2006. **80**(20): p. 9962-9.

74.   Cristea, I.M., et al., *Host factors associated with the Sindbis virus RNA-dependent RNA polymerase: role for G3BP1 and G3BP2 in virus replication.* J Virol, 2010. **84**(13): p. 6720-32.

75.   Johnson, D.C. and M.J. Schlesinger, *Vesicular stomatitis virus and sindbis virus glycoprotein transport to the cell surface is inhibited by ionophores.* Virology, 1980. **103**(2): p. 407-24.

76.   Griffiths, G., et al., *The dynamic nature of the Golgi complex.* J Cell Biol, 1989. **108**(2): p. 277-97.

77.   Chen, K.C., et al., *Comparative analysis of the genome sequences and replication profiles of chikungunya virus isolates within the East, Central and South African (ECSA) lineage.* Virol J, 2013. **10**: p. 169.

78.   Firth, A.E., et al., *Discovery of frameshifting in Alphavirus 6K resolves a 20-year enigma.* Virol J, 2008. **5**: p. 108.

79.   Snyder, J.E., et al., *Functional characterization of the alphavirus TF protein.* J Virol, 2013. **87**(15): p. 8511-23.

80.   Yap, M.L., et al., *Structural studies of Chikungunya virus maturation.* Proc Natl Acad Sci U S A, 2017. **114**(52): p. 13703-13707.

81.   Zhang, R., et al., *Mxra8 is a receptor for multiple arthritogenic alphaviruses.* Nature, 2018. **557**(7706): p. 570-574.

82.   Sanz, M.A. and L. Carrasco, *Sindbis virus variant with a deletion in the 6K gene shows defects in glycoprotein processing and trafficking: lack of complementation by a wild-type 6K gene in trans.* J Virol, 2001. **75**(16): p. 7778-84.

83.   Loewy, A., et al., *The 6-kilodalton membrane protein of Semliki Forest virus is involved in the budding process.* J Virol, 1995. **69**(1): p. 469-75.

84.   Leung, J.Y., M.M. Ng, and J.J. Chu, *Replication of alphaviruses: a review on the entry process of alphaviruses into cells.* Adv Virol, 2011. **2011**: p. 249640.

85.   Taylor, A., et al., *Effects of an In-Frame Deletion of the 6k Gene Locus from the Genome of Ross River Virus.* J Virol, 2016. **90**(8): p. 4150-4159.

86.   Radoshitzky, S.R., et al., *siRNA Screen Identifies Trafficking Host Factors that Modulate Alphavirus Infection.* PLoS Pathog, 2016. **12**(3): p. e1005466.

87.   Wahlberg, J.M., W.A. Boere, and H. Garoff, *The heterodimeric association between the membrane proteins of Semliki Forest virus changes its sensitivity to low pH during virus maturation.* J Virol, 1989. **63**(12): p. 4991-7.

88.   Andersson, H., et al., *Oligomerization-dependent folding of the membrane fusion protein of Semliki Forest virus.* J Virol, 1997. **71**(12): p. 9654-63.

89.   Sánchez-San Martín, C., C.Y. Liu, and M. Kielian, *Dealing with low pH: entry and exit of alphaviruses and flaviviruses.* Trends Microbiol, 2009. **17**(11): p. 514-21.

90.   Zhang, X., et al., *Furin processing and proteolytic activation of Semliki Forest virus.* J Virol, 2003. **77**(5): p. 2981-9.

91.   Lobigs, M. and H. Garoff, *Fusion function of the Semliki Forest virus spike is activated by proteolytic cleavage of the envelope glycoprotein precursor p62.* J Virol, 1990. **64**(3): p. 1233-40.

92.   Kielian, M., et al., *Biosynthesis, maturation, and acid activation of the Semliki Forest virus fusion protein.* J Virol, 1990. **64**(10): p. 4614-24.

93.   Salminen, A., et al., *Membrane fusion process of Semliki Forest virus. II: Cleavage-dependent reorganization of the spike protein complex controls virus entry.* J Cell Biol, 1992. **116**(2): p. 349-57.

94.   Jose, J., J.E. Snyder, and R.J. Kuhn, *A structural and functional perspective of alphavirus replication and assembly.* Future Microbiol, 2009. **4**(7): p. 837-56.

95.   Wengler, G., et al., *Establishment and analysis of a system which allows assembly and disassembly of alphavirus core-like particles under physiological conditions in vitro.* Virology, 1984. **132**(2): p. 401-12.

96.   Wengler, G., *The regulation of disassembly of alphavirus cores.* Arch Virol, 2009. **154**(3): p. 381-90.

97.   Klenk, H.D. and W. Garten, *Host cell proteases controlling virus pathogenicity.* Trends Microbiol, 1994. **2**(2): p. 39-43.

98.   Suomalainen, M., P. Liljeström, and H. Garoff, *Spike protein-nucleocapsid interactions drive the budding of alphaviruses.* J Virol, 1992. **66**(8): p. 4737-47.

99.   Sjöberg, M. and H. Garoff, *Interactions between the transmembrane segments of the alphavirus E1 and E2 proteins play a role in virus budding and fusion.* J Virol, 2003. **77**(6): p. 3441-50.

100.   Marquardt, M.T., T. Phalen, and M. Kielian, *Cholesterol is required in the exit pathway of Semliki Forest virus.* J Cell Biol, 1993. **123**(1): p. 57-65.

101.   Vashishtha, M., et al., *A single point mutation controls the cholesterol dependence of Semliki Forest virus entry and exit.* J Cell Biol, 1998. **140**(1): p. 91-9.

102.   Lu, Y.E., T. Cassese, and M. Kielian, *The cholesterol requirement for sindbis virus entry and exit and characterization of a spike protein region involved in cholesterol dependence.* J Virol, 1999. **73**(5): p. 4272-8.

103.   Liljeström, P., et al., *In vitro mutagenesis of a full-length cDNA clone of Semliki Forest virus: the small 6,000-molecular-weight membrane protein modulates virus release.* J Virol, 1991. **65**(8): p. 4107-13.

104.   Ramsey, J. and S. Mukhopadhyay, *Disentangling the Frames, the State of Research on the Alphavirus 6K and TF Proteins.* Viruses, 2017. **9**(8).

105.   Taylor, G.M., P.I. Hanson, and M. Kielian, *Ubiquitin depletion and dominant-negative VPS4 inhibit rhabdovirus budding without affecting alphavirus budding.* J Virol, 2007. **81**(24): p. 13631-9.

106.   Frolov, I., E. Frolova, and S. Schlesinger, *Sindbis virus replicons and Sindbis virus: assembly of chimeras and of particles deficient in virus RNA.* J Virol, 1997. **71**(4): p. 2819-29.

107.   Martinez, M.G., et al., *Imaging the alphavirus exit pathway.* J Virol, 2014. **88**(12): p. 6922-33.

108.   Martinez, M.G. and M. Kielian, *Intercellular Extensions Are Induced by the Alphavirus Structural Proteins and Mediate Virus Transmission.* PLoS Pathog, 2016. **12**(12): p. e1006061.

109.   Ammerman, N.C., M. Beier-Sexton, and A.F. Azad, *Growth and maintenance of Vero cell lines.* Curr Protoc Microbiol, 2008. **Appendix 4**: p. Appendix 4E.

110.   Lieber, M., et al., *A continuous tumor-cell line from a human lung carcinoma with properties of type II alveolar epithelial cells.* Int J Cancer, 1976. **17**(1): p. 62-70.

111.   Kruse, C.A., et al., *Characterization of a continuous human glioma cell line DBTRG-05MG: growth kinetics, karyotype, receptor expression, and tumor suppressor gene analyses.* In Vitro Cell Dev Biol, 1992. **28a**(9-10): p. 609-14.

112.   Nakabayashi, H., et al., *Growth of human hepatoma cells lines with differentiated functions in chemically defined medium.* Cancer Res, 1982. **42**(9): p. 3858-63.

113.   Pontén, J. and E.H. Macintyre, *Long term culture of normal and neoplastic human glia.* Acta Pathol Microbiol Scand, 1968. **74**(4): p. 465-86.

114.   Pontén, J. and B. Westermark, *Properties of human malignant glioma cells in vitro.* Med Biol, 1978. **56**(4): p. 184-93.

115.   Laue, M.M., L. , *The VirusExplorer - A database for diagnostic electron microscopy of viruses.* 2015, Zenodo.

116.   Noranate, N., et al., *Characterization of chikungunya virus-like particles.* PLoS One, 2014. **9**(9): p. e108169.

117. Bassetto, M., et al., *Computer-aided identification, design and synthesis of a novel series of compounds with selective antiviral activity against chikungunya virus.* Antiviral Res, 2013. **98**(1): p. 12-8.

118. Das, P.K., et al., *Design and Validation of Novel Chikungunya Virus Protease Inhibitors.* Antimicrob Agents Chemother, 2016. **60**(12): p. 7382-7395.

119. Briolant, S., et al., *In vitro inhibition of Chikungunya and Semliki Forest viruses replication by antiviral compounds: synergistic effect of interferon-alpha and ribavirin combination.* Antiviral Res, 2004. **61**(2): p. 111-7.

120. Gallegos, K.M., et al., *Chikungunya Virus: In Vitro Response to Combination Therapy With Ribavirin and Interferon Alfa 2a.* J Infect Dis, 2016. **214**(8): p. 1192-7.

121. Franco, E.J., et al., *The effectiveness of antiviral agents with broad-spectrum activity against chikungunya virus varies between host cell lines.* Antivir Chem Chemother, 2018. **26**: p. 2040206618807580.

122. Marlina, S., et al., *Development of a Real-Time Cell Analysing (RTCA) method as a fast and accurate screen for the selection of chikungunya virus replication inhibitors.* Parasit Vectors, 2015. **8**: p. 579.

123. Delang, L., et al., *Mutations in the chikungunya virus non-structural proteins cause resistance to favipiravir (T-705), a broad-spectrum antiviral.* J Antimicrob Chemother, 2014. **69**(10): p. 2770-84.

124. BAuA, *TRBA 462 "Einstufung von Viren in Risikogruppen".* 2012, Ausschuss für Biologische Arbeitsstoffe (ABAS) & Bundesausschuss für Arbeitsschutz und Arbeitsmedizin (BAuA).

125. BAuA, *TRBA 100 „Schutzmaßnahmen für Tätigkeiten mit biologischen Arbeitsstoffen in Laboratorien".* 2013, Ausschuss für Biologische Arbeitsstoffe (ABAS) & Bundesausschuss für Arbeitsschutz und Arbeitsmedizin (BAuA).

126. Sourisseau, M., et al., *Characterization of reemerging chikungunya virus.* PLoS Pathog, 2007. **3**(6): p. e89.

127.   Olagnier, D., et al., *Inhibition of dengue and chikungunya virus infections by RIG-I-mediated type I interferon-independent stimulation of the innate antiviral response.* Journal of virology, 2014. **88**(8): p. 4180-4194.

128.   Solignat, M., et al., *Replication cycle of chikungunya: a re-emerging arbovirus.* Virology, 2009. **393**(2): p. 183-97.

129.   Sudeep, A.B., et al., *Differential susceptibility & replication potential of Vero E6, BHK-21, RD, A-549, C6/36 cells & Aedes aegypti mosquitoes to three strains of chikungunya virus.* Indian J Med Res, 2019. **149**(6): p. 771-777.

130.   Lin, J., et al., *Comparative analysis of phase I and II enzyme activities in 5 hepatic cell lines identifies Huh-7 and HCC-T cells with the highest potential to study drug metabolism.* Arch Toxicol., 2012 **86**(1): p. 87-95.

131.   Acharya, D., et al., *Loss of Glycosaminoglycan Receptor Binding after Mosquito Cell Passage Reduces Chikungunya Virus Infectivity.* PLoS Negl Trop Dis, 2015. **9**(10): p. e0004139.

132.   Hsieh, P., M.R. Rosner, and P.W. Robbins, *Host-dependent variation of asparagine-linked oligosaccharides at individual glycosylation sites of Sindbis virus glycoproteins.* J Biol Chem, 1983. **258**(4): p. 2548-54.

133.   Nunes, M.R., et al., *Emergence and potential for spread of Chikungunya virus in Brazil.* BMC Med, 2015. **13**: p. 102.

134.   Spriggs, K.A., M. Bushell, and A.E. Willis, *Translational Regulation of Gene Expression during Conditions of Cell Stress.* Molecular Cell, 2010. **40**(2): p. 228-237.

135.   Weller, M., et al., *Predicting chemoresistance in human malignant glioma cells: the role of molecular genetic analyses.* Int J Cancer, 1998. **79**(6): p. 640-4.

136.   Graci, J.D. and C.E. Cameron, *Mechanisms of action of ribavirin against distinct viruses.* Rev Med Virol, 2006. **16**(1): p. 37-48.

137.   Librelotto, C.S., et al., *Chromosomal instability and cytotoxicity induced by ribavirin: comparative analysis in cell lines with different drug-metabolizing profiles.* Drug Chem Toxicol, 2019. **42**(4): p. 343-348.

138. Scheidel, L.M. and V. Stollar, *Mutations that confer resistance to mycophenolic acid and ribavirin on Sindbis virus map to the nonstructural protein nsP1.* Virology, 1991. **181**(2): p. 490-9.

139. Furuta, Y., et al., *Mechanism of action of T-705 against influenza virus.* Antimicrob Agents Chemother, 2005. **49**(3): p. 981-6.

140. Mendenhall, M., et al., *Effective oral favipiravir (T-705) therapy initiated after the onset of clinical disease in a model of arenavirus hemorrhagic Fever.* PLoS Negl Trop Dis, 2011. **5**(10): p. e1342.

141. Baranovich, T., et al., *T-705 (favipiravir) induces lethal mutagenesis in influenza A H1N1 viruses in vitro.* J Virol, 2013. **87**(7): p. 3741-51.

142. Arias, A., L. Thorne, and I. Goodfellow, *Favipiravir elicits antiviral mutagenesis during virus replication in vivo.* Elife, 2014. **3**: p. e03679.

143. Sangawa, H., et al., *Mechanism of action of T-705 ribosyl triphosphate against influenza virus RNA polymerase.* Antimicrobial agents and chemotherapy, 2013. **57**(11): p. 5202-5208.

144. Jin, Z., et al., *The ambiguous base-pairing and high substrate efficiency of T-705 (Favipiravir) Ribofuranosyl 5'-triphosphate towards influenza A virus polymerase.* PLoS One, 2013. **8**(7): p. e68347.

145. Tardugno, R., et al., *Design, synthesis and evaluation against Chikungunya virus of novel small-molecule antiviral agents.* Bioorg Med Chem, 2018. **26**(4): p. 869-874.

146. Verheijen, M., et al., *DMSO induces drastic changes in human cellular processes and epigenetic landscape in vitro.* Sci Rep, 2019. **9**(1): p. 4641.

147. De Jong, W.H. and P.J. Borm, *Drug delivery and nanoparticles:applications and hazards.* Int J Nanomedicine, 2008. **3**(2): p. 133-49.

148. Lee, M.S., E.C. Dees, and A.Z. Wang, *Nanoparticle-Delivered Chemotherapy: Old Drugs in New Packages.* Oncology (Williston Park), 2017. **31**(3): p. 198-208.

149. Hucke, F.I.L. and J.J. Bugert, *Current and Promising Antivirals Against Chikungunya Virus.* Frontiers in Public Health, 2020. **8**(916).

150.   Preston, S.L., et al., *Pharmacokinetics and absolute bioavailability of ribavirin in healthy volunteers as determined by stable-isotope methodology.* Antimicrob Agents Chemother, 1999. **43**(10): p. 2451-6.

151.   Lindahl, K., et al., *High-dose ribavirin in combination with standard dose peginterferon for treatment of patients with chronic hepatitis C.* Hepatology, 2005. **41**(2): p. 275-9.

152.   Sung, H., M. Chang, and S. Saab, *Management of Hepatitis C Antiviral Therapy Adverse Effects.* Curr Hepat Rep, 2011. **10**(1): p. 33-40.

153.   Aslantürk, Ö.S., *In Vitro Cytotoxicity and Cell Viability Assays: Principles, Advantages, and Disadvantages.* Genotoxicity - A Predictable Risk to Our Actual World, 2018.

154.   Payne, S., *Chapter 4 - Methods to Study Viruses*, in *Viruses*, S. Payne, Editor. 2017, Academic Press. p. 37-52.

155.   Ryu, W.-S., *Chapter 4 - Diagnosis and Methods*, in *Molecular Virology of Human Pathogenic Viruses*, W.-S. Ryu, Editor. 2017, Academic Press: Boston. p. 47-62.

156.   Berkowitz, F.E. and M.J. Levin, *Use of an enzyme-linked immunosorbent assay performed directly on fixed infected cell monolayers for evaluating drugs against varicella-zoster virus.* Antimicrobial agents and chemotherapy, 1985. **28**(2): p. 207-210.

157.   MacLachlan, N.J. and E.J. Dubovi, *Chapter 2 - Virus Replication*, in *Fenner's Veterinary Virology (Fifth Edition)*, N.J. MacLachlan and E.J. Dubovi, Editors. 2017, Academic Press: Boston. p. 17-45.

158.   Ke, N., et al., *The xCELLigence system for real-time and label-free monitoring of cell viability.* Methods Mol Biol, 2011. **740**: p. 33-43.

159.   Kho, D., et al., *Application of xCELLigence RTCA Biosensor Technology for Revealing the Profile and Window of Drug Responsiveness in Real Time.* Biosensors (Basel), 2015. **5**(2): p. 199-222.

160.   Lucas-Hourani, M., et al., *A phenotypic assay to identify Chikungunya virus inhibitors targeting the nonstructural protein nsP2.* J Biomol Screen, 2013. **18**(2): p. 172-9.

161.   Yactayo, S., et al., *Epidemiology of Chikungunya in the Americas.* J Infect Dis, 2016. **214**(suppl 5): p. S441-s445.

162.   Cassadou, S., et al., *Emergence of chikungunya fever on the French side of Saint Martin island, October to December 2013.* Euro Surveill, 2014. **19**(13).

163.   Weaver, S.C., *Arrival of chikungunya virus in the new world: prospects for spread and impact on public health.* PLoS Negl Trop Dis, 2014. **8**(6): p. e2921.

164.   Staples, J.E. and A.M. Powers, *217 - Togaviridae: Alphaviruses*, in *Principles and Practice of Pediatric Infectious Diseases (Fifth Edition)*, S.S. Long, C.G. Prober, and M. Fischer, Editors. 2018, Elsevier. p. 1126-1128.e2.

XII. APPENDIX

1. List of materials

1.1. Working compounds

1.1.1. Series 1: *in silico* nsP2 protease inhibitors

Molecule No.	Structure	Internal Code	Primary Code	Molar mass g/mol
1		MB-58	AB-224	362.429
2		MB-59	AB-228	363.417
3		MB-60	AB-233	352.394
4		MB-61	AB-237	396.531
5		MB-62	AB-244	394.515
6		MB-63	AB-246	320.436
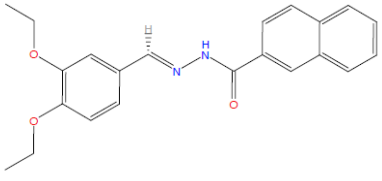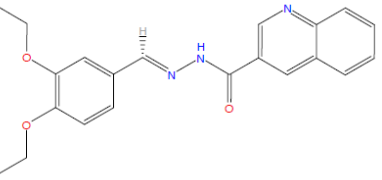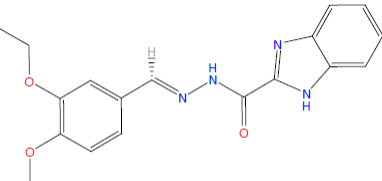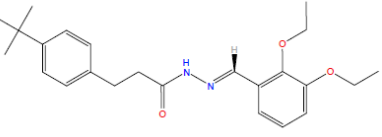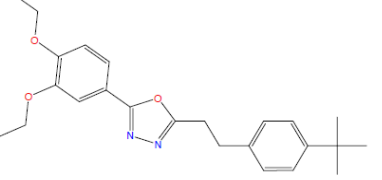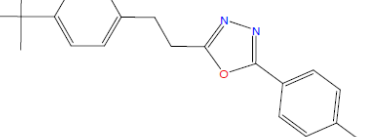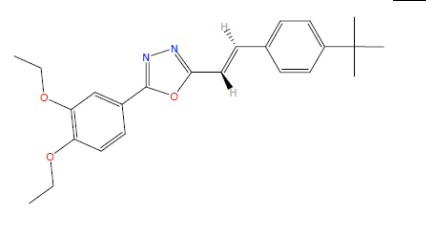
7		MB-64	AB-248	392.499
8		MB-65	AB-249	380.488
9		MB-66	AB-252	420.514
10		MB-67	AB-260	320.436
11		MB-68	AB-274	363.417
12		MB-69	AB-280	351.406
13		MB-70	AB-287	308.425
14		MB-71	AB-293	362.517
15		MB-72	AB-295	367.489
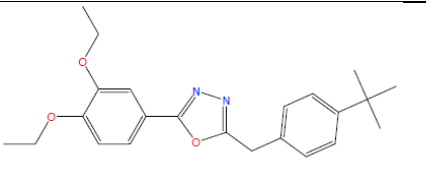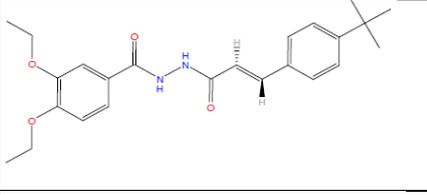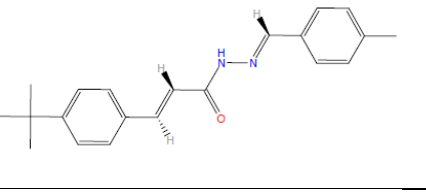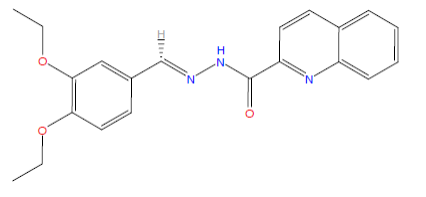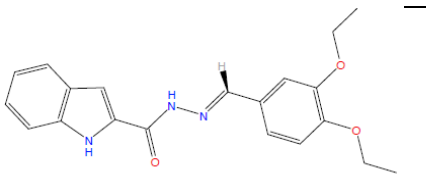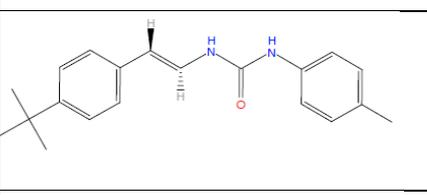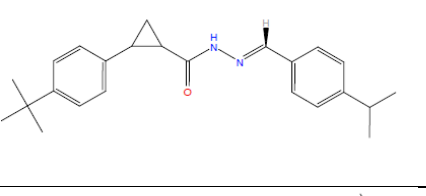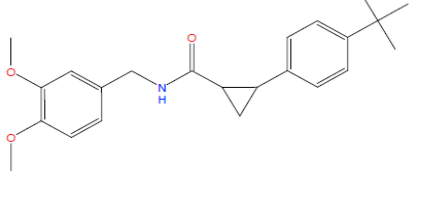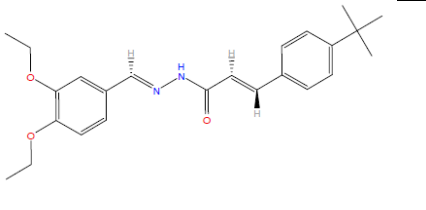
16		MB-73	AB-297	394.515
17		MB-74	AB-298	334.463
18		MB-75	AB-581	410.514
19		MB-76	AB-582	322.452
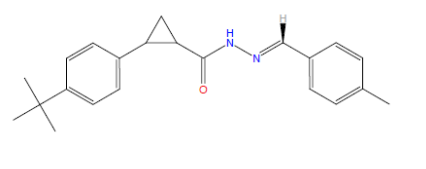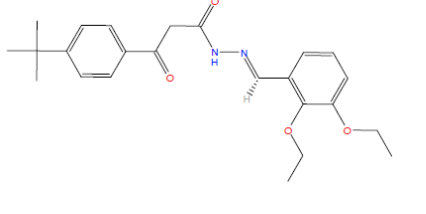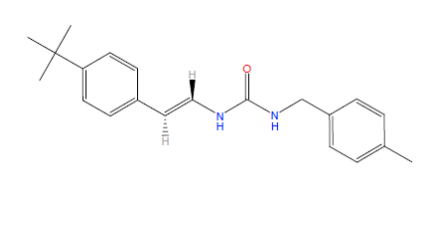
1.1.2. Series 2: Nucleoside analogues and ProTides of favipiravir (T-1105)

Molecule No.	Structure	internal code	primary code	Series	Molar mass g/mol
20		MB-85	AB-1717	T-1105-nuc	285.25598
21		MB-86	AB-1718	T-1105-nuc	271.229
22		MB-87	AB-1719	T-1105-nuc	287.24698
23		MB-88	AB-1720	T-1105-nuc	287.24698
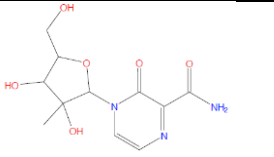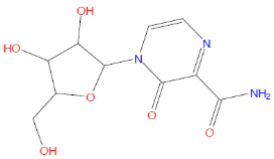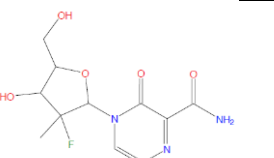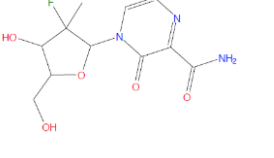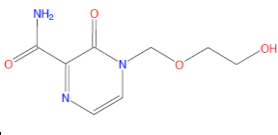
24		MB-89	AB-1721	T-1105-nuc	213.19299
25		MB-90	AB-1723	T-1105 Reference	139.114
26		MB-91	AB-1724	T-1105-nuc	285.25598
27		MB-101	AB-1884	T-1105-ProTide	530.474
28		MB-102	AB-1885	T-1105-ProTide	482.42999
29		MB-103	AB-1886	T-1105-ProTide	604.52802
30		MB-104	AB-1887	T-1105-ProTide	604.52802
31		MB-105	AB-1888	T-1105-ProTide	560.5
32	Atom limit exceeded	MB-106	AB-1889	T-1105-ProTide	877.78101
33		MB-107	AB-1890	T-1105-ProTide	602.53699
34		MB-108	AB-1891	T-1105-ProTide	602.53699
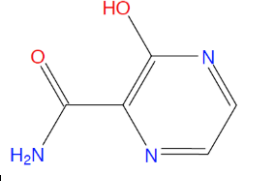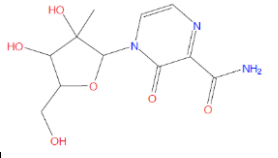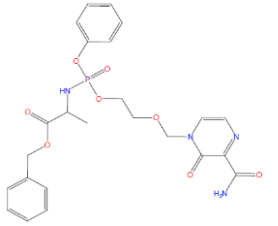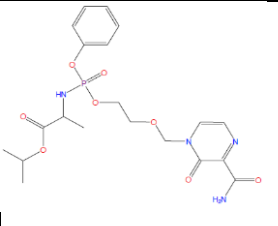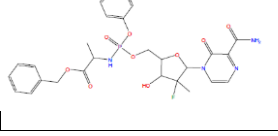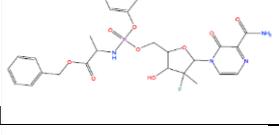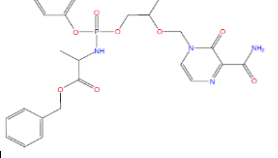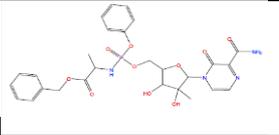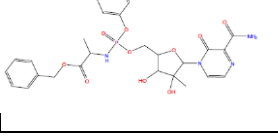
1.2.   Commercial chemicals, enzymes and solutions

Tab. 35: Commercial chemicals, enzymes, media and solutions

Name	Manufacturer/ Source
Alcian-blue 8 GX, C.I. 74240	Sigma-Aldrich (Schnelldorf, Germany)
Antibodies: anti-CHIKV (IgG) antibody F160129BF Alexa Fluor 488 goat α-human IgG	 Euroimmun (Lübeck, Germany) Invitrogen (Carlsbad, CA, USA)
Crystal violet (C.I. 42555)	Merck (Darmstadt, Germany)
Dimethyl sulfoxide (DMSO)	Sigma-Aldrich, UK
Dulbecco's Modified Eagle Medium (DMEM(1X) + GlutaMAX™-I medium with 1 g/L of D-glucose Ref# 21885-025	Thermo Fisher Scientific Ltd, UK
Dulbecco's Modified Eagle Medium (DMEM(1X) + GlutaMAX™-I medium with 4.5 g/L of D-glucose Ref# 61965-06	Thermo Fisher Scientific Ltd, UK
Dulbecco's Phosphate Buffered Saline (DPBS) ohne $CaCl_2$ und $MgCl_2$	Sigma-Aldrich (Schnelldorf, Germany)
Ethanol (99.9%)	Roth (Karlsruhe, Germany)
Foetal Bovine Serum	Sigma-Aldrich, Hilden, Germany
Formaldehyde (37%)	Merck (Darmstadt, Germany)
Glacial acetic acid (99%)	Merck (Darmstadt, Germany)
Glutaraldehyde (25%) G5882	Merck (Darmstadt, Germany)
Hydroxychloroquine	Sigma-Aldrich, Hilden, Germany
Ivermectine	Sigma-Aldrich, Hilden, Germany
Loading Buffer (5X) 0.4 % Trypan blue	Invitrogen (Carlsbad, CA, USA) ICN Biomedicals Inc. (CA, USA)
Methyl cellulose (M0262-250G) (Viscosity 400 cP)	Sigma-Aldrich (Schnelldorf, Germany)
Paraformaldehyde	Merck (Darmstadt, Germany)
Phosphotungstic acid (1%)	Merck (Darmstadt, Germany)
Ribavirin	Merck (Darmstadt, Germany)
RNase-free water	Qiagen (Hilden, Germany)
Trysin: TrypLE™ Express, Ref# 12604-013	Gibco, Life Technologies Limited, UK

1.3.   Commercial kits

Tab. 36: Commercial kits

Name	Manufacturer/ Source of supply
CellTiter 96®AQ$_{ueous}$ Non-Radioactive Cell Proliferation Assay (MTS)	Promega (Madison, Wisconsin, USA)
QIAmp® DNA Mini Kit	Qiagen (Hilden, Germany)
QuantiTect®Probe RT PCR Kit	Qiagen (Hilden, Germany)
ReadyMix™ Taq PCR Reaction Mix	Sigma-Aldrich (Missouri, USA)
RealStar® Chikungunya RT-PCR Kit 2.0	Altona diagnostics (Hamburg, Germany)
TOPO TA Cloning® Kit for Sequencing	Thermo Fischer Scientific (MA, USA)
TopTaq™ Master Mix Kit	Qiagen (Hilden)

1.4.   **Buffers and solutions**

Tab. 37: Buffers and solutions

Name	Composition	
0.2% Crystal violet, 20% Formaldehyde	460 mL miliQ water 2 gr Crystal violet 540 mL Formaldehyde (37%)	
2.5 % Methyl celluloses	25 gr of Methyl celluloses in 1000 mL of miliQ water	
NaCl-Solution (5M)	5 M NaCl	
TE-Buffer (1X)	10 mM Tris, pH 8 0,1 mM EDTA	
Alcian-blue (1%) 1:1 Mixture of Solution I and Solution II	**Solution I**: 2% alcian blue ddH$_2$O Dissolve by using an ultrasonic bath (10 min) Centrifuge Solution I for 1h at 14150×g or full speed rpm at RT Carefully collect the supernatant	**Solution II**: 2% glacial acetic acid ddH$_2$O

1.5.   **Consumables**

Tab. 38: Consumables

Name	Manufacturer/ Source of supply
24-Well Cell Culture Plates (Cellstar®)	Greiner bio-one (Frickenhausen, Germany)
96-Well Plates clear (Costar®)	Corning Inc. (NY, USA)
Cell culture flask (75 m^2) with vented caps: NUNC™ EasY Flask™ 75 m^2 Nunclon™ Delta Surface, Cat#. 156499	Thermo Fischer Scientific, Denmark
Conical Tubes (15 ml, 50 ml): Cellstar® Tubes, Cat#. 188271	Greiner Bio-one, Germany
Desinfectant: Pursept® AXpress	Schülke & Mayr GmbH, Germany
Disposable gloves, Nitril	UNIGLOVES® Arzt- und Klinikbedarf (Troisdorf)
Mikro Tubes (1.5 mL, 2 mL)	Eppendorf, (Hamburg Germany)
Neubauer cell counting chamber	NanoEnTek Inc. South Korea
PCR-Tubes	Eppendorf, (Hamburg Germany)
Pipet tips (10 – 1000 µl)	Thermo Scientific, UK
real time-PCR-Tubes	Sarstedt (Nümbrecht)
Serological pipets (5 mL, 10 mL, 25 mL)	Falcon corning incorporated – Life Sciences, USA
Trash bags	Carl Roth (Karlsruhe)

1.6.   **Machines and software**

Tab. 39: Machines and software

Name	Model/ Type	Manufacturer/ Source of supply
Biosafety cabinets	Berner Claire® pro & Berner Claire® pure	Berner International GmbH, Germany
Cell Resistance	xCELLigence RTCS RTCA Software 2.0	PerkinElmer (MA, USA) ACEA Biosciences Inc. (USA)
Centrifuges	Heraeus MultifugeX1R Centrifuge Centrifuge 5424 R	Unity™Lab Services, Part of Thermo Fischer Scientific, (MA, USA). Eppendorf (Hamburg, Germany)
Data Programmes	Microsoft Office 2013 GraphPad Prism6 Adobe-Reader 11 VirusExplorer20151127	Microsoft (Redmond, USA) GraphPad Software, (La Jolla, CA, USA) Adobe Systems (San Jose, USA) Robert Koch Intitute, Germany
DNR/RNA purification	QIAcube classic	Qiagen, Hilden, Deutschland
Incubators	Heraeus® HeraCell®	Thermo Scientific (Waltham, MA, USA)
Micropipets (10 – 1000 µL)	Research plus	Eppendorf, (Hamburg, Germany)
Microplate-Readers	iMark™ Microplate Reader Victor™X5 PerkinElmer 2030 Manager Software	Bio-Rad (München, Germany PerkinElmer (MA, USA)
Microscopes:	Axiovert25 LSM-TPMT Leica DM3000 (inverted) Zeiss Libra 120 TEM ImageSp Software WinTEM™ control software	Zeiss (Oberkochen, Germany) Zeiss (Oberkochen, Germany) Leica, (Wetzlar, Germany) Zeiss (Oberkochen, Germany)
PCR-Cycler real time PCR-Cycler	RotorGeneQ RotorGeneQ Version 2.3.1 Software Light Cycler® 480	Qiagen, (Hilden, Germany) Qiagen, (Hilden, Germany) Roche, Germany
Pipetting Aid	Pipetus®	Hirschmann Laborgeräte (Eberstadt, Germany)

Preparation of nucleic acids	MagnNA Pure LC MagNa Pure LC Total Nucleic Acid Isolation Kit REF# 03038505001	Roche Diagnostics GmbH, (Mannheim, Germany)
Vortexer	IKA®MS3 basic	IKA, IKA-Werke GmbH & Co. KG (Staufen, Germany)

2. Tables and figures

Tables:

Figures:

XIII. ACKNOWLEDGEMENTS

I am forever grateful to

Dr. Bugert for his ready mentoring and professional input.

Prof. Dr. Brack-Werner from the Helmholtz Institute for a loan of U138 and U251 cells.

Paola Zanetta, for her friendship, technical help with the CLSM and in the statistical analysis.

Malena Bestehorn-Willmann for backing me up, helping me in the L3**, sequencing my CHIKV strains, giving professional input and experimental support.

Marcella Bassetto for her friendship and helping me understand chemistry.

The Bugert Lab members for their practical support, ready offered help and the hearty atmosphere.

Claudia Kalhofer, for her technical support with the TEM.

All colleagues of the IMB for their ready support, patience and comradeship.